DETERMINING THE ROLE OF ACIDIC PH SENSING AND RESISTANCE IN UROPATHOGENIC ESCHERICHIA COLI PATHOGENESIS

By

Michelle Alyse Wiebe

Dissertation

Submitted to the Faculty of the

Graduate School of Vanderbilt University

in partial fulfillment of the requirements

for the degree of

DOCTOR OF PHILOSOPHY

in

Microbe-Host Interactions

May 10, 2024

Nashville, Tennessee

Approved:

John Karijolich, Ph.D., Chair

Mariana Byndloss, Ph.D., DVM

Timothy Cover, M.D.

John McLean, Ph.D.

Maria Hadjifrangiskou, Ph.D.

Dedication

To my parents and brother. Thanks for believing in me.

Acknowledgements

First, I want to thank my advisor, Dr. Maria Hadjifrangiskou, for all her support over the past 5.5 years. Her dedication to science and her students inspires me. She has created an amazing lab environment where we can feel comfortable being who we are. Thank you to my thesis committee, Dr. John Karjiolich, Mariana Byndloss, Tim Cover, and John McLean, for all their support and suggestions.

Thank you to all the goofballs who have made my time in lab so amazing: Grace Morales, Hamilton Green, Jamisha Francis, Tomás Bermudez, Seth Reasoner, Sarah Comer, Mollie Gidney, and Robert Mann. Thank you all for being the reason 80% of the tears I shed in lab were because I was crying from laughing so hard. You all are amazing scientists and the best coworkers I could have asked for to get through grad school. I would also like to thank the former members of the lab, Dr. John Brannon, Dr. Connor Beebout, and Dr. Melanie Hurst, for showing me the ropes, being my coffee buddies, and helping me become the scientist I am now.

Thank you to my brother, George. My first friend, my best pal, and the owner of my favorite dog. Thanks for all the reality checks when I doubt myself and all your encouragement. Most importantly, I would like to thank my parents. I wouldn't be here if it weren't for the hours that you spent helping me with my homework, taking me to the library, museums, and all my sporting events, reading with me for mother-daughter book club, driving me to and from boarding school on the weekends, and the countless other sacrifices you made to spend time with me. Thank you for showing me the world and encouraging me to explore. No matter how smart you think I am, I could not have accomplished this without the discipline, perseverance, and stubbornness you instilled in me. Everything you have done is more valuable than anything else you could have possibly given me.

Table of Contents

List of Tables

List of Figures

List of Abbreviations

%	Percent
℃	Degrees Celsius
Δ	Deletion
μ	Micro
AFAB	Assigned Female at Birth
AMAB	Assigned Male at Birth
ANOVA	Analysis of Variance
APEC	Avian pathogenic *Escherichia coli*
AR	Acid Resistance
ASB	Asymptomatic bacteriuria
AV	Aerobic vaginitis
BV	Bacterial vaginosis
cAMP	Cyclic adenosine monophosphate
cDNA	Complementary DNA
CFA	Cyclopropane fatty acid
CFU	Colony Forming Unit
CRP	cAMP receptor protein
C_T	Cycle Threshold
DNA	Deoxyribonucleic Acid
E. coli	*Escherichia coli*
EHEC	Enterohemorrhagic *Escherichia coli*
EMSA	Electrophoretic mobility shift assay
EPEC	Enteropathogenic *Escherichia coli*
et al	And Others
EtBr	Ethidium Bromide
ETC	Electron transport chain
ExPEC	Extraintestinal pathogenic *Escherichia coli*
GABA	γ-amino butyric acid
GI	Gastrointestinal
GTP	Guanosine triphosphate
H^+	Hydrogen ion
HEPES	N-2-hydroxyethylpiperazine-N-2-ethane sulfonic acid
HK	Histidine kinase
IACUC	Institutional Animal Care and Use Committee
IBC	Intracellular Bacterial Communities
Ig	Immunoglobulin
IL	Interleukin
kan	Kanamycin
kDa	Kilodaltons
LB	Lysogeny Broth
LC-MS/MS	Liquid Chromotography Tandem Mass Spectrometry
MFS	Major Facilitator Superfamily
mg	Milligram
mL	Milliliter

MLST	Multi locus sequence type
mm	Millimeter
mM	Millimolar
MOPS	3-(N-morpholino)propanesulfonic acid
NIH	National Institutes of Health
NMEC	neonatal meningitis causing *Escherichia coli*
OD_{600}	Optical Density at 600 nanometers
OMP	Outer membrane protein
PAGE	Polyacrylamide Gel Electrophoresis
PBS	Phosphate Buffered Saline
PCR	Polymerase Chain Reaction
pH	Potential of Hydrogen
PLP	Pyridoxal-5'-phosphate
polyp	Inorganic polyphosphate
QIR	Quiescent Intracellular Reservoir
RLU	Relative Luminescence Unit
RNA	Ribonucleic Acid
RR	Response regulator
RT-qPCR	Reverse Transcription Quantitative Polymerase Chain Reaction
rUTI	Recurrent urinary tract infection
SD	Standard deviation
SDS	Sodium Dodecyl Sulfate
SEM	Standard Error of the Mean
Spp.	Species
ST	Sequence type
TBST	Tris Buffered Saline Tween 20
TCA	Tricarboxylic Acid Cycle
TCS	Two-component system
TLR	Toll like receptor
TTC	Triphenyl Tetrazolium Chloride
UPEC	Uropathogenic *Escherichia coli*
UTI	Urinary tract infection
UUTI	Uncomplicated urinary tract infection
VUMC	Vanderbilt University Medical Center
VUTI	Vanderbilt Urinary Tract Isolate
WT	Wild-type
YESCA	Yeast Extract Casamino Acids

Chapter 1: Introduction

1.1 Urinary Tract Infections

Urinary tract infections (UTIs) are among the most common bacterial infections of adult humans in the world. Approximately 150 million people experience these infections every year.[1-3] This amounts to billions of dollars in healthcare costs and hours of time in missed work.[4] UTIs are characterized by the presence of pathogenic bacteria in the urinary tract, which includes the urethra, bladder, ureters, and kidneys. UTIs can manifest across a spectrum of symptoms from asymptomatic bacteriuria (ASB) to uncomplicated cystitis, or in some cases, pyelonephritis, bacteremia and urosepsis.[5,6] ASB patients shed over 10^4 bacteria per milliliter of urine, yet report no symptoms commonly associated with UTI.[6,7] In uncomplicated cystitis, or uncomplicated UTI (UUTI), patients have a positive urine culture (>10^4 bacteria per milliliter of urine), along with symptoms of urinary frequency, urgency, and painful urination.[6] This is the most common form of UTI, accounting for 95% of general practice visits. Consequently, antibiotic prescriptions for UUTI are among the highest globally.[8] Even patients with ASB are oftentimes prescribed antibiotics, given that uropathogens can ascend to the kidneys, where they can cause more severe sequelae associated with pyelonephritis.[7,9] Pyelonephritis patients typically experience back and flank pain, nausea, and vomiting in addition to the symptoms of cystitis. Urosepsis is a bloodstream infection caused by infection of the urinary tract. Like other forms of sepsis, the severity of urosepsis is dependent on the patient's immune response. Of all sepsis cases, up to 31% are urosepsis cases.[6] The leading cause of urosepsis is urinary obstruction.

UTIs disproportionately affect people assigned female at birth (AFAB), with 80% of all UTIs being reported in people AFAB. It is hypothesized that the disparate rates of infection between people AFAB and people assigned male at birth (AMAB) is due to the shorter distance

between the urethra and anus in people AFAB compared to that in people AMAB.[10] Other factors that contribute to this disparity in occurrences between the sexes include differences in sex hormones, incontinence rates and vaginal dysbiosis.[10,11] About 50% of people AFAB will experience at least one UTI in their lifetime.

A major problem in the UTI field is recurrence of infection. Recurrent UTIs are defined as at least three episodes of UTI in one year or two episodes in six months. Approximately 20-30% of people AFAB who have a UTI will have a recurrent UTI. Not only do recurrent UTIs greatly diminish the quality of life of those infected, but also perpetuate the continued use of antibiotics, leading oftentimes to the evolution of multidrug resistant clones colonizing the rUTI patient.[12,13]

First line antibiotics for cystitis include nitrofurantoin, trimethoprim-sulfamethoxazole, and fosfomycin. However, these antibiotic treatments can result in long-lasting changes in the vaginal and gut microbiota because of their broad-spectrum activities. Global antibiotic use as treatments for UTIs has led to resistant bacteria, exacerbating the antimicrobial resistance public health threat. Unfortunately, multi-drug resistant uropathogens are increasing, leaving many doctors to prescribe last resort antibiotics. The rise in antibiotic resistance has highlighted the importance of discovering potential new drug targets to mitigate infection.

1.2 The pathogenesis and host response to uropathogenic *E. coli* in the urinary tract

Many different bacteria have the potential to cause UTIs, including *Escherichia coli*, *Klebsiella pneumoniae, Pseudomonas aeruginosa, Proteus mirabilis,* and *Enterococcus faecalis.* All of these pathogens must overcome several barriers to colonization prior to establishing infection, including traversing the distance to get to the bladder and withstanding the shear forces imposed on bacterial cells by the process of urination. The natural flow of urine that can wash

away nonattached or weakly adherent bacteria from the bladder. Additionally, the composition of urine can be nutritionally challenging for uropathogens. High osmolarity, high concentrations of salts and urea, and organic acids can help prevent growth of uropathogens. Not surprisingly, all uropathogens have strategies to adhere to the urothelial cells, although studies to illuminate the chemotaxis mechanisms guiding ascension to the bladder are lacking.

Over 80% of UTIs however are caused by uropathogenic *E. coli* (UPEC). UPEC uses type 1 pili, encoded by the *fimAICDFGH* operon to adhere to uroplakins on bladder epithelial cells. UPEC then becomes internalized by the bladder epithelial cells. Upon internalization, UPEC become encapsulated in $Rab27^{+}$ vesicles that have non-lytic exocytic properties that rid most bladder cells of the bacterial invaders.[14,15] However, UPEC can escape the vesicles through an undefined mechanism. When this escape happens, the bacteria may be recognized by the host cell and targeted for autophagy. However, UPEC can withstand – somehow – the low pH of the phagolysosomes and eventually escape into the host cell cytosol, where UPEC can divide and expand rapidly. This population expansion allows UPEC to form intracellular bladder communities (IBC), which are biofilm-like, cocooning bacteria in a self-produced extracellular matrix. Inside IBCs, UPEC avoids the host immune response and gains an additional protective layer against host cell impermeable antibiotics.[16] UPEC resides in the IBC for ~24h based on murine models[17,18], during which time the UPEC population keeps expanding taking up almost the entirety of the host cell volume. While bladder cells can initiate a pyroptosis-like mode of cell death early during intracellular infection, the rapid expansion of UPEC leads to a transient hypoxic state that stabilizes HIF-1α and blocks host cell death and exfoliation of infected cells converting them into a replicative niche for UPEC.[19] Eventually, upon receiving some unknown signal, the bacteria in the IBC filament and can flux out from the bladder epithelial cell killing the urothelial host cell in the

process. The filamentous state also allows UPEC to resist killing by neutrophils. The fluxed filaments complete cell division once outside the host cell and can repeat the cycle of bladder cell invasion, IBC formation, and fluxing. This pathogenic cascade describes the acute phase of infection.

In the bladder lumen, neutrophils are the first immune cell recruited to the bladder once bacteria are detected by bladder epithelial cells. An inflammatory response is triggered when lipopolysaccharide (LPS) on the outer membrane of UPEC is detected by Toll like receptor (TLR) 4 on host bladder epithelial cells. TLR-4 activation leads to NFκB pathway activation, which results in the production of interleukin (IL) 1, IL-6, and IL-8, among other proinflammatory cytokines and chemokines.[15] TLR-5 stimulation by bacterial flagella can also contribute the inflammatory response.[15] IL-8 is the primary chemokine that recruits neutrophils to the bladder. Neutrophils have been detected in urine as soon as 2 hours post infection and their numbers peak around 6 hours. The primary job of the neutrophils is to phagocytose bacteria. Macrophages also infiltrate the bladder within 24-48 hours of infection.

Once the intracellular pathogenic cascade begins, UPEC can infect naïve epithelial cells, destroying the protective barrier of the bladder and exposing the transitional intermediate cells underneath. In 20-30% of the patients, an overactive immune response may prevent proper terminal cell differentiation, leading to a compromised urothelium that exhibits a distinct genetic program and is prone to chronic infection.[20,21] UPEC can also invade transitional cells, forming asymptomatic quiescent reservoirs that can re-seed infection. Several studies including human subjects have also elucidated the ability of UPEC to asymptomatically occupy different niches within the body, including the gut[22,23] and the vagina[24], where from they can re-emerge, transverse the genitourinary tract and ascend the urethra to establish an infection. The ability of UPEC to

form reservoirs within the gut and the vaginal spaces contributes to recurrent infection, which is experienced by 27% of the patients with UTI.[11,25,26] How does UPEC manage to persist in so many different host niches?

1.3 *E. coli* is a versatile colonizer

E. coli is arguably one of the most well-studied model organisms in basic science research. Countless discoveries in microbiology have been made, using laboratory-adapted nonpathogenic strains of *E. coli*. However, this phenomenon oftentimes masks the fact that the species *E. coli* is exceptionally diverse.

Given the great diversity that exists in the *E. coli* species, the field has developed a few different classification systems to describe *E. coli* strains. One classification is serotyping. Serotypes are determined by the version of H (flagella), K (capsule), and O (LPS) antigens the strain of *E. coli* expresses. UTI89, the strain of UPEC utilized for all studies described in this body of work, is serotype O18:K1:H7. Another classification system used to describe *E. coli* strains is multi locus sequence typing (MLST). MLST approaches sort *E. coli* into nine phylogenetic groups (A, B1, B2, C, D, E, F, G, H) by measuring the sequence variation of 6 housekeeping genes.[27,28] Unique sequences (alleles) are assigned a random number, and a unique combination of alleles at each locus creates the allelic profile for the strain tested.[28] The allelic profile determines the sequence type (ST). The majority of UPEC strains belong to the B2 and D phylogroups while the lab model strain of *E. coli*, K12, belongs to phylogroup A.

Pathotyping is another classification system for *E. coli*. With this classification, strains are divided into commensal and pathogenic strains, with pathogenic strains being further divided into intestinal and extra-intestinal pathogens. The pathogenic strains are characterized based on the

type of disease they cause, and these distinctions are what determines the pathotype. Examples include enteropathogenic *E. coli* (EPEC), enterohemorrhagic *E. coli* (EHEC), and uropathogenic *E. coli* (UPEC). EPEC and EHEC establish infection in the intestines of humans and are rarely found in other parts of the body. Meanwhile, UPEC causes infection in the bladder, but it can live in the intestines alongside commensal strains of *E. coli* and other members of the microbiota.

The term ExPEC for Extra-intestinal pathogenic *E. coli* is used as a blanket term to describe *E. coli* that causes disease outside the intestinal tract, encompassing UPEC, avian pathogenic *E. coli* (APEC) and neonatal meningitis causing *E. coli* (NMEC) among others.[29] It is therefore obvious that *E. coli* strains are versatile, harboring the ability to thrive in different environments both within and outside the host. This thesis dissertation focuses on dissecting how UPEC acid resistance mechanisms may be influencing the ability of this pathogen to thrive in multiple host niches.

UPEC, like all *E. coli,* is a facultative anaerobe, meaning it is able to grow in both the presence and absence of oxygen.[30] This ability to survive with or without oxygen allows UPEC to thrive in many different host niches, including the gastrointestinal (GI) tract, vagina, bladder, kidneys, and blood.

The gastrointestinal tract is anaerobic.[31,32] Under normal host conditions, *E. coli* can thrive in the gut by respiration using alternate electron acceptors or fermentation, depending on alternate electron acceptor availability.[33] During an infection state, the gut becomes more aerobic due to inflammation that leads to increases in ROS production.[34] In this aerobic state, *E. coli* can survive and outcompete the obligate anaerobes in the gut.[34,35]

The vaginal microenvironment is microaerophilic, so both aerobes and anaerobes can survive. Bacterial vaginosis (BV), a state of vaginal microbiome dysbiosis, is characterized by an

overgrowth of anaerobic bacteria, particularly *Gardnerella vaginosis*. During BV, *E. coli* can thrive in multispecies biofilms with *G. vaginosis*.[36] Aerobic vaginitis (AV), another state of vaginal microbiome dysbiosis, is characterized by increases in aerobic, enteric bacteria, vaginal inflammation, and deficient epithelial maturation.[37,38] *E. coli* are some of the most common bacteria identified in AV.[38,39]

The bladder and kidneys are microaerophilic, with 4-5.5% oxygen in the bladder.[30,40,41] Obligate anaerobes are rarely identified in the bladder, although they are more commonly identified in catheterized patients.[42] UPEC relies on aerobic respiration in the bladder.[19,43-45] Overall, the versatility of UPEC allows it to be a successful uropathogen.

1.4 Acid stress response in *E. coli*

E. coli strains are thought to colonize the human host early in life, through ingestion. Therefore, *E. coli* strains must have the ability to survive the low pH in the stomach prior to colonizing the small and large intestine. Moreover, in the gut, *E. coli* must contend with the variation in pH caused by the secretion bile acids and organic acid metabolites by the microbiota. UPEC strains have additional encounters with acidic conditions in the vagina and bladder, as described below.

People AFAB who experience recurrent UTIs have a higher frequency of *E. coli* colonization of the vagina, suggesting the vagina can serve as a reservoir for recurrent infections. In people AFAB, the vaginal lumen is highly colonized by *Lactobacillus spp.*, which produce lactic acid to acidify the vaginal environment, along with secreting toxins that are cytotoxic to UPEC.[46-48] UPEC must be able to detect and respond appropriately to the decreased pH of the vaginal niche. In the bladder, the host immune response to UPEC exposes the bacteria to acidic pH stress in both the lumen and inside the bladder epithelial cells. As described in section 1.2, neutrophils and

macrophages are the primary immune cell responders to UPEC infection in the bladder lumen. Both cell types use mechanisms of bacterial killing that involve low pH. Inside the bladder cell, UPEC are encapsulated in phagolysosomes where the pH is also low. However, UPEC has been shown to neutralize phagolysosomes in bladder epithelial cells. This neutralization prevents bacterial cell death, although the mechanism through which UPEC can accomplish it remains unknown. Elucidating mechanisms by which UPEC strains withstand a barrage of stresses from the time of gut colonization to extra-intestinal transit, is critical in facilitating our ability to thwart extra-intestinal infection.

At an acidic pH, the concentration of protons is high and can lead to the protonation of biological molecules. This protonation will change the charge of the molecules and thus affect the structure and function adversely. Acidic conditions in the bacterial cell interior disturb vital physiological processes, such as enzymatic activity, protein folding, membrane- and DNA maintenance, all of which are needed for cellular function and can cause bacterial death. Lipid membranes are generally good at preventing ions (ie: H^+) from freely diffusing through to protect the cell interior from drastic pH shifts.[49,50] However, organic acids present a challenge to this lipid membrane barrier. If the environment is acidic, organic acids will exist in the protonated (uncharged) state. Protonated organic acids are able to freely diffuse across cell membranes. When diffusion occurs, the protonated organic acid enters an environment that is less acidic than outside the cell, and the organic acid will dissociate into a free H^+ and its conjugate base inside the cytoplasm of the bacteria. As a result, organic acids are a distinct challenge for bacteria. Not surprisingly, *E. coli* has developed several strategies to mitigate protein and DNA damage imposed by acidic conditions **(Figure 1)**.

To begin, the composition of the *E. coli* membranes can be altered to decrease the membrane fluidity, thus reducing the influx of protons. This membrane stabilization occurs when cells decrease the concentration of unsaturated lipids, while increasing the concentration of cyclopropane fatty acids that are incorporated into the membrane. The global stress response regulator, RpoS, activates transcription of the cyclopropane fatty acid (CFA) synthase.[51-53]

E. coli can also block proton influx by blocking outer membrane porins (OMPs). Binding of polyphosphate or cadaverine to OMPs can prevent the diffusion of ions into the periplasmic space.[49] Inorganic polyphosphate (polyP) is a key component of general stress response in *E. coli.* PolyP acts as a protein stabilizing chaperone, metal chelator, and as a regulator of RNA and DNA polymerases, ribosomal translation fidelity, and transcription.[54] The regulation of polyP is not completely understood. DksA and (p)ppGpp have both been shown to positively regulate polyp production.[54-56] Cadaverine is produced through lysine decarboxylation, an acid resistance mechanism discussed in detail below, and has been shown to induce porins to close.[57,58]

To ensure that proteins remain folded and functional under acidic conditions, *E. coli* expresses chaperone proteins in the periplasm and cytoplasm. HdeA and HdeB are periplasmic chaperone proteins that undergo activating conformational changes under acidic conditions and help prevent aggregation and denaturation of proteins.[59-61] HdeA and HdeB are among the most abundant proteins found in the periplasmic space. In the cytoplasm, chaperone protein Hsp31 plays an important role in acid resistance.[62] To protect DNA under stress conditions, *E. coli* expresses Dps, a DNA binding protein.[63] Both acid stress and oxidative stress can lead to the production of hydroxyl radicals which can lead to single and double stranded DNA breaks. In addition to protecting DNA by directly biding to it, Dps also has iron sequestration and ferroxidase properties to prevent the production of damaging hydroxyl radicals.[63-66]

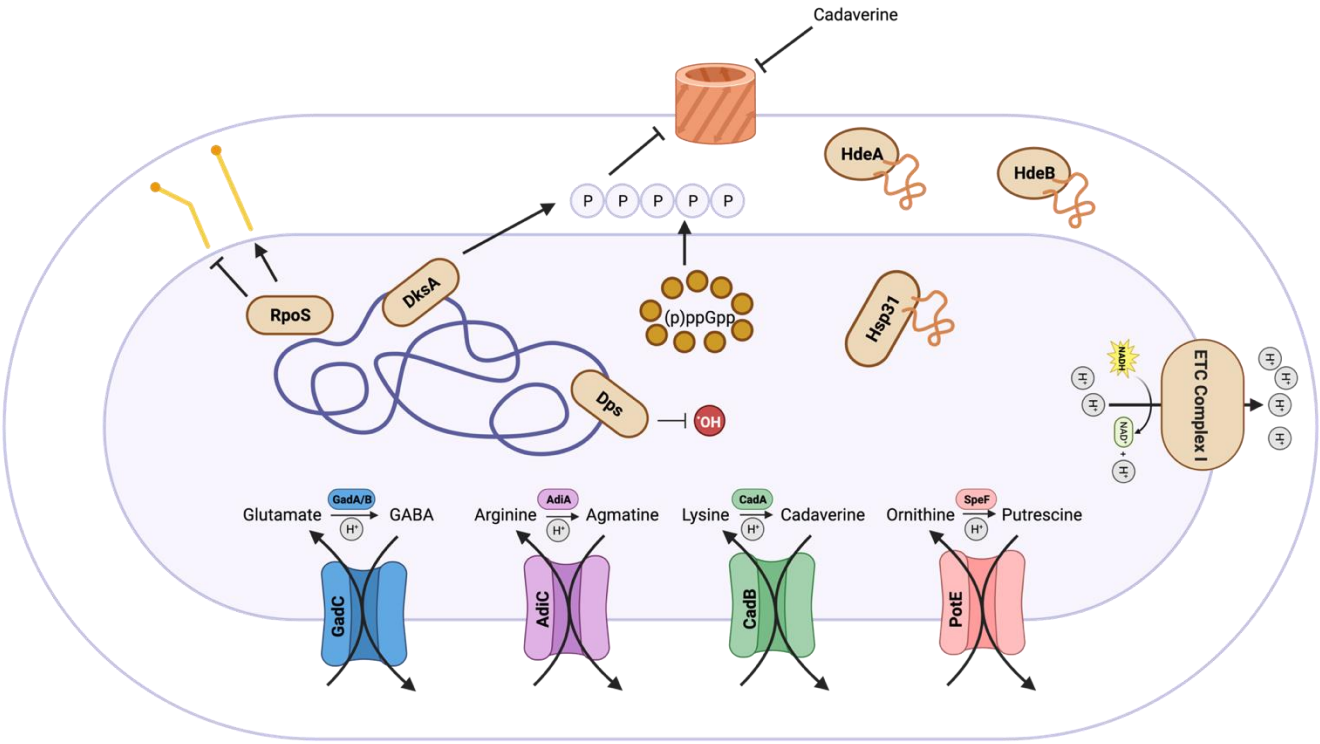

Figure 1. Diagram of characterized acid resistance mechanisms in *E. coli*
Outer membrane protection: DksA and (p)ppGpp signaling lead to the accumulation of polyphosphate and lysine decarboxylation leads to the export of cadaverine. Polyphosphate and cadaverine inhibit the function of outer membrane transporters (OMPs) to prevent the influx of protons. Inner membrane protection: Under acidic pH stress conditions, RpoS leads to the activation of pathways that increase the production of saturated fatty acids, such as CFA, and the downregulation of unsaturated fatty acids. Incorporation of saturated fatty acids into the membrane increases membrane stability. Chaperone proteins: HdeA, HdeB, and Hsp31 help to protect and repairs proteins damaged by acidic pH stress. DNA protection: Dps binds to DNA and protects against hydroxyl radicals. Proton flux: genes in the electron transport chain are upregulated under acidic pH stress conditions. It is believed that upregulation of the ETC results in increased proton pumping out of the cell which helps alleviate acidic pH stress inside the cell. Proton consumption: amino acid decarboxylation consumes a proton which neutralizes the interior of the cell.

E. coli also changes its metabolism under acidic conditions to mitigate stress. The primary changes are through the induction of stress response systems. Activation of genes in the periplasmic stress response and oxidative stress response systems occurs. *E. coli* also upregulates pathways involved in the transport and metabolism of secondary carbon sources (ie: ribose, arabinose, mannitol, etc.) and down regulates glucose utilization pathways. This is because the metabolism of these secondary carbon sources results in the production of fewer acidic metabolites, thus decreasing the cell's contribution of protons to the acidic environment. Another metabolic change *E. coli* makes under acidic conditions is the upregulation of the electron transport chain (ETC).[67] One of the primary outcomes of running the ETC is the formation of a proton gradient, with a higher concentration of protons outside of the cell compared to inside the cell. By increasing the ETC, the cell is able to export more protons to help neutralize the cell interior.

Although physiological and metabolic changes are crucial for *E. coli* to tolerate acidic conditions, the main focus of this body of work will focus on proton consuming mechanisms in *E. coli* as a way to survive acidic pH stress. Most of the proton consuming mechanisms in *E. coli* rely on the activity of pyridoxal-5'-phosphate (PLP) dependent amino acid decarboxylase systems. There are 4 PLP dependent decarboxylase systems, or acid resistance mechanisms (AR), in *E. coli*: AR2, AR3, AR4, and AR5. These AR systems all contain a PLP that catalyzes a proton dependent decarboxylation of an amino acid to produce a biproduct and CO_2. The biproduct is then exported through an amino acid/bioproduct antiporter. The decarboxylation reaction consumes one proton, thereby increasing the cytoplasmic pH. AR2 involves the decarboxylation of glutamate to form γ-amino butyric acid (GABA). AR3 involves the decarboxylation of arginine to produce agmatine. AR4 involves the decarboxylation of lysine to produce cadaverine. Finally, ornithine decarboxylation to putrescine is the basis of AR5.

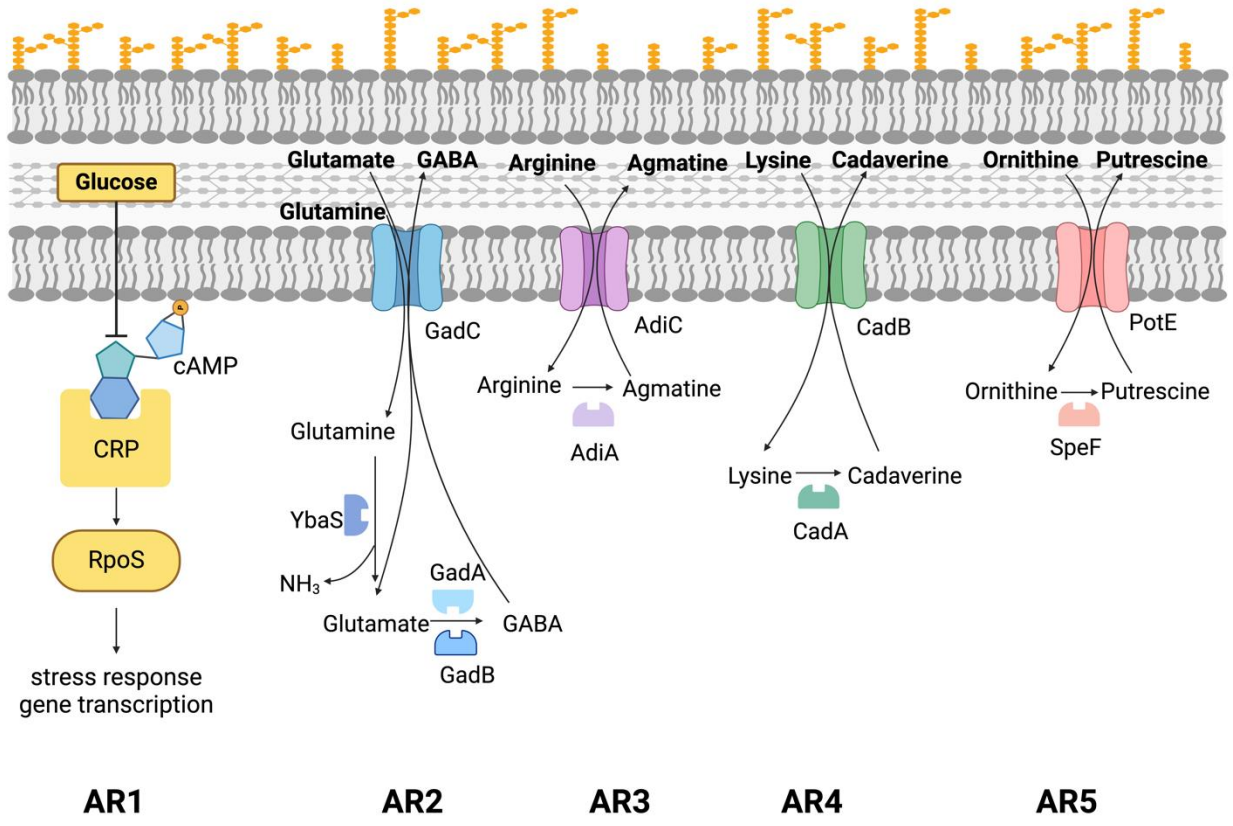

Figure 2. Defined acid resistance mechanisms in *E. coli*
AR1: Glucose repressed/oxidative acid resistance mechanism. AR2: Glutamate is imported by GadC and is decarboxylated by GadA and GadB to produce GABA. Glutamine can also be imported by GadC and is deaminated by YbaS to glutamate. The glutamate can then be decarboxylated by GadA and GadB. AR3: Arginine is imported by AdiC and decarboxylated by AdiA to produce agmatine. AR4: Lysine is imported by CadB and decarboxylated by CadA to produce cadaverine. AR5: Ornithine is imported by PotE and decarboxylated by SpeF to produce putrescine.

Acid resistance mechanism 1

Acid resistance mechanism 1 (AR1) is not well characterized **(Figure 2)**. In 1993, Gorden and Small demonstrated that *E. coli* could survive in pH 2.0 for 2 hours if the cells were in stationary phase when exposed to acidic pH.[68] The following year, Small et al. determined that the survival of *E. coli* at pH 2 was dependent on RpoS.[69] In 1995, Lin et al. showed that *E. coli* exhibited acid resistance at pH 2 when cells were grown oxidatively (in complex media) before acid stress was applied.[70] The protection they observed in oxidatively grown cells was not observed

when the cells were grown fermentatively (in complex media containing glucose).[70] cyclic-AMP (cAMP) and cAMP reactive protein (CRP) regulate gene expression under glucose limited conditions. In 1999, Castanie-Cornet et al. found that deletion of *crp* (gene encoding CRP) and *cya* (gene encoding the Class I adenylyl cyclase that produces cAMP) ablated survival of the *E. coli* that were grown to express the AR1 system, thus revealing that AR1 is dependent on RpoS and cAMP-CRP.[71] Since 1999, not much more has been elucidated about how AR1 works.

Acid resistance mechanism 2

The decarboxylase isoenzymes of the AR2 mechanism are GadA and GadB **(Figure 2)**. These enzymes share 98% sequence homology.[72] The glutamate/GABA antiporter is GadC. GadC recognizes the net charge of the substrates it transports. Under acidic conditions, glutamate carries a net 0 charge.[73,74] GABA is exported through GadC with a +1 net charge.[73,74] The import of glutamate (0 charge) followed by its decarboxylation to GABA (+1 charge) not only helps increase the pH inside the cell, but also reverse the transmembrane potential to prevent proton import into the cell.[72,75] The genes encoding GabB and GadC are found in an operon together, while *gadA* is found in the *E. coli* acid fitness island along with other genes involved in AR2 gene regulation and the genes encoding the HdeA and HdeB chaperones described above.[76] GadA and GadB are optimally active at pH 3.7-3.8.[77] The AR2 system is activated during stationary phase by RpoS. However, under acidic conditions, AR2 is activated in exponential and stationary phase in an RpoS independent manner.[71] GadB expression is more affected by RpoS while GadA expression is more affected by acidic pH.[71] GadX, GadW, GadE, YdeO, and EvgA are all involved in the regulation of AR2 expression.

Acid resistance mechanism 3

The decarboxylase enzyme of AR3 is AdiA and the arginine/agmatine antiporter is AdiC **(Figure 2)**. The *adiA* and *adiC* genes are clustered near each other and separated by *adiY,* which encodes the AdiY regulator of *adiA* and *adiC.* The AR3 system is maximally expressed at pH 4.4 under anaerobic conditions. AdiA oligomerizes at acidic pH.[78] As pH increase, AdiA dissociates into inactive dimers.[78] AdiC transport activity is pH dependent, with a pH <6 allowing for the import of arginine inside the cell.[79]

Acid resistance mechanism 4

AR4 is regulated through CadC, a membrane integrated transcription regulator. CadC detects low pH and, indirectly, the presence of lysine to promote transcription of *cadA* and *cadB*.[80] CadB imports lysine then CadA decarboxylates lysine to cadaverine, which is exported by CadB **(Figure 2)**. LysP, a constitutively expressed lysine importer, has been shown to inhibit *cadBA* expression through interactions with CadC. When extracellular lysine is absent or concentrations are low, LysP inhibits CadC activation of the *cadBA* operon.[81] CadA is optimally active at pH 5.7.[82]

Acid resistance mechanism 5

Ornithine decarboxylation to putrescine is performed by the PLP enzyme, SpeF **(Figure 2)**. SpeF has an optimal pH of 7.0[83,84], a property which has resulted in SpeF being characterized as the least effective acid resistance mechanism in *E. coli.* Induction of *speF* transcription is regulated by GTP levels.[85] The ornithine/putrescine antiporter, PotE, is encoded in an operon with *speF*.[84]

While decarboxylation of amino acids appears to be the primary means of acid resistance in *E. coli*, there is evidence that deamination of amino acids can also serve to increase the intracellular pH. This is evident in AR2_Q, in which the cell imports glutamine and then de-

aminates it to provide the glutamate that is then decarboxylated **(Figure 2)**.[86,87] Glutamine deamination also produces ammonia which consumes a proton and diffuses out of the cell as ammonium **(Figure 2)**.[86,87]

This thesis focuses on delineating the role of the known AR systems in UPEC pathogenesis. Moreover, Chapter 2 will detail how I discovered another amino acid deamination reaction, serine deamination, which contributes to acidic pH tolerance in UPEC. We have termed this newly discovered mechanism AR6.

1.5 Acidic pH sensing by two-component systems

Bacteria must be able to quickly sense and respond to their environment. Two-component signal transduction is one of the most dominant forms of signaling in bacteria. TCSs are – in their simplest form - composed of a sensor histidine kinase (HK) that serves as the signal receptor, and a response regulator protein that carries out the output response.[88,89] The HK auto-phosphorylates at a conserved histidine residue, in response to signal reception and transfers the phosphoryl group to a conserved aspartate on the response regulator (RR) to activate RR function. Unlike eukaryotic signaling pathways, TCSs are usually highly insulated and specific. HKs and RRs undergo co-evolution that allow for this specificity.[90] Molecular and spatial determinants also enforce the fidelity of phosphotransfer between the HK-RR pair, but as is true for eukaryotic signal transduction systems, molecular "infidelity" or cross-interaction can occur between the HK of one system and the RR of another.[91] The net result of this non-cognate partner interaction is the ability to expand the range of responses a bacterium can have at a given environment.

Detection of pH changes through TCSs have been reported in *E. coli* and other bacteria. For example, induction of AR2 is mediated in part by the two-component system EvgSA **(Figure**

3).[92-94] EvgS is a histidine kinase that is activated by changes in external pH and phosphorylates the response regulator EvgA.[94] Phosphorylated EvgA induces transcription of YdeO which acts to induce expression of GadE.[93,95] GadE induces expression of glutamate decarboxylases, GadA and GadB, and the glutamate/GABA antiporter, GadC.[95] YdeO also induces the expression of SafA, a protein that activates the PhoPQ two-component system.[92] PhoPQ activation is thought to contribute to acid resistance by modulating levels of RpoS, a stationary phase regulator of general stress response.[96] PhoPQ does this by activating IraM which interacts with RpoS to promote its activity.[97,98] There is also evidence that activation of PhoPQ leads to induction of *gad* genes and *hdeA* and *hdeB*.[96,99]

Chapter 4 will detail the discovery of another regulatory system, BtsS-YpdB, that responds to acid stress. The sensor histidine kinase BtsS, of the BtsSR two-component system, senses changes in extracellular pyruvate and in response interacts with the YpdB transcription factor from the YpdAB two-component system. The net result of BtsS-YpdB cross-interaction is the induction of a yet uncharacterized gene, *yhjX*, as well as the repression of cysteine metabolism.

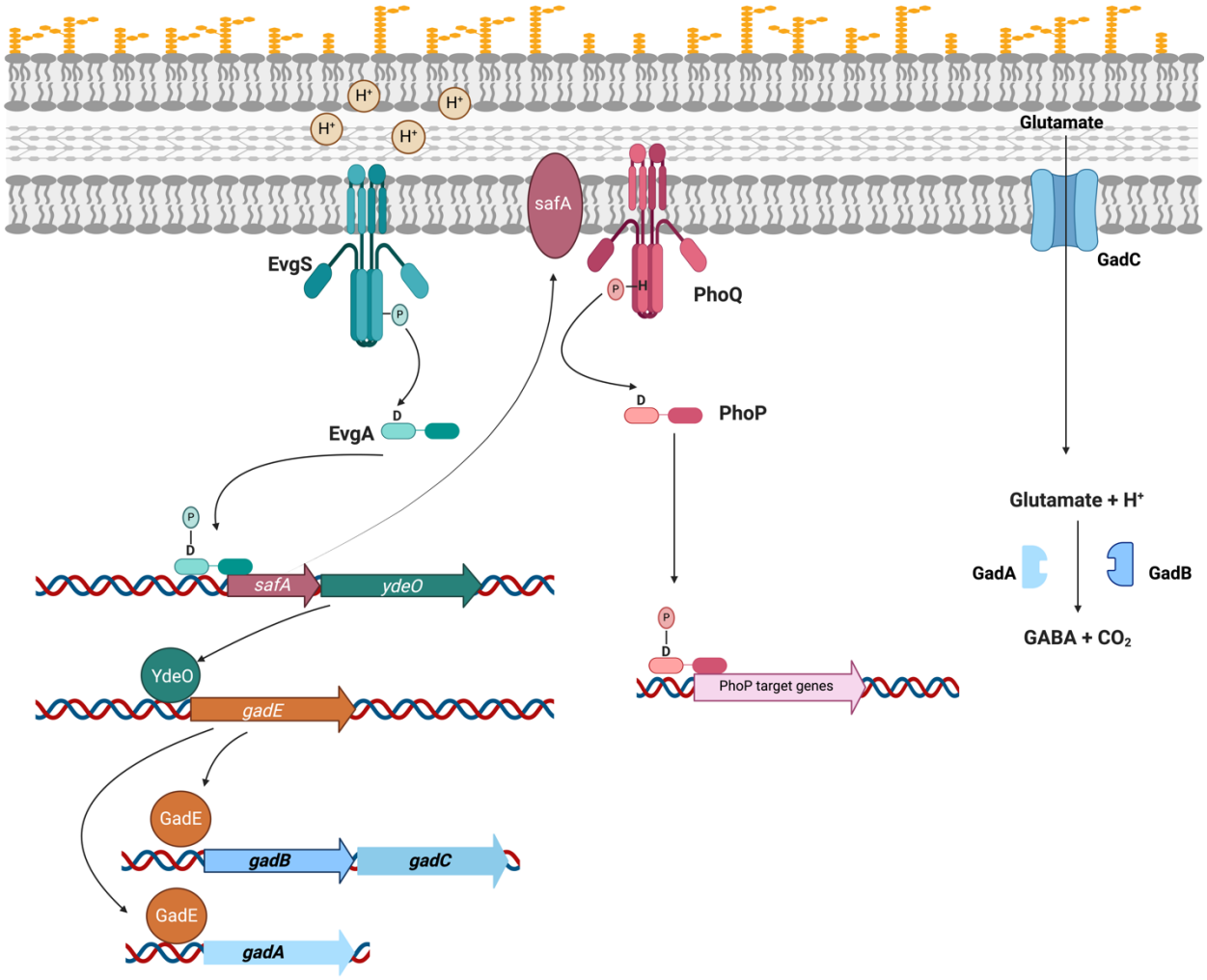

Figure 3. *E. coli* two-component system signaling in response to acidic conditions
Histidine kinase, EvgS, senses acidic pH and activates EvgA. EvgA is a transcription factor that activates many genes, including those involved in regulating the glutamate decarboxylase system. EvgA also activates transcription of *safA*. SafA is an accessory protein required for the activation of the histidine kinase PhoQ. PhoQ activation by acidic pH and SafA leads to phosphorylation of PhoP, a transcription factor that activates transcription of many genes, including genes encoding regulators of the glutamate decarboxylase system.

1.6 Unanswered questions that this thesis attempts to bridge

Although the chemical mechanisms for most AR mechanisms in of *E. coli* have been elucidated, there are limited studies to investigate when each AR mechanism is active during colonization of the host. A study by John Foster's group has shown the AR2 is important for *E. coli* colonization of the bovine intestine, but AR3 was not.[100]

Critically, in UPEC pathogenesis, only a handful of studies[101,102] have addressed the importance of some ARs during UTI. As mentioned in section 1.2 above, UPEC undergoes a complex pathogenic cascade that encompasses extracellular and intracellular stages, all replete with acid-stresses. Moreover, the metabolic inventory available to UPEC in the bladder versus the gut is vastly different. How does that affect responses to acid stress during infection? The following questions arise:

- Are there other amino acids - more relevant to UPEC during infection - that can be protective against acidic pH stress? Chapter 2 will present evidence of a serine de-amination system that mitigates acid stress in UPEC. We term this system AR6.
- What AR systems are used by UPEC during the different stages of infection? Chapter 3 will elucidate systems that are critical for early colonization of the host.
- Are there other TCSs that can sense pH changes in the environment? Chapter 4 will describe a newly discovered non-cognate TCS pair that is active under acidic stress and interfaces with known AR regulators.

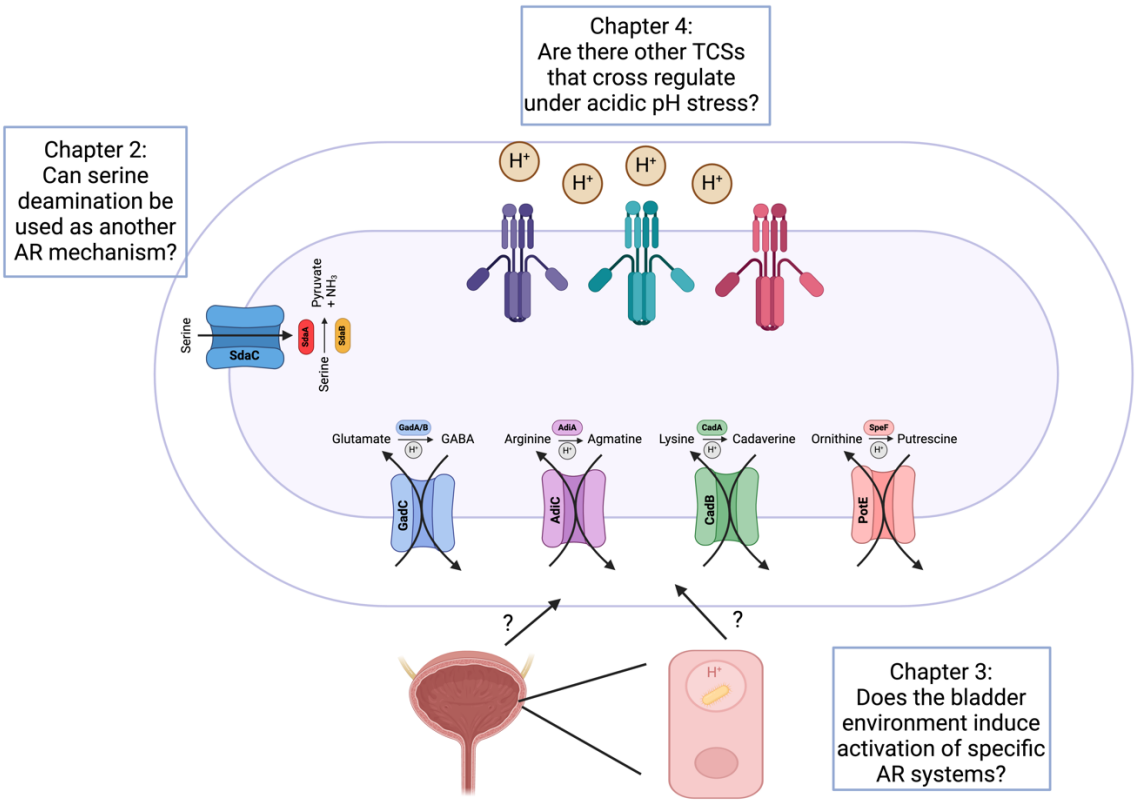

Figure 4. Questions addressed in this thesis

Chapter 2: Serine Deamination is a New Acid Tolerance Mechanism Observed in Uropathogenic *Escherichia coli*

Wiebe MA, Brannon JR, Steiner BD, Bamidele A, Schrimpe-Rutledge AC, Codreanu SG, Sherrod SD, McLean JA, Hadjifrangiskou M. Serine Deamination Is a New Acid Tolerance Mechanism Observed in Uropathogenic *Escherichia coli*. mBio. 2022 Dec 20;13(6):e0296322. doi: 10.1128/mbio.02963-22. Epub 2022 Dec 5. PMID: 36468870; PMCID: PMC9765748.

Abstract

Escherichia coli associates with humans early in life and can occupy several body niches either as a commensal in the gut and vagina, or as a pathogen in the urinary tract. As such, *E. coli* has an arsenal of acid response mechanisms that allow it to withstand the different levels of acid stress encountered within and outside the host. Here, we report the discovery of an additional acid response mechanism that involves the deamination of L-serine to pyruvate by the conserved L-serine deaminases SdaA and SdaB. L-serine is the first amino acid to be imported in *E. coli* during growth in laboratory media. However, there remains a lack in knowledge as to how L-serine is utilized. Using a uropathogenic strain of *E. coli*, UTI89, we show that in acidified media, L-serine is brought into the cell via the SdaC transporter. We further demonstrate that deletion of the L-serine deaminases SdaA and SdaB renders *E. coli* susceptible to acid stress, similar to other acid stress deletion mutants. The pyruvate produced by L-serine de-amination activates the pyruvate

sensor BtsS, which in concert with the non-cognate response regulator YpdB upregulates the putative transporter YhjX. Based on these observations, we propose that L-serine deamination constitutes another acid response mechanism in *E. coli*.

Importance

The observation that L-serine uptake occurs as *E. coli* cultures grow is well-established, yet the benefit *E. coli* garners from this uptake remains unclear. Here, we report a novel acid tolerance mechanism, where L-serine is deaminated to pyruvate and ammonia, promoting survival of *E. coli* under acidic conditions. This study is important as it provides evidence of the use of L-serine as an acid response strategy, not previously reported for *E. coli*.

Introduction

Acid stress is a substantial challenge to bacterial life. Acidic conditions can damage the bacterial cell envelope, rendering membrane-embedded proteins and the proton motive force established across the membrane dysfunctional or non-functional.[103] Acidic conditions in the bacterial cell interior disturb vital physiological processes, such as enzymatic activity, protein folding, membrane- and DNA maintenance, all of which are needed for cellular function and can cause bacterial death. As a result, bacteria are equipped to withstand acidic conditions. One of the model bacterial organisms, *Escherichia coli*, occupies numerous environmental and host niches and encounters a range of acidic conditions in a niche-dependent manner. For example, all *E. coli* harbored in the gut are thought to be acquired via ingestion[104], indicating that *E. coli* must be able to survive the low pH of the stomach, which ranges from pH 1.5-3.5.[50] It is therefore not surprising

that five acid resistance (AR) mechanisms, termed AR1-AR5, have been identified in *E. coli*, all of which have been shown to be active in the gut.[100,105,106]

The most well characterized AR mechanisms, AR2-5, depend on the import and subsequent decarboxylation of specific amino acids. The decarboxylation reaction consumes one proton, thereby increasing the cytoplasmic pH. AR2, which has been shown to be the most effective AR mechanism in *E. coli*, involves the deamination of glutamine to glutamate, which is then decarboxylated to form γ-amino butyric acid (GABA).[50,70,106,107] AR3 involves the decarboxylation of arginine to produce agmatine, while AR4 leads to decarboxylation of lysine to produce cadaverine. Finally, ornithine decarboxylation to putrescine is the basis of AR5.[106] The AR1 mechanism of action is not well understood.

While decarboxylation of amino acids appears to be the primary means of acid resistance in *E. coli*, there is evidence that deamination of amino acids can also serve to increase the intracellular pH. This is evident in AR2, where glutamine deamination not only provides the glutamate that is then decarboxylated (AR2_Q)[86,108], but also produces ammonia which consumes a proton and diffuses out of the cell as ammonium.[86,87] Here we demonstrate that the deamination of L-serine is an additional acid response mechanism in *E. coli*.

Notably, L-serine is the first amino acid consumed by *E. coli* when grown in complex media.[109] Under aerobic conditions, it is known that L-serine is deaminated by SdaA and SdaB to produce pyruvate and ammonia.[110] However, to date no metabolic role for serine deamination in *E. coli* has been described[111], as most of the pyruvate derived carbon is subsequently excreted from the cell.[109] In *Klebsiella aerogenes* and *Streptococcus pyogenes* serine deamination has been shown to be important for regulating nitrogen balance and maintaining extracellular pH[112,113] but the full import of serine deamination in these pathogens remains unclear.

Uropathogenic *E. coli* (UPEC) is a extraintestinal pathotype of *E. coli*, responsible for over 75% of reported urinary tract infections.[1] UPEC strains have developed strategies to persist for years in the host[12,114,115], colonizing the gut, the vaginal space and the bladder in asymptomatic reservoirs for long periods of time.[116] UPEC has been reported to persist within the acidic environment of the vagina (pH 3.8-5)[48,117] before ascending to and colonizing the urinary tract (pH 5.5-7).[118,119] No studies have elucidated the mechanisms of acid tolerance in UPEC. In this work, we demonstrate that L-serine deamination is a previously unrecognized acid tolerance mechanism in UPEC. We show that under acidic conditions, serine is transported into the cell by the SdaC transporter and deaminated by the L-serine deaminases SdaA and SdaB, a process that imparts *E. coli* with protection from acid.

Methods

Bacterial Strains and Growth Conditions

All studies were performed in the well characterized UPEC cystitis isolate UTI89[114] and derived isogenic deletion mutants. UTI89 is of the sequence type ST95 and is serotyped as O18:K1:H7.[114] For all analyses, strains were propagated from a single colony in unbuffered lysogeny broth (LB) (Fisher Scientific), at pH 7.4. Inoculated strains were grown overnight at 37°C with shaking unless otherwise noted. Strains containing the luciferase reporter plasmid were grown in LB + 50 μg/ml gentamicin at 37°C, 220 rpm overnight. The pH at the beginning of the culture (pH 7.4) and end of the culturing (pH 8.56) was measured using Thermo Scientific Orion Star A211 pH meter with an Orion™ Green pH Combination Electrode. Specific growth conditions for reporter and survival assays are described in the relevant sections below. Gene deletions were created using the λ-red recombinase system.[120] The Δ*btsS*Δ*ypdB* and Δ*yhjX* mutant strains were

created in previous studies.[121] The *yhjX*::lux reporter, which was previously constructed[122], was introduced into each strain via electroporation and validated by PCR.

A complete list of strains, primers, and plasmids used for in this study can be found in Tables 1 and 2.

Luciferase reporter assay

Overnight cultures were spun at 3220 x g for 10 minutes. Pellets were resuspended in 5 ml 1X PBS and re-pelleted. Pellets were resuspended in 5 ml 1X PBS and normalized to a starting OD_{600} = 0.05 in 1 ml of the indicated media (LB, LB + 10 mM HCl, or LB + 50 mM MOPS or HEPES buffer + 10 mM HCl). Each suspension was used to seed black, clear bottomed 96 well plates at 200 µl per well from and grown at 37°C with shaking. OD_{600} and luciferase readings were taken every hour for 8 hours using a Molecular Devices SpectraMax i3 plate reader. At least 3 biological replicates were assayed.

Acid Tolerance Assays

Acid tolerance assays were performed as follows: Bacteria were grown overnight as described above and diluted 1:100 in 5 ml of fresh, unbuffered LB at pH 7.4. Cultures were incubated at 37°C with shaking. When strains reached mid exponential growth phase (OD_{600} of ~3.0 at 3 hours), 1 ml of the culture was centrifuged at 16,000 x g for 5 minutes, washed in 1X PBS, serially diluted and plated for CFUs to determine colony forming units prior to acid exposure (Input sample). The pH of the remaining 4-ml culture was adjusted to a pH of 3 using 5 M HCl, and acidified cultures were incubated at 37°C, with shaking for 30 minutes. Following incubation, 1 ml of the acidified sample was centrifuged, washed in PBS, and plated for CFUs. Percent survival

was calculated by dividing the CFU/ml after acid stress by the CFU/ml of the input sample. Statistical analysis was performed by 1-way ANOVA with post hoc Dunnett's multiple comparisons correction test.

RNA Extraction and RT-qPCR

Growth conditions for RNA sample collection: To collect samples for transcriptional analysis, strains were grown aerobically in LB to an OD_{600} = 0.5 and then split into two conditions: continued growth in LB alone, or in LB in which HCl was added to a final concentration of 10 mM. Samples were taken for RNA extraction at time = 0, 15, 30, 60, and 120 minutes after splitting the culture. All samples were centrifuged at 6000 x g for 7 minutes at 4°C. The supernatant fractions were decanted, and cell pellets were flash frozen in dry ice and ethanol and stored at -80°C until RNA extraction.

RNA was extracted using the RNeasy mini kit from Qiagen, following the manufacturer's extraction protocol. A total of 3 µg of RNA was DNAse treated using 2 units of Turbo DNase I enzyme (Invitrogen). A total of 1 µg of DNAse-treated RNA was reverse transcribed using Superscript III reverse transcriptase (Invitrogen/Thermo Fisher). cDNA was amplified in an Applied Biosystems StepOne Plus Real-Time instrument using TaqMan MGB chemistry with primers and probes listed in Table S1. All reactions were performed in triplicate with four different cDNA concentrations (100, 50, 25, or 12.5 ng per reaction). Relative fold difference in transcript abundance was determined using the ΔΔCT method of Pfaffl et al., with a PCR efficiency of >95%.[123] Transcripts were normalized to *gyrB* abundance. At least 3 biological replicates were performed for each transcript. Results were statistically analyzed using a two-way ANOVA with Sidak's multiple comparisons test.

Metabolomics

UTI89, Δ*btsS*Δ*ypdB*, and Δ*sdaC* were grown in LB and incubated at 37°C with shaking, until cultures reached an OD_{600} = 0.5. Then, 1 M HCl was added to the culture to a final concentration of 10 mM (pH=5). Cultures were incubated for another 15 minutes and then 1 ml of culture was collected. Cells were pelleted and supernatant was flash frozen and stored at -80°C until analyzed via Liquid Chromatography-Mass Spectrometry (LC-MS)-based metabolomics in the Vanderbilt Center for Innovative Technology (CIT). Isotopically labeled phenylalanine-D8 and biotin-D2 were added to 200 µL of culture supernatant per sample, and protein was precipitated by addition of 800 µL of ice-cold methanol followed by overnight incubation at -80°C. Precipitated proteins were pelleted by centrifugation (15,000 rpm, 15 min), and supernatants were dried down in vacuo and stored at -80°C. Individual samples were reconstituted in 120 µL of reconstitution buffer (acetonitrile/water, 90:10, v/v) containing tryptophan-D3, pyruvate-C13, valine-D8, and inosine-4N15. A quality control (QC) sample was prepared by pooling equal volumes from each individual sample. Quality control samples were used for column conditioning, retention time alignment and to assess mass spectrometry instrument reproducibility throughout the sample set and for individual batch acceptance.

LC-MS and LC-MS/MS analyses were performed on a high-resolution Q-Exactive HF hybrid quadrupole-Orbitrap mass spectrometer (Thermo Fisher Scientific, Bremen, Germany) equipped with a Vanquish UHPLC binary system and autosampler (Thermo Fisher Scientific, Germany). Metabolite extracts were separated on ACQUITY UPLC BEH Amide HILIC 1.7µm, 2.1 × 100 mm column (Waters Corporation, Milford, MA) held at 30°C. Liquid chromatography was performed at a 200 µL min−1 using solvent A (5 mM Ammonium formate in 90% water, 10%

acetonitrile and 0.1% formic acid) and solvent B (5 mM Ammonium formate in 90% acetonitrile, 10% water and 0.1% formic acid) with a gradient length of 30 min.

Full MS analyses (6 µL injection volume) were acquired over 70-1050 mass-to-charge ratio (m/z) in negative ion mode. Full mass scan was acquired at 120K resolution with a scan rate of 3.5 Hz, automatic gain control (AGC) target of 10e6, and maximum ion injection time of 100 ms. MS/MS spectra were collected at 15K resolution, AGC target of 2e5 ions, and maximum ion injection time of 100 ms.

The acquired raw data were imported, processed, normalized, and reviewed using Progenesis QI v.3.0 (Non-linear Dynamics, Newcastle, UK). All MS and MS/MS sample runs were aligned against a QC (pooled) reference run. Unique ions (retention time and m/z pairs) were de-adducted and de-isotoped to generate unique "features" (retention time and m/z pairs). Data were normalized to all features using Progenesis QI.

Experimental data for measured serine (i.e., retention time and MS^2 fragmentation pattern) and pyruvate (i.e., retention time) was consistent with reference standards.

Pyruvate Quantification

To collect samples for extracellular pyruvate quantification, strains were grown aerobically in LB to an OD_{600} = 0.5 and then split into two conditions: continued growth in LB alone, or in LB in which HCl was added to a final concentration of 10 mM. Samples were taken at time = 0, 15, 60, and 180 minutes after splitting the culture and normalized to an OD_{600} = 1.0. Samples were then centrifuged, and cell pellets and supernatant were separated, flash frozen, and stored at -80°C until assay was performed. Pyruvate Assay kits (MAK071-1KT, Sigma Aldrich) were used to quantify pyruvate in the supernatant fraction according to manufacturer's protocol. Fold change in

pyruvate concentration was calculated by dividing the concentration of pyruvate in cells grown in acidic conditions over the concentration of pyruvate in cells grown in LB alone for each time point. Data were analyzed using 2-way ANOVA with a Dunnett's post hoc multiple comparison test to compare the mutants to WT at each time point.

Statistical analysis

Statistical analyses were performed in GraphPad Prism, using the most appropriate test as indicated in the sections above and in the results. Details of sample size, test used, error bars, and statistical significance cutoffs are presented in the text or figure legends. All experiments were performed in at least three biological replicates. Representative graphs are shown for the luminescence reporter assays. qPCR data were analyzed using 2-way ANOVA with a Sidak's multiple comparison test to compare individual time points. LC-MS abundance values were plotted as ArcSinh normalized values.

Graphics

All graphical models and drawings were generated using BioRender.com.

Results

YhjX is upregulated in response to low pH in a manner that depends on the non-cognate two-component system BtsS and YpdB

Previous work indicated that L-serine induces the activation of the BtsS pyruvate sensor kinase[124], presumably due to production of pyruvate via SdaA/B mediated L-serine de-amination. BtsS has been shown to induce the upregulation of the uncharacterized gene *yhjX*, in concert with

a non-cognate response regulator partner, YpdB.[121] Interestingly, natural induction of *yhjX* has been previously reported by the Jung group to occur in *E. coli* culture during mid-logarithmic growth phase[122], when bacterial cell density is high and nutrient depletion of LB begins to occur. Moreover, previous studies have shown that *yhjX* is among the genes upregulated in response to acidic pH in K-12 *E. coli*.[125] To confirm that these previous observations hold true in UPEC, we first assessed induction of *yhjX* in cystitis strain UTI89.[114] UTI89 is a sequence type ST95 strain, isolated from a patient with cystitis.[114] UTI89 is an O18:K1:H7 serotype, typical of UPEC strains and its genome has been sequenced.[114,126] To monitor whether *yhjX* induction is indeed acid-responsive in UPEC, we used a previously constructed strain UTI89/P*yhjX*::lux[121] that harbors a plasmid containing the *yhjX* promoter fused to the *luxCDABE* operon.[122] Luminescence and bacterial growth were monitored over time in unbuffered lysogeny broth (LB) with shaking. Cultures inoculated at near-neutral pH 7.4 to 7.6 **(Figure 5C, right y-axis)** showed a peak in *yhjX* promoter activity at 180 minutes, coincident with late logarithmic phase of growth **(Figure 5B, Figure 6)**. Addition of increasing concentrations of HCl to the media led to an increase in *yhjX* promoter activity that was proportional to the drop in pH **(Figure 5B)**. The addition of HCl in the conditions tested did not affect bacterial growth **(Figure 6)**. Addition of buffer - either MOPS or HEPES – to the acidified culture media restored neutral pH and suppressed *yhjX* promoter activity to levels observed when grown in LB with pH 7.4 **(Figure 5C)**. These results indicate that *yhjX* is indeed an acid-induced target in UPEC and corroborate previous observations in K-12 strains of *E. coli*.

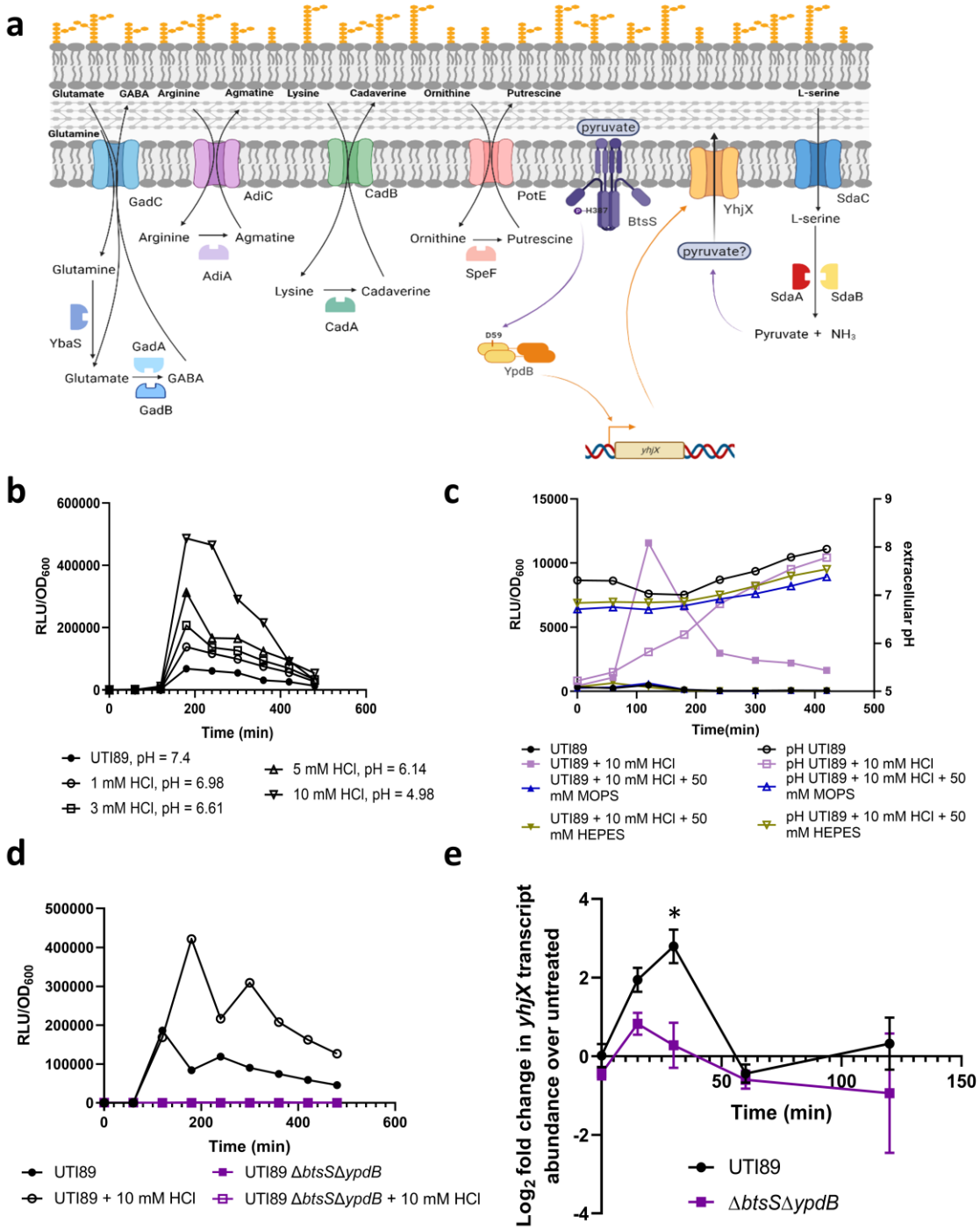

Figure 5. *yhjX* is upregulated in response to low pH in a manner that depends on the non-cognate two-component system BtsS and YpdB

A) Cartoon depicts currently known acid tolerance mechanisms in *E. coli*. Also depicted is our proposed novel acid tolerance mechanism that depends on L-serine import and de-amination. The signaling system BtsS-YpdB and its downstream target *yhjX* that codes for a putative transporter, are also induced during acid stress. Cartoon was created using BioRender.com B-C) Graphs depict relative luminescence units (RLU) normalized to growth (OD_{600}) over time, of UPEC strain UTI89

harboring the P*yhjX-lux* reporter in increasing concentration of HCl (B) or during growth in LB buffered to a pH of 7 with either 50 mM MOPS or 50 mM HEPES (C). D) Luciferase reporter assay of UPEC strain UTI89 the isogenic Δ*btsS*Δ*ypdB* strain grown in the presence (initial pH of 5.0) or absence (initial pH of 7.4) of HCl. Graphs are representative of 3 independent biological repeats. E) RT-qPCR analysis of *yhjX* transcript abundance after acid stimulation (pH of 5) in wild-type UTI89 (black) and Δ*btsS*Δ*ypdB* (purple) strains. Relative fold change was determined by the $\Delta\Delta C_T$ method, where transcript abundances were normalized to *gyrB* housekeeping gene transcripts. **P* = 0.0165 calculated by two-way ANOVA with Sidak's multiple comparisons test. Error bars indicate SEM of three biological replicates.

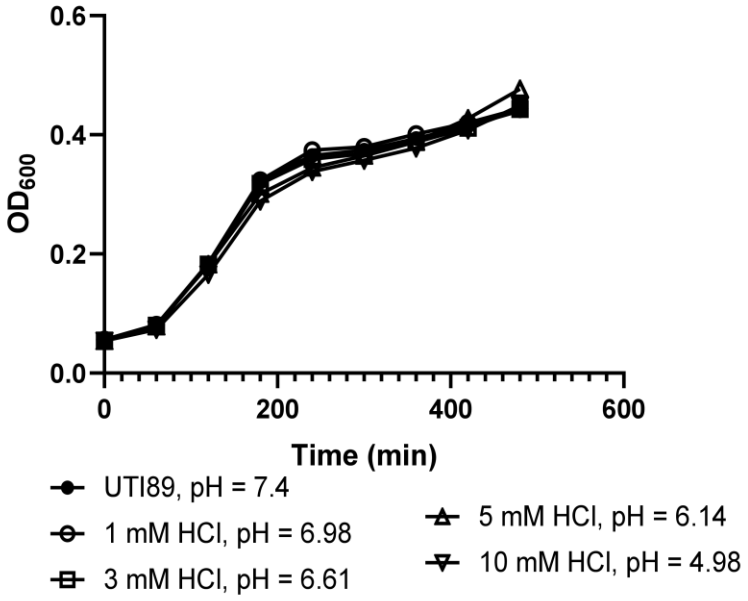

Figure 6. Growth of strains depicted in figure 5, under acidic conditions.
OD_{600} was measured over time of UTI89 cultures in the presence of increasing concentrations of HCl during growth in LB. Growth curves are representative of 3 biological replicates.

The *yhjX* gene encodes a putative pyruvate transporter of the major facilitator superfamily that has not yet been shown to import or export pyruvate.[122,127] Studies have shown that pyruvate increases in the extracellular milieu as the bacterial culture reaches late exponential growth[122], and that this pyruvate is directly sensed by the BtsS histidine kinase, leading to subsequent upregulation of *yhjX* via the action of the YpdB response regulator.[121] To determine whether acid-

mediated induction of *yhjX* is dependent on BtsS and YpdB, a mutant lacking both *btsS* and *ypdB* (Δ*btsS*Δ*ypdB*)[121] was tested via our luminescence reporter assay in acidic and neutral conditions. These experiments showed no induction of *yhjX* in the Δ*btsS*Δ*ypdB* strain, regardless of pH in the culture media **(Figure 5D)**. To validate these findings, *yhjX* steady-state transcript over time was also monitored by RT-qPCR and TaqMan based chemistry in acidified and non-acidified cultures of wild-type UTI89 and the isogenic Δ*btsS*Δ*ypdB* mutant. Transcript abundance of *yhjX* was compared between acid stimulated and unstimulated growth conditions and normalized to the *gyrB* housekeeping gene. These analyses revealed a characteristic transcription surge[128] for *yhjX* in acidified wildtype UTI89 cultures, which was not apparent in the isogenic Δ*btsS*Δ*ypdB* **(Figure 5E)**. To further confirm that *yhjX* is induced by low pH and not just HCl, we utilized the luminescent reporter to monitor *yhjX* induction in UTI89 and Δ*btsS*Δ*ypdB* in the presence of lactic acid, acetic acid, and pyruvic acid **(Figure 7)**. All organic acids tested resulted in strong *yhjX* induction in UTI89. However, the Δ*btsS*Δ*ypdB* strain did not induce *yhjX* under any of these acidic conditions **(Figure 7)**. Notably, addition of HCl, or acetic acid occasionally leads to two peaks in luminescence **(Figure 5D and 7)** in wild-type UTI89, indicative of two activation surges for *yhjX* transcription. This phenomenon is likely connected to BtsS signaling, but why it occurs only in response to HCl or acetic acid is unknown. Together, these data confirm that *yhjX* is induced in low-pH growth conditions and that this induction depends on the presence of BtsS and YpdB.

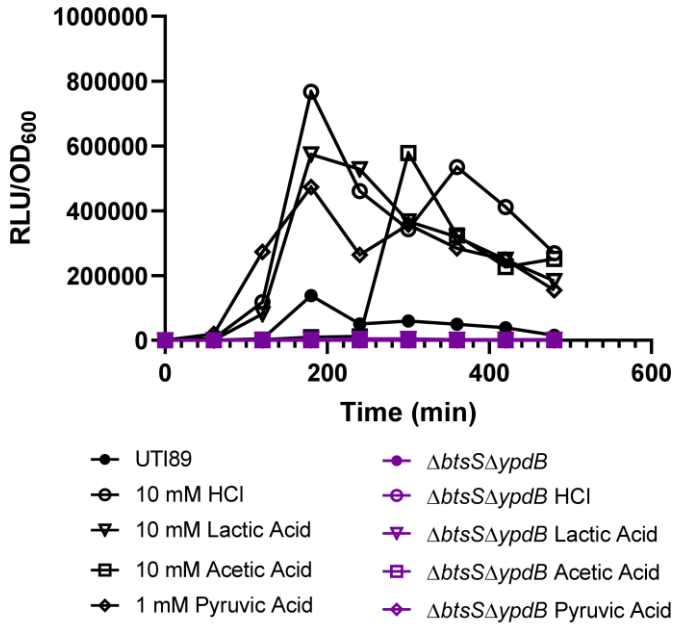

Figure 7. *yhjX* induction in response to organic acids
Wild-type UTI89 (black) and the isogenic Δ*btsS*Δ*ypdB* (purple) containing the P_{yhjX} luminescence reporter fusion were cultured in LB in the absence (filled shapes) or presence (open shapes) of 10 mM HCl (circles), 10 mM acetic acid (squares), 10 mM lactic acid (upside down triangles), or 1 mM pyruvic acid (diamonds). Luminescence and OD_{600} were measured every hour and luminescence normalized to OD_{600} is plotted. Graphs are representative of four biological replicates.

Induction of BtsS-YpdB in response to acid results from pyruvate produced during L-serine deamination

Previous work demonstrated that BtsS signaling is affected by L-serine levels in the growth medium.[129] These studies postulated that L-serine, which is the first amino acid to be consumed by *E. coli* during growth in laboratory media[109], is converted to pyruvate by the L-serine deaminases SdaA and SdaB and could then presumably exported by YhjX to serve as a positive feedback signal for BtsS[110,130,131] **(Figure 5A)**. Given that the de-amination of L-serine also produces ammonia, which can raise intracellular pH **(Figure 5A)**, we asked whether the mechanism of acid stress alleviation observed in our studies depends on the import and

deamination of L-serine. To test this hypothesis, we first created a series of mutants lacking the SdaC transporter (Δ*sdaC*), the SdaA or SdaB de-aminases (Δ*sdaA* and Δ*sdaB*) or both de-aminases (Δ*sdaA*Δ*sdaB*). The induction of *yhjX* in these mutants was tested via luciferase reporter assays either in media in which exogenous L-serine was added **(Figure 8A)**, or in media acidified with HCl **(Figure 8B)**. Addition of L-serine did not induce *yhjX* promoter activity in any of the *sda* mutants **(Figure 8A)**. Addition of acid to the media led to decreased *yhjX* induction compared to wild-type UTI89 in all the single mutants tested and led to no *yhjX* induction in the Δ*sdaA*Δ*sdaB* strain **(Figure 8B)**. Given that pyruvate is the known ligand of the BtsS sensor, our data suggests that in-vivo it is the de-amination of L-serine into pyruvate that actually leads to *yhjX* being induced. As further evidence that it is the generation of pyruvate driving *yhjX* induction, sodium pyruvate was added to the media of the Δ*sdaA*Δ*sdaB* strain, which caused – as expected – *yhjX* induction **(Figure 9)**.

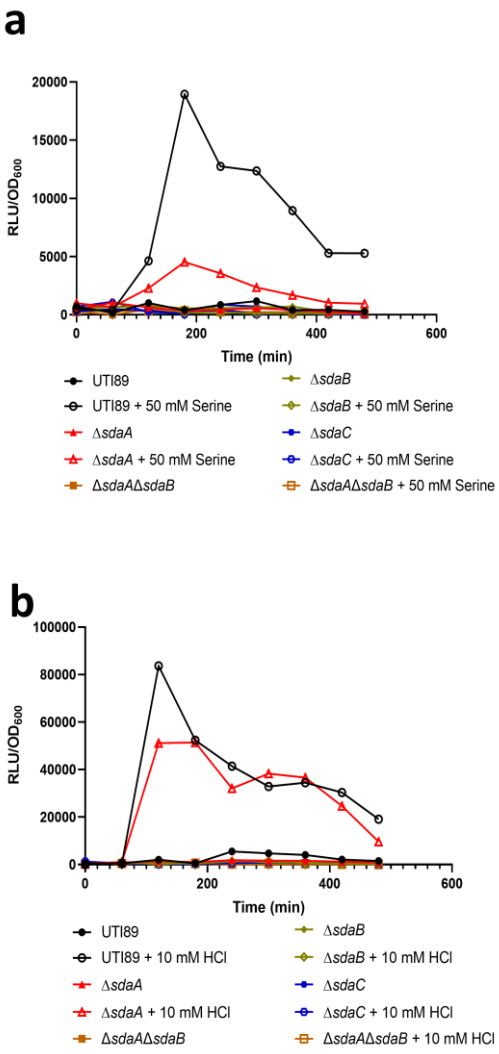

Figure 8. Induction of BtsS-YpdB in response to acid results from pyruvate produced during L-serine deamination

Graphs depict luciferase reporter assay performed over time of strains harboring the *yhjX* promoter reporter during growth in media supplemented with 50 mM serine (a) or 10 mM HCl (b). Deletion of serine import (*sdaC*, blue) or de-amination genes (*sdaA*, red; *sdaB*, gold) diminishes *yhjX* promoter activity. Results are representative of 3 biological repeats.

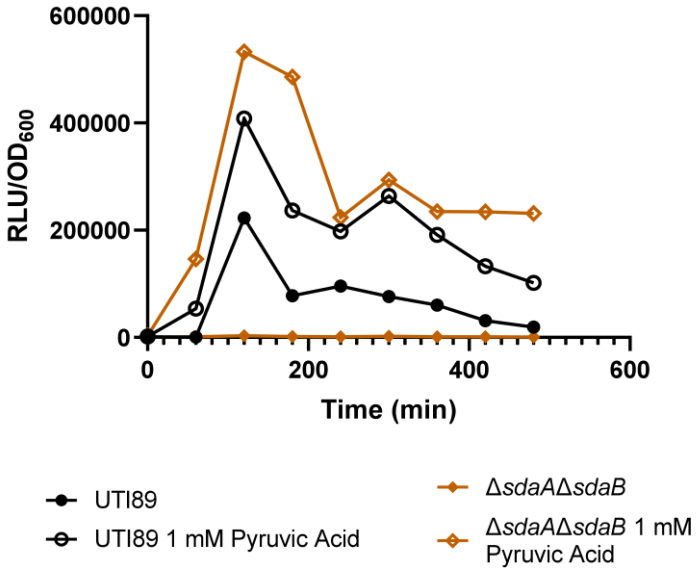

Figure 9. Sodium pyruvate induces the *yhjX* reporter in the absence of SdaA and SdaB
Wild-type UTI89 (black) and the isogenic Δ*sdaA*Δ*sdaB* (brown) strains containing the P_{yhjX} luminescence reporter fusion were cultured in LB in the absence (filled shapes) or presence (open shapes) of 1 mM sodium pyruvate. Luminescence and OD_{600} were measured every hour and luminescence normalized to OD_{600} is plotted. Graphs are representative of three biological replicates.

L-serine deamination is a mechanism that protects E. coli from acid stress

If L-serine deamination is a component of the *E. coli* acid response, we reasoned that the mutant lacking the SdaA/B enzymes would display a survival defect in acidic conditions. We first determined the acid tolerance profile of UTI89, given that we have not previously tested this strain for acid sensitivity. To do this, we sub-cultured UTI89 in fresh, unbuffered LB (pH 7.4) for 3 hours then adjusted the culture pH to 7, 6, 5, 4, 3, or 2 using HCl. We then assessed survival of UTI89 after 30 minutes or 2 hours of exposure. As expected, wild-type UPEC survival did not get substantially affected during 30 min incubation at pH 3 but decreased by 2 logs during the 2h incubation **(Figures 10 and 11A)**. Incubation at pH 2 for 30 minutes and 2h both had substantial impact on UPEC growth **(Figures 10A and 11A)**. To compare the effects of *sda* deletion on acid tolerance, we picked 30-minute incubation at pH 3, since these conditions do not significantly

impact survival of wild-type UTI89. Under the selected conditions, we observed the Δ*sdaA*Δ*sdaB* strain exhibiting the most pronounced acid survival defect compared to any of the single Δ*sdaA*, Δ*sdaB* or Δ*sdaC* mutants **(Figure 12)**. The acid susceptibility profile of Δ*sdaA*Δ*sdaB* is similar to known acid resistance mutants cultured under the same conditions **(Figure 10B)**. The survival defect of Δ*sdaA*Δ*sdaB* was also observed when the strain was incubated for 2h in pH 3, compared to wild-type UTI89 or an isogenic Δ*gadA*Δ*gadB* strain **(Figure 11B – pH 3 data)**. Intriguingly, when we tested Δ*sdaA*Δ*sdaB* and Δ*gadA*Δ*gadB* in pH 2 for 30 minutes, we observed a similar decline in CFUs that was not statistically different from wild-type UTI89 **(Figure 11C – pH 2 30-minute data)**. These observations indicate a different susceptibility profile for UPEC, compared to commensal *E. coli*[67,75] and demonstrate that L-serine de-amination becomes an important acid tolerance mechanism for UPEC.

To determine if serine is imported by *E. coli* in response to a drop in pH, cell culture supernatants were then analyzed for relative serine abundance by LC-MS and compared to acidified media alone as a control. Mass spectrometric measurements of serine in media alone demonstrated that baseline serine abundance level can be detected with this method **(Figure 10C)**. Measurements of serine in acidified media revealed a significant reduction in extracellular serine abundance in the supernatant fractions of WT UTI89, but not the Δ*sdaC* mutant **(Figure 10C)**. These data indicate that serine is imported – in an SdaC-dependent manner – into the bacterial cell in response to acid stress.

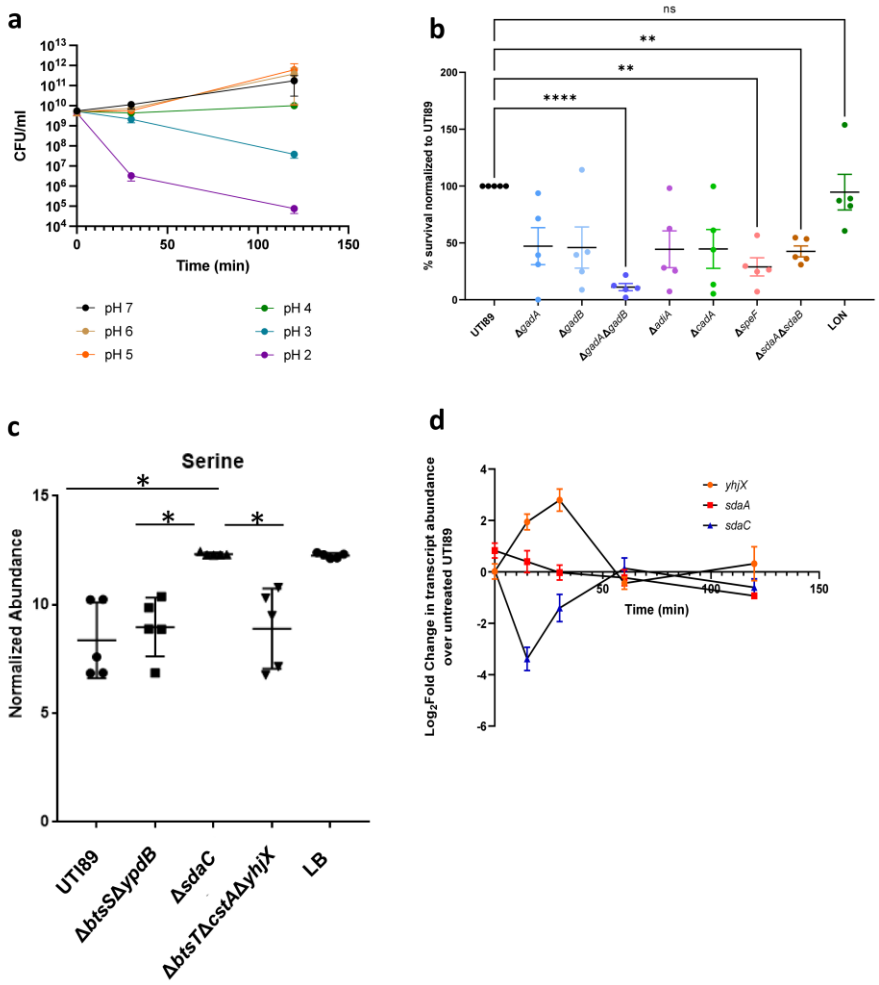

Figure 10. L-serine deamination is another acid resistance mechanism in *E. coli*
A) CFU/ml of UTI89 grown in LB adjusted to the indicated pHs with HCl (n=4 biological replicates). B) Graph depicts survival in acidic conditions, compared to the wild-type strain, of mutants deleted for decarboxylases or serine deaminases. For these assays, cultures were incubated for three hours, at which point an aliquot was collected for CFU enumeration before acid treatment. The remaining culture was treated with HCl to adjust the pH to three. Samples were incubated for an additional 30 minutes, after which they were plated for CFUs. Percent survival in acid is calculated as the number of CFUs in acid treatment, compared to untreated input control. Statistical analysis was performed by 1-way ANOVA with *post hoc* Dunnett's multiple comparisons correction test (***P*<0.005, *****P* <0.0001). Error bars indicate SEM of 5 biological replicates. C) UTI89, Δ*btsS*Δ*ypdB*, and Δ*sdaC* were grown until cultures reached an OD_{600} = 0.5, then 1 M HCl was added to the culture to a final concentration of 10 mM (pH=5). Cultures were incubated for another 15 minutes, then 1 ml of culture was collected. Cells were pelleted and supernatant was flash frozen and stored at -80°C prior to sample preparation. Following MS sample preparation, extracellular serine abundance was detected by LC-MS. D) qPCR analysis of *yhjX* (orange), *sdaA* (red), and *sdaC* (blue) transcript abundance after acid stimulation in wildtype UTI89. The relative fold change was determined by the $\Delta\Delta C_T$ method where transcript abundances were normalized to *gyrB* housekeeping gene transcripts. Error bars indicate SEM of three biological replicates (**P*< 0.005, ANOVA).

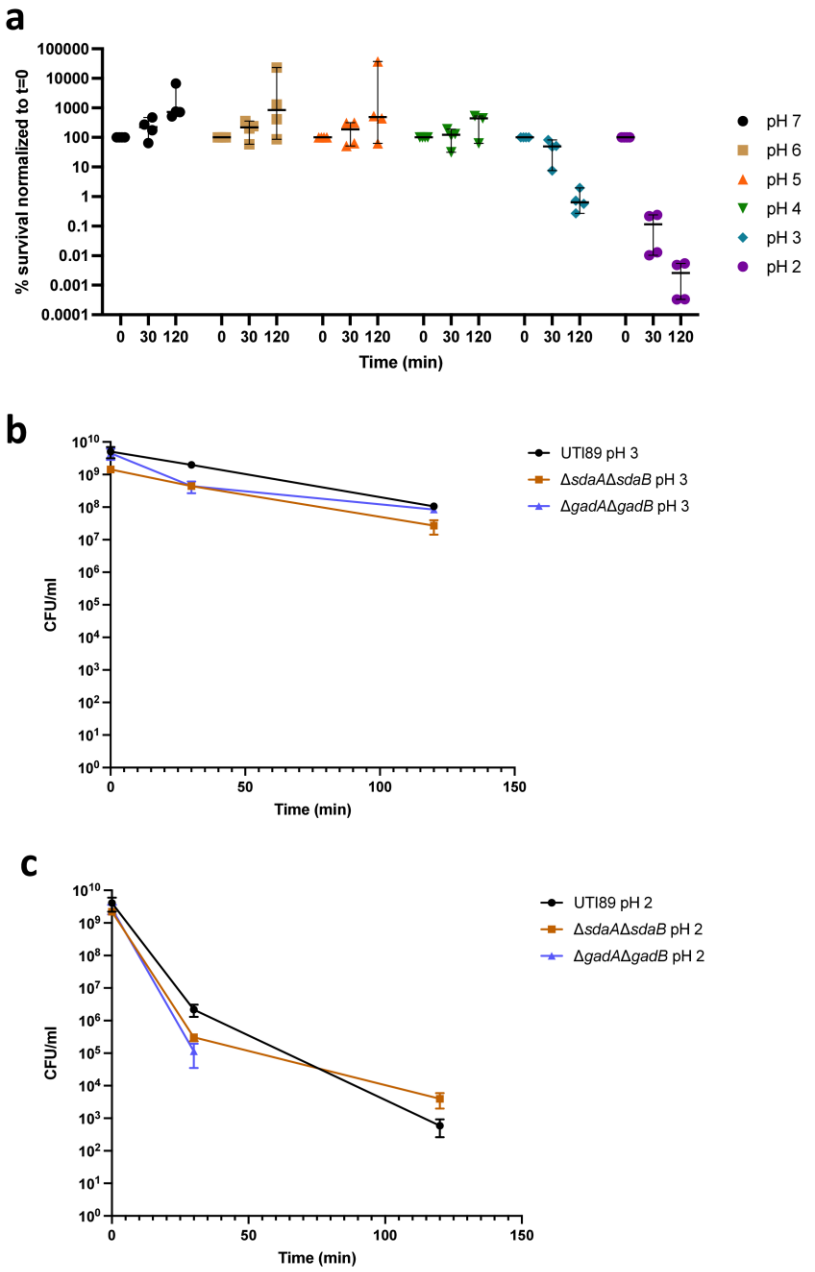

Figure 11. Δ*sdaA*Δ*sdaB* has similar acid resistance profile to Δ*gadA*Δ*gadB*

A) Graph depicts survival of UTI89 in increasingly acidic conditions. For these assays, cultures were incubated for three hours, at which point an aliquot was collected for CFU enumeration before acid treatment. The remaining culture was adjusted to the indicated pH using HCl. Samples were incubated for 30 minutes and 120 minutes. Percent survival in acid is calculated as the number of CFUs in acid treatment, compared to untreated input control. (n=4 biological replicates). B) Graph depicts CFU/ml of UTI89, UTI89 Δ*sdaA*Δ*sdaB*, and UTI89 Δ*gadA*Δ*gadB* at t=0, 30, and 120 minutes after pH of the culture was adjusted to 3 with HCl. C) Graph depicts CFU/ml of UTI89, UTI89 Δ*sdaA*Δ*sdaB*, and UTI89 Δ*gadA*Δ*gadB* at t=0, 30, and 120 minutes after pH of the culture was adjusted to 2 with HCl.

Extracellular serine levels also drop in the Δ*btsS*Δ*ypdB* mutant under acidic conditions **(Figure 10C)**. This observation is consistent with the notion that L-serine is imported independent of BtsS-YpdB signaling. Subsequent qPCR showed that in the wild-type strain *sdaA* transcript abundance does not significantly change in response to acid stress **(Figure 10D)**, in sharp contrast to *yhjX* that displays an activation surge **(Figure 10D)**. These data indicate that *sdaA* transcription is not acid inducible. Interestingly, *sdaBC* transcript abundance sharply drops at 15 minutes post addition of acid to the media, displaying a fold-change that is the opposite of *yhjX* **(Figure 10D)**. Maurer et al, previously reported *sdaB* and *sdaC* as "acid-low" transcripts.[67] Our data indicated drop in transcript shortly after addition of acid and coincident to the time that L-serine is brought into the cell **(Figure 10B)**. This could indicate that acidic conditions lead to downregulation of *sdaBC* via an unknown regulator, or that production of pyruvate or ammonia by L-serine de-amination has a negative impact on s*daBC* transcription.

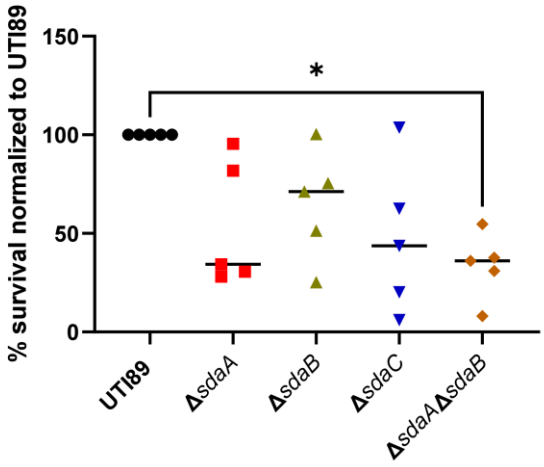

Figure 12. Acid tolerance profile of serine deaminase and serine import mutants
Graph depicts survival in acidic conditions, compared to the wild-type strain, of mutants deleted serine deaminases (*sdaA* and *sdaB*) or serine importer (*sdaC*). For these assays, cultures were incubated for three hours, at which point an aliquot was collected for CFU enumeration before acid treatment. The remaining culture was treated with HCl to adjust the pH to three. Samples were incubated for an additional 30 minutes, after which they were plated for CFUs. Percent survival in acid is calculated as the number of CFUs in acid treatment, compared to untreated input control. Statistical analysis was performed by 1-way ANOVA with *post hoc* Dunnett's multiple comparisons correction test (*$P<0.05$).

YhjX is induced in response to pyruvate detection by the BtsS sensor histidine kinase.[129] Given that L-serine de-amination leads to the production of pyruvate, which is the known ligand for BtsS[129], we hypothesized that SdaA/SdaB-mediated L-serine deamination increases intracellular pyruvate levels that could then be exported via YhjX if the function of YhjX is to transport pyruvate **(Figure 13A)**. To determine if extracellular pyruvate abundance changes in response to acid treatment, we measured pyruvate levels in the extracellular milieu over time, following acidification of the culture media, in the same samples used for the serine measurements in Figure 10C. Cell culture supernatants were analyzed for changes in pyruvate abundance using Pyruvate Assay kits (MAK071-1KT, Sigma Aldrich) and fold change compared to non-treated controls was determined. In wildtype UTI89, an increase in extracellular pyruvate is observed at 15 minutes following acidification, compared to the untreated isogenic control **(Figure 13B)**. Following this pyruvate surge, pyruvate levels are not significantly higher between treated and untreated UTI89 cells at 60 and 180 minutes post acidification. In the mutant lacking the SdaC transporter, extracellular levels are significantly lower than those of wild-type UTI89 at 15 minutes post acidification, but still increase, suggesting that pyruvate is exported from the cell even when L-serine import is disrupted. In sharp contrast, the supernatant fractions of the Δ*btsS*Δ*ypdB* mutant, which as demonstrated in Figure 5D, has no observable *yhjX* promoter activity **(Figure 13B)**, show no increase in extracellular pyruvate levels at 15 minutes following acidification. Instead, we observe an increase in extracellular pyruvate at 60 minutes post acidification for Δ*btsS*Δ*ypdB*. These data suggest that YhjX may indeed export pyruvate, although additional studies are needed to prove this biochemically. Our data also indicate that in the absence of YhjX, other transporters can presumably fulfill the function of pyruvate export, since extracellular pyruvate levels do increase at a later timepoint in the acid-treated Δ*btsS*Δ*ypdB* strain.

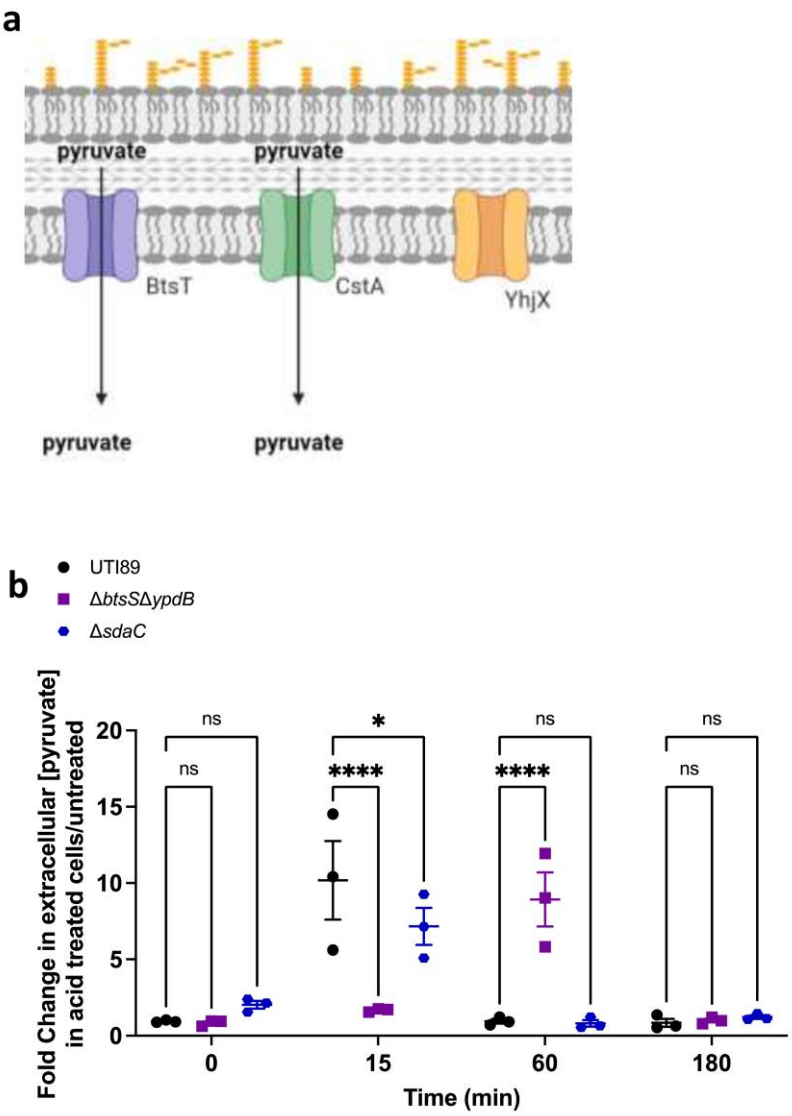

Figure 13. Pyruvate export is delayed in Δ*btsS*Δ*ypdB*

a) Cartoon depicts currently known pyruvate transporters (BtsT and CstA) and a putative pyruvate transporter (YhjX) in *E. coli.* Created with BioRender.com b) UTI89, Δ*btsS*Δ*ypdB*, and Δ*sdaC* strains were grown until cultures reached an OD_{600} = 0.5, then split so that 1 M HCl was added to half of the culture while the other half continued to grow in LB alone. Supernatant was collected after 0, 15, 60, and 180 minutes. Pyruvate concentration in the supernatant was quantified for all time points. Fold change in pyruvate concentration in the acid treated samples over the unstimulated samples is graphed. Error bars indicate SEM of 3 biological replicates (****P<0.001, *P<0.05).

In conclusion, our data demonstrate that the import and deamination of L-serine provides protection from acid stress to uropathogenic *E. coli* and we provide circumstantial evidence for export of pyruvate via YhjX under acidic conditions.

Discussion

In this work, we show that L-serine deamination serves as an additional acid response mechanism in *E. coli*. Serine is the first amino acid consumed by *E. coli* when grown in complex media, despite its toxicity at higher concentrations.[109] L-serine can be deaminated by the SdaA and SdaB enzymes to yield pyruvate and ammonia. *E. coli* encodes multiple serine deaminase genes that function under a variety of environmental conditions.[132] For instance, while both *sdaA* and *sdaB* are expressed under aerobic conditions, *sdaA* is expressed in nutrient limited minimal media, and in contrast, *sdaB* is expressed in the nutrient rich LB.[111,131,133] The redundancy of these enzymes indicates that the deamination of serine is important for these bacteria. In this paper, we propose that L-serine import into *E. coli* serves as an acid tolerance mechanism through the production of ammonia and pyruvate. Maurer et al. profiled gene expression in K-12 *E. coli* in response to pH changes. Their work showed that serine deaminases were upregulated in basic conditions when compared to acidic conditions.[67] This is reflected in our qPCR data **(Figure 10D)**, where we show that *sdaC* is downregulated shortly after acidification. However, we see that sustained growth in acidic media led to an increase in *sdaC* transcript abundance over time **(Figure 10D)**. It is possible that acidic conditions lead to downregulation of *sdaBC* via an unknown regulator, or that production of pyruvate or ammonia by L-serine de-amination exerts negative feedback on *sdaBC* transcription.

Various bacteria are known to use ammonia to neutralize their intracellular pH, including *E. coli*.[86,134,135] We postulate that the ammonia produced via L-serine deamination functions as a base which increases the cytoplasmic pH of *E. coli* when under acid stress. A similar role has been reported for glutamine (AR2_Q) in *E. coli*.[86,87] Deletion of the serine deaminase genes, *sdaA* and *sdaB*, results in a significant decrease in cell survival in acidic conditions compared to the wildtype strain. This decrease in cell survival is comparable to that observed in other AR mutants of *E. coli*. All together, these data suggest that L-serine deamination serves as a previously uncharacterized acid tolerance mechanism in *E. coli*. Loss of serine deaminase activity was previously shown to result in changes to cell shape due to interference with cell wall synthesis.[111,132] These serine deaminase mutants exhibit increased filamentation. In the context of UTI, filamentous UPEC are deficient in invading bladder cells, forming secondary intracellular bacterial communities, and in establishing quiescent intracellular reservoirs.[17,136] Thus, loss of serine deamination could detrimentally affect the ability of UPEC to form reservoirs in addition to its ability to tolerate low pH. Evolution of mechanisms that utilize various amino acids for tolerating acid stress would allow bacteria to seamlessly adapt to different host niches with differing resource availabilities during the infection process.

It has been shown that up to 51% of serine flux is directed to the production of pyruvate[109], which can presumably be shunted into the TCA cycle for energy production. Here we demonstrate a connection between serine deamination and the pyruvate responsive cross regulating two-component system, BtsS-YpdB. BtsS-YpdB activation occurs in response to increased pyruvate and leads to the upregulation of *yhjX* transcription. Loss of L-serine deaminases result in ablation of *yhjX* promoter induction in response to serine, indicating that pyruvate produced via serine deamination induces activation of the BtsS-YpdB system. Our metabolomics analyses demonstrate

that extracellular serine levels drop in the Δ*btsS*Δ*ypdB* mutant under acidic conditions indicating that BtsS-YpdB activation occurs after L-serine is imported. In this work we also show that *yhjX* is also induced by the BtsS-YpdB system in response to acidic pH **(Figure 5B-D)**. Although this activation in response to low pH was dose dependent, considering the data that suggests *yhjX* is induced through serine deamination and that pyruvate is a known ligand for BtsS, *yhjX* activation in response to low pH appears to be a response to the pyruvate produced by serine deaminases. The function of YhjX remains elusive. We, and others, have hypothesized that YhjX could serve as a pyruvate transporter. Here we provide preliminary evidence that YhjX may function as a pyruvate transporter, but it is not necessary for the L-serine mediated acid response, as extracellular pyruvate levels do increase – albeit in a delayed fashion – in the Δ*btsS*Δ*ypdB* strain **(Figure 13B)**.

In summary we show that in acidified media, cells import L-serine from the growth media via the SdaC transporter and de-aminate it via the action of SdaA and SdaB. Deletion of both deaminase genes renders *E. coli* susceptible to acid stress similarly to known AR system deletion mutants. We therefore propose that the importation and deamination of serine represents a previously uncharacterized acid response mechanism in *E. coli*.

Table 1: Primers used in this study

Primer name	Sequence 5'-3'	Purpose
btsS_KO_f	GGCCTGTTCGCTGTCGCGGCGGATCACCGCTTTAA TGGTGTTAAGCGCGTGTAGGCTGGAGCTGCTTC	Deletion of *btsS*
btsS_KO_r	GTGTGGTTTGCGGGTATGTACGATTTTAATCTGGT GTTGCTGCTGCTTCACATATGAATATCCTCCTTAG	Deletion of *btsS*
btsS_KO_test_f	GATAAGCGTTCACATGTTCAATTTCGTC	Validation of *btsS* deletion
btsS_KO_test_r	GCAAGAGTTCAAAGAAAGTTAAACGCAAG	Validation of *btsS* deletion
ypdB_KO_f	CAGGAACTGAGCTGGCTAATTAAAGAGCACAGCC AGATGGAGATTGTCGGCGTGTAGGCTGGAGCTGC TTC	Deletion of *ypdB*
ypdB_KO_r	TTACAGATGCATTAACTGGCGGAATTCTTTAACTT TGCTACGGCTGACCGCATATGAATATCCTCCTTAG	Deletion of *ypdB*
ypdB_KO_test_f	GCCGGAGTGATATTGTGAAAGTCAT	Validation of *ypdB* deletion
ypdB_KO_test_r	AATTGTTGATCGGCGGGCAAGC	Validation of *ypdB* deletion
sdaA_KO_f	GTTATTAGTTCGTTACTGGAAGTCCAGTCACCTTG TCAGGAGTATTATCGTGTAGGCTGGAGCTGCTTC	Deletion of *sdaA*
sdaA_KO_r	AAGCGGGAATAAATTCGCCCATCCGTTGCAGATG GGCGAATAAGAAGATCATATGAATATCCTCCTTAG	Deletion of *sdaA*
sdaA_KO_test_f	CATCTGGGTCGTTATCATCCT	Validation of *sdaA* deletion
sdaA_KO_test_r	GTAACGAGTGCGCAAATCG	Validation of *sdaA* deletion
sdaB_KO_f	CGCGCCGCTTTCGGGCGGCGCTTCCTCCGTTTTAA CGCGATGTATTTCCTGTGTAGGCTGGAGCTGCTTC	Deletion of *sdaB*
sdaB_KO_r	GGATGAGAAATCGGGAAGAGGCCTCGCAAAAAGA GGCCTCTGGAGAGCGACATATGAATATCCTCCTTA G	Deletion of *sdaB*
sdaB_KO_test_f	GTTCCTGATGCCGATGTAC	Validation of *sdaB* deletion
sdaB_KO_test_r	CCAGAACAGGCTATGGCT	Validation of *sdaB* deletion
sdaC_KO_f	GGCTGAACTGGCTAAAAGCTGAATTATTTGCATTC CTCCAGGAGAAATAGGTGTAGGCTGGAGCTGCTT C	Deletion of *sdaC*
sdaC_KO_r	ACATCGCGTTAAAACGGAGGAAGCGCCGCCCGAA AGCGGCGCGAAAGGACCATATGAATATCCTCCTT AG	Deletion of *sdaC*
sdaC_KO_test_f	CATCGCCGATAGACAGAT	Validation of *sdaC* deletion
sdaC_KO_test_r	GAACTCCACTTCATGCTGAC	Validation of *sdaC* deletion
gadB_KO_FOR	CAGGTGTGTTTAAAGCTGTTCTGCTGGGCAATACC CTGCAGTTTCGGGTGTGTAGGCTGGAGCTGCTTC	Deletion of *gadB*
gadB_KO_REV	CAAGTAACGGATTTAAGGTCGGAACTACTCGATTC ACGTTTTGGTGCGAACATATGAATATCCTCCTTAG	Deletion of *gadB*

gadB_KO_Test_FOR	GTGAACAGACTTTGGAAATTGTCCC	Validation of *gadB* deletion
gadB_KO_Test_REV	ACTTGCTTACTTTATCGATAAATCCTA	Validation of *gadB* deletion
gadA_KO_FOR	GTTTAAAGCTGTTCTGCTGGGCAATACCCTGCAGT TTCGGGTGGTCGCTGGTGTAGGCTGGAGCTGCTTC	Deletion of *gadA*
gadA_KO_REV	AAATGGACCAGAAGCTGTTAACGGATTTCCGCTCA GAACTACTCGATTCACATATGAATATCCTCCTTAG	Deletion of *gadA*
gadA_KO_Test_FOR	CAATTAATAAGTAGCCGAATACCCACC	Validation of *gadA* deletion
gadA_KO_Test_REV	TGTAATACCTTGCTTCCATTGCG	Validation of *gadA* deletion
adiA_ko_f	ATGATGAAAGTATTAATTGTTGAAAGCGAGTTTCT CCATCAAGACACCTGGTGTAGGCTGGAGCTGCTTC	Deletion of *adiA*
adiA_ko_r	TTACGCTTTCACACACATAACGTGGTAAATACCGT CAATAATTTCTGTCCCTTCCATATGAATATCCTCCT TAG	Deletion of *adiA*
adiA_kotest_f	GAAGATACTTGCCCGCAAC	Validation of *adiA* deletion
adiA_kotest_r	CTCGCTAAAGCGAAGCGATAC	Validation of *adiA* deletion
cadA_ko_f	ATGACTATGAACGTTATTGCAATATTGAATCACAT GGGGGTTTATTTTAAAGAAGGTGTAGGCTGGAGCT GCTTC	Deletion of *cadA*
cadA_ko_r	TTATTTTTTGCTTTCTTCTTTCAATACCTTAACGGT ATAGCGGCCATCAGCATATGAATATCCTCCTTAG	Deletion of *cadA*
cadA_kotest_f	GTACCTTCATCGTCAGCCTG	Validation of *cadA* deletion
cadA_kotest_r	GTGTTCTCCTTATGAGC	Validation of *cadA* deletion
speF_ko_f	ATGACGAGTATAGCCAGTTACCGGGCTGGTCTGG GTTATTGCATCTGCGTGTAGGCTGGAGCTGCTTC	Deletion of *speF*
speF_ko_r	AATTTTTCCCCTTTCAACAGGGCGCTTTGCGCATC ACGAGGCTTGATGACCATATGAATATCCTCCTTAG	Deletion of *speF*
speF_kotest_f	GGTGCTCATATACTGCTAAC	Validation of *speF* deletion
speF_kotest_r	GTTGACCATCGTCAGTATG	Validation of *speF* deletion
gyrB_qPCR_f	GATGCGCGTGAAGGCCTGATTG	qPCR housekeeping gene
gyrB_qPCR_r	CACGGGCACGGGCAGCATC	qPCR housekeeping gene
gyrB_qPCR_probe	VIC-ACGAACTGCTGGCGGA-MGBNFQ	qPCR housekeeping gene
yhjX_qPCR_f	TCGCTACACCAATCACATACAGAC	*yhjX* qPCR
yhjX_qPCR_r	GAAGCAGGAAGTGAAAACCAGC	*yhjX* qPCR

yhjX_qPCR_probe	FAM-GCATCGACTCTGCCAGGGTGTAGTC-MGBNFQ	*yhjX* qPCR
sdaA_qPCR_f	TGCAAATCCACGCCTATAACG	*sdaA* qPCR
sdaA_qPCR_r	CAGTACGCGAGCAGTTCG	*sdaA* qPCR
sdaA_qPCR_probe	FAM-CGAAGTGAGCGTGCCGTATCCG-MGBNFQ	*sdaA* qPCR
sdaC_qPCR_f	GATGCTGCTGGCTCTGTACC	*sdaC* qPCR
sdaC_qPCR_r	ATGATCGGAGAGTGGTTGAACG	*sdaC* qPCR
sdaC_qPCR_probe	NED-GCTGTCTCTGGACACTGCATCTG-MGBNFQ	*sdaC* qPCR

Table 2: Strains and plasmids in this study

E. coli strain	Relevant genotype	plasmid	Plasmid description
UTI89			
Δ*btsS*Δ*ypdB*	Δ*btsS*Δ*ypdB*		
Δ*sdaA*	Δ*sdaA*		
Δ*sdaB*	Δ*sdaB*		
Δ*sdaC*	Δ*sdaC*		
Δ*sdaA*Δ*sdaB*	Δ*sdaA*Δ*sdaB*		
Δ*gadA*	Δ*gadA*		
Δ*gadB*	Δ*gadB*		
Δ*gadA*Δ*gadB*	Δ*gadA*Δ*gadB*		
Δ*adiA*	Δ*adiA*		
Δ*cadA*	Δ*cadA*		
Δ*speF*	Δ*speF*		
UTI89		pBBR *yhjX-lux*	PyhjX -264/+36 cloned in the BamHI and EcoRI sites of pBBR1-MCS5-TTRBS-lux; Gm^r [24]

Chapter 3: Lysine decarboxylation is a key contributor to UPEC pathogenesis during intracellular infection

At the time of this thesis submission, this chapter is in preparation for submission for publication at Infection and Immunity

Michelle A. Wiebe[a], Seth Reasoner[a], Tomas Bermudez[a], John R. Brannon[b], Grace Morales[a], Faith Guice[c], Erin Q. Jennings[b], Jeffery C. Rathmell[b], and Maria Hadjifrangiskou[b,d,e,*]

Abstract

Acid stress is a substantial challenge to bacterial life. Acidic conditions can damage the bacterial cell envelope and disturb vital physiological processes, such as enzymatic activity, protein folding, membrane- and DNA maintenance. *Escherichia coli* occupies numerous environmental and host niches with varying pH. Consequently, *E. coli* strains are equipped with multiple acid resistance (AR) mechanisms to withstand acidic conditions. Uropathogenic *E. coli* (UPEC), which accounts for >75% of urinary tract infections (UTIs) persist for years in the host, colonizing the gut and the vagina asymptomatically for long periods of time, while causing acute or chronic infection in the bladder. While these host niches have variable pH, no studies elucidated which AR mechanisms are used by UPEC during infection. Here, focusing on the acute stage of bladder infection we uncover which AR mechanisms are induced during intracellular UPEC replication. We show that in human urothelial cells, the AR4 mechanism, which involves lysine decarboxylation to cadaverine, is upregulated during intracellular infection. Consequently, deletion of AR4 leads to fewer bacteria associating with urothelial cells and decreases colonization in the murine bladder during acute UTI. Deletion of AR4 is epistatic to other AR deletions *in vivo*,

suggesting that AR4 is utilized for the initial stages of infection. Moreover, we demonstrate that bafilomycin treatment rescues the AR4 deletion phenotype intracellularly, suggesting that AR4 is important for UPEC survival inside the lysosome. Collectively this work identifies AR4 as a ket AR mechanism for UPEC survival during UTI establishment.

Introduction

Urinary tract infections (UTIs) are among the most common bacterial infections of adult humans in the world. These infections most commonly occur in the bladder (cystitis), but bacteria can ascend the ureters and infect the kidneys, occasionally leading to pyelonephritis. UTIs disproportionately affect people assigned female at birth (AFAB), with approximately 80% of all UTIs being reported in people AFAB.[137] The majority of UTIs are caused by uropathogenic *E. coli* (UPEC).[1] The majority of UPEC strains belong to the B2 and D phylogenetic clades, members of which can colonize the human host for years.[104,138,139]

It is hypothesized that UTI-causing *E. coli* strains can be acquired through ingestion of contaminated food[140], which implies that UPEC can survive the acidic conditions of the stomach and the variable pH encountered in the gastrointestinal and genitourinary tracts.[11,141] In the gastrointestinal tract, stomach acid, bile acids, and organic acid metabolites from the gut microbiota all present pH challenges for UPEC.[107,108,142] In the human vaginal space, where UPEC can form transient asymptomatic reservoirs[143], different *Lactobacillus spp.*[48] excrete large concentrations of lactic acid that lowers the vaginal pH.[48,144,145] In the bladder lumen **(Figure 14A)**, the primary immune responders during UPEC infection are neutrophils and macrophages[15], which use mechanisms of bacterial killing that involve low pH. Inside urothelial cells, where UPEC expands during acute infection, the phagolysosome has been shown to kill or expel invading

UPEC.[15] However, UPEC has been shown to neutralize phagolysosomes in bladder epithelial cells.[15,146] This neutralization prevents bacterial cell death, although the mechanism through which UPEC can accomplish it remains unknown. In this study, we present evidence that lysine decarboxylation contributes to increased intracellular survival during the early stages of acute UTI, specifically in the lysosome.

The most well characterized AR mechanisms, AR2-5 **(Figure 14B)**, depend on the import and subsequent decarboxylation of specific amino acids. The decarboxylation reaction consumes one proton, thereby increasing the cytoplasmic pH.[50,83,103,108,147] Decarboxylation of lysine to cadaverine is catalyzed by the AR4 mechanism, which comprises the CadB lysine/cadaverine antiporter and the CadA enzyme that decarboxylates lysine to produce cadaverine **(Figure 14B** and [50,148]**)**.

AR4 is regulated through CadC, a membrane integrated transcription regulator. CadC responds to low pH and changes in lysine abundance to promote transcription of *cadA* and *cadB*.[80] CadB imports lysine then CadA decarboxylates lysine to cadaverine, which is exported by CadB **(Figure 14C)**. LysP, a constitutively expressed lysine importer, has been shown to inhibit *cadBA* expression through interactions with CadC. When extracellular lysine is absent or concentrations are low, LysP inhibits CadC activation of the *cadBA* operon.[81]

In this work we present new insights into the role of AR4 during acute UPEC infection. We show that *cadBA* is upregulated inside human urothelial cells and that inactivation of AR4 via the deletion of the *cadA* lysine decarboxylase gene impairs acute infection. We demonstrate that mutants deleted for *cadA* have a fitness defect in the intracellular environment of the urothelial cell, which is restored upon treatment with bafilomycin, an agent that blocks vesicle acidification.

We conclude that AR4 specifically is the AR mechanism used during the early stages of intracellular infection.

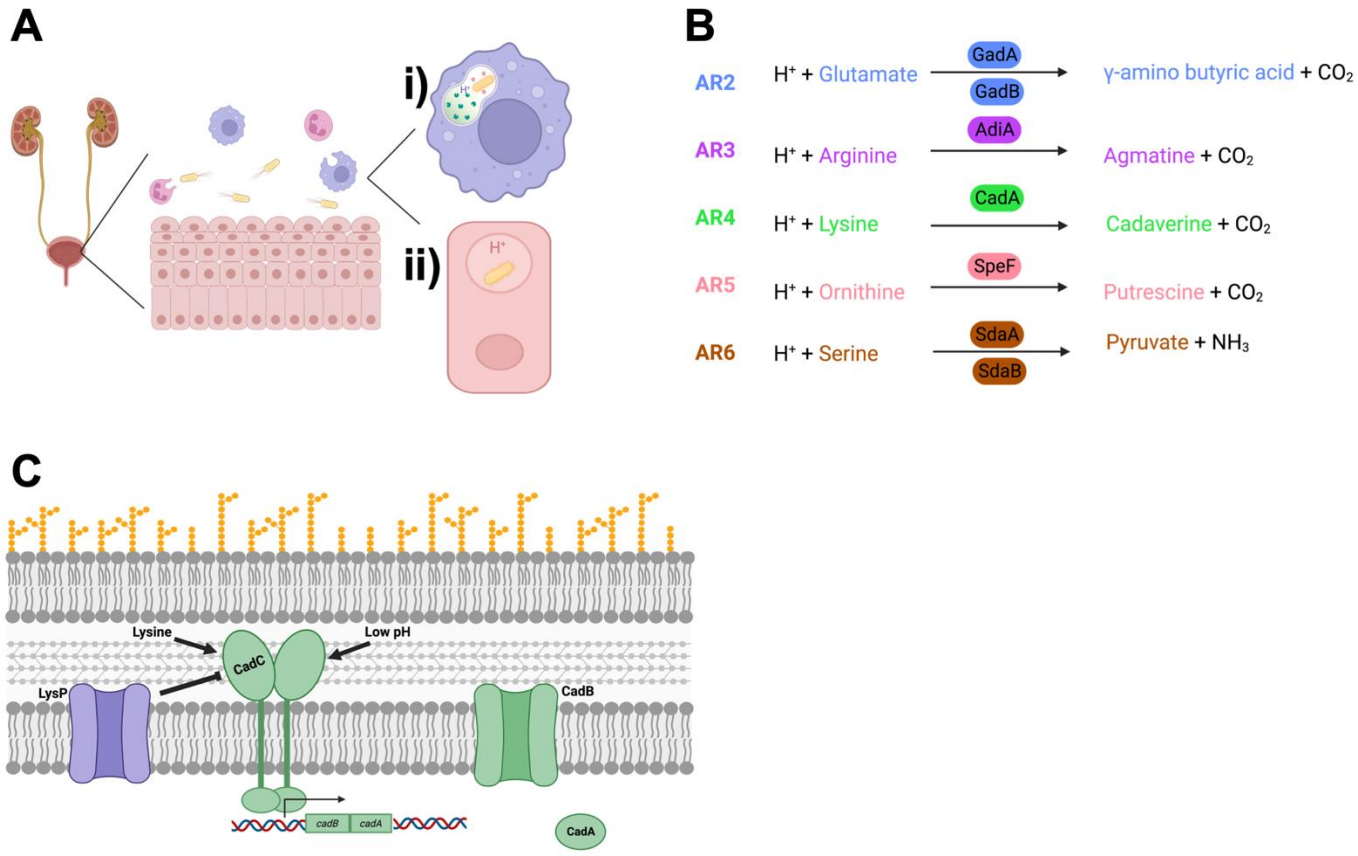

Figure 14. Acidic pH stress in the bladder and E. coli acid resistance mechanisms
A) During bladder colonization, the major acidic pH stress UPEC encounters is due to the innate immune response to infection (model made with biorender). Ai) macrophages and neutrophils phagocytose UPEC. Fusion of the phagosome with the lysosome induces a pH decrease in the newly formed compartment. The pH decrease is meant to be bactericidal. Aii) During its pathogenic cascade, UPEC invades bladder epithelial cells. In order to expand into intracellular bladder communities, UPEC must be able to survive and escape from endocytic vesicles that become acidified in response to infection. B) Chemical reactions of previously described acid resistance mechanisms in *E. coli.* AR2-AR5 are all decarboxylation reactions that consume a proton to produce CO_2 . The resulting product is then exported by amino acid antiporters. AR6 involves the deamination of serine to produce NH_3 (model made with biorender). C) Model of AR4 regulation (made with biorender). Membrane embedded transcriptional regulator, CadC, activates transcription of *cadBA* under high lysine concentration and low pH conditions. LysP, a constitutively expressed lysine importer, inhibits CadC under low lysine concentrations.

Results

AR4 is upregulated during intracellular infection.

The acute infection cycle of UPEC encompasses a transient intracellular stage in urothelial cells, where the pathogen replicates in the host cell cytoplasm by consuming oxygen.[19] To expand intracellularly, cells must first escape the phagolysosome, where they would encounter a change in pH **(Figure 14A)**. To test whether any of the AR systems are induced once UPEC enters the bladder cell, RNA was isolated from intracellular bacteria following invasion of the urothelial cell line 5637 (ATCC HTB-9) by the prototypic cystitis isolate UTI89.[149] For these studies, urothelial cells were seeded in 24 well plates and infected with UTI89 at an MOI of 10 and incubated for 2 hours at 37°C with 5% CO_2. After 2 hours of incubation with the bacteria, wells were treated with gentamicin for 2 hours to kill extracellular bacteria and washed to remove the antibiotic. RNA was extracted from the treated bladder cells and converted to cDNA following DNAse treatment. Following reverse transcription, transcript abundance of key components of each AR systems was determined using probe-based qPCR. Specifically, *gadA, gadC* (AR2)*, adiA (*AR3)*, cadA* (AR4)*, speF* (AR5)*, sdaA* and *sdaC* (AR6) abundance were quantified, using the housekeeping gene *gyrB* as a normalizer, as we previously described.[19,150] Transcript abundance intracellularly was compared to the transcript abundance of the same gene in bacterial cDNA prepared from the bacterial input. These analyses revealed that UPEC *cadA* transcript abundance is increased in the host intracellular environment, compared to the inoculum **(Figure 15**, Log_2 fold change = 3.774**)**. Conversely, there was a decrease in *gadC* transcript abundance intracellularly **(Figure 15**, Log_2 fold change = -4.37**)**. The transcripts of the other AR system components remained unchanged, although the *speF* transcript (AR5) appeared to have a nominal, yet not-statistically significant increase **(Figure 15)**.

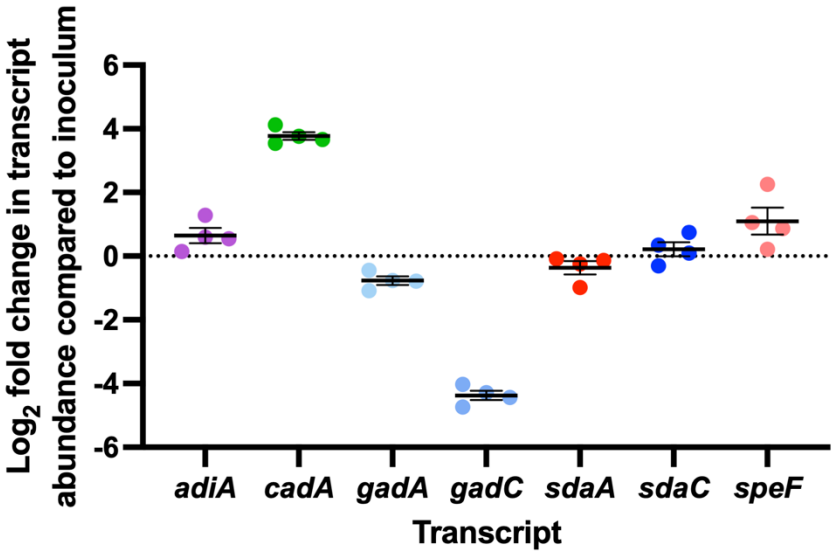

Figure 15. Transcript analysis of acid resistance genes during intracellular bladder cell infection

HTB9 cells were infected with WT UTI89 for 2 hours. Following infection, unattached extracellular bacteria were washed away, and cells were treated with gentamicin to kill extracellular bacteria for 2 hours. RNA was extracted from infected HTB9 cells. qPCR analysis of *adiA* (purple), *cadA* (green), *gadA* (pale blue), *gadC* (light blue), *sdaA* (red), *sdaC* (royal blue), and *speF* (coral) transcript abundance in UTI89 after infection relative to transcript abundance before infection. The relative fold change was determined by the $\Delta\Delta C_T$ method where transcript abundances were normalized to *gyrB* housekeeping gene transcripts. *cadA* was highly upregulated (Log_2 fold change = 3.77) during intracellular colonization compared to before infection. Graph shows analysis of 4 biological replicates.

AR4 deletion results in decreased bladder colonization in a murine model of infection

Our *in vitro* data suggest that the AR4 mechanism is induced during intracellular replication of UPEC, a stage which is critical for the establishment of acute infection. We therefore asked whether mutants in AR4, or AR5 would have defects in infection. To further address the role of AR4 and the other AR systems in acute bladder infection, we leveraged a series of existing[151] and newly created **(Table 3)** AR deletion mutants. Before evaluating the effects of each deletion mutant to adherence and invasion of bladder cells, we determined the effects of each deletion on bacterial

growth in laboratory media (lysogeny broth (LB) **Figure 16A**), human urine **(Figure 16B)**, or the tissue culture medium used in our studies (RPMI, **Figure 16C**). Growth, measured by OD_{600}, in LB is not affected for any of the AR mutants **(Figure 16A)**, indicating that deletion of only one or two AR systems is not sufficient to sensitize *E. coli* to changes in pH during *in vitro* growth in rich media. Similarly, during growth in human urine **(Figure 16B)** or RPMI **(Figure 16C)**, none of the strains display significant difference in growth compared to the wild-type parent strain, although most strains exhibited a slower growth rate in urine **(Figure 17).** Together, these data indicate that loss of one or two AR systems does not impair growth in the *in vitro* tested conditions.

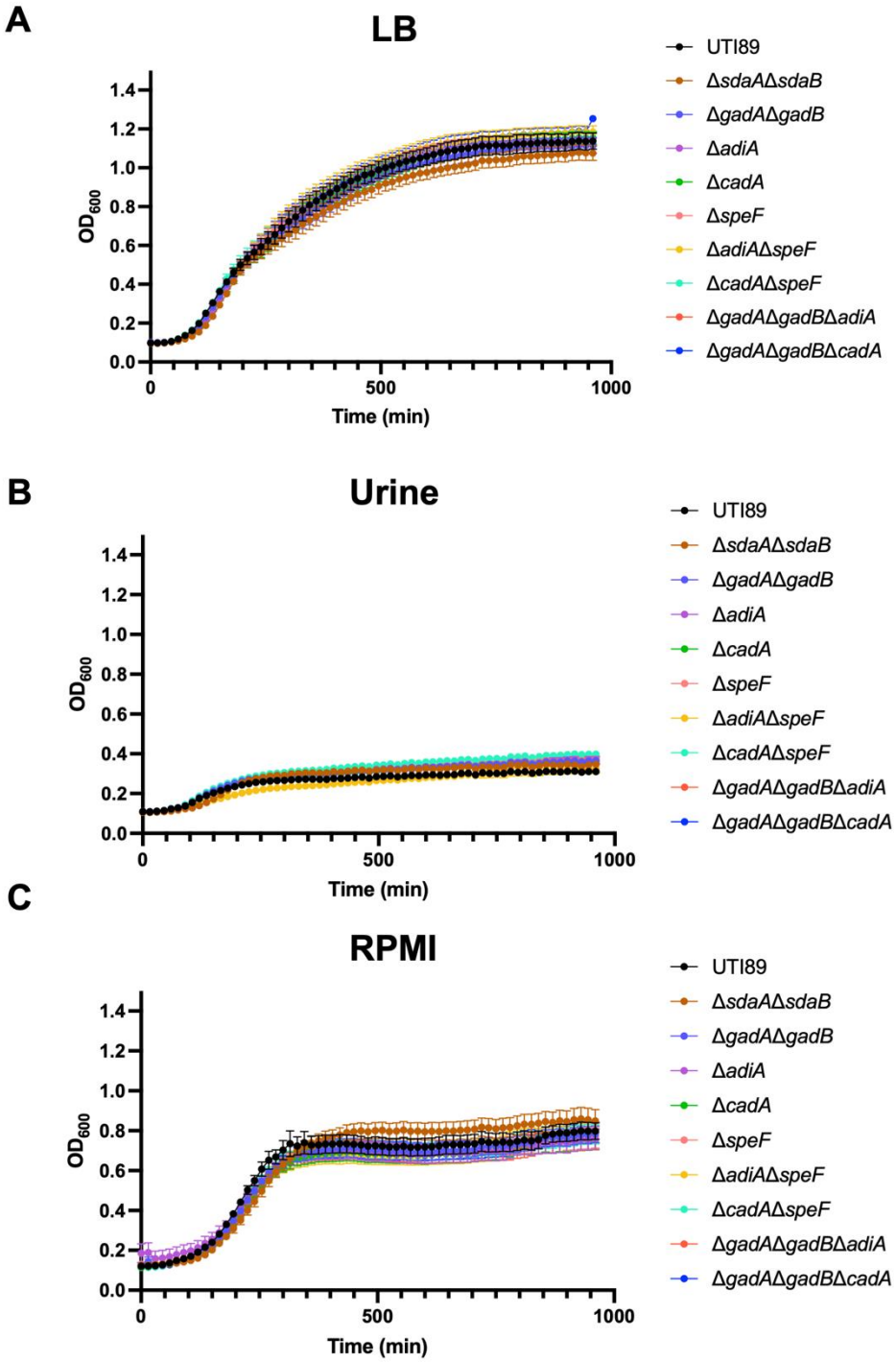

Figure 16. Growth curves of UTI89 Acid Resistance Mechanism Mutants
UTI89 and the indicated AR mutants were grown in LB (A), pooled human urine (B), and RPMI (C) in 96 well plates for 16 hours. OD_{600} was measured using the plate reader every 15 minutes. Graphs depict 2 biological replicates.

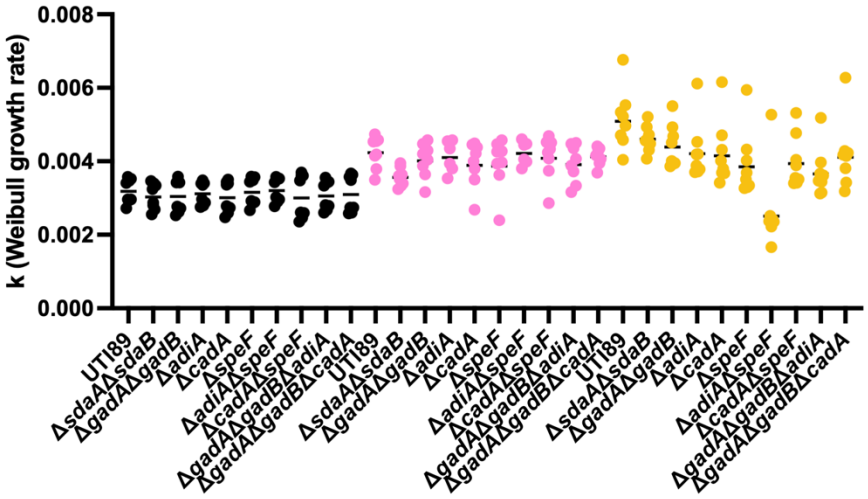

Figure 17. Growth rates of AR mutants
Growth rates for cells grown in LB (black), RPMI (pink), or pooled human urine (yellow) were calculated using the Weibull growth curve formula.

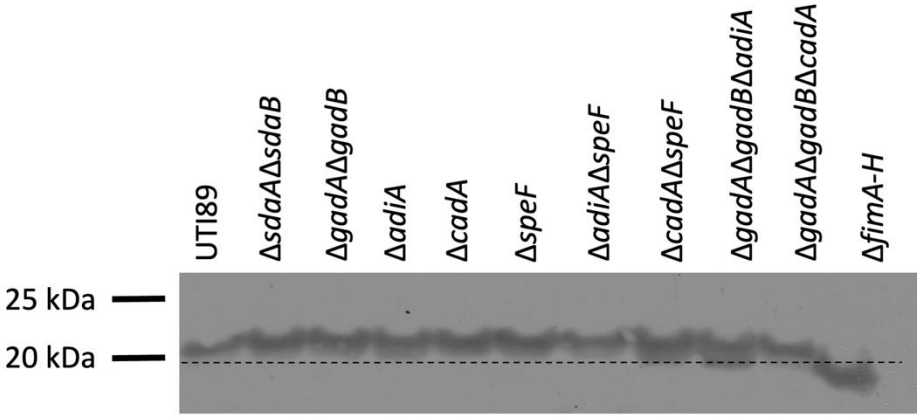

Figure 18. Type 1 pilus production is not altered in AR mutants
Cell pellets were normalized to an OD_{600} = 1 and denatured in Laemmli sample buffer containing beta-mercaptoethanol. Samples were acidified with 1N HCl at room temperature for 15 minutes then neutralized with NaOH. The samples were then boiled for 10 minutes at 100ºC. Samples were run on 14% SDS-PAGE gels and transferred to nitrocellulose membranes. After transfer, membranes were blocked overnight at 4ºC. The membrane was then washed followed by incubation with the primary anti-FimA antibody for 1 hour at room temperature. The membrane was then washed again followed by incubation with the horseradish peroxidase conjugated goat anti-rabbit secondary antibody for 1 hour at room temperature. The membrane was then treated with SuperSignal West Pico chemiluminescent substrate and visualized on X-ray film.

We then assessed the ability of the AR mutants to produce type 1 pili. UPEC must adhere to the urothelium during acute infection[115], a process that is essential to prevent voiding during urination.[115,152] Binding primarily depends on FimH adhesin interactions with uroplakin, which induces a TLR4-mediated uptake of bacteria by the urothelial cells.[14,153] FimH is the tip adhesin of type 1 pili encoded by the *fim* operon.[154] To determine if any of the AR deletions influences production of type 1 pili, we analyzed the abundance of the primary pilin subunit FimA in each of the AR mutants by immunoblot analysis. No significant differences were observed in FimA abundance in any of the strains tested **(Figure 18)**, suggesting that these specific AR deletions do not impair expression of type 1 pili under the conditions tested.

Following the *in vitro* analyses, we assessed the ability of strains lacking AR4 (Δ*cadA*), AR5 (Δ*speF*), or both (Δ*cadA* Δ*speF*) to cause acute infection. For this work, 7-8 week-old female C3H/HeN mice were transurethrally inoculated with 10^7 CFU of WT UTI89 or each of the isogenic mutants. After 24 hours, mice were sacrificed and the bladders, kidneys, and vaginas were harvested, homogenized, and plated for CFUs. Compared to the WT-infected mice, the mice infected with the AR mutants had significantly lower (1-log) bladder bacterial titers **(Figure 19A)**. Similarly, the mutants had decreased titers in the kidney **(Figure 20A)**. By contrast, no differences were observed in vaginal titers among strains **(Figure 20B)**, suggesting that deletion of AR4 and AR5 impairs establishment of acute infection, but not necessarily transition of the UPEC to the vaginal space.

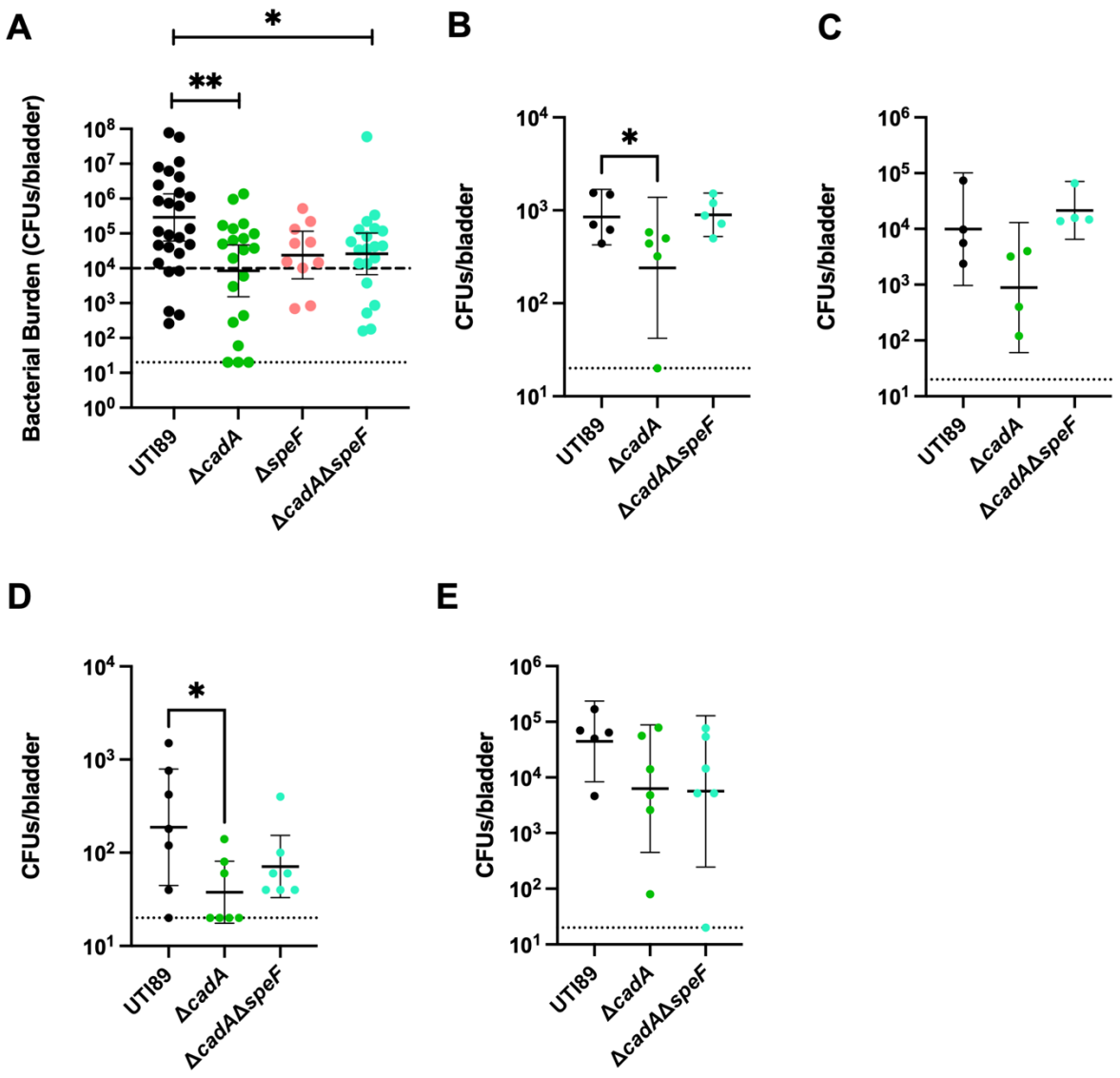

Figure 19. AR4 mutants have bladder colonization defect

A) Graph depicts bacterial burden in the bladder 24 hours post infection. Δ*cadA* and Δ*cadA*Δ*speF* are significantly decreased compared to WT (*p=0.028, **p=0.007, Mann-Whitney). B) Total bacterial burden in mouse bladder 1 hour post infection. Δ*cadAq* is significantly decreased compared to WT (*p=0.0397 , Mann-Whitney). C) Total bacterial burden in mouse bladders 6 hours post infection. There is no significant difference between WT and the AR mutants (Mann-Whitney). D) Intracellular bacterial burden in mouse bladder 1 hour post infection. Δ*cadA* is significantly decreased compared to WT (*p=0.0478 , Mann-Whitney). E) Intracellular bacterial burden in mouse bladder 6 hours post infection. There is no significant difference between WT and the AR mutants (Mann-Whitney).

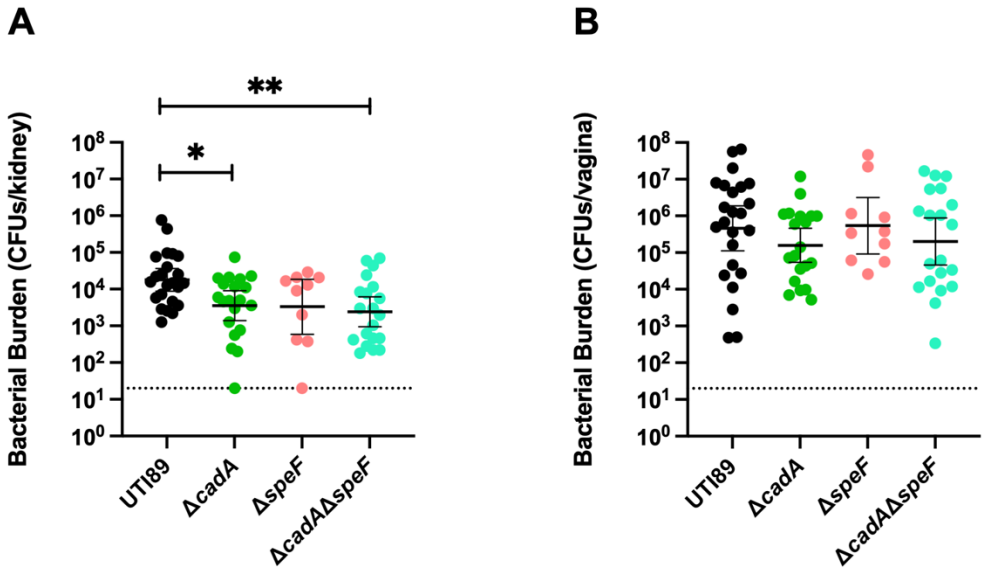

Figure 20. AR mutants have a kidney colonization defect
Mice were infected with UTI89, Δ*cadA,* Δ*speF*, or Δ*cadA*Δ*speF* for 24 hours. Kidneys and vaginas were harvested, homogenized, and plated for CFU enumeration. A) Δ*cadA* and Δ*cadA*Δ*speF* bacterial burdens are significantly reduced in the kidney compared to WT (*p=0.0146, **p=0.0018, Mann-Whitney). B) no significant difference in bacterial burden in the vagina between WT and the AR mutants (Mann-Whitney).

A decrease in acute infection titers may stem from a disadvantage in the bladder lumen, or in the bladder interior. In the lumen, bacteria encounter acid stress if phagocytosed by PMNs that infiltrate the site of infection[155], while inside the bladder cell, UPEC would encounter acidic conditions in the lysosome.[146] To begin to sort where the defect for each AR mutant may arise, we repeated the transurethral inoculations, but sacrificed the mice at 1 hour and 6 hours post infection. These time points were selected because the 1 hour timepoint coincides with the time of initial adherence and internalization, while the 6 hour timepoint coincides with intracellular replication into the cytosolic space.[19,156] For these studies we only used Δ*cadA* and the Δ*cadA*Δ*speF* double mutant since all mutants displayed a similar defect at 24 hours post infection, and to minimize the numbers of animals used. To determine intracellular titers for each time point, half the cohort bladders for each strain were randomly selected upon sacrifice, bisected, and treated with

gentamicin, followed by washes and organ homogenization for intracellular CFUs. The bladders of the remaining mice were homogenized without gentamicin treatment to quantify the total numbers of cell-associated bacteria (intracellular and extracellular). In parallel, urines were collected from the mice prior to sacrifice for PMN scoring. Our data revealed that by 1 hour post infection the Δ*cadA* mutant exhibited infection a significant decrease in both total and intracellular colonization, compared to WT UTI89 **(Figure 19B and D)**. At 6 hours, both mutants had lower total and intracellular bacterial burdens, compared to WT, although these decreases were not statistically significant **(Figures 19C and E)**. These data suggest that AR4 and AR5 are playing a role in UPEC's ability to withstand acidic stress as it establishes acute infection.

Given that we saw lower total and intracellular CFUs in the mutants during the early infection stages, we assessed the PMN response to each of the strains we used, in vivo and in vitro. As mentioned above, urine was collected from each infected mouse at 1 and 6 hours post infection (prior to sacrifice) and urine smears were prepared for PMN scoring. These results revealed similar PMN scores at 1 hour post infection **(Figure 21A).** However, we observed lower PMN scores for the mutant strains for the 6 hour samples **(Figure 21B)**, consistent with lower bacterial titers. Because macrophages are also part of the innate immune response to acute UTI[157], we investigated the ability of the AR4 and AR5 mutants to survive inside macrophages *in vitro*. For these assays, RAW246 macrophages were infected with UTI89, Δ*cadA*, Δ*speF*, and Δ*cadA*Δ*speF* at an MOI of 10 and incubated for 30 minutes. After 30 minutes, one set of wells was lysed to determine internalized bacterial CFUs. Another set of wells was treated with gentamycin for 1 hour. After 1 hour, the cells were lysed and the surviving bacterial CFUs were enumerated. These experiments showed that there was no difference in the AR4 or AR5 mutants' ability to survive macrophage killing compared to WT UTI89 **(Figure 21C)**. Collectively, these data point towards AR4 and

AR5 being important for intracellular expansion and not for survival inside white blood cells recruited to the bladder lumen during infection.

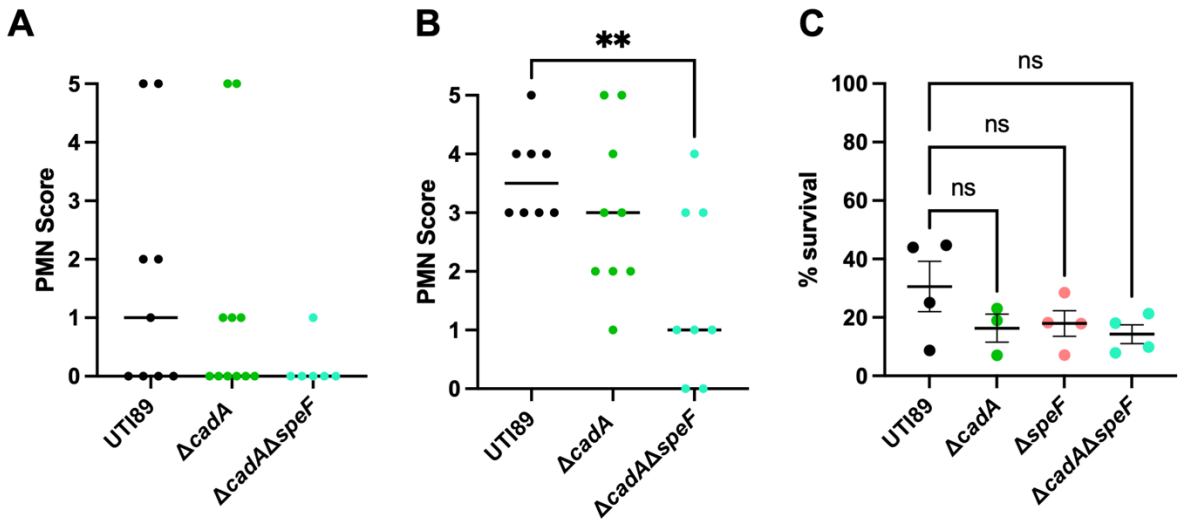

Figure 21. Immune response to AR mutants is not significantly altered compared to WT
Urine was collected from infected mice at A) 1 hour or B) 6 hours post infection. 20 ul of urine was smeared onto a glass slide and fixed and stained with Quick Diff. PMNs were counted in 10 frames of view per slide. PMN score was assigned as previously described.[158] A) PMN scores trend lower in cadA and cadAspeF infected mice than WT infected mice at 1 hour post infection (ns, One-Way ANOVA with Dunnett's multiple comparisons test). B) PMN score was significantly lower in cadAspeF infected mice compared to WT infected mice at 6 hours post infection (**p=0.0090, One-Way ANOVA with Dunnett's multiple comparisons test). C) *in vitro* macrophage survival after 90 minutes was not significantly different between WT and the AR mutants (One-Way ANOVA with Dunnett's multiple comparisons test).

Deletion of cadA (AR4) *and speF* (AR5) *impairs UPEC intracellular expansion*

To elucidate the roles of AR4 and AR5 inside the urothelial cells, we turned to the human urothelial tissue culture model, using the 5637 (ATCC HTB-9) bladder cell line. In this assay, approximately 1% of cells typically become internalized to seed intracellular infection.[159] Of these internalized UPEC cells, the majority becomes expelled via a non-lytic mechanism[14,160], leaving a small portion of cells that drive intracellular expansion. To determine if AR mutants have defects in at any stage during bladder infection, urothelial cells were infected with wild-type (WT) UTI89, or each of the isogenic AR mutants as described for the transcriptional profiles above, and in previous studies.[143,159] Following infection for 2 hours and a 2 hour treatment with gentamicin to kill the extracellular cohort[159], we enumerated total, adherent and intracellular bacterial titers. Our analyses revealed that, although total and adherent titers did not differ among strains **(Figure 22A and B)**, Δ*cadA*Δ*speF* intracellular titers were significantly lower, compared to the WT parent **(Figure 23A)**. Complementation of Δ*cadA*Δ*speF* with a plasmid expressing *cadA* restored the WT phenotype **(Figure 23B)**, indicating that, AR4 complementation is sufficient to restore wild-type levels of replication intracellularly.

UPEC enter the bladder epithelial cell in RAB27b$^+$ fusiform vesicles[14,160], leading to activation of Toll-like receptor 4 (TLR4), an increase in intracellular cyclic AMP (cAMP) levels and subsequent expulsion of UPEC-containing RAB27b$^+$ vesicles.[160] Intracellular UPEC that escape the RAB27b$^+$ vacuole are targeted by autophagy and delivered into the lysosomes that have a lower pH. [161] UPEC neutralize these lysosomes via a yet uncharacterized mechanism.[146]

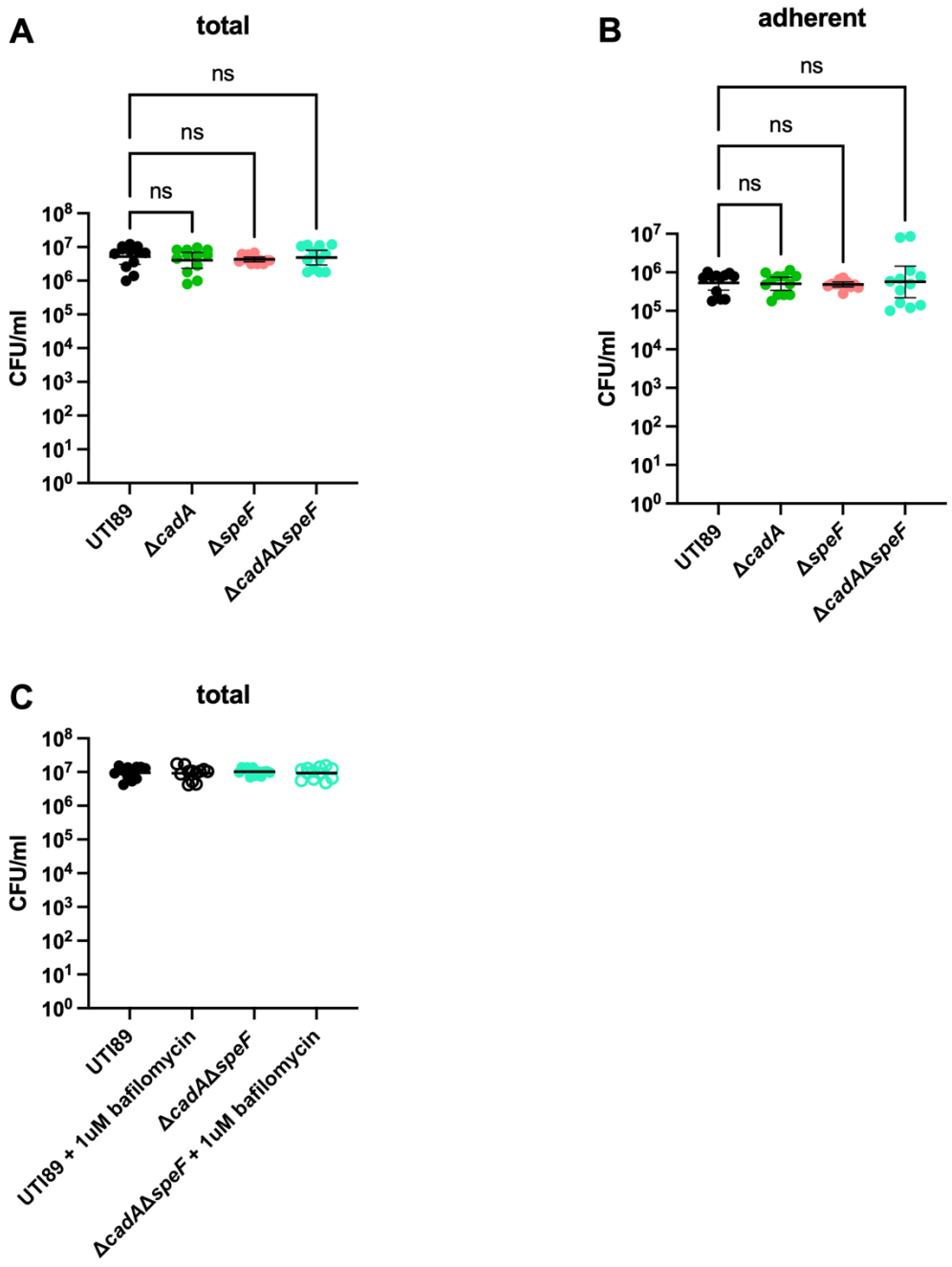

Figure 22. AR mutants do not have a defect extracellularly during bladder cell culture infection

HTB9 cells were infected with UTI89 (black), Δ*cadA* (green), Δ*speF* (coral), or Δ*cadA*Δ*speF* (turquoise) at an MOI of 7.5. A) No significant difference in total bacterial CFUs between WT and AR mutant infected cells (One-Way ANOVA with Dunnett's multiple comparisons test). B) No significant difference in adherent bacterial CFUs between WT and AR mutant infected cells (One-Way ANOVA with Dunnett's multiple comparisons test). C) No significant difference in total bacterial CFUs in bladder cells and bladder cells treated with bafilomycin between WT and AR mutant infected cells.

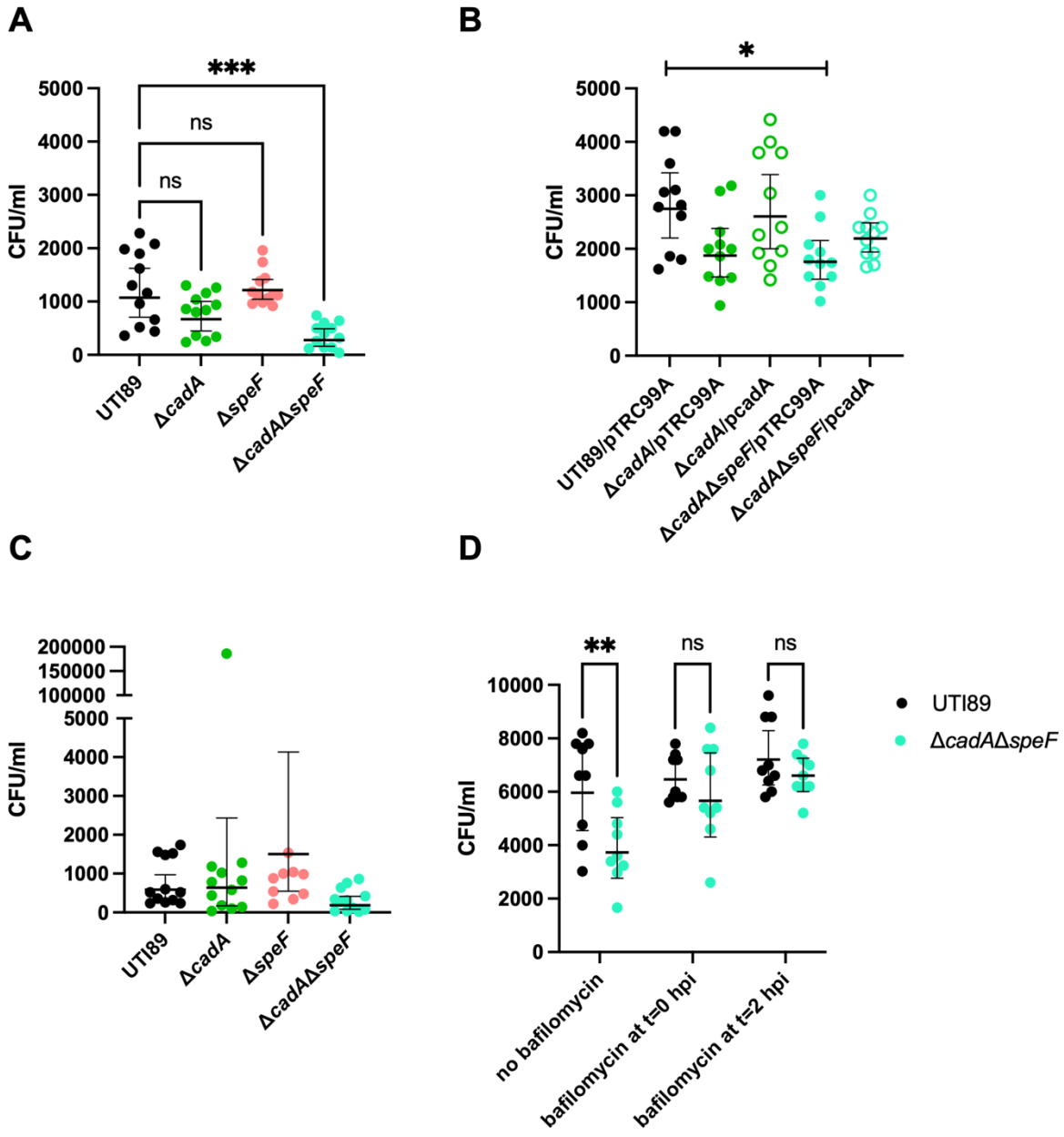

Figure 23. Δ*cadA*Δ*speF* intracellular survival defect due to inability to survive in acidic vacuole

HTB9 cells were infected with UTI89 (black), Δ*cadA* (green), Δ*speF* (coral), or Δ*cadA*Δ*speF* (turquoise) at an MOI of 7.5. A) Δ*cadA*Δ*speF* is significantly decreased intracellularly compared to WT (***p=0.0003, Kruskal Wallis with Dunn's multiple comparisons test). B) complementation of *cadA* in the Δ*cadA*Δ*speF* strain rescues intracellular survival (*p=0.0165, Kruskal Wallis with Dunn's multiple comparisons test). C) cytoplasmic bacterial burdens were not significantly different in AR mutants compared to WT (Kruskal Wallis with Dunn's multiple comparisons test). D) addition of bafilomycin rescues Δ*cadA*Δ*speF* intracellular survival (**p=0.0036, two-way ANOVA with Sidak's multiple comparisons test).

To determine if the intracellular defect observed in the bladder cells is due to increased susceptibility to the low pH of the lysosome, we performed modified adherence and invasion assays using chloroquine treatment. Chloroquine is a lysosomotropic drug that accumulates in the acidic endosomes and not in the cytosol.[162] Chloroquine has been shown to be bactericidal by inhibiting DNA and RNA synthesis.[163] Previous work successfully used chloroquine to evaluate cytoplasmic versus vacuolar UPEC.[164-166] This experiment revealed that while a difference was observed with gentamicin treatment **(Figure 23A)**, chloroquine treatment revealed no difference in cytoplasmic CFUs **(Figure 23C).** Combined, these data suggest that the intracellular titer defect in AR4 and AR5 mutants likely stems due to lower numbers in the lysosomal vacuole.

To assess whether deletion of AR4 and AR5 impairs UPEC survival in the lysosome, we performed modified adherence and invasion assays using bafilomycin treatment. Bafilomycin is an inhibitor of phagosome-lysosome fusion by targeting the V-ATPase to inhibit lysosomal acidification.[167] Addition of bafilomycin at the time of infection did not affect total bacterial burden **(Figure 22C)**. We observed that addition of bafilomycin at the time of infection or at the time of gentamicin treatment restored intracellular survival of the Δ*cadA*Δ*speF* mutant to WT levels (**Figure 23D**). Together, these data demonstrate that AR4 and AR5 mediate UPEC survival in the host cell lysosome.

We next wanted to determine if the reason we observe reduced survival of AR4 mutants in bladder cells but not macrophages was due to availability of lysine inside the cells. To test this, we quantified free intracellular lysine in RAW246 macrophages and HTB9 bladder cells by LC-MS/MS. Our results showed that lysine concentration was significantly higher in RAW246 macrophages compared to HTB9 bladder cells **(Figure 24A)**. Thus, free lysine is less available for bacteria to utilize inside bladder cells. We next wanted to determine if we could detect differences

in free lysine concentration in bladder cells infected with WT bacteria versus our AR mutants. We observed a nominal increase in lysine concentration in bladder cells infected with Δ*cadA* **(Figure 24B)**.

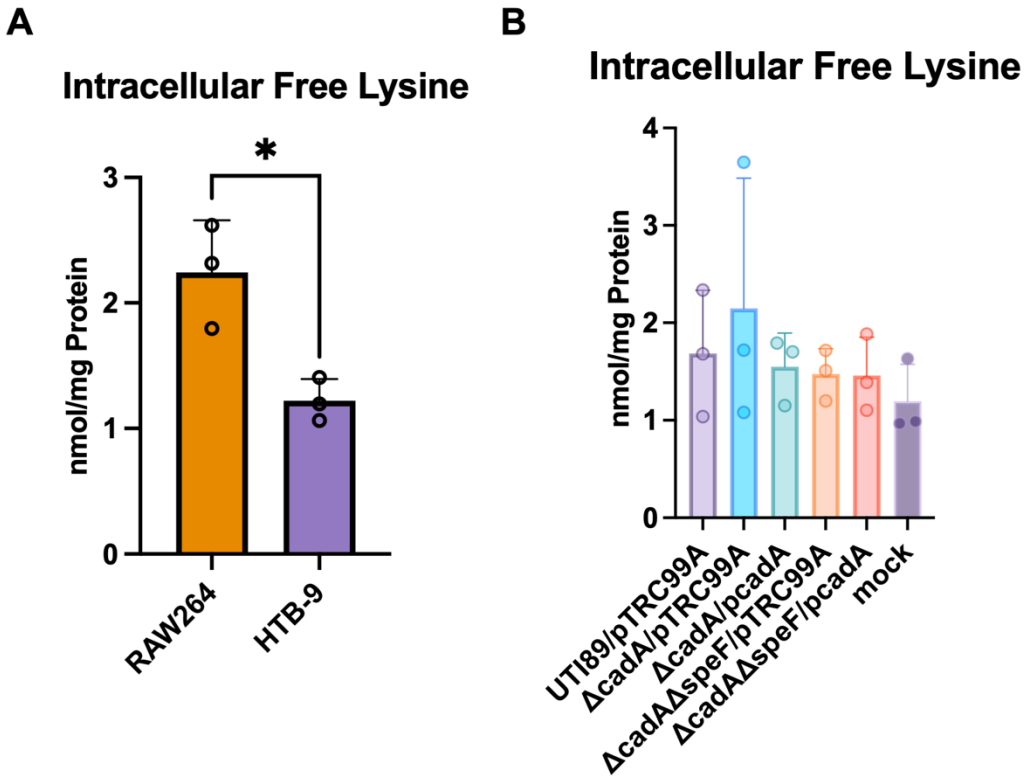

Figure 24. Free intracellular lysine concentrations are not affected during infection
A) Free intracellular lysine was quantified by LC-MS/MS in RAW246 macrophages (orange) and HTB9 bladder cells (purple). Macrophages had a significantly higher free intracellular lysine concentration (n=3 biological replicatesm *p=0.0363, Welch's t-test). B) HTB9 bladder cells were infected with the indicated strain of UTI89 or mock infected with PBS as described in the methods. After 2 hours of infection followed by 2 hours of treatment with gentamycin, cells were harvested for free intracellular lysine quantification. Δ*cadA* infected bladder cells had nominally higher intracellular lysine (blue bar). Complementation of *cadA* on a plasmid in the Δ*cadA* strain resulted in reduced intracellular lysine concentrations (green bar) (n=3 biological replicates, One-Way ANOVA with Tukey multiple comparisons test).

Discussion

In this study, we investigated the role of acid resistance (AR) mechanisms in UPEC pathogenesis, as no study has evaluated the role of each AR system in UPEC. We identify the AR4 mechanism as the primary AR mechanism UPEC relies on, at the early stages of intracellular infection within bladder epithelial cells. We show that lysine decarboxylation protects UPEC from acidic conditions within the bladder epithelial cell vacuoles **(Figure 23)**. Thus, lysine decarboxylation contributes to the early colonization of the bladder by protecting UPEC from damaging acidic pH conditions. Our data using a combination of chloroquine and bafilomycin treatments suggest that UPEC needs AR4 – and possibly AR5 when inside the lysosomal compartment, where pH is low. AR4 gene expression is dependent upon both a low pH and the presence of lysine in the environment; here we show that AR4 is the most highly induced AR system when UPEC is inside the host cell **(Figure 15)**, and we demonstrate that sufficient levels of free lysine are present in the urothelial cell to support AR4 activation **(Figure 24)**. Defects in lysine decarboxylation have previously been shown to impair UPEC survival under nitrosative stress conditions.[101,168] However, a mechanism for cadaverine-mediated protection to nitrosative stress was not determined, and no experiments to distinguish intracellular versus extracellular defects were performed.[101,168] Our study builds upon the prior findings, demonstrating that AR4 deletion impacts intracellular bacterial burden, by impairing UPEC survival in the acidic vacuole of bladder epithelial cells. Our data indicate that lysine decarboxylation is critical for surviving acidic pH inside of host cells. It is possible that neutralization of the lysosomal compartment via the decarboxylation of lysine allows for UPEC survival, affording the pathogen time to escape into the cytoplasm. No studies have previously elucidated how UPEC manages to neutralize the host cell vacuole. We propose that UPEC achieves this via the AR4 mechanism.

Cadaverine, like other polyamines, has been shown to influence many cellular processes. Due to its polycationic properties, cadaverine can bind to and regulate DNA, RNA, protein, and phospholipid synthesis.[169] Due to their pleiotropic roles, polyamines have been characterized in many contrasting physiologic phenomena. In some cases, polyamines have also been shown to improve gastrointestinal barrier integrity to protect host cells from infection.[169] In other cases, bacterially derived polyamines increased the abundance of anti-inflammatory macrophages in the gut and prevented the formation of the NLRP3 inflammasome, leading to improved bacterial colonization of the host.[170,171] Our results indicate that UPEC derived cadaverine may be altering ability of bladder cells to clear bacteria.

Other organisms have been shown to rely on lysine decarboxylation, including *Salmonella enterica*. However, in contrast with what we observe for UPEC, studies in Salmonella indicate that lysine decarboxylation genes are downregulated in the *Salmonella* containing vacuole (SCV). It was shown that OmpR inhibits lysine decarboxylation mediated pH neutralization in *Salmonella*.[172] Neutralization of the pH of the SCV does not allow for secretion of the *Salmonella* pathogenicity island (SPI)-2 effector proteins that are essential for bacterial replication in the vacuole.[173] As UPEC does not utilize a T3SS for pathogenesis, lysine decarboxylation is not inhibitory to its pathogenicity. In fact, we demonstrate that lysine decarboxylation by UPEC is critical for bladder colonization.

It is important to note that there are differences in survival phenotypes in our single lysine decarboxylase mutant and our lysine and ornithine decarboxylase mutant in our murine model versus our *in vitro* bladder epithelial cell culture model. Deletion of just *cadA* was sufficient to lead to decreased bacterial burden in the mouse model **(Figure 19)**, while deletion of both *cadA* and *speF* was necessary to see a defect in cell culture experiments **(Figure 23A)**. We expect this

can be explained by the robust innate response that occurs in the mouse compared to the lack of immune cells in our bladder cell culture model.

We showed that in the bladder, AR4 mutants had a significant colonization defect **(Figure 19A)**. Surprisingly, these mutants did not have a defect in vaginal colonization **(Figure 20B)**. One of the potential explanations for this is that our established mouse model, conventionally reared C3H/HeN mice, are devoid of *Lactobacilli* and the murine vaginal pH is near neutral, unlike the human vaginal pH.[145,174] So, while our mouse model can be used to investigate vaginal colonization after transurethral bladder inoculation, the pH in the mouse vagina may be higher than what is observed in humans. Other labs have addressed this concern with the use of mice with humanized vaginal microbiomes.[175,176] Future experiments may utilize mice with humanized vaginal microbiomes to determine if a more acidic environment inhibits growth of AR mutant UPEC more that WT. Alternately, it is possible that AR4 is not used to combat the acidic environment in the vagina. Future studies will address the role of AR2, AR3, AR5 and AR6 in vaginal colonization.

In this work we focused our attention to investigating the role of acid resistance mechanisms in early UPEC bladder colonization. We found that the lysine decarboxylation is important for intracellular bacterial survival. We speculate that the other acid resistance mechanisms are not expendable but are needed at different times during infection. For example, previous work by Jeff Purkerson has shown that the AR mechanisms that produce polyamines are important for UPEC colonization of the kidneys in a murine model of kidney acidosis.[102]

We also hypothesize that deletion of one or two acid resistance mechanisms in one strain may not be enough to uncover the necessity of AR systems for the establishment of infection. Future studies are planned with strains deficient in all but one AR mechanism, so no other system

is able to compensate. Such experiments should provide more insight into how the AR systems are utilized during UTI.

Materials and Methods

Bacterial Strains and Growth Conditions

All studies were performed in the well characterized UPEC cystitis isolate UTI89 and derived isogenic deletion mutants. UTI89 is of the sequence type ST95 and is serotyped as O18:K1:H7.[149] Strains were propagated in unbuffered lysogeny broth (LB) (Fisher Scientific), at pH 7.4. Inoculated strains were grown overnight at 37ºC with shaking unless otherwise noted. Gene deletions were created using the λ-red recombinase system.[120] A complete list of strains, primers, and plasmids used for in this study can be found in Tables 3 and 4.

For growth analyses in pooled urine, urine was collected from healthy human volunteers in accordance with approved protocols (IRB #180973). A healthy volunteer is defined as an individual who is urologically asymptomatic, not menstruating, and who has not taken antibiotics in the last 90 days. An equal volume of male and female urine was pooled from multiple volunteers then filtered through a 0.22 um filter before use.

Western Blot

Strains were grown in LB at 37ºC with shaking for 4 hours then subcultures 1:1000 in 10 ml of LB and grown statically at 37ºC for 24 hours. The static cultures were subcultured 1:1000 in 10 ml of LB and grown statically at 37ºC for an additional 24 hours. Cultures were then resuspended in PBS to an OD_{600} = 1.0. The normalized cell suspension was then pelleted and resuspended in 100 ul of Laemmli sample buffer containing beta-mercaptoethanol. Samples were acidified with 1N HCl at room temperature for 15 minutes then neutralized with NaOH. The samples were then boiled for 10 minutes at 100ºC. Samples were run on 14% SDS-PAGE gels and

transferred to nitrocellulose membranes with the Bio-Rad Trans-Blot Turbo transfer system. After transfer, membranes were blocked overnight at 4ºC in 5% milk and 1% BSA in TBST. The membrane was then washed followed by incubation with the primary anti-FimA antibody diluted 1:5000 in TBST+5% milk for 1 hour at room temperature. The membrane was then washed again followed by incubation with the horseradish peroxidase conjugated goat anti-rabbit secondary antibody for 1 hour at room temperature. The membrane was then treated with SuperSignal West Pico chemiluminescent substrate and visualized on X-ray film.

Mammalian Cell Lines

Cell culture infections were performed using 5637 human transitional bladder epithelial cells (ATCC HTB-9) originally derived from a 68-year old white male with Grade II bladder carcinoma. 5637 cells were propagated and infected in RPMI 1640 (Gibco) supplemented with 10% fetal bovine serum (Gibco).

Macrophage survival assays were performed using RAW246.7 murine macrophage cell line (ATCC TIB-71) derived from a tumor in a male mouse induced with the Abelson murine leukemia virus.

Adherence and invasion assay

HTB-9 bladder epithelial cells were seeded at $1.0x10^5$ cells/well in 24 well plates. Once cells reach at least 80% confluence, they were infected with UTI89 or the UTI89 acid resistance mutants at an MOI of 7.5. The plates were then centrifuged at 600xg for 5 minutes to facilitate and synchronize attachment. The cells were then incubated for 2 hours at 37ºC in 5% CO_2. To quantify total CFUs, monolayers were treated with 0.1% Triton X-100 and serially diluted to enumerate

CFUs/ml. To determine adherent CFUs, monolayers were washed with PBS three times to remove extracellular bacteria, lysed with 0.1% Triton X-100 and serially diluted. To determine intracellular CFUs, monolayers were washed with PBS three times then treated with PBS containing 100 ug/ml gentamycin to kill extracellular bacteria. After incubation in gentamycin for 2 hours, the monolayers were washed three times in PBS then lysed with 0.1% Triton X-100 and serially diluted to enumerate CFUs/ml.

Macrophage survival assay

RAW246.7 macrophage cells were seeded at $1.0x10^5$ cells/well in 24 well plates. Once cells reach at least 80% confluence, they were infected with UTI89 or the UTI89 acid resistance mutants at an MOI of 5. The plates were then centrifuged at 600xg for 5 minutes to facilitate and synchronize attachment. The cells were then incubated for 30 minutes at 37ºC in 5% CO_2 to allow for internalization. Then, one set of wells/strain of bacteria was washed 3 times with PBS, lysed with 0.1% TritonX-100, serially diluted, and plated to enumerate CFUs of the internalized bacteria. A second set of wells/strain of bacteria were treated with 100 μg/ml of gentamycin for 60 minutes to kill any extracellular bacteria. The cells were then washed 3 times with PBS, lysed with 0.1% TritonX-100, serially diluted, and plated to enumerate CFUs of the surviving bacteria. Percent survival was calculated by dividing the CFUs of surviving bacteria by the CFUs of internalized bacteria.

Murine infections

Murine infections were performed as described previously.[177] Briefly, UTI89 and each mutant strain were inoculated into 5 mL of LB and grown shaking at 37C overnight. Next, the

overnight cultures were diluted 1:1000 in 10 mL of fresh LB and grown statically at 37ºC for 24 hours. These static cultures were then diluted 1:1000 in 10 mL of fresh LB and grown statically at 37C for another 24 hours. Next, each culture was normalized to 10^7 CFU in PBS. 6-7 week old C3H/HeN female mice (Envigo) were transurethrally inoculated with 50 ul of the normalized bacteria in PBS. Mice were sacrificed at 24 hours post infection. The bladders, kidneys, and vaginas were harvested and homogenized for CFU enumeration.

For chronic infections, bacteria were grown and mice were infected as stated above. On days 1, 3, 7, 14, 21, and 27 post infection urine was collected from each mouse and plated for CFUs. On day 28 post infection mice were sacrificed. The bladders, kidneys, and vaginas were harvested and homogenized for CFU enumeration.

All animal studies were approved by the Vanderbilt University Medical Center Institutional Animal Care and Use Committee (IACUC) (protocol number # M1800101-01) and carried out in accordance with all recommendations in the Guide for the Care and Use of Laboratory Animals of the National Institutes of Health and the IACUC.

Intracellular Free Lys Quantitation

Using a targeted metabolomics method to measure intracellular free lysine, 3×10^6 cells were seeded in T75 flasks. The next day, media was removed, flasks were washed twice with room temperature PBS and cells were scraped into PBS to harvest. The cells were then pelleted in 15 mL conical tubes, flash frozen in liquid N_2, and stored at -80°C until ready for metabolite extraction. 30 nmol of internal standard ($^{13}C_6$,$^{15}N_2$-Lysine, Thermo Fisher Scientific, Waltham, MA) was spiked into each sample. Metabolites were extracted by adding 2 mL of -80°C 80:20 MeOH:H_2O to the cell pellets, vortexed vigorously, and then placed in a -80°C freezer to extract

for 15 minutes. After 15 minutes, samples were pelleted by centrifugation at 3,500 x rpm for 10 minutes at 4°C. Supernatant containing extracted metabolites and internal standard was transferred to new 15 mL conical tubes and dried under N_2. Precipitated protein pellets were resolubilized and protein concentration was measured via BCA assay (Thermo Fisher Scientific, Waltham, MA). Samples were resuspended in 80 µL 3:2 mobile buffer A: mobile buffer B (see below). 18 µL of the sample was then chromatographed with a Shimadzu LC system equipped with a 100 x 2.1mm, 3.5µm particle diameter XBridge Amide column (Waters, Milford, MA). Mobile phase A: 20 mM NH_4OAc, 20 mM NH_4OH, 5% acetonitrile in H_2O, pH 9.45; mobile phase B: 100% acetonitrile. With a flow rate of 0.45 mL/min the following gradient was used: 2.0 min, 95% B; 3.0 min, 85% B; 5.0 min, 85% B; 6.0 min, 80% B; 8.0 min, 80% B; 9.0 min, 75% B; 10 min, 75% B; 11 min, 70% B; 12 min, 70% B; 13 min, 50% B; 15 min, 50% B; 16 min 0% B; 17.5 min, 0% B; 18 min, 95% B. The column was equilibrated for 3 minutes at 95% B between each sample. Scheduled MRM was conducted in negative mode with a detection window of 120 seconds using an AB SCIEX 6500 QTRAP with the analyte parameters below. Lysine was then quantified via LC-MS/MS using the $^{13}C_6$,$^{15}N_2$-Lysine internal standard and normalized to the protein in each respective sample's cell pellet. Outliers were removed using interquartile range.

Table 3. Lysine m/z LC-MS/MS

Species	Q1 (m/z)	Q3 (m/z)	RT (min)
Lysine	147	84	14
$^{13}C_6$,$^{15}N_2$-Lysine [Internal Standard]	155	90	14

Table 4: Strains and plasmids used in this study

***E. coli* strain**	**Relevant genotype**	**Plasmid**
UTI89	WT	
UTI89 Δ*sdaA*Δ*sdaB*	Δ*sdaA*Δ*sdaB*[151]	
UTI89 Δ*gadA*Δ*gadB*	Δ*gadA*Δ*gadB*[151]	
UTI89 Δ*adiA*	Δ*adiA*[151]	
UTI89 Δ*cadA*	Δ*cadA*[151]	
UTI89 Δ*speF*	Δ*speF*[151]	
UTI89 Δ*cadA*Δ*speF*	Δ*cadA*Δ*speF*	
UTI89 Δ*gadA*Δ*gadB*Δ*cadA*	Δ*gadA*Δ*gadB*Δ*cadA*	
UTI89/pTRC99A	WT	pTRC99A
UTI89 Δ*cadA*/pTRC99A	Δ*cadA*	pTRC99A
UTI89 Δ*cadA*/pTRC_cadA	Δ*cadA with cadA* complementation	pTRC99A
UTI89 Δ*cadA*Δ*speF*/pTRC99A	Δ*cadA*Δ*speF*	pTRC99A
UTI89 Δ*cadA*Δ*speF*/pTRC_cadA	Δ*cadA*Δ*speF* with *cadA* complementation	pTRC99A

Table 5. Primers used in this study

Primer name	Primer sequence (5'→3')	Primer function
sdaA_KO_f	GTTATTAGTTCGTTACTGGAAGTCCAG TCACCTTGTCAGGAGTATTATCGTGTA GGCTGGAGCTGCTTC	Deletion of *sdaA*
sdaA_KO_r	AAGCGGGAATAAATTCGCCCATCCGT TGCAGATGGGCGAATAAGAAGATCAT ATGAATATCCTCCTTAG	Deletion of *sdaA*
sdaA_KO_test_f	CATCTGGGTCGTTATCATCCT	Validation of *sdaA* deletion
sdaA_KO_test_r	GTAACGAGTGCGCAAATCG	Validation of *sdaA* deletion
sdaB_KO_f	CGCGCCGCTTTCGGGCGGCGCTTCCTC CGTTTTAACGCGATGTATTTCCTGTGT AGGCTGGAGCTGCTTC	Deletion of *sdaB*
sdaB_KO_r	GGATGAGAAATCGGGAAGAGGCCTCG CAAAAAGAGGCCTCTGGAGAGCGACA TATGAATATCCTCCTTAG	Deletion of *sdaB*
sdaB_KO_test_f	GTTCCTGATGCCGATGTAC	Validation of *sdaB* deletion
sdaB_KO_test_r	CCAGAACAGGCTATGGCT	Validation of *sdaB* deletion
sdaC_KO_f	GGCTGAACTGGCTAAAAGCTGAATTA TTTGCATTCCTCCAGGAGAAATAGGT GTAGGCTGGAGCTGCTTC	Deletion of *sdaC*
sdaC_KO_r	ACATCGCGTTAAAACGGAGGAAGCGC CGCCCGAAAGCGGCGCGAAAGGACC ATATGAATATCCTCCTTAG	Deletion of *sdaC*
sdaC_KO_test_f	CATCGCCGATAGACAGAT	Validation of *sdaC* deletion
sdaC_KO_test_r	GAACTCCACTTCATGCTGAC	Validation of *sdaC* deletion
gadB_KO_FOR	CAGGTGTGTTTAAAGCTGTTCTGCTGG GCAATACCCTGCAGTTTCGGGTGTGT AGGCTGGAGCTGCTTC	Deletion of *gadB*
gadB_KO_REV	CAAGTAACGGATTTAAGGTCGGAACT ACTCGATTCACGTTTTGGTGCGAACAT ATGAATATCCTCCTTAG	Deletion of *gadB*
gadB_KO_Test_FOR	GTGAACAGACTTTGGAAATTGTCCC	Validation of *gadB* deletion
gadB_KO_Test_REV	ACTTGCTTACTTTATCGATAAATCCTA	Validation of *gadB* deletion
gadA_KO_FOR	GTTTAAAGCTGTTCTGCTGGGCAATAC CCTGCAGTTTCGGGTGGTCGCTGGTGT AGGCTGGAGCTGCTTC	Deletion of *gadA*

gadA_KO_REV	AAATGGACCAGAAGCTGTTAACGGATTTCCGCTCAGAACTACTCGATTCACATATGAATATCCTCCTTAG	Deletion of *gadA*
gadA_KO_Test_FORC	CAATTAATAAGTAGCCGAATACCCACC	Validation of *gadA* deletion
gadA_KO_Test_REV	TGTAATACCTTGCTTCCATTGCG	Validation of *gadA* deletion
adiA_ko_f	ATGATGAAAGTATTAATTGTTGAAAGCGAGTTTCTCCATCAAGACACCTGGTGTAGGCTGGAGCTGCTTC	Deletion of *adiA*
adiA_ko_r	TTACGCTTTCACACACATAACGTGGTAAATACCGTCAATAATTTCTGTCCCTTCCATATGAATATCCTCCTTAG	Deletion of *adiA*
adiA_kotest_f	GAAGATACTTGCCCGCAAC	Validation of *adiA* deletion
adiA_kotest_r	CTCGCTAAAGCGAAGCGATAC	Validation of *adiA* deletion
cadA_ko_f	ATGACTATGAACGTTATTGCAATATTGAATCACATGGGGGTTTATTTTAAAGAAGGTGTAGGCTGGAGCTGCTTC	Deletion of *cadA*
cadA_ko_r	TTATTTTTTGCTTTCTTCTTTCAATACCTTAACGGTATAGCGGCCATCAGCATATGAATATCCTCCTTAG	Deletion of *cadA*
cadA_kotest_f	GTACCTTCATCGTCAGCCTG	Validation of *cadA* deletion
cadA_kotest_r	GTGTTCTCCTTATGAGC	Validation of *cadA* deletion
speF_ko_f	ATGACGAGTATAGCCAGTTACCGGGCTGGTCTGGGTTATTGCATCTGCGTGTAGGCTGGAGCTGCTTC	Deletion of *speF*
speF_ko_r	AATTTTTCCCCTTTCAACAGGGCGCTTTGCGCATCACGAGGCTTGATGACCATATGAATATCCTCCTTAG	Deletion of *speF*
speF_kotest_f	GGTGCTCATATACTGCTAAC	Validation of *speF* deletion
speF_kotest_r	GTTGACCATCGTCAGTATG	Validation of *speF* deletion

Chapter 4: BtsS-YpdB Cross interaction induces target gene expression in response to acidic pH

Adebisi Bamidele contributed to the work presented in this chapter

Introduction

As discussed in Chapter 1.5, two-component systems are the dominant signaling systems bacteria used to detect and respond to these different environments. TCSs are composed of a sensor histidine kinase (HK) that perceives a signal, autophosphorylates at a conserved histidine residue, and transfers the phosphate to a conserved aspartate residue on its cognate response regulator (RR). RRs typically function as transcription factors to alter gene expression in response to a stimulus. Molecular "infidelity" or cross-regulation can occur between the HK of one system and the RR of another. The net result of this non-cognate partner interaction is the ability to expand the range of responses a bacterium can have at a given environment. This chapter will focus on the cross regulation between the HK of the BtsSR system and the RR of the YpdAB system.

In K12 *E. coli* the sensor histidine kinase BtsS of the BtsSR (named after **B**renz**t**raubens**ä**ure, the name given to pyruvic acid when it was first synthesized)[129] two-component system senses changes in extracellular pyruvate and activates its cognate response regulator, BtsR. BtsR induces transcription of *btsT*, a gene that encodes a pyruvate importer **(Figure 25)**.[178] Previous studies had also implicated BtsS in serine sensing, but it was later demonstrated that this is indirect sensing of pyruvate.[129,179] Serine is imported in the cell by SdaC and converted to pyruvate via the action of serine deaminases, SdaA and SdaB. In agreement with these studies, deletion of serine deaminases, or the serine transporter, abolishes BtsS signaling in response to serine **(Chapter 2)**. *E. coli* contains a second pyruvate sensing system, YpdAB, in which YpdA (HK) senses changes in extracellular pyruvate and activates YpdB (RR) to induce

transcription of *yhjX* **(Figure 25)**. The gene *yhjX* encodes a protein of unknown function, but based on sequence homology, YhjX is classified as a Major Facilitator Superfamily (MFS) transporter.[122]

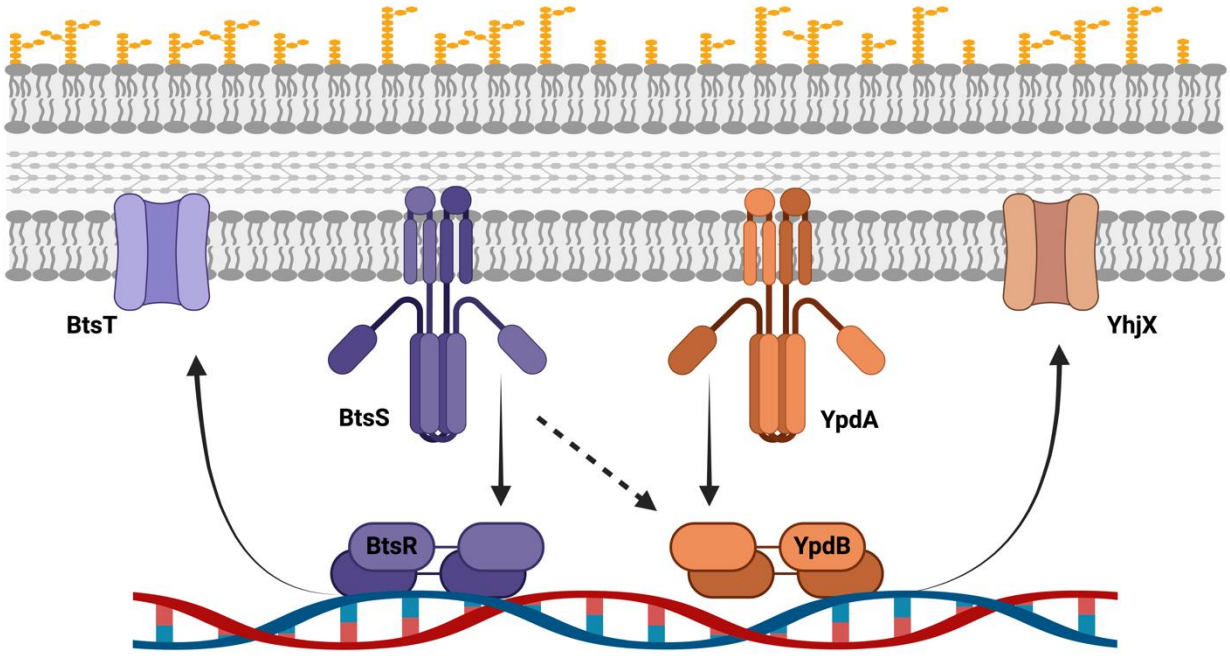

Figure 25. Model of BtsS/BtsR and YpdA/YpdB two-component systems
BtsS is a histidine kinase that senses pyruvate, autophosphorylates, and transfers the phosphate to BtsR. BtsR is a response regulator and transcription factor. Upon phosphorylation, BtsR binds to the *btsT* promoter and activates *btsT* transcription. BtsT is a pyruvate importer. YpdA is a histidine kinase that senses pyruvate, autophosphorylates, and transfers the phosphate to YpdB. Upon phosphorylation, YpdB binds to the *yhjX* promoter and activates *yhjX* transcription. YhjX is a predicted transport protein, but the substrate it transports has yet to be identified. We have shown that BtsS cross regulates YpdB to lead to activation of *yhjX* transcription.

In UPEC, the sensor histidine kinase BtsS, of the BtsSR two-component system, senses changes in extracellular pyruvate and in response interacts with the YpdB transcription factor from the YpdAB two-component system **(Figure 25)**. The net result of BtsS-YpdB cross-regulation is the induction of *yhjX*.[121] Deletion of the noncognate pair BtsS and YpdB ablates *yhjX* expression, while deletion of the other noncognate pair, BtsR and YpdA, results in elevated and sustained *yhjX* expression.[121]

In a transcriptomic profile in K12 *E. coli* performed by Kannan et al., it was determined that *yhjX* expression was significantly upregulated under acidic pH conditions.[125] In chapter 2, I describe how we discovered that *yhjX* expression was also induced by acidic pH conditions. In response to HCl, lactic acid, acetic acid, and pyruvic acid BtsS-YpdB cross regulation is critical for *yhjX* upregulation, as determined by luminescent reporter assays. I confirmed *yhjX* upregulation in response to acidic pH by qPCR analyses **(Figure 5 and 7)**. This chapter will expand on the activating signals of the BtsS-YpdB system that I have identified. This chapter will also discuss the interactions between the BtsS-YpdB system with other TCSs.

Methods

Luciferase reporter assay

Overnight cultures were spun at 3220 x g for 10 minutes. Pellets were resuspended in 5 ml 1X PBS and re-pelleted. Pellets were resuspended in 5 ml 1X PBS and normalized to a starting OD_{600} = 0.05 in 1 ml of the indicated media (LB, LB + 10 mM HCl, or LB + 50 mM MOPS or HEPES buffer + 10 mM HCl, LB + 10 mM Lactic Acid, LB + 10 mM Acetic Acid, LB + 1mM Pyruvic Acid). For *Lactobacillus* spent media experiments, 100 µl of spent media obtained from the indicated *Lactobacillus* species was added to 900 µl of LB. Each suspension was used to seed black, clear bottomed 96 well plates at 200 µl per well from and grown at 37°C with shaking. OD_{600} and luciferase readings were taken every hour for 8 hours using a Molecular Devices SpectraMax i3 plate reader. At least 3 biological replicates were assayed.

RNA Extraction and RT-qPCR

To collect samples for transcriptional analysis, strains were grown aerobically in LB to an OD_{600} = 0.5 and then split into two conditions: continued growth in LB alone, or in LB in which

HCl was added to a final concentration of 10 mM. Samples were taken for RNA extraction at time = 0, 15, 30, 60, and 120 minutes after splitting the culture. All samples were centrifuged at 6000 x g for 7 minutes at 4°C. The supernatant fractions were decanted, and cell pellets were flash frozen in dry ice and ethanol and stored at -80°C until RNA extraction.

RNA was extracted using the RNeasy mini kit from Qiagen, following the manufacturer's extraction protocol. A total of 3 μg of RNA was DNAse treated using 2 units of Turbo DNase I enzyme (Invitrogen). A total of 1 μg of DNAse-treated RNA was reverse transcribed using Superscript III reverse transcriptase (Invitrogen/Thermo Fisher). cDNA was amplified in an Applied Biosystems StepOne Plus Real-Time instrument using TaqMan MGB chemistry with primers and probes listed in Table S1. All reactions were performed in triplicate with four different cDNA concentrations (100, 50, 25, or 12.5 ng per reaction). Relative fold difference in transcript abundance was determined using the ΔΔCT method of Pfaffl et al., with a PCR efficiency of >95%.[123] Transcripts were normalized to *gyrB* abundance. At least 3 biological replicates were performed for each transcript. Results were statistically analyzed using a two-way ANOVA with Sidak's multiple comparisons test.

RNAseq

Wildtype UTI89 and Δ*btss*Δ*ypdB* strains were grown in LB until the culture reached an OD_{600} = 0.5. The cultures were then split into 2 flasks and one flask had the pH of the culture shifted to 5 with 1 M HCl. Cells were collected 0 and 60 minutes after induction with HCl and RNA was extracted and converted to cDNA as described above. Samples were sent to VANTAGE where all samples are sequenced and performed at multiplex Paired-End 150 bp on the Illumina NovaSeq 6000. Sequenced reads were uploaded to PATRIC (Bacterial and Viral Bioinformatics

Resource Center) and analyzed by Patric's RNA-seq analysis tool. This analysis utilizes the Tuxedo suite of programs.[180]Briefly the TopHat program aligned the reads to UTI89 genome. Then the Cufflinks program determined which genes were differentially expressed using the t-test analogical method.[181] Significantly differentially expressed genes were called with a q value < 0.05.

Motility assays

LB agar (pH=7)was made at a concentration of 0.25% agar. 10 ml of LB agar was added to each well of a 6 well plate. Motility needles were inoculated with overnight cultures of UTI89 or the indicated mutants then stabbed through the center of the motility agar, with care taken to not touch the bottom of the well. Plates were incubated at 37℃ for up to 7 hours. 2 measurements of the diameter were averaged for each biological replicate.

Results and Discussion

Roles of BtsS/BtsR and YpdA/YpdB in yhjX regulation under acidic conditions

In chapter 2, I demonstrated that *yhjX* transcription could be induced under a variety of different acidic conditions **(Figure 5 and 7)**. I also showed that *yhjX* induction was dependent on BtsS-YpdB signaling, as deletion of both *btsS* and *ypdB* did not result in *yhjX* induction **(Figure 5)**. To further demonstrate that *yhjX* upregulation is dependent on BtsS and YpdB, I performed the same luminescence reporter assay in strains lacking BtsR and YpdA. When both *btsR* and *ypdA* are deleted, *yhjX* promoter activity is elevated beyond levels observed for wildtype UTI89, indicating BtsR and YpdA enact inhibitory effects on *yhjX* expression **(Figure 26A)**.

I next wanted to determine if BtsS was responsible for acidic pH sensing. When YpdA is missing from the cell, *yhjX* promoter activity is high in neutral LB **(Figure 26B)**. Upon addition of HCl to the media, *yhjX* promoter activity increases in the *ypdA* mutant **(Figure 26B)**. However, when BtsS is missing from cells, *yhjX* promoter activity becomes elevated with or without acidification **(Figure 26B)**. Acid sensing therefore appears to be controlled by BtsS. Quantitative PCR analysis of wildtype and UTI89Δ*btsS*Δ*ypdB* confirmed the observations of the luminescence reporter assay: the wildtype strain showed a surge in *yhjX* transcript abundance after exposure to acidified media that was lost in the Δ*btsS*Δ*ypdB* mutant strain **(Figure 5**).

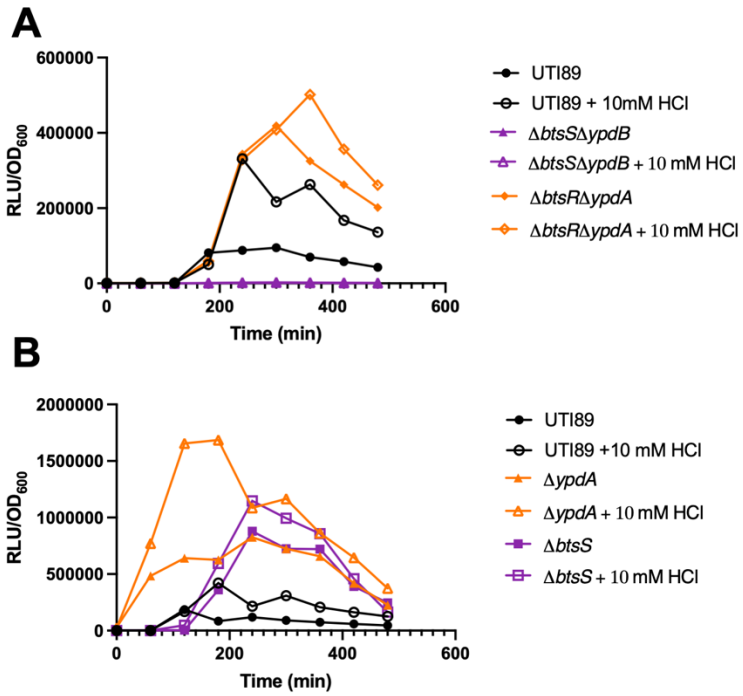

Figure 26. Contribution of BtsSR and YpdAB component to *yhjX* expression
Graphs depict relative luminescence units (RLU) normalized to growth (OD_{600}) over time, of UPEC strains harboring the P*yhjX*-lux reporter grown in LB or LB + 10 mM HCl. A) Deletion of *btsS* and *ypdB* (purple) abolish *yhjX* promoter activity. Deletion of *btsR* and *ypdA* resulted in elevated *yhjX* promoter activity compared to WT (black). B) Deletion of *btsS* (purple) results in elevated, but acid insensitive, *yhjX* expression compared to WT. Deletion of *ypdA* (orange) results in elevated, but acid sensitive, *yhjX* expression compared to WT. Graphs are representative of 3 biological replicates.

Physiologically relevant acid stress conditions and BtsS-YpdB signaling

Organic acids are abundant in both the gastrointestinal and vaginal spaces, both of which are niches that UPEC will encounter and establish reservoirs in route to the urinary tract. In the gut, the bacteria of the microbiome release a variety of organic acids as they metabolize dietary fibers in the gut. The most prevalent SCFAs produced by the gut microbiota are acetate, propionate, and butyrate.

In the vagina, *Lactobacillus*, the dominant genus, produces lactic acid to acidify the environment. 75% of people AFAB are predominantly vaginally colonized by *Lactobacillus spp.*[182,183] Colonization rates vary by ethnicity.[183] Most of the L-lactic acid and nearly all D-lactic acid in the vagina is produced by *Lactobacillus* but vaginal epithelial cells can produce up to 20% of the L-lactic acid. People AFAB with bacterial vaginosis (BV) exhibit a decrease in lactic acid in the vagina and an increase in other SCFAs such as acetic acid, propionic acid, butyric acid, and succinic acid.[184] UPEC is better able to colonize the vagina under BV conditions as compared to healthy microbiome conditions.[36,185]

In chapter 2, I demonstrated that these physiologically relevant organic acids were able to induce the upregulation of *yhjX.* To study the effect of other acidic conditions on *yhjX* expression, I utilized a luminescence reporter fused to the *yhjX* promoter to track *yhjX* expression over time **(Figure 7)**. Investigation of different organic acids – acetic acid, lactic acid, and pyruvic acid- revealed that all lead to upregulation of *yhjX,* as observed by the increase in luminescence as compared to the untreated control. Acetic acid not only increased *yhjX* expression, but it also delayed peak expression from 180 minutes to 300 minutes **(Figure 7)**.

As opposed to inorganic acids, organic acids can potentially lead to changes in BtsS-YpdB signaling due to the changes they induce to UPEC metabolism. To determine if the upregulation

of *yhjX* was due to the pH changes caused by the organic acids, I modified the luminescence reporter assay to include buffers, to keep the pH of the culture neutral even after the addition of organic acids to the media. Addition of buffers to media that is acidified by acetic acid did not reduce *yhjX* expression levels, but they did return the timing of peak *yhjX* expression to 180 minutes **(Figure 27A)**. This phenomenon may be explained by the fact that acetic acid leads to an increased lag phase. When buffers were added to acetic acid treated media, the growth of UTI89 is the same as UTI89 grown in LB alone. Addition of buffers to media that is acidified by lactic acid returns the pH to neutral **(Table 5)** and returns *yhjX* expression to similar levels observed in the untreated control **(Figure 27B)**.

Buffering 1 mM pyruvic acid treated media did not result in changes to *yhjX* expression as compared to pyruvic acid alone **(Figure 27C)**. This was expected for two reasons. The first is that 1 mM pyruvic acid nominally decreased the pH of the LB from 7.35 to 7.03. The second is that pyruvate has been shown to directly bind to BtsS and lead to an increased expression of *yhjX*. 1 mM pyruvic acid was initially used due to prior work done in BtsS signaling. By increasing the concentration of pyruvic acid to 10 mM, the pH of the media decreased to 5.50. Buffering 10 mM pyruvic acid still did not reduce *yhjX* expression levels back to those of the untreated control **(Figure 27D)**. Together these data suggest that various acids can induce *yhjX* expression. Additionally, they suggest that pyruvate and pH are two distinct signals that can lead to *yhjX* upregulation.

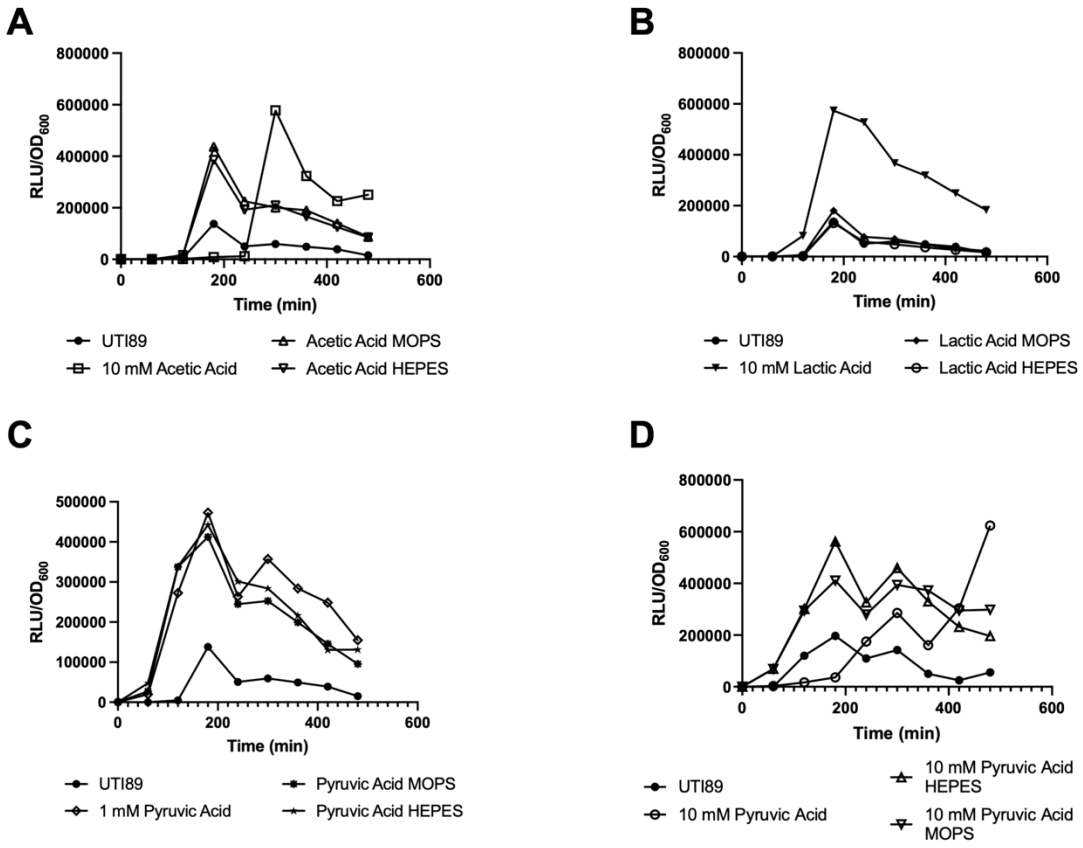

Figure 27. Organic acids induce *yhjX* expression in a pH dependent manner
Graphs depict relative luminescence units (RLU) normalized to growth (OD_{600}) over time, of UTI89 harboring the P*yhjX*-lux reporter grown in LB or (A) LB + 10 mM Acetic Acid, (B) LB + 10 mM Lactic Acid, (C) LB + 1 mM Pyruvic Acid, or (D) LB + 10 mM Pyruvic Acid. Each organic acid treatment was also buffered with either 50 mM MOPS or 50 mM HEPES buffer. Graphs are representative of 3 biological replicates.

In the GI tract, UPEC would encounter lower oxygen concentrations than it experienced in the assays I have performed thus far.[186] To determine if *yhjX* induction by acidic pH occurs anaerobically, I performed qPCR on RNA samples that I collected from WT UTI89 and Δ*btsS*Δ*ypdB* cultures grown anaerobically until they reached mid-log phase then exposed the cells to 10 mM HCl for 60 minutes. In wildtype UTI89, anaerobic growth led to downregulation of *yhjX* after 60 minutes of exposure to acid compared to UTI89 grown aerobically **(Figure 28)**. I also grew UTI89 anaerobically in LB supplemented with nitrate then exposed the culture to 10 mM

HCl for 60 minutes. The nitrate treatment acted as an alternate electron acceptor since oxygen was not available. Thus, the nitrate ensured that the ETC would run. Under these conditions, *yhjX* was downregulated compared to cells grown aerobically **(Figure 28)**. *yhjX* was downregulated in the Δ*btsS*Δ*ypdB* strain under all conditions **(Figure 28)**. These findings indicate that BtsS-YpdB regulation of *yhjX* in response to acid occurs only under aerobic conditions and it corroborates previous observations ascribing differential acid responses under aerobic and anaerobic conditions.[67,187]

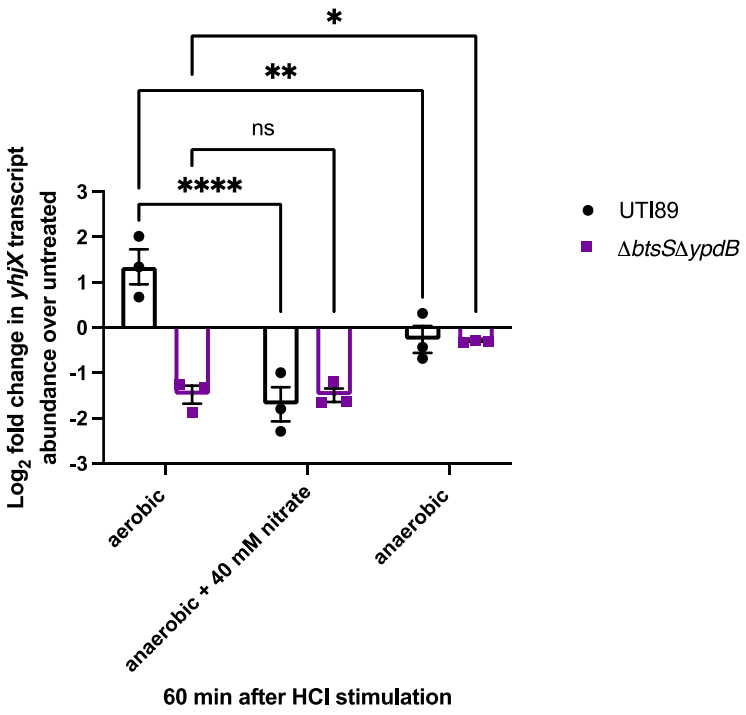

Figure 28. transcript abundance of yhjX under anaerobic conditions.
Wildtype UTI89 and Δ*btsS*Δ*ypdB* mutant (purple) were grown to mid log phase then exposed to 10 mM HCl for 60 minutes before samples were collected for RNA extraction. Relative fold change was determined by the $\Delta\Delta C_T$ method, where *yhjX* transcript abundances were normalized to *gyrB* housekeeping gene transcripts. Three biological replicates were performed for each transcript. (* $p = 0.0177$, ** $p = 0.0024$, **** $p < 0.0001$ 2 way ANOVA with Dunnett's multiple comparisons)

Another niche where pH sensing may play an important role in UPEC colonization and pathogenesis is the vagina. *Lactobacillus spp.* are dominant in the vaginal microbiome and produce lactic acid to drop the pH. To determine if *Lactobacilli* could induce *yhjX,* I modified the luminescence reporter assay to include spent media from 7 different *Lactobacillus* clinical isolates in the UPEC culture media. Each *lactobacillus* isolate was grown in MRS media for 3 days. The *Lactobacillus* culture was then centrifuged, and the supernatant was filter sterilized to exclude bacteria. The spent media was then diluted 1:10 in LB and this media was used to grow either WT or Δ*btsS*Δ*ypdB* UTI89 strains containing the *yhjX* luminescent reporter plasmid. I observed upregulation of *yhjX* in WT UTI89 when the culture was grown with *L. acidophilus, L. brevis, L. delbrueckeii, L. gasseri,* and *L. reuteri* spent media*. L. johnsonii* and *L. rhamnosis* did not show any *yhjX* promoter activity **(Figure 29A)**. Upon further investigation this lack of activation was explained by the fact that UTI89 was unable to grow in media mixtures that contained spent media from *L. johnsonii* and *L. rhamnosis* **(Figure 29B)**. When I performed the same luminescence reporter assay with the Δ*btsS*Δ*ypdB* strain, I observed no activation of *yhjX* expression, consistent with the experiments presented previously **(Figure 29C)**. The lack of *yhjX* expression was not due to Δ*btsS*Δ*ypdB* strain being unable to grow **(Figure 29D)**.

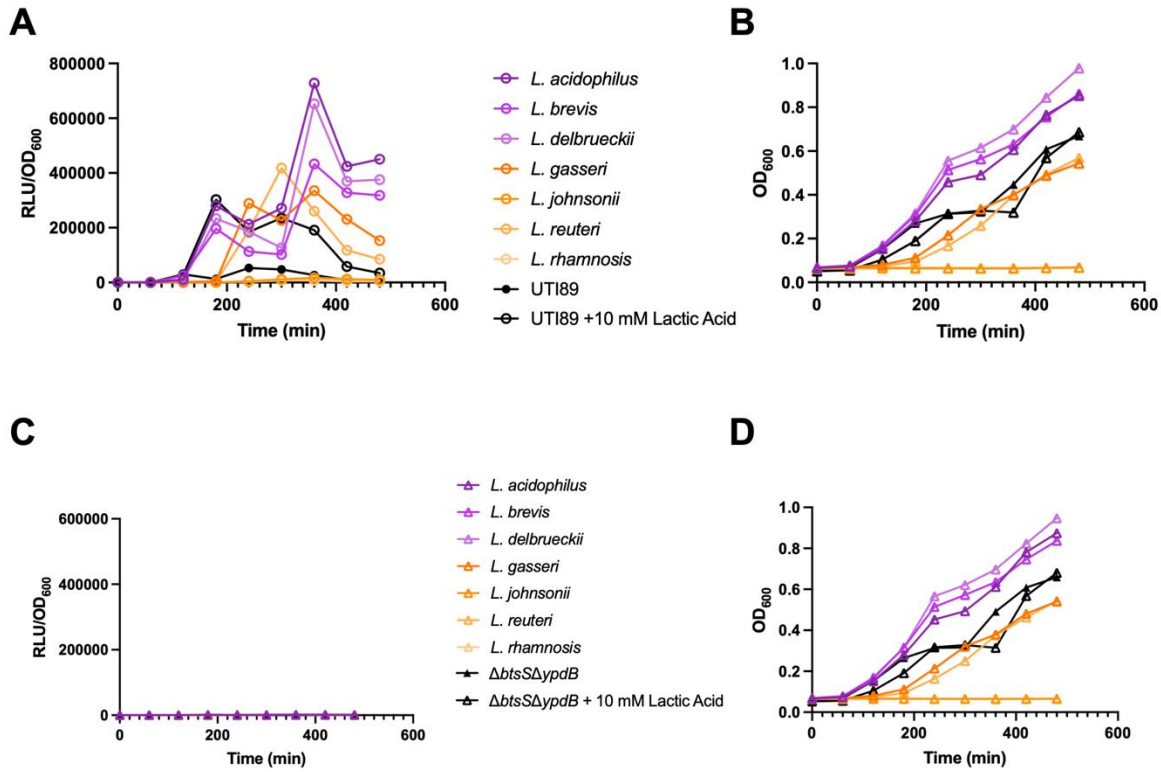

Figure 29. *Lactobacillus spp.* spent media induces *yhjX* expression
Graphs A and C depict relative luminescence units (RLU) normalized to growth (OD_{600}) over time, of UTI89 harboring the P*yhjX*-lux reporter (A) or Δ*btsS*Δ*ypdB* harboring the P*yhjX*-lux reporter (C) grown in 90% LB + 10% spent media from the indicated *Lactobacillus spp.* Graphs B and D depict the corresponding growth curves (OD_{600}) for graphs A and C. Graphs are representative of 3 biological replicates.

To begin to investigate why some *Lactobacillus spp.* produced spent media that inhibited UPEC growth, I measured the pH of the LB mixture with *L. johnsonii* spent media and discovered that *L. johnsonii* spent media dropped the pH of the media to around 4.5 **(Figure 30A)**. When a buffer was added to the *L. johnsonii* spent media LB mixture, the pH returned to near 7 **(Figure 30A)** and growth of UTI89 was restored, indicating that the low pH of *L. johnsonii* spent media was inhibitory to UPEC growth **(Figure 30B)**. Buffering the media also resulted in attenuated *yhjX* expression in UTI89 compared to the unbuffered culture conditions **(Figure 30C)**. Overall, this experiment demonstrates that *yhjX* expression is induced by metabolites produced by bacteria that UPEC would encounter in the vaginal space.

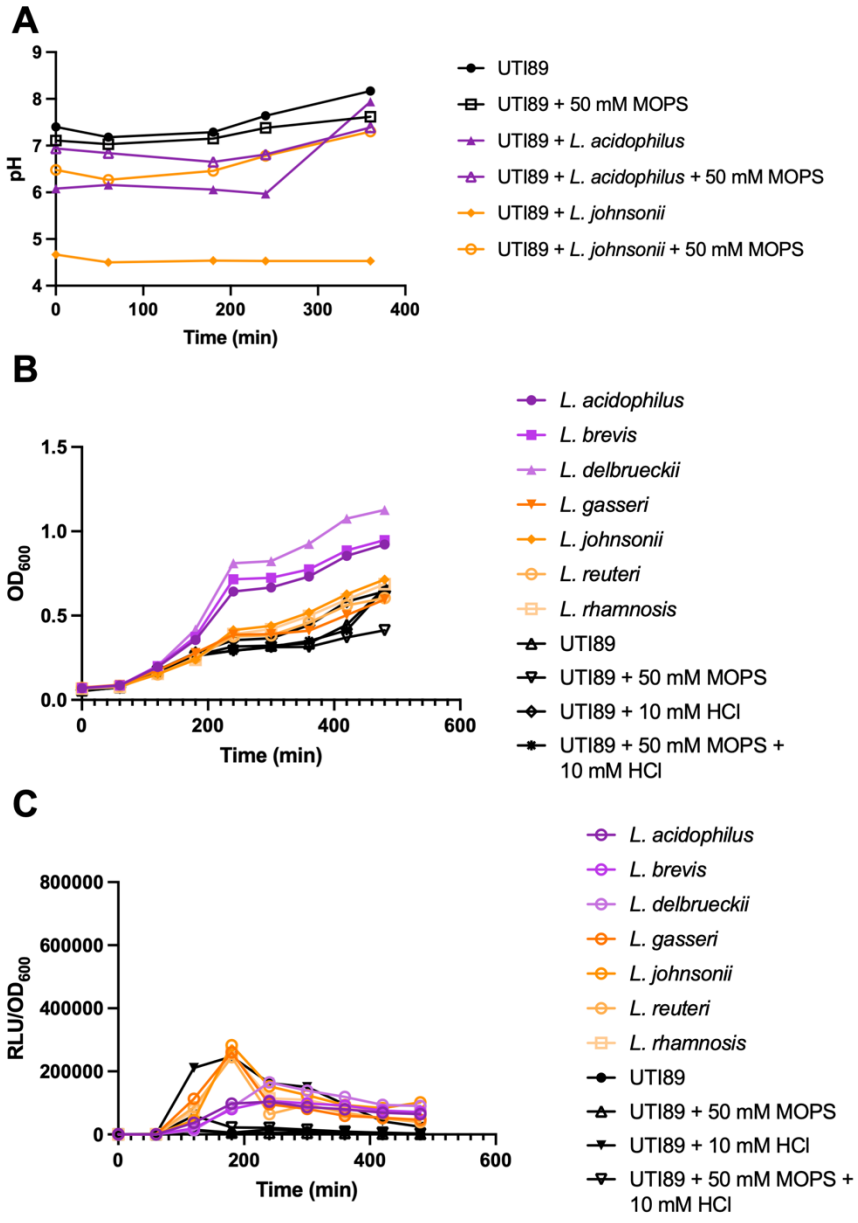

Figure 30. pH of *Lactobacillus* spent media is responsible for elevated *yhjX* expression
A) pH of cultures of UTI89 grown in LB, LB + 50 mM MOPS, 90%LB+10% *Lactobacillus* spent media, or 90%LB+10% *Lactobacillus* spent media + 50 mM MOPS. B) Growth curves (OD_{600}) of UTI89 grown in 90% LB + 10% spent media from the indicated *Lactobacillus spp.* + 50 mM MOPS. C) relative luminescence units (RLU) normalized to growth (OD_{600}) over time, of UTI89 harboring the P*yhjX*-lux reporter grown in 90% LB + 10% spent media from the indicated *Lactobacillus spp.* + 50 mM MOPS. Graphs are representative of 3 biological replicates.
Interaction between Btss-Ypdb and other acid sending TCSs

Four TCSs, BarA, CpxRA, EvgSA, and PhoPQ, were previously implicated in acidic pH sensing. To determine the contribution of these systems on BtsSR and YpdAB signaling, deletion mutants of each system were created then transformed with the *yhjX* luminescent reporter plasmid. The expression of the *yhjX* gene was measured over the course of eight hours as the deletion mutants were challenged with 10 mM hydrochloric acid. Deletion of either *evgSA* or *phoPQ* resulted in loss of *yhjX* induction in both neutral and acidified media **(Figure 31A and B)**. Both the *cpxRA* and *barA* deletion mutants had not change in *yhjX* activity compared to wildtype **(Figure 31C and D)**.

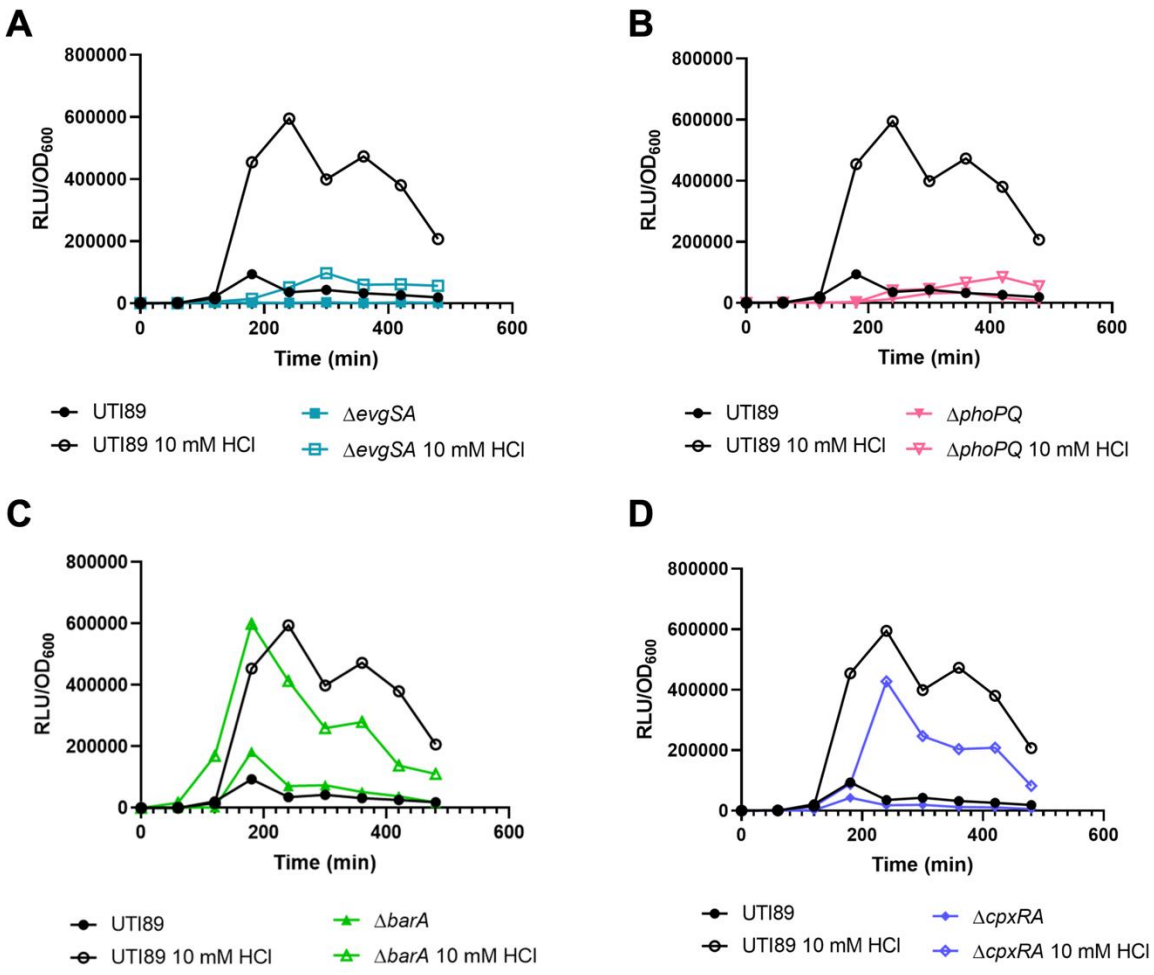

Figure 31. Δ*evgSA* and Δ*phoPQ* do not induce *yhjX* expression under acidic pH conditions
Graphs depict relative luminescence units (RLU) normalized to growth (OD_{600}) over time, of UTI89, Δ*evgSA* (A), Δ*phoPQ* (B), Δ*barA* (C), or Δ*cpxRA* (D) harboring the P*yhjX*-lux reporter grown in LB or LB + 10 mM HCl. Graphs are representative of 3 biological replicates.

I next wanted to determine if the influence these acid sensing TCSs had on *yhjX* expression was specific to acidic pH inducing conditions. To do this I performed the same luminescence reporter assay but supplementing the media with pyruvate – the known activator of the BtsSR and YpdAB systems – instead of HCl. I observed *yhjX* induction similar to WT levels in all of the TCS deletion strains **(Figure 32A-D)**.

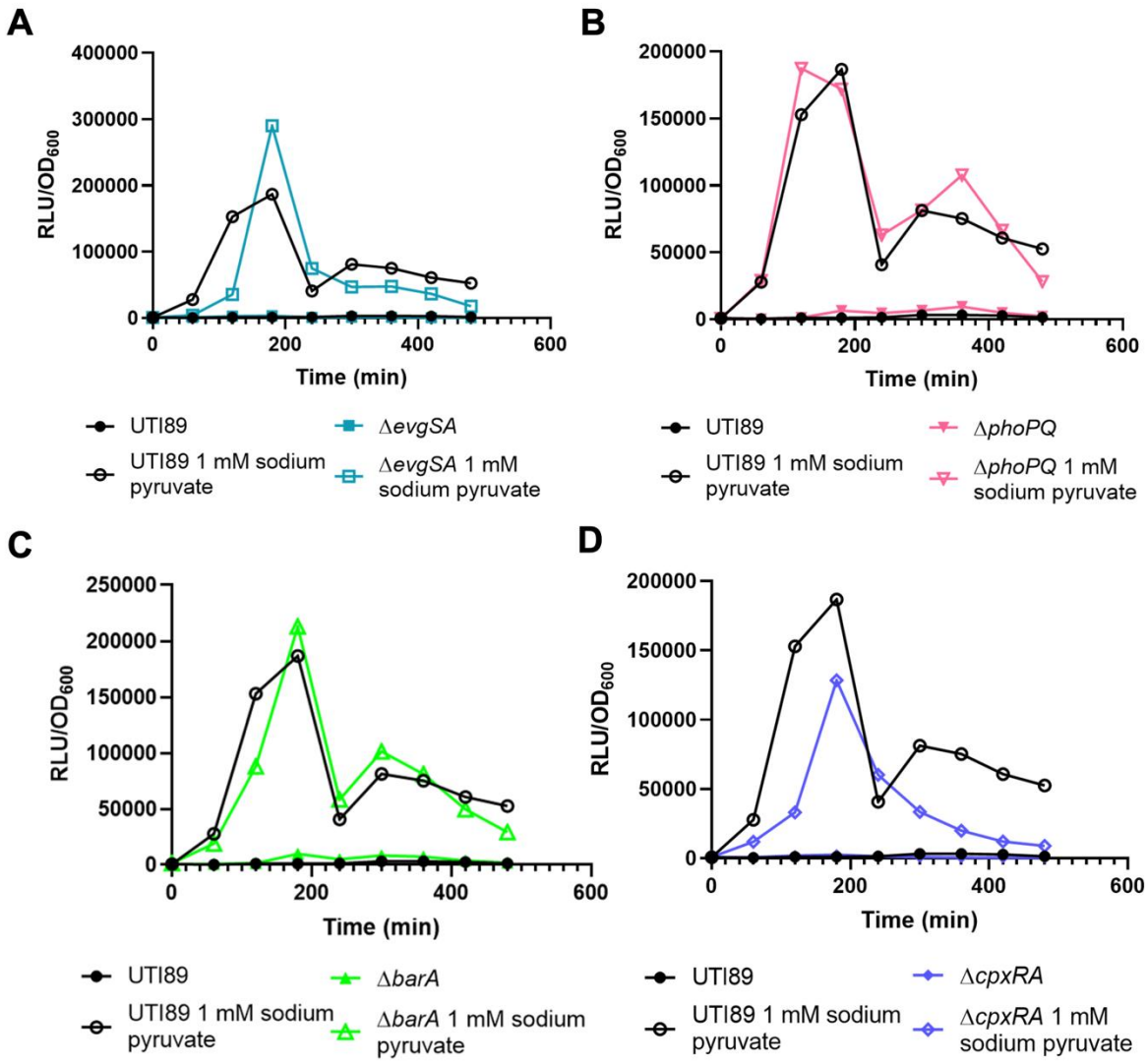

Figure 32. Other acidic pH sensing TCSs do not impact *yhjX* expression under pyruvate induction conditions
Graphs depict relative luminescence units (RLU) normalized to growth (OD_{600}) over time, of UTI89, Δ*evgSA* (A), Δ*phoPQ* (B), Δ*barA* (C), or Δ*cpxRA* (D) harboring the P*yhjX*-lux reporter grown in LB or LB + 1 mM sodium pyruvate. Graphs are representative of 3 biological replicates.

I confirmed that both Δ*evgSA* and Δ*phoPQ* strains were unable to induce *yhjX* expression by qPCR. These qPCR analyses showed that Δ*evgSA* and Δ*phoPQ* strains had the same *yhjX* expression patterns as the Δ*btsS*Δ*ypdB* strain **(Figure 33)**. Combined, these results indicate that

the EvgSA and PhoPQ systems interact with the BtsSR and YpdAB systems to modulate *yhjX* expression under acidic conditions only.

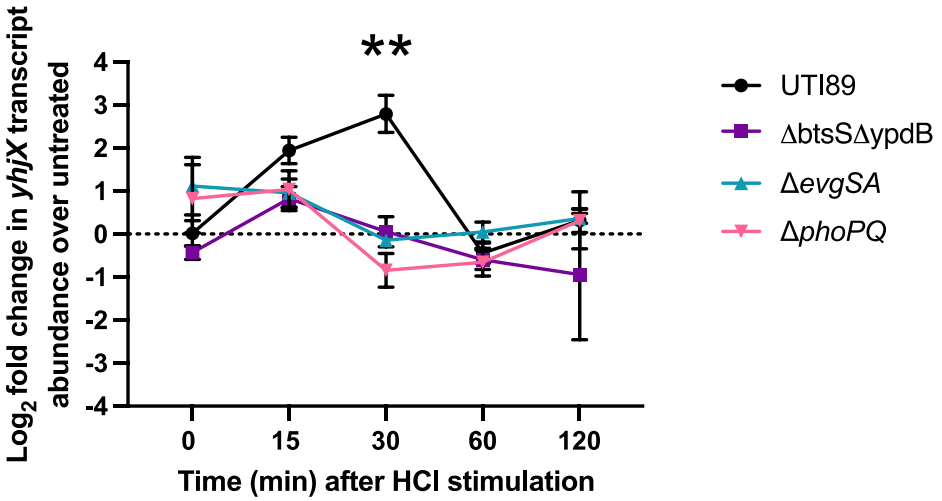

Figure 33. Deletion of *evgSA* or *phoPQ* decreases *yhjX* expression
WT UTI89 (black), Δ*evgSA* (teal), Δ*phoPQ* (pink), and Δ*btsS*Δ*ypdB* (purple) were grown to mid log phase then exposed to 10 mM HCl and samples were collected for RNA extraction at T = 0, 15, 30, 60, and 120 minutes after acidic pH exposure. Relative fold change was determined by the $\Delta\Delta C_T$ method, where *yhjX* transcript abundances were normalized to *gyrB* housekeeping gene transcripts. Three biological replicates were performed for each transcript. (Δ*btsS*Δ*ypdB* p=0.0014, Δ*evgSA* p=0.0006, Δ*phoPQ* p<0.0001, Two-way ANOVA with Dunnett's multiple comparisons test)

Since *yhjX* is under the regulation of the BtsS-YpdB pathway, qPCR analysis was performed to determine if EvgSA and PhoPQ played role in this BtsS-YpdB acid sensing pathway by altering either *btsS* or *ypdB* expression. RNA samples were collected from Δ*evgSA* and Δ*phoPQ* strains grown in the presence or absence of 10 mM HCl. The RNA samples were then reversed transcribed to cDNA which were used in the qPCR which probed for *btsS* and *ypdA*. The results of the qPCR show that there is no statistical difference between the fold change in *btsS* or *ypdA* transcript abundance when EvgSA and PhoPQ deletion mutants are placed under acidic conditions compared to the wildtype **(Figure 34 A and B)**. This leads to the conclusion that while EvgSA and

PhoPQ somehow participate in the regulation of *yhjX*, they do not do so by affecting the transcription of *btsS* or *ypdA*. The mechanism with which EvgSA and PhoPQ influence *yhjX* is still to be determined, and future studies to investigate this are proposed in Chapter 5.

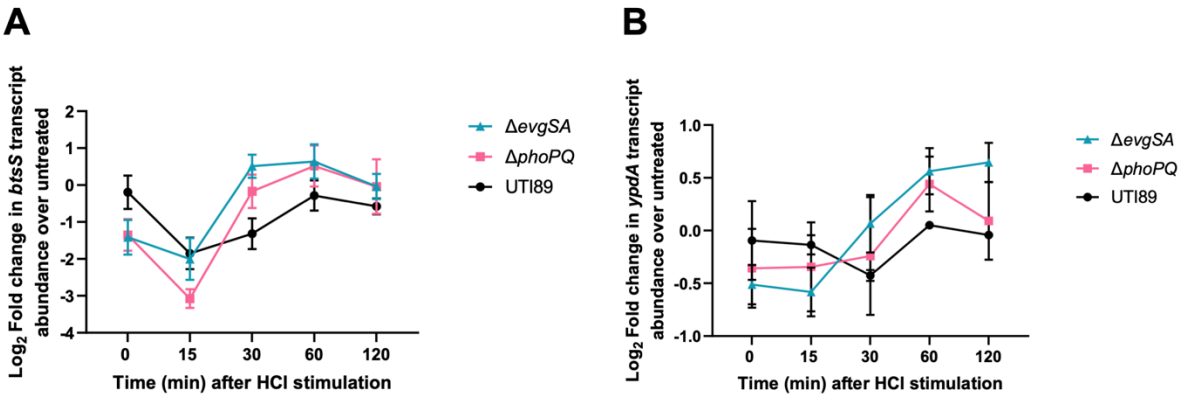

Figure 34. EvgSA and PhoPQ have no effect on *btsSR* or *ypdAB* expression
WT UTI89 (black), Δ*evgSA* (teal), and Δ*phoPQ* (pink)were grown to mid log phase then exposed to 10 mM HCl and samples were collected for RNA extraction at T = 0, 15, 30, 60, and 120 minutes after acidic pH exposure. Relative fold change was determined by the $\Delta\Delta C_T$ method, where *btsS* (A) and *ypdA* (B) transcript abundances were normalized to *gyrB* housekeeping gene transcripts. Three biological replicates were performed for each transcript.

BtsS-YpdB regulates cysteine metabolism under acidic conditions

In the preceding sections I have shown that BtsS-YpdB cross regulation in response to acidic conditions leads to upregulation of *yhjX.* Previous literature suggests that cross regulation of two-component systems can result in expanded cellular responses to a single stimulus.[121,188-190] To determine if BtsS-YpdB signaling in response to acid affects any other cellular processes, I performed RNA-seq. RNA was collected from WT and Δ*btss*Δ*ypdB* cell cultures at 0 minutes and 60 minutes after the cell cultures were acidified to a pH of 5 with HCl. I performed 4 different comparisons: WT t=0 min vs Δ*btss*Δ*ypdB* t=0 min **(Figure 35)** to determine if there were any differences in baseline gene regulation between WT and Δ*btss*Δ*ypdB*, WT t=0 min vs WT t=60

min + HCl **(Figure 36)** to determine which genes were differentially regulated in WT cells in response to acid stress, Δ*btss*Δ*ypdB* t=0 min vs Δ*btss*Δ*ypdB* t=60 min + HCl **(Figure 37)** to determine which genes were differentially regulated in Δ*btss*Δ*ypdB* cells in response to acid stress, and WT t=60 min + HCl vs Δ*btss*Δ*ypdB* t=60 min + HCl **(Figure 38)** to determine the differentially expressed genes between WT and Δ*btss*Δ*ypdB* under acidic conditions. Analyses of RNA reads is described in the methods. Briefly, all sequencing reads were uploaded to PATRIC and Tuxedo was run to compare the indicated samples. When comparing WT transcripts to Δ*btss*Δ*ypdB,* I saw that *yhjX* was significantly downregulated in the Δ*btss*Δ*ypdB* mutant, as expected.

To get a better idea of what pathways were affected by the differential gene expression, significantly differentially expressed genes were then submitted to PANTHER for gene ontology enrichment analysis. At the t=0 minute time point, pathways involving motility and flagella genes were downregulated in the Δ*btss*Δ*ypdB* strain compared to the WT strain. Additionally, anaerobic respiration and nitrogen metabolism genes were upregulated in the Δ*btss*Δ*ypdB* strain at the t=0 minute time point. After 60 minutes of exposure to pH 5, the Δ*btsS*Δ*ypdB* mutant showed upregulation of sulfur assimilation and cysteine metabolism genes compared to WT, while carbohydrate and alcohol metabolism genes were downregulated in the mutant strain.

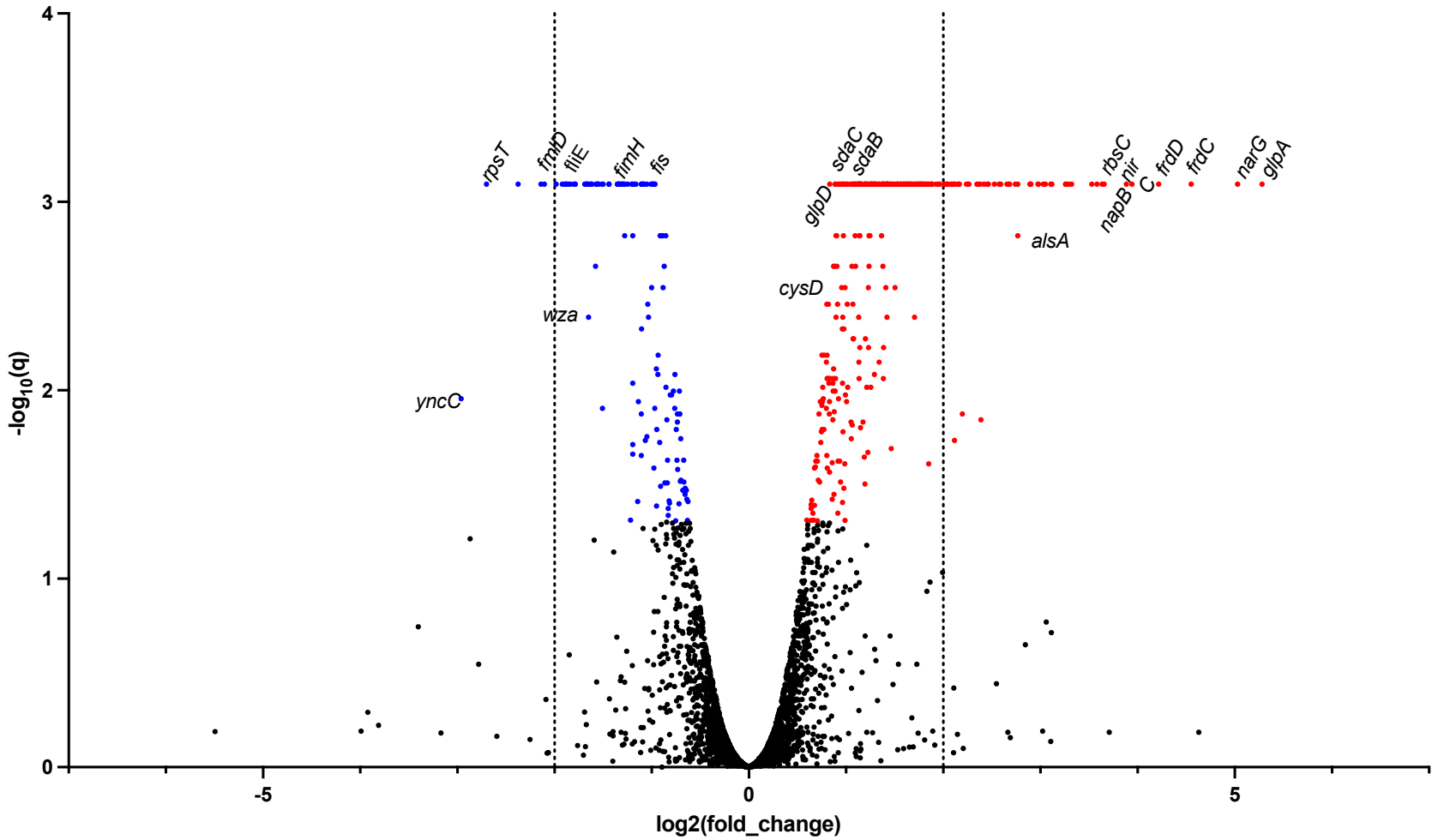

Figure 35. Differentially expressed genes in Δ*btsS*Δ*ypdB* compared to WT 0 minutes after HCl exposure
Significantly downregulated genes in Δ*btsS*Δ*ypdB* are highlighted in blue. Significantly upregulated genes in Δ*btsS*Δ*ypdB* are highlighted in red. Vertical dashed lines indicate Log_2FoldChange cutoff of -2 and 2.

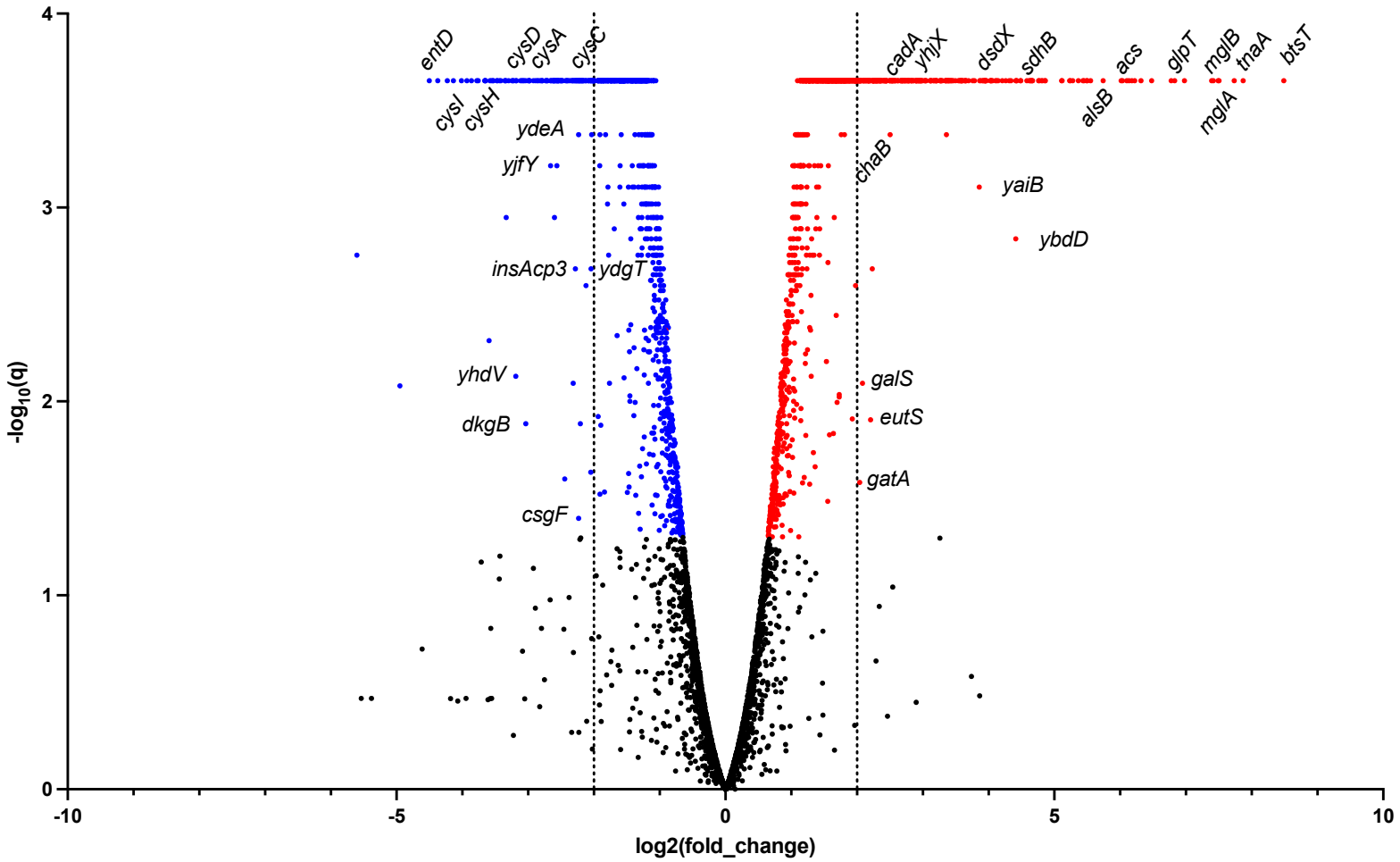

Figure 36. Differentially expressed genes in WT 60 minutes after HCl exposure compared to WT 0 minutes after HCl exposure
Significantly downregulated genes in WT 60 minutes after HCl exposure are highlighted in blue. Significantly upregulated genes in WT 60 minutes after HCl exposure are highlighted in red. Vertical dashed lines indicate Log_2FoldChange cutoff of -2 and 2.

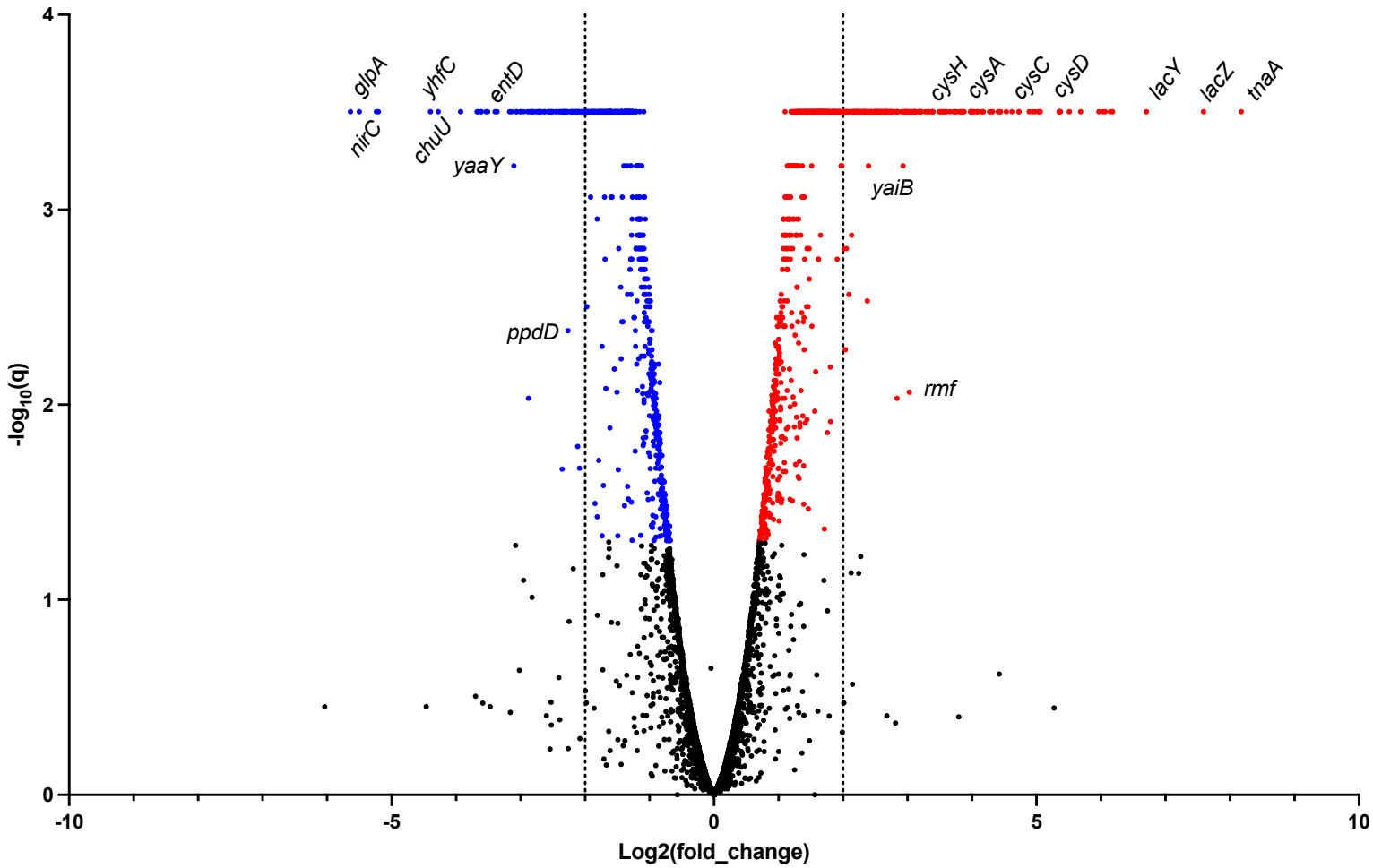

Figure 37. Differentially expressed genes in Δ*btsS*Δ*ypdB* 60 minutes after HCl exposure compared to Δ*btsS*Δ*ypdB* 0 minutes after HCl exposure

Significantly downregulated genes in Δ*btsS*Δ*ypdB* 60 minutes after HCl exposure are highlighted in blue. Significantly upregulated genes in Δ*btsS*Δ*ypdB* 60 minutes after HCl exposure are highlighted in red. Vertical dashed lines indicate Log_2FoldChange cutoff of -2 and 2.

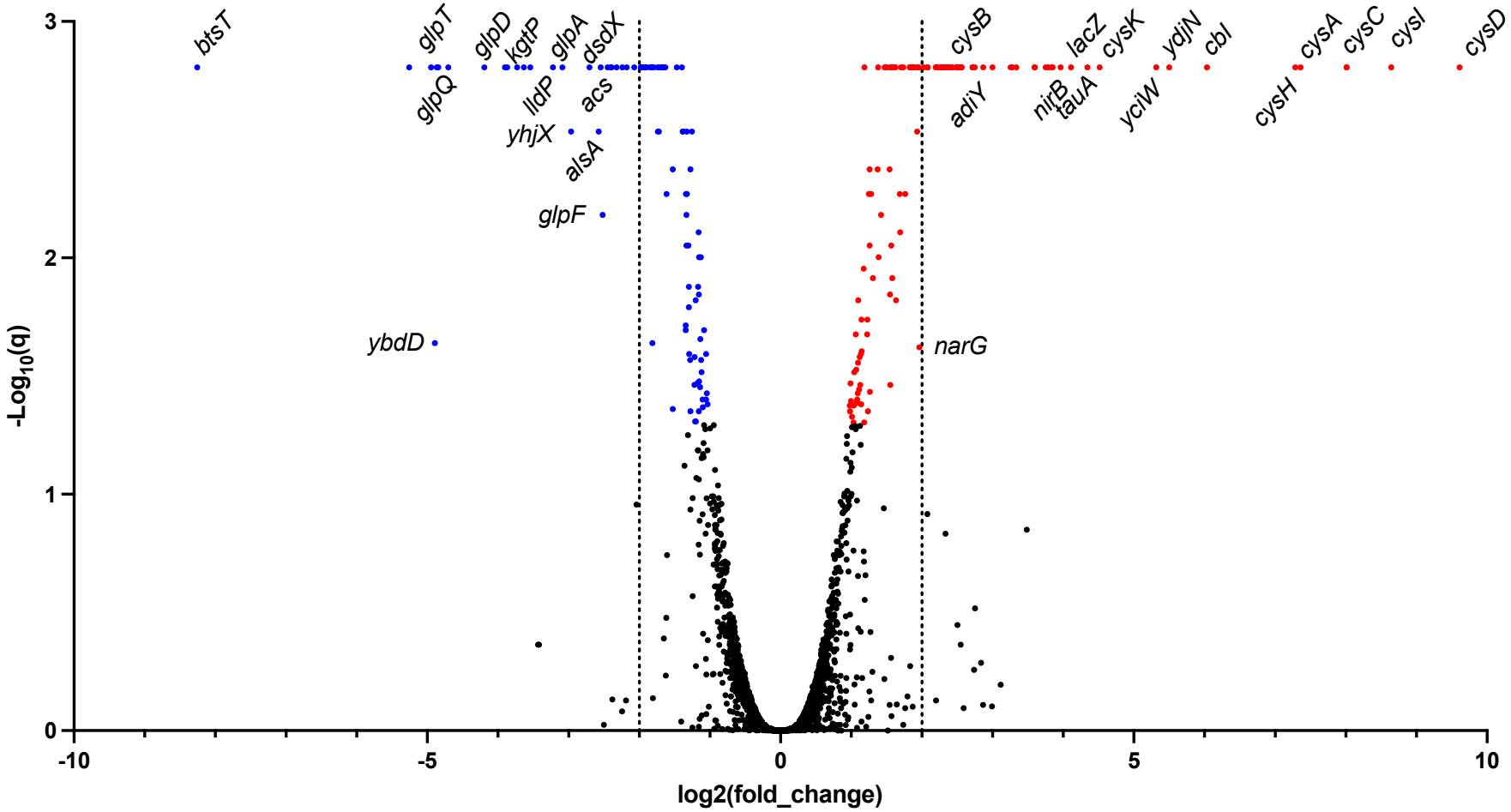

Figure 38. Differentially expressed genes in Δ*btsS*Δ*ypdB* 60 minutes after HCl exposure compared to WT 60 minutes after HCl exposure

Significantly downregulated genes in Δ*btsS*Δ*ypdB* 60 minutes after HCl exposure are highlighted in blue. Significantly upregulated genes in Δ*btsS*Δ*ypdB* 60 minutes after HCl exposure are highlighted in red. Vertical dashed lines indicate Log_2FoldChange cutoff of -2 and 2.

As one of the classes of genes downregulated in the Δ*btsS*Δ*ypdB* mutant was motility, I performed motility assays for WT UTI89, Δ*btsS*Δ*ypdB,* Δ*sdaA,* Δ*sdaB,* Δ*sdaC,* and Δ*sdaA*Δ*sdaB* strains. Although the transcriptomic results showed downregulation of flagellar genes, the motility assay did not reveal any significant difference in motility between WT UTI89 and the Δ*btsS*Δ*ypdB* strain **(Figure 39)**.

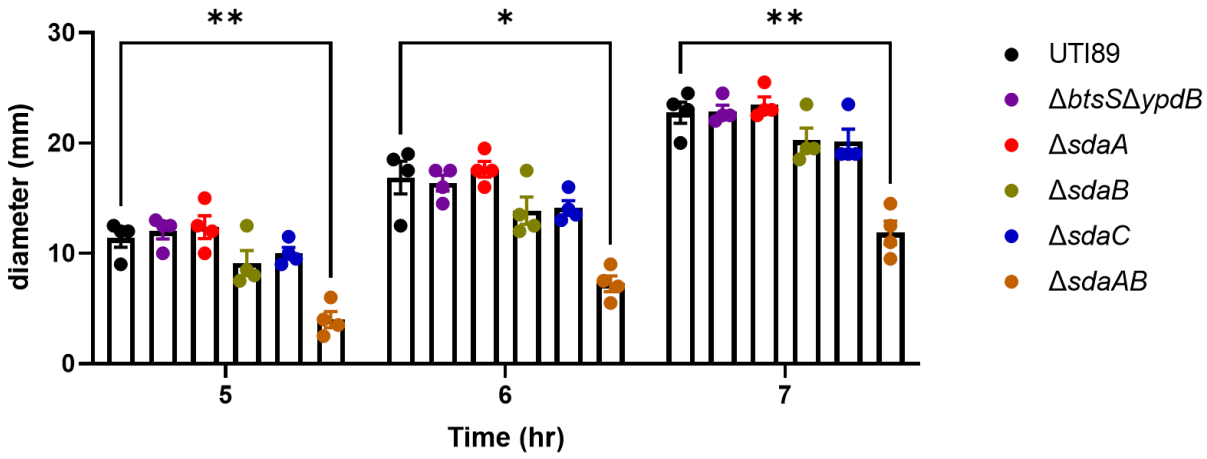

Figure 39. Δ*btsS*Δ*ypdB* does not have a motility defect
Motility plates were inoculated with overnight cultures using a motility needle. Graph depicts results of 4 independent biological replicates (2-way ANOVA with Dunnett's multiple comparisons test).

When comparing RNA transcripts 60 minutes post acid exposure from strains UTI89 and Δ*btsS*Δ*ypdB*, I observed that the most upregulated genes in the Δ*btsS*Δ*ypdB* strain were in the CysB regulated operon **(Figure 38)**. Conversely, in the wildtype strain the CysB regulon is among the most strongly downregulated gene clusters in the WT strain 60 minutes after acidic pH exposure compared to the WT strain at 0 minutes.

CysB is a transcription factor that upregulates genes that encode proteins involved in sulfate assimilation and cysteine metabolism.[191-193] Sulfur is an essential element for life. Sulfur can be assimilated in *E. coli* from many sources, with sulfate and cysteine being the preferred

sources.[191,194] Sulfate is taken up by the cell through the sulfate permease complex encoded by *cysPUWA* and *sbp.*CysD and CysN are responsible for the conversion of sulfate into adenosine 5' phosphosulfate (APS).[194,195] APS is then phosphorylated by CysC to generate 3'phosphoadenosin 5'phophosulfate (PAPS).[194,195] PAPS is converted to sulfite and adenosine 3'5'bisphosphate (PAP) by CysH.[194,195] Sulfite is reduced to sulfide by CysI and CysJ. Sulfide is reacted with O-acetylserine (OAS) to produce cysteine by CysK[194,195] OAS is generated by CysE, which reacts serine with acytl-CoA.[194,195] Importantly, *cysPUWA, cysM, cysDNC,, cysH, cysIJ, cysK,* and sbp were all upregulated in the Δ*btsS*Δ*ypdB* mutant 60 minutes post acidic pH exposure.

Cysteine is the most important sulfur containing amino acid. It plays an important role in protein structure due to its ability to form disulfide bonds.[193] Cysteine also required for iron-sulfur cluster containing proteins, including the serine deaminases SdaA and SdaB.[193,196] Additionally, cysteine is a key component of glutathione, a cofactor involved in protecting cells during oxidative stress.[193] Previous work showed that the CysB regulon is induced in response to exposure to hydrogen peroxide.[197] Thus, I hypothesized that the upregulation of cysteine metabolism genes in the Δ*btsS*Δ*ypdB* mutant may enhance the cells' ability to overcome oxidative stress. To test this hypothesis, I grew UTI89 and the Δ*btsS*Δ*ypdB* strains in M9 minimal media +/- increasing concentrations of H_2O_2 **(Figure 40A-F and Table 6)**. Growth curves were performed 5 times and were analyzed with the Weibull non-linear regression in GraphPad Prism. When UTI89 and the Δ*btsS*Δ*ypdB* mutant strains were grown in M9 media alone, they had a lag time of 295.42 and 296.91 minutes, respectively **(Figure 40A, Table 6)**. When the concentration of H_2O_2 was raised to 1.75 mM, the Δ*btsS*Δ*ypdB* mutant showed improved growth compared to the WT strain. The lag time for WT was 422.83 minutes while it was 351.25 minutes for the mutant **(Figure 40B, Table 6)**. Growth for WT UTI89 was completely inhibited at 2.5 mM and 2.75 mM H_2O_2 while

the Δ*btsS*Δ*ypdB* mutant was still able to grow **(Figure 40E and F)**. These results indicate that BtsS-YpdB signaling leads to a repression of cysteine metabolism genes. However, in the absence of BtsS-YpdB, the upregulation of the *cysB* regulon appears to allow for cysteine to be utilized to combat H_2O_2 induced stress.

It has also been shown that high concentrations of intracellular cysteine promote the Fenton reaction which is toxic to cells.[197] Thus, cysteine metabolism and its regulation are important for cell survival. At present, it remains unclear how BtsS-YpdB signaling is playing a role in regulating cysteine metabolism and how this regulation is contributing to acid resistance. Potential experiments to address these unknowns will be discussed in chapter 5.

Conclusions

Overall, these studies show that the BtsS-YpdB cross regulating TCS is activated by conditions UPEC encounters within the human host, namely, SCFAs and *Lactobacillus* spent media. These physiologically relevant stimuli act in a pH dependent manner, as buffering of media containing the stimuli to a neutral pH resulted in reduced *yhjX* expression (the readout for BtsS-YpdB signaling). In addition to BtsS-YpdB, acid sensing TCSs EvgSA and PhoPQ are also involved in *yhjX* regulation under acidic pH conditions. Future experiments proposed in Chapter 5 will work to uncover how multiple TCSs work to regulate *yhjX.*

Additionally, studies in this chapter revealed that BtsS-YpdB are involved in the regulation of sulfur assimilation and cysteine metabolism. Deletion of both *btsS* and *ypdB* led to significant upregulation of *cysB* and CysB regulated genes. This finding indicates that YpdB may act as a repressor of *cysB*. Experiments to test this hypothesis are proposed in Chapter 5.

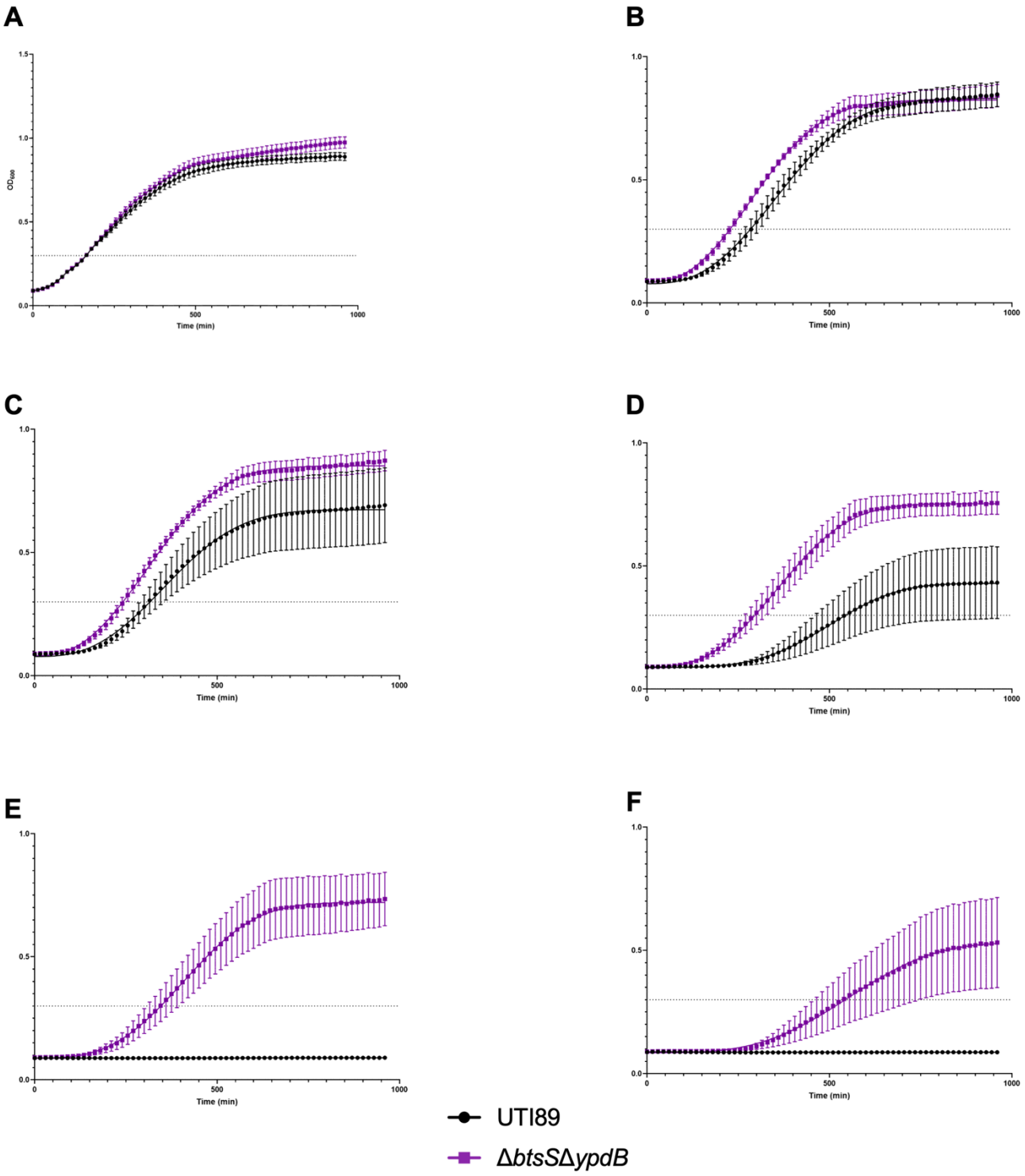

Figure 40. H_2O_2 growth curves
Growth curves (OD_{600}) of WT UTI89 and Δ*btsS*Δ*ypdB* grown in M9 minimal media + 0 (A), 1.75 (B), 2 (C), 2.25 (D), 2.5 (E), or 2.75 (F) mM H_2O_2. Cultures were grown in 96 well plates for 16 hours in the plate reader at 37 ℃. Graphs depict the mean and SEM of 5 biological replicates.

Table 6. Starting pH of cultures after acid and buffers were added

Media Conditions	Starting pH	Starting pH with 50 mM HEPES added	Starting pH with 50 mM MOPS added
Acetic Acid (10 mM)	5.49	6.85	6.77
Lactic Acid (10 mM)	5.21	6.92	6.84
Pyruvic Acid (1 mM)	7.03	7.20	7.13
Pyruvic Acid (10 mM)	5.50	6.91	6.80
HCl (10 mM)	5.00	6.75	6.59
LB	7.35	7.37	7.35

Table 7. Lag times for H_2O_2 growth curves

[H_2O_2] (mM)	Lag time (min) UTI89	Lag time (min) Δ*btsS*Δ*ypdB*
0	295.42	296.91
1	340.72	351.12
1.5	362.45	364.70
1.75	422.83	351.25
2	418.76	374.53
2.25	548.55	415.63
2.5	622.28	463.39
2.75	700.28	615.38

Chapter 5: Conclusions and Future Directions

Conclusions

Uropathogenic *Escherichia coli* (UPEC) is one of the most prevalent human pathogens, causing about 80% of urinary tract infections (UTI) in the world. To establish an infection in the bladder, UPEC must survive in the gastrointestinal tract and genitourinary tract. Traversing these bodily niches presents significant stressors to UPEC, including acidic pH stress. UPEC are equipped with multiple acid resistance mechanisms, however, the role these systems play during UTIs has not been elucidated. Understanding how UPEC survives in the human host is critical for the development of new antimicrobials to prevent or treat UTIs.

In this work, I describe a new acid resistance mechanism in UPEC that utilizes serine deamination. Through *in vitro* methods, I determined that loss of serine deamination leads to reduced survival in acidic media conditions. I show that serine is imported by UPEC under acidic media conditions to mediate this survival. This novel acid resistance mechanism is important for the activation of a cross-regulating two-component system, BtsS-YpdB. Through RNAseq analyses, I showed that BtsS-YpdB crosstalk is involved in regulating cysteine metabolism in acidic conditions, providing additional evidence of how acidic conditions impact cellular metabolism.

Additionally, through systematic deletion of UPEC's acid resistance mechanism genes, I determined that lysine decarboxylation plays a key role in early bladder colonization. During bladder cell infection, the lysine decarboxylase, *cadA,* is upregulated in UPEC. Deletion of *cadA* reduces UPEC's ability to survive within bladder cells compared to wildtype strains. Collectively, this work helps to elucidate how UPEC utilizes its acid resistance mechanisms during infection and identifies lysine decarboxylation as a critical mechanism for early bladder colonization.

Future directions

My work has advanced our knowledge of how UPEC handles acidic pH stress during UTI pathogenesis but has opened up many questions. The following thoughts can serve as a roadmap for future investigations:

Project 1: Serine deamination as an acid tolerance mechanism in UPEC

In chapter 2, my results led me to propose that serine deamination can serve as an acidic pH tolerance mechanism for UPEC. To further support this claim, I believe it is important to perform studies concerning the fate of the ammonium produced in the serine deamination reaction. Ammonium buffering has been shown to be an effective acid resistance mechanism used by other bacteria. In *Helicobacter pylori*, urea is hydrolyzed to ammonia and carbon dioxide by urease enzymes.[135] In *Streptococcus, Lactobacillus,* and *Pseudomonas spp.*, arginine deiminases produce ammonia and citrulline.[198,199] In *E. coli*, glutamine deamination by YbaS results in the production of ammonia and glutamate.[86,87] In all of these instances, the ammonia that is produced has been shown to play a proton consuming role inside of the cell. In this project, I propose to clarify how serine deamination is acting as an acid tolerance mechanism in UPEC.

Aim 1. Determine the amount of ammonia produced through serine deamination under acidic conditions

In acidic conditions, ammonia (NH_3) has a high affinity for protonation and will become ammonium (NH_4^+) Ammonia is also the preferred nitrogen source for *E. coli* and constitutes an important metabolite as an energy source. Understanding how much ammonia/ammonium is produced while under acid stress could give insight as if the production of ammonia as a downstream product of acid tolerance could also be beneficial in nutrient acquisition as well. I

propose to quantify ammonium produced by serine deamination under acidic conditions by comparing WT to the Δ*sdaA*Δ*sdaB* mutant grown in acidified media in the presence or absence of excess serine. To measure ammonium, I would use an ammonium ion probe. Alternatively, it is possible to measure ammonia/ammonium by HPLC. Understanding the amount of ammonium produced will give us a clearer mechanism for ammonia buffering by serine deamination.

Aim 2. Elucidate the role of ammonia in pH neutralization

To determine if Sda-mediated serine de-amination serves to neutralize the bacterial cell cytosol under conditions of mild acid stress, I propose to track pH changes in the wild-type and isogenic Δ*sda* strains, using a previously validated fluorimetry approach.[200,201] Specifically, I propose to use a derivative of green fluorescent protein (GFP), GFPmut3[202] in a commercially available plasmid. The pH dependence of fluorescence intensity is based on protonation of the phenolate moiety of the fluorophore; this exchange reaction occurs in less than a millisecond, facilitating the measurement of the cellular rate of pH change in response to a rapid shift in extracellular pH.[200,203] The plasmid containing GFPmut3 will be introduced in the wildtype and Δ*sdaA*Δ*sdaB* strains. Bacterial cytoplasmic pH measurements can be performed as previously described[203] under acidic or buffered conditions with or without supplemented serine. In addition to fluorimetry, pH-dependent fluorescence of cells can be tracked by microscopy to determine if signal is uniform within the population.

In parallel, I propose isotope labeling to track the fate of ammonia produced from serine deamination. Ammonium is a key source of nitrogen for bacteria. Nitrogen assimilation is critical for protein synthesis. I expect that some of the ammonia produced by serine deamination will be protonated then assimilated into other amino acids for protein synthesis. To test this, I propose

using nitrogen heavy isotope labeling to track where ammonia from serine gets incorporated. Completion of this project will support observations I made in chapter 2.

Project 2: Determine the contribution of each AR mechanism to UPEC fitness in the bladder

As discussed in chapter 3, I investigated the role of acid resistance mechanisms in early UPEC bladder colonization. I found that the lysine decarboxylation is important for intracellular bacterial survival. We speculate that the other acid resistance mechanisms are not expendable but are needed at different times during infection. For example, previous work by Jeff Purkerson has shown that the AR mechanisms that produce polyamines are important for UPEC colonization of the kidneys in a murine model of kidney acidosis.[102]

I also hypothesize that deletion of one or two acid resistance mechanisms in one strain may not be enough to uncover the necessity of AR systems for the establishment of infection. Future studies are planned with strains deficient in all but one AR mechanism, so no other system is able to compensate. Such experiments should provide more insight into how the AR systems are utilized during UTI.

Aim 1. Examine spatiotemporal dynamics in the phagolysosome during UTI

In Chapter 3, I showed that inhibition of phagolysosome formation rescued the Δ*cadA* and Δ*cadA*Δ*speF* mutants from intracellular bacterial burden. Utilizing confocal microscopy, I propose analyzing GFP producing WT or Δ*cadA* infected cells over time. Bladder cell staining with $LAMP^+$ and $Rab27^+$ markers would allow for colocalization of bacteria with the vacuole. Across the course of the infection, we could observe the entrance, proliferation, expansion, or lack thereof, of the bacteria within the vacuole. Additionally, I propose utilizing fluorescent reporters for other AR mechanisms to determine if other AR mechanisms are active within the vacuole.

Aim 2. Elucidate compensatory acid resistance systems in ΔcadA strain

In chapter 3, I discover that lysine decarboxylation is critical for early bladder colonization by UPEC. However, experiments with chronic mouse UTIs showed that over time, the Δ*cadA* mutant strain was able to catch up to WT levels of bacterial burden in the bladder, kidneys, and vagina **(Figure 41A-C)**. I also observed no difference in the mice's ability to resolve their UTIs. This led me to wonder if the other AR systems were becoming activated in the surviving bacteria to compensate for the loss of lysine decarboxylation.

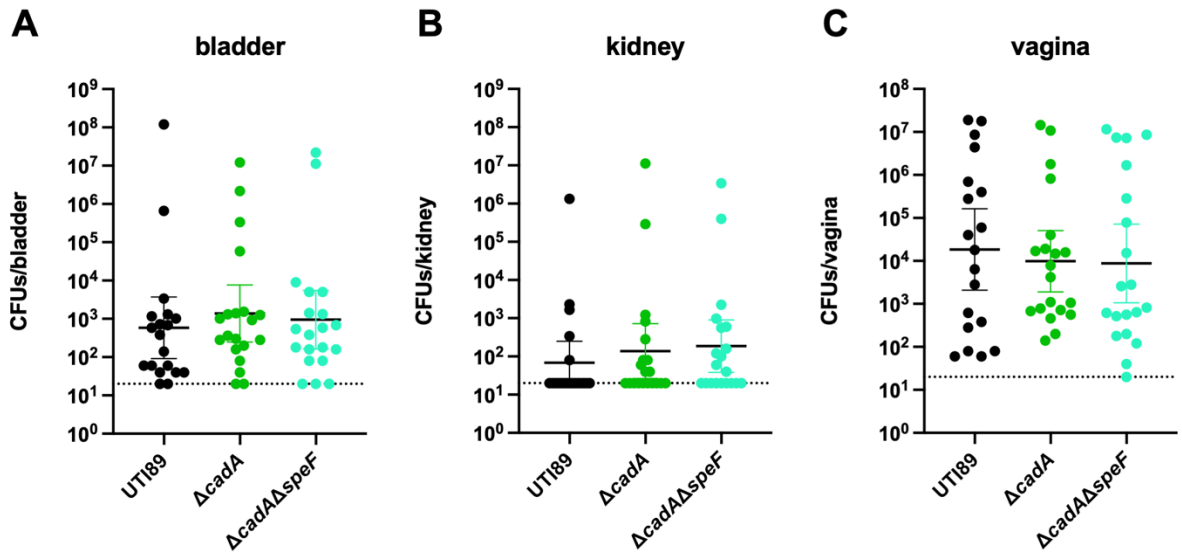

Figure 41. Chronic mouse model of UTI
To investigate the role of lysine decarboxylase on bacterial persistence, 6-8 week old female mice were transurethrally infected with 10^7 CFU of UTI89, Δ*cadA*, or Δ*cadA*Δ*speF.* Infections were allowed to continue for 28 days, after which bladders, kidneys, and vaginas were harvested and homogenized for CFU enumeration. (dashed line indicated limit of detection, N=20 mice per strain, ns by Mann-Whitney).

To address this question, I propose transcription profiling of Δ*cadA* bacterial RNA that has been isolated from infected bladder cells. I have begun to perform these transcriptional profiles *in vitro*. So far, I have concluded that Δ*cadA* grown in RPMI exhibits no difference in *gadA* or *speF* transcript abundance compared to WT cells **(Figure 42B and C)**. However, when I performed similar transcriptional analyses on cells that had been grown in LB, I observed that Δ*cadA* significantly upregulated *gadA* and *gadC* transcription compared to WT **(Figure 43A and B)**. I believe it would be worthwhile to perform these transcriptional profiles in bacteria that have infected bladder cells *in vitro* and in the mouse. As discussed in chapter 3, differences in *in vivo* and *in vitro* assays are not negligible due to differences in nutrient availability or immune responses. Therefore, differences in AR gene regulation may be observed under infection conditions. In parallel, I also propose utilizing fluorescent reporters of *gadA, gadB, adiA,* and *speF* to track activation of the system inside infected bladder cells. The Jung group recently utilized such fluorescent reporters to track AR system activation in *E. coli* cultured *in vitro*.[204]

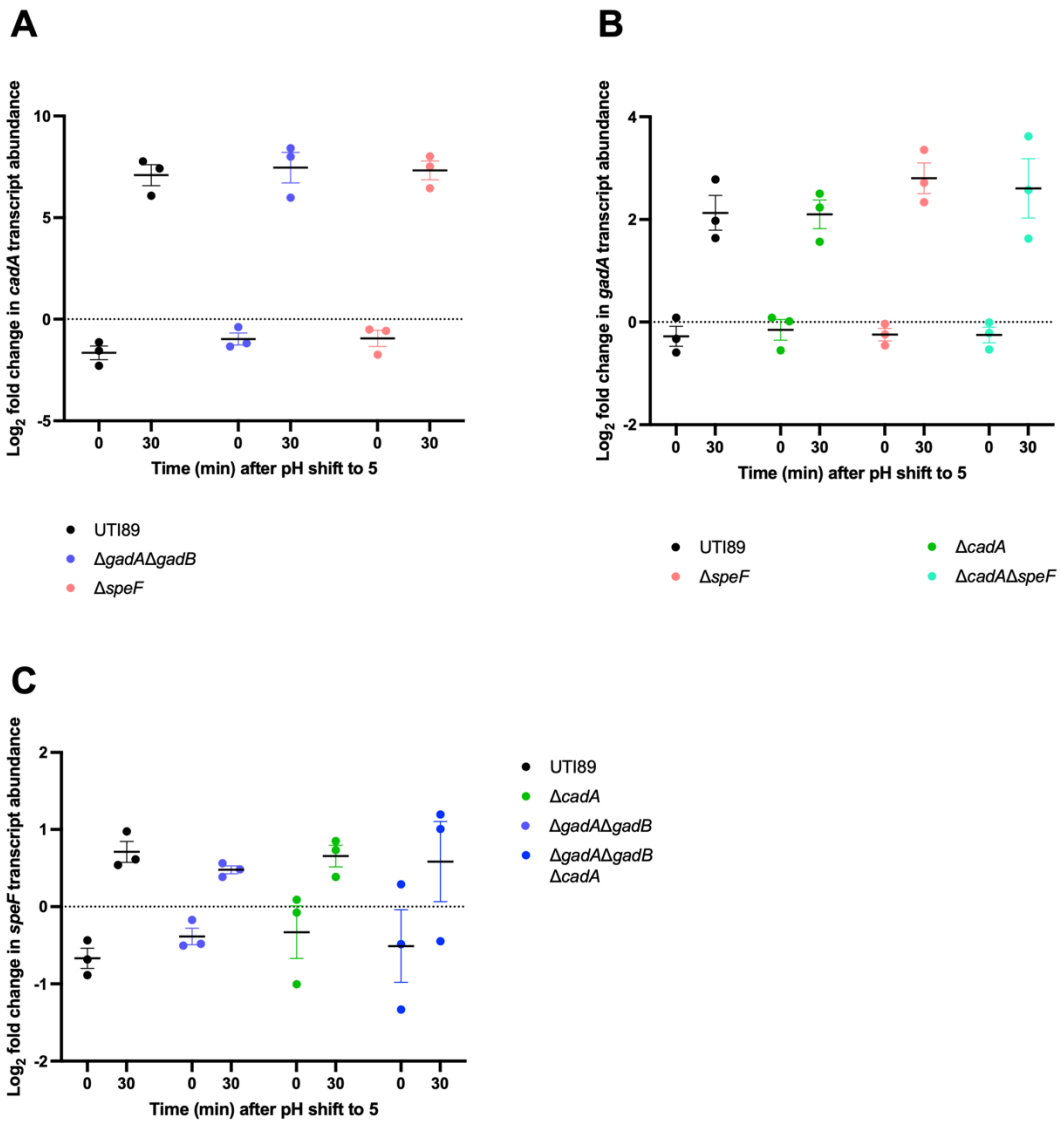

Figure 42. qPCR analysis of AR genes in various AR mutant backgrounds grown in RPMI
A) RT-qPCR analysis of *cadA* transcript abundance after acid stimulation (pH of 5) in WT, Δ*gadA*Δ*gadB*, and Δ*speF* strains grown in RPMI. B) RT-qPCR analysis of *gadA* transcript abundance after acid stimulation (pH of 5) in WT, Δ*cadA*, Δ*speF*, Δ*cadA*Δ*speF* strains grown in RPMI. C) RT-qPCR analysis of *speF* transcript abundance after acid stimulation (pH of 5) in WT, Δ*cadA*, Δ*gadA*Δ*gadB*, Δ*gadA*Δ*gadB*Δ*cadA* strains grown in RPMI. Relative fold change was determined by the $\Delta\Delta C_T$ method, where transcript abundances were normalized to *gyrB* housekeeping gene transcripts. Two-way ANOVA with Sidak's multiple comparisons test. Error bars indicate SEM of three biological replicates.

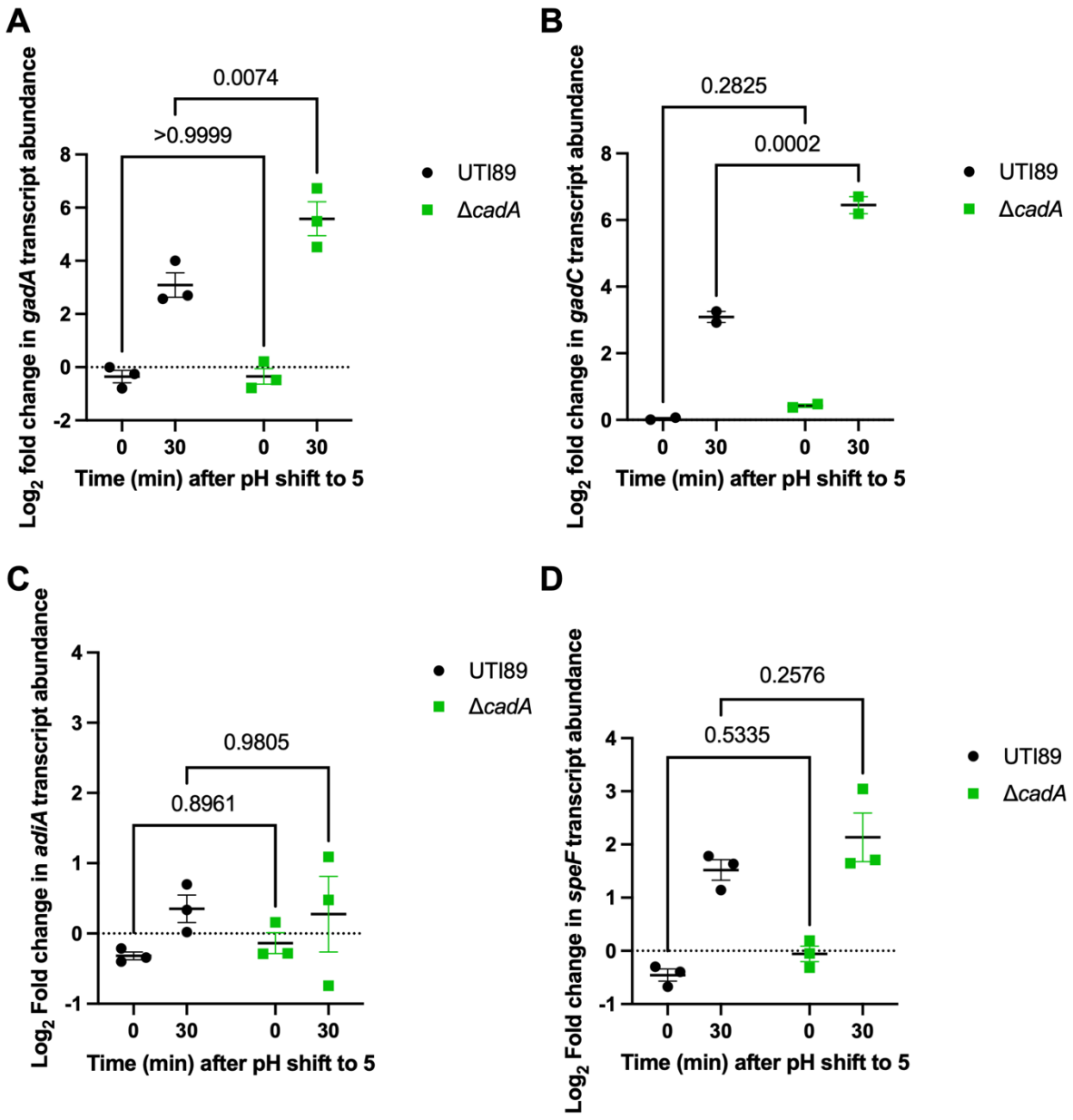

Figure 43. Δ*cadA* upregulates AR2 in acidified LB
RT-qPCR analysis of A) *gadA*, B) *gadC*, C) *adiA*, and D) *speF* transcript abundance after acid stimulation (pH of 5) in wild-type UTI89 (black) and Δ*cadA* (green) strains grown in LB. Relative fold change was determined by the $\Delta\Delta C_T$ method, where transcript abundances were normalized to *gyrB* housekeeping gene transcripts. Two-way ANOVA with Sidak's multiple comparisons test. Error bars indicate SEM of three biological replicates.

Project 3: Determine the role of UPEC acid resistance mechanisms in colonization of alternate host niches

My work in chapter 3 showed that in a UTI mouse model, *cadA* deletion impaired UPEC bladder colonization at early time points. During these acute experiments, I also enumerated bacterial CFUs from the kidneys and vaginas of the infected mice. Although I observed impairments in kidney colonization by some of the acid resistance system mutants **(Figure 44A)**, I did not see significant differences in the vagina **(Figure 44B)**. At first, this was unexpected because I predicted the vagina, which is more acidic than the bladder, to present a greater challenge to strains deficient in acid resistance. Upon further consideration, the lack of difference observed may be because any bacteria that were able to colonize the vagina were pre-exposed to a challenging environment in the bladder and this pre-exposure may have primed the bacteria to better adapt when they reached the vagina. The current mouse model of UTI is reliable and tractable model for cystitis and pyelonephritis caused by UPEC. This model involves the direct instillation of bacteria into the bladders of female mice through transurethral catheterization. One of the limitations of the mouse model used for these UTI studies is direct instillation of bacteria into the bladder. By bypassing the gut and vagina, the model may be missing potential bottlenecks to bladder colonization that are exacerbated in the AR system mutant strains. To test this hypothesis, I propose the following experiments:

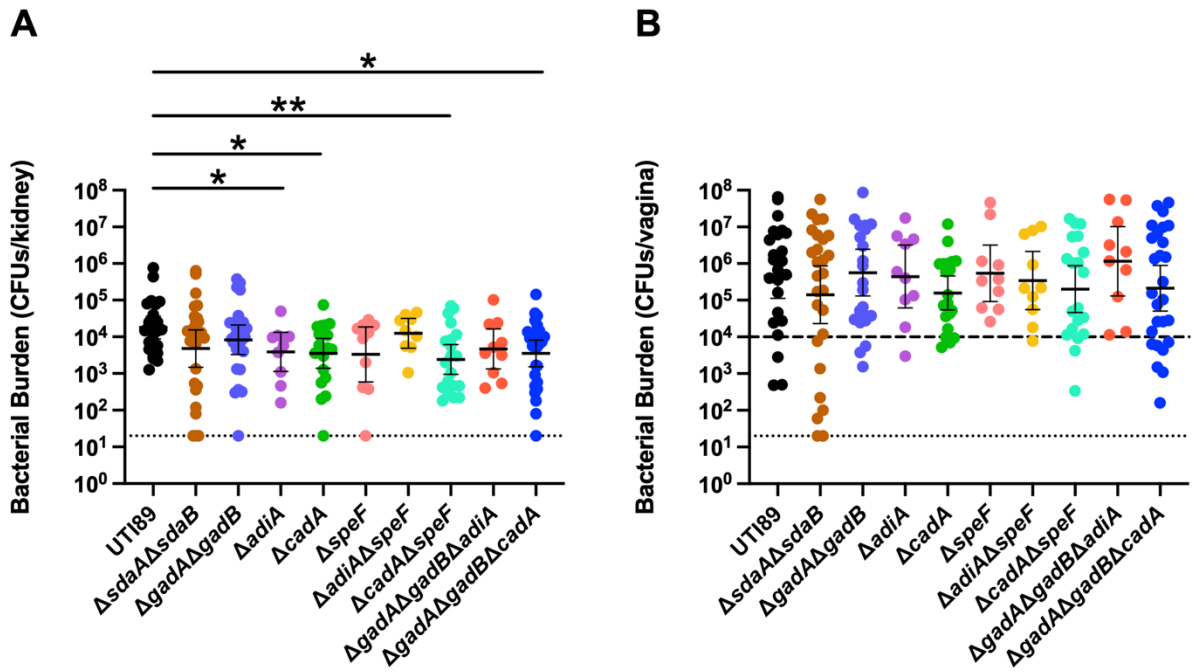

Figure 44. Deletion of AR mechanisms reduces bacterial burden in kidneys but not vagina
To investigate the role of AR mechanisms in organ colonization during acute UTI, female mice were in fected with 10^7 CFU of UTI89 or an isogenic AR deletion mutant. Mice were sacrificed 24 hours post infection and organs were harvested, homogenized, and plated for CFU enumeration. A) Δ*adiA*, Δ*cadA*, Δ*cadA*Δ*speF*, and Δ*gadA*Δ*gadB*Δ*cadA* were all significantly decreased in the kidney compared to UTI89 (dashed line indicates limit of detection, ns by Mann-Whitney). B) No significant differences between WT and any of the AR mutant strains was observed in the vagina (upper dashed line indicates threshold for chronicity, lower dashed line indicates limit of detection, ns by Mann-Whitney).

Aim 1. Determine the role of acid resistance in the ability to traverse the gut-bladder axis

We understand that in human UTIs, many of the infections originate from bacteria that traverse the gastrointestinal and urogenital tract to colonize the bladder. To date, it has been challenging to develop a mouse model of UTI that recapitulates the natural infection process. Some of the factors that have hindered this development include early clearance of UPEC and colonization resistance in the gut due to the mouse microbiome. Students in our lab are currently working to establish a gut colonization model of UTI. We have observed that mice from different vendors have different microbiome compositions. Mice from Jackson Labs, which are

Enterobacteriaceae free, allowed for more robust gut colonization by UPEC. These mice were also observed to have UPEC present in their urine, indicating that it is possible for them to develop UTIs following oral gavage with UPEC (Bermudez, T. A., et al., unpublished). Work to optimize a gut colonization mouse model of UTI is still ongoing. If a reliable and reproducible model is developed, I believe infecting mice orally with my AR system deletion mutants will struggle to colonize both the gut and urinary tract due to their reduced ability to combat the acid stress experienced from exposure to stomach acid and SCFAs in the intestines.

Aim 2. Determine the role of acid resistance in the ability of UPEC to navigate the female urogenital tract

Our lab has previously shown that bacteria instilled in the mouse vagina can traverse the urinary tract and cause UTI.[143] In future studies I propose comparing bladder colonization rates after vaginal instillation of the AR mutants I have generated to WT UTI89. One of the potential pitfalls for this project is that our established mouse model, conventionally reared C3H/HeN mice, are devoid of *Lactobacilli* and the murine vaginal pH is maintained low by the action of *Enterococci*. In the human vaginal microbiome, *Lactobacillus spp.* are the dominant community members that acidify the environment with lactic acid. So, while our mouse model can be used to investigate vaginal colonization followed by UPEC egress, the pH may be higher than what is observed in humans. Other labs have addressed this concern with the use of mice with humanized vaginal microbiomes. In the gnotobiotic background we can mono-colonize mice with human-associated urogenital *Lactobacilli* and observe how the induction of ARs changes and how our corresponding mutants behave in the presence of *Lactobacilli* within the host. The use of the

gnotobiotic mice is also critical to elucidate the baseline induction of the AR systems in a mouse model that lacks microbiota in the vaginal niche.

Project 4: Elucidate the function of cysteine metabolism during acid stress

In chapter 4, I discovered that *cysB* regulated genes were highly upregulated in Δ*btsS*Δ*ypdB*. It is still unclear whether activated YpdB directly represses *cysB* transcription, or if the induction of the CysB regulon occurs due to increased levels of H_2O_2 in the mutant cells. To begin to investigate how YpdB controls cysteine metabolism, I have performed site directed mutagenesis to change the phospho-accepting aspartate to a glutamate (YpdB_D59E) **(Figure 45)**. Such a mutation is phosphomimetic, so the YpdB_D59E variant protein should behave as a constitutively active protein. I performed the luminescence reporter assay in which the promoter for the target gene of YpdB is fused to the *luxCDABE* operon and monitored luminescence over time in UTI89 expressing the WT form of YpdB and in UTI89 expressing the D59E mutant version of YpdB **(Figure 45)**. My data indicate that this variant protein induces a higher luminescence peak compared to the WT control. To determine how YpdB is regulating *cysB* I propose the following experiments:

Aim 1. Elucidate if YpdB *directly regulates cysB*

To begin to investigate how YpdB controls cysteine metabolism, I propose performing qPCR assessing the transcript levels of *cysB* and CysB target genes (*cysK, cysA, cysI, cysD*) in the Δ*btss*Δ*ypdB* strain harboring pBAD_YpdB_D59E, a plasmid that expresses a mutant version of YpdB that mimics constitutively active YpdB. I would expect that in this strain there would be robust downregulation of *cysB* and its targets. I have also used site directed mutagenesis to generate *ypdB* with a D59A mutation. This mutation will produce a constitutively inactive version of YpdB

because the aspartate has been mutated to alanine, which is unable to become phosphorylated. I propose performing qPCR assessing the transcript levels of CysB in the Δ*btss*Δ*ypdB* strain harboring pBAD_YpdB_D59A. I expect if YpdB is repressing *cysB*, then the YpdB D59A mutant strain will have much higher *cysB* transcript compared to WT. In parallel, electrophoretic mobility shift assay (EMSA) analyses can be performed to determine if YpdB can bind to the *cysB* promoter region.

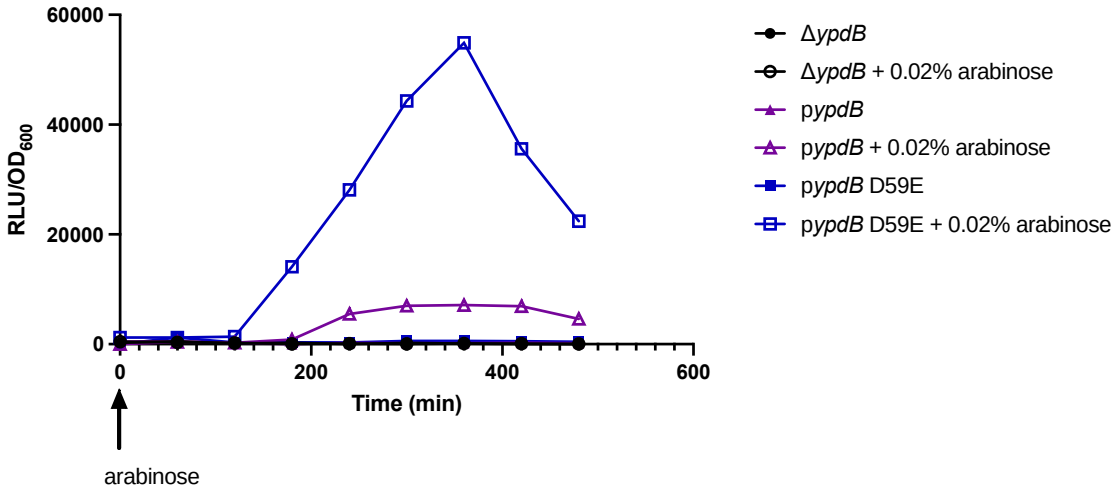

Figure 45. YpdB_D59E results in elevated *yhjX* expression
UTI89 Δ*ypdB* containing the *yhjX* luminescence reporter plasmid and empty vector pBAD plasmid (black), *ypdB* complemented on the pBAD plasmid (purple), or *ypdB*_D59E complemented on the pBAD plasmid (blue) was cultured in LB and luminescence and OD_{600} were measured every hour and luminescence normalized to OD_{600} is plotted. Graph is a representative of three biological replicates.

Aim 2. Investigate cysteine metabolism as a novel acid resistance regulator

Cysteine is a sulfur containing amino acid and plays an important role in protein structure due to its ability to form disulfide bonds. Cysteine is also the main way sulfur becomes available for cells for iron-sulfur cluster containing proteins. Additionally, cysteine is the main substrate providing sulfur for coenzyme-A and methionine biosynthesis. Cysteine metabolism has been

shown to play a role in relieving oxidative stress in bacteria. Cysteine can react with H_2O_2 in the periplasm to produce H_2O and cystine, thus preventing H_2O_2 from participating in harmful Fenton reactions in the cell.[197]

Additionally, previous literature has shown that CysB, the transcriptional regulator of cysteine metabolism genes, also works in concert with AdiY to regulate responses to acidic pH.[205,206] Given these two stress responses involve cysteine metabolism, I would want to determine if cysteine metabolism genes upregulated in the Δ*btsS*Δ*ypdB* as a way for the cell to combat acidic pH stress. To address this question, I propose performing acid resistance assays as described in Chapter 2 with UTI89 and mutant strains with deletions in the *cysB* regulon. In parallel, I propose analyzing transcript abundance of AR genes in *cysB* deletion background.

Project 5: Cross regulation between acidic pH sensing two-component systems

In chapter 4, I determined that Btss, EvgA, and PhoP all impact *yhjX* expression, presumably due to their interaction/activation of YpdB. Histidine kinase interactions with noncognate response regulators have been reported before. Such cross regulation between two-component systems allows bacteria to activate multiple responses. This led me to question whether these noncognate histidine kinases are able to phosphotransfer to YpdB.

To elucidate the determinants that enable BtsS, EvgA, and PhoP to interact with YpdB, I propose to subject BtsS, EvgA, or PhoP-enriched membrane fractions to phosphotransfer assays with YpdB in the presence of pyruvate, HCl, or lactic acid in buffered or unbuffered conditions. I selected hydrochloric acid because *E. coli* encounters this acid during its transit through the stomach following ingestion. I selected lactic acid, given that it is produced by *Lactobacillus* species in the vagina of female humans, a recently appreciated niche for recurrent UTI.[11,26,143] In

parallel to using the WT proteins, I will evaluate YpdB variants that lack the phospho-accepting aspartate as a control, given that this interaction should yield no phosphorylated protein.

It is however possible to not observe phosphotransfer from BtsS to YpdB, as it has previously been experienced for other LytS-type histidine kinases.[207] Unlike canonical histidine kinases, BtsS and other LytS-type histidine kinases have a mutation in the G1 box of the ATP binding domain that could prevent the ability to phosphotransfer.[127,179] Notably, two accessory genes – *ypdC* and *yehT* – are co-transcribed with *btsS* and *ypdB* and harbor domains that could facilitate phosphotransfer. If BtsS-YpdB phosphotransfer is not observed in this proposed study, experiments can be repeated in the presence of purified YpdC or YehT (constructs already made). BtsS-loaded membrane fractions will be incubated with γ-^{32}P labeled ATP plus YpdC or YehS and autokinase/phosphotransfer activities of BtsS will be resolved by PAGE and and phosphor-imaging as I previously described.[150,208-210]

An alternate approach to determine if interaction occurs between BtsS and YpdB is to use a bacterial two-hybrid system in a *cya* deficient strain of UTI89. I would express a fusion of the histidine dimerization domain of BtsS to one fragment of the adenylyl cyclase protein (T25). I would also express a fusion of the receiver domain of YpdB to the other fragment of the adenylyl cyclase protein (T18).[211] If BtsS and YpdB interact, Cya function will be restored, cAMP will be produced, bind to CAP, and lacZ will be transcribed. LB indicator plates containing x-gal will be used to screen transformants for BtsS – YpdB interaction. If an interaction is detected, SDM will be utilized to alter residues surrounding the conserved histidine of BtsS or the conserved aspartate of YpdB in an attempt to prevent their interaction. This SDM will allow me to determine residues that are important for allowing cross-regulation between the BtsSR and YpdAB systems.

Final Thoughts

The work I have presented in this thesis and proposed future studies improve our understanding of how UPEC senses and responds to environmental stresses, specifically pH stress. Furthering these studies is necessary for increasing our ability to develop novel targets to prevent and treat UTI.

Appendix

A. Genes significantly downregulated in WT UTI89 60 minutes after HCl exposure compared to WT at 0 minutes

gene symbol	locus	sample_1	sample_2	value_1	value_2	log2(fold_cha	test_stat	p_value	q_value	logq
ydjN	NC_007946:1	0	60hcl	1012.97	44.6577	-4.50354	-8.71985	5.00E-05	0.00022207	3.65351206
entD	NC_007946:5	0	60hcl	269.354	12.9831	-4.3748	-8.52189	5.00E-05	0.00022207	3.65351206
ndh	NC_007946:1	0	60hcl	771.48	41.1265	-4.22949	-8.0963	5.00E-05	0.00022207	3.65351206
ybdB	NC_007946:6	0	60hcl	433.264	24.6421	-4.13605	-7.89896	5.00E-05	0.00022207	3.65351206
cysI	NC_007946:3	0	60hcl	249.168	15.4251	-4.01376	-8.1828	5.00E-05	0.00022207	3.65351206
nirB	NC_007946:3	0	60hcl	154.754	10.1375	-3.9322	-3.66828	5.00E-05	0.00022207	3.65351206
entB	NC_007946:6	0	60hcl	2744.24	188.889	-3.86079	-7.14822	5.00E-05	0.00022207	3.65351206
ybiX	NC_007946:8	0	60hcl	144.831	10.5512	-3.77889	-7.3384	5.00E-05	0.00022207	3.65351206
ycfJ	NC_007946:1	0	60hcl	629.723	46.5356	-3.75831	-7.28849	5.00E-05	0.00022207	3.65351206
chuU	NC_007946:3	0	60hcl	438.005	34.6317	-3.66078	-7.30618	5.00E-05	0.00022207	3.65351206
yhdX	NC_007946:3	0	60hcl	106.3	8.42004	-3.65817	-6.97661	5.00E-05	0.00022207	3.65351206
entE	NC_007946:6	0	60hcl	555.541	44.2327	-3.65071	-7.02524	5.00E-05	0.00022207	3.65351206
fepA	NC_007946:5	0	60hcl	1014.79	80.9692	-3.64767	-6.89989	5.00E-05	0.00022207	3.65351206
yhdY	NC_007946:3	0	60hcl	96.663	8.08561	-3.57953	-6.6247	5.00E-05	0.00022207	3.65351206
	NC_007946:5	0	60hcl	602.66	51.2267	-3.55638	-5.4987	5.00E-05	0.00022207	3.65351206
yhiF	NC_007946:3	0	60hcl	46.1473	3.97727	-3.5364	-5.91664	5.00E-05	0.00022207	3.65351206
rpmD	NC_007946:3	0	60hcl	2478.63	214.902	-3.52779	-5.09053	5.00E-05	0.00022207	3.65351206
yifB	NC_007946:4	0	60hcl	154.681	13.8966	-3.47649	-6.74313	5.00E-05	0.00022207	3.65351206
cysH	NC_007946:3	0	60hcl	112.845	10.1968	-3.46815	-6.73484	5.00E-05	0.00022207	3.65351206
cirA	NC_007946:2	0	60hcl	1119.78	103.582	-3.43438	-6.33751	5.00E-05	0.00022207	3.65351206
intD	NC_007946:5	0	60hcl	209.482	19.6416	-3.41485	-6.0498	5.00E-05	0.00022207	3.65351206
pdhR	NC_007946:1	0	60hcl	1119.46	109.561	-3.353	-5.99961	5.00E-05	0.00022207	3.65351206
ybiL	NC_007946:8	0	60hcl	376.425	36.9397	-3.34912	-6.35009	5.00E-05	0.00022207	3.65351206
ybaA	NC_007946:4	0	60hcl	1809.33	179.288	-3.3351	-5.52178	5.00E-05	0.00022207	3.65351206
cysD	NC_007946:3	0	60hcl	38.048	3.85079	-3.3046	-6.16746	5.00E-05	0.00022207	3.65351206
	NC_007946:4	0	60hcl	66.3745	6.76266	-3.29497	-4.53656	5.00E-05	0.00022207	3.65351206
entC	NC_007946:6	0	60hcl	599.103	63.3098	-3.2423	-6.278	5.00E-05	0.00022207	3.65351206
yafT	NC_007946:2	0	60hcl	799.125	85.0017	-3.23286	-5.60632	5.00E-05	0.00022207	3.65351206
chuW	NC_007946:3	0	60hcl	229.698	24.6964	-3.21737	-6.16879	5.00E-05	0.00022207	3.65351206
entF	NC_007946:5	0	60hcl	500.527	55.2158	-3.18029	-2.10148	5.00E-05	0.00022207	3.65351206
aceE	NC_007946:1	0	60hcl	6588.2	726.91	-3.18004	-4.30673	5.00E-05	0.00022207	3.65351206
chuX	NC_007946:3	0	60hcl	926.396	106.861	-3.11589	-6.05699	5.00E-05	0.00022207	3.65351206
yjjQ	NC_007946:4	0	60hcl	79.8445	9.33609	-3.0963	-5.64287	5.00E-05	0.00022207	3.65351206
yhfC	NC_007946:3	0	60hcl	454.313	53.7334	-3.07979	-5.59385	5.00E-05	0.00022207	3.65351206
nirC	NC_007946:3	0	60hcl	38.1424	4.56784	-3.06181	-5.69413	5.00E-05	0.00022207	3.65351206
fis	NC_007946:3	0	60hcl	3438.18	417.964	-3.04019	-5.58696	5.00E-05	0.00022207	3.65351206
	NC_007946:1	0	60hcl	519.419	64.7938	-3.00297	-5.85662	5.00E-05	0.00022207	3.65351206
appA	NC_007946:1	0	60hcl	494.813	62.6347	-2.98185	-4.888	5.00E-05	0.00022207	3.65351206
rpsT	NC_007946:2	0	60hcl	1706.4	216.09	-2.98125	-4.46152	5.00E-05	0.00022207	3.65351206
tfaQ	NC_007946:5	0	60hcl	49.4379	6.27278	-2.97844	-4.67188	5.00E-05	0.00022207	3.65351206
ackA	NC_007946:2	0	60hcl	1871.44	247.24	-2.92017	-5.09483	5.00E-05	0.00022207	3.65351206
cysA	NC_007946:2	0	60hcl	310.412	41.8969	-2.88927	-5.66522	5.00E-05	0.00022207	3.65351206
yjaA	NC_007946:4	0	60hcl	240.685	33.0703	-2.86354	-4.78765	5.00E-05	0.00022207	3.65351206
yfgJ	NC_007946:2	0	60hcl	127.749	17.7748	-2.84541	-3.98589	5.00E-05	0.00022207	3.65351206
yfaZ	NC_007946:2	0	60hcl	292.921	41.5611	-2.81721	-5.38312	5.00E-05	0.00022207	3.65351206
	NC_007941:5	0	60hcl	70.7729	10.1722	-2.79857	-3.70798	5.00E-05	0.00022207	3.65351206
	NC_007946:4	0	60hcl	226.595	32.8965	-2.78411	-4.9638	5.00E-05	0.00022207	3.65351206
aceF	NC_007946:1	0	60hcl	10002.6	1452.28	-2.784	-3.5279	5.00E-05	0.00022207	3.65351206
	NC_007946:2	0	60hcl	310.184	46.7565	-2.72989	-5.5454	5.00E-05	0.00022207	3.65351206
yhiM	NC_007946:3	0	60hcl	14.6098	2.20327	-2.72922	-4.83602	5.00E-05	0.00022207	3.65351206
yjfI	NC_007946:4	0	60hcl	14.0224	2.14103	-2.71136	-3.46646	5.00E-05	0.00022207	3.65351206
gspM	NC_007946:3	0	60hcl	126.287	19.3779	-2.70422	-4.98484	5.00E-05	0.00022207	3.65351206
priB	NC_007946:4	0	60hcl	8477.45	1343.22	-2.65794	-4.60097	5.00E-05	0.00022207	3.65351206
aslB	NC_007946:4	0	60hcl	169.825	26.9217	-2.65721	-4.80791	5.00E-05	0.00022207	3.65351206
ykiA	NC_007946:4	0	60hcl	96.6652	15.5355	-2.63743	-4.5083	5.00E-05	0.00022207	3.65351206
ydcX	NC_007946:1	0	60hcl	41.3977	6.68777	-2.62995	-3.43822	5.00E-05	0.00022207	3.65351206
ydfZ	NC_007946:1	0	60hcl	49.4758	8.11046	-2.60887	-2.98982	5.00E-05	0.00022207	3.65351206
gspG	NC_007946:3	0	60hcl	158.106	25.9207	-2.60871	-4.9256	5.00E-05	0.00022207	3.65351206
tdcR	NC_007946:3	0	60hcl	13.5378	2.22042	-2.6081	-3.00915	5.00E-05	0.00022207	3.65351206
fimG	NC_007946:1	0	60hcl	91.1723	14.9744	-2.6061	-4.11122	5.00E-05	0.00022207	3.65351206
fhuC	NC_007946:1	0	60hcl	2062.28	339.638	-2.60217	-3.80253	5.00E-05	0.00022207	3.65351206
yebB	NC_007946:1	0	60hcl	14.5757	2.43287	-2.58284	-3.87506	5.00E-05	0.00022207	3.65351206
chuT	NC_007946:3	0	60hcl	170.595	28.6988	-2.57151	-5.11426	5.00E-05	0.00022207	3.65351206
chuA	NC_007946:3	0	60hcl	454.828	76.6124	-2.56967	-5.06036	5.00E-05	0.00022207	3.65351206
atpI	NC_007946:4	0	60hcl	1625.13	275.786	-2.55894	-4.68063	5.00E-05	0.00022207	3.65351206
aslA	NC_007946:4	0	60hcl	35.5968	6.08796	-2.54772	-4.89376	5.00E-05	0.00022207	3.65351206
gspL	NC_007946:3	0	60hcl	368.189	63.0083	-2.54683	-4.23885	5.00E-05	0.00022207	3.65351206
yhhQ	NC_007946:3	0	60hcl	49.3797	8.47272	-2.54302	-4.79915	5.00E-05	0.00022207	3.65351206

yhdZ	NC_007946:3	0	60hcl	87.8343	15.0978	-2.54045	-4.94945	5.00E-05	0.00022207	3.65351206
gspI	NC_007946:3	0	60hcl	338.944	59.0285	-2.52157	-4.5407	5.00E-05	0.00022207	3.65351206
metA	NC_007946:4	0	60hcl	128.607	22.6354	-2.50632	-4.82412	5.00E-05	0.00022207	3.65351206
pspG	NC_007946:4	0	60hcl	489.493	86.6049	-2.49877	-4.24257	5.00E-05	0.00022207	3.65351206
yjeN	NC_007946:4	0	60hcl	50.0509	8.88131	-2.49455	-3.97345	5.00E-05	0.00022207	3.65351206
yegD	NC_007946:2	0	60hcl	401.153	71.6815	-2.48448	-4.47616	5.00E-05	0.00022207	3.65351206
yfcC	NC_007946:2	0	60hcl	66.9498	12.046	-2.47452	-4.77955	5.00E-05	0.00022207	3.65351206
yjcB	NC_007946:4	0	60hcl	117.065	21.6914	-2.43211	-4.20757	5.00E-05	0.00022207	3.65351206
	NC_007946:1	0	60hcl	59.5414	11.1438	-2.41765	-4.30303	5.00E-05	0.00022207	3.65351206
ansP	NC_007946:1	0	60hcl	347.005	65.3688	-2.40828	-4.74501	5.00E-05	0.00022207	3.65351206
yjeO	NC_007946:4	0	60hcl	157.824	29.8848	-2.40083	-4.57107	5.00E-05	0.00022207	3.65351206
fliQ	NC_007946:2	0	60hcl	252.808	48.5379	-2.38086	-4.52649	5.00E-05	0.00022207	3.65351206
cysC	NC_007946:3	0	60hcl	116.787	22.7666	-2.35889	-4.13289	5.00E-05	0.00022207	3.65351206
cspG	NC_007946:1	0	60hcl	6475.44	1287.32	-2.33061	-4.59985	5.00E-05	0.00022207	3.65351206
	NC_007946:1	0	60hcl	373.097	74.1826	-2.3304	-3.98638	5.00E-05	0.00022207	3.65351206
rhuM	NC_007946:4	0	60hcl	332.579	66.8876	-2.31388	-4.60927	5.00E-05	0.00022207	3.65351206
ygfE	NC_007946:3	0	60hcl	960.584	194.03	-2.30763	-4.69278	5.00E-05	0.00022207	3.65351206
ycgX	NC_007946:1	0	60hcl	21.056	4.3106	-2.28827	-3.43126	5.00E-05	0.00022207	3.65351206
	NC_007946:1	0	60hcl	40.6597	8.32837	-2.28749	-3.39727	5.00E-05	0.00022207	3.65351206
yqhH	NC_007946:3	0	60hcl	81.8688	16.9531	-2.27177	-3.61427	5.00E-05	0.00022207	3.65351206
yjeB	NC_007946:4	0	60hcl	3207.19	666.988	-2.26558	-4.18865	5.00E-05	0.00022207	3.65351206
	NC_007946:2	0	60hcl	35.8251	7.4802	-2.25982	-4.15431	5.00E-05	0.00022207	3.65351206
rpmB	NC_007946:4	0	60hcl	3294.84	692.84	-2.24962	-3.83231	5.00E-05	0.00022207	3.65351206
ecpD	NC_007946:1	0	60hcl	8.39385	1.77934	-2.23799	-3.32439	5.00E-05	0.00022207	3.65351206
yjfK	NC_007946:4	0	60hcl	10.5532	2.24834	-2.23075	-3.50449	5.00E-05	0.00022207	3.65351206
slyX	NC_007946:3	0	60hcl	121.745	26.0956	-2.22198	-3.39916	5.00E-05	0.00022207	3.65351206
yhdG	NC_007946:3	0	60hcl	2938.2	630.58	-2.22018	-3.61943	5.00E-05	0.00022207	3.65351206
rpsR	NC_007946:4	0	60hcl	4055.71	873.326	-2.21536	-4.17893	5.00E-05	0.00022207	3.65351206
ydgQ	NC_007946:1	0	60hcl	932.402	202.893	-2.20023	-4.18238	5.00E-05	0.00022207	3.65351206
ycfR	NC_007946:1	0	60hcl	86.4545	18.8539	-2.19708	-3.73757	5.00E-05	0.00022207	3.65351206
yihF	NC_007946:4	0	60hcl	50.0977	10.9548	-2.19318	-4.43413	5.00E-05	0.00022207	3.65351206
	NC_007946:2	0	60hcl	332.259	73.2808	-2.1808	-4.14674	5.00E-05	0.00022207	3.65351206
fhuE	NC_007946:1	0	60hcl	30.6018	6.79317	-2.17146	-4.40303	5.00E-05	0.00022207	3.65351206
yhdW	NC_007946:3	0	60hcl	39.6096	8.79311	-2.17141	-4.20629	5.00E-05	0.00022207	3.65351206
yeeF	NC_007946:2	0	60hcl	938.024	209.794	-2.16065	-3.44686	5.00E-05	0.00022207	3.65351206
	NC_007946:3	0	60hcl	833.417	186.939	-2.15647	-4.34345	5.00E-05	0.00022207	3.65351206
yaaH	NC_007946:9	0	60hcl	241.712	55.142	-2.13207	-4.26218	5.00E-05	0.00022207	3.65351206
	NC_007946:2	0	60hcl	290.813	66.8989	-2.12004	-4.24479	5.00E-05	0.00022207	3.65351206
pin	NC_007946:9	0	60hcl	25.2531	5.82594	-2.1159	-3.70307	5.00E-05	0.00022207	3.65351206
	NC_007946:1	0	60hcl	13.7952	3.25592	-2.08304	-2.95997	5.00E-05	0.00022207	3.65351206
cspA	NC_007946:3	0	60hcl	89168.1	21059.3	-2.08207	-3.55617	5.00E-05	0.00022207	3.65351206
ybdO	NC_007946:6	0	60hcl	3.08833	0.735864	-2.06932	-2.74044	5.00E-05	0.00022207	3.65351206
ydgI	NC_007946:1	0	60hcl	228.219	55.0799	-2.05082	-3.74435	5.00E-05	0.00022207	3.65351206
ycgF	NC_007946:1	0	60hcl	83.5674	20.1759	-2.05031	-4.05195	5.00E-05	0.00022207	3.65351206
rpsN	NC_007946:3	0	60hcl	22800.9	5542.75	-2.04042	-3.57926	5.00E-05	0.00022207	3.65351206
	NC_007941:2	0	60hcl	537.919	130.805	-2.03997	-3.96081	5.00E-05	0.00022207	3.65351206
yhdJ	NC_007946:3	0	60hcl	52.8598	13.0116	-2.02237	-3.77443	5.00E-05	0.00022207	3.65351206
rnfD	NC_007946:1	0	60hcl	403.02	99.2276	-2.02204	-3.85392	5.00E-05	0.00022207	3.65351206
secG	NC_007946:3	0	60hcl	21000.7	5189.95	-2.01665	-3.52833	5.00E-05	0.00022207	3.65351206
fmlD	NC_007946:1	0	60hcl	19.4648	4.82841	-2.01125	-3.53852	5.00E-05	0.00022207	3.65351206
	NC_007946:1	0	60hcl	310.522	77.4334	-2.00367	-4.03993	5.00E-05	0.00022207	3.65351206
fhuA	NC_007946:1	0	60hcl	934.241	233.055	-2.00312	-3.7045	5.00E-05	0.00022207	3.65351206
recO	NC_007946:2	0	60hcl	377.679	94.3887	-2.00047	-3.79448	5.00E-05	0.00022207	3.65351206
ydeA	NC_007941:7	0	60hcl	38.7158	8.23543	-2.23301	-2.86234	0.0001	0.0004213	3.37540751
ybiN	NC_007946:8	0	60hcl	306.113	74.6925	-2.03503	-2.76157	0.0001	0.0004213	3.37540751
yjfY	NC_007946:4	0	60hcl	18.5381	2.93524	-2.65894	-2.75763	0.00015	0.00060833	3.21585862
	NC_007946:3	0	60hcl	6.15308	1.04176	-2.56228	-2.95538	0.00015	0.00060833	3.21585862
	NC_007946:1	0	60hcl	97.0051	9.62018	-3.33393	-4.15007	0.0003	0.0011257	2.94857733
	NC_007946:4	0	60hcl	47.8956	7.90898	-2.59833	-2.67289	0.0003	0.0011257	2.94857733
	NC_007946:2	0	60hcl	70.279	1.44679	-5.60217	-4.66394	0.0005	0.00175942	2.75463048
insAcp3	NC_007946:4	0	60hcl	28.6957	5.898	-2.28254	-2.66352	0.0006	0.00207315	2.68336927
ydgT	NC_007946:1	0	60hcl	29.0128	7.03548	-2.04397	-2.36029	0.0006	0.00207315	2.68336927
	NC_007946:2	0	60hcl	17.1879	3.95597	-2.11928	-2.44763	0.00075	0.00252622	2.59752883
	NC_007946:1	0	60hcl	73.6588	6.09911	-3.59419	-5.68591	0.00155	0.00485812	2.31353176
yhdV	NC_007946:3	0	60hcl	22.8091	2.50355	-3.18756	-4.39752	0.0025	0.00742419	2.12935092
	NC_007946:4	0	60hcl	6.25931	1.25884	-2.31391	-2.2434	0.00275	0.00806519	2.0933854
	NC_007946:2	0	60hcl	115.727	3.74953	-4.94787	-3.268	0.00285	0.008322	2.07977229
	NC_007946:4	0	60hcl	15.1047	3.65559	-2.04682	-1.6158	0.00925	0.0231683	1.63510583
	NC_007946:1	0	60hcl	16.7238	3.07089	-2.44518	-3.10156	0.01015	0.0250937	1.6004353
csgF	NC_007946:1	0	60hcl	2.77523	0.590521	-2.23255	-2.13398	0.0175	0.0400356	1.39755366

B. Genes significantly upregulated in WT UTI89 60 minutes after HCl exposure compared to WT at 0 minutes

gene symbol	function	locus	sample_1	sample_2	value_1	value_2	log2(fold_cha	test_stat	p_value	q_value	significant	logq
dapB	4-hydroxy-tet	NC_007946:3	0	60hcl	92.7861	371.396	2.00098	4.05831	5.00E-05	0.00022207	yes	3.65351206
kduI	4-deoxy-L-thr	NC_007946:3	0	60hcl	14.0602	56.4078	2.00428	3.99766	5.00E-05	0.00022207	yes	3.65351206
		NC_007946:4	0	60hcl	9.81773	39.5072	2.00866	3.18092	5.00E-05	0.00022207	yes	3.65351206
pntB	NAD(P) transh	NC_007946:1	0	60hcl	151.677	611.182	2.0106	3.9817	5.00E-05	0.00022207	yes	3.65351206
yeaD	Aldose 1-epim	NC_007946:1	0	60hcl	59.8989	241.542	2.01167	3.93204	5.00E-05	0.00022207	yes	3.65351206
		NC_007946:2	0	60hcl	5.94968	24.0015	2.01224	3.2392	5.00E-05	0.00022207	yes	3.65351206
hsdR	Type I restrict	NC_007946:4	0	60hcl	63.9254	260.391	2.02622	3.91283	5.00E-05	0.00022207	yes	3.65351206
	NAD-depende	NC_007946:1	0	60hcl	7.10215	29.0155	2.0305	3.83185	5.00E-05	0.00022207	yes	3.65351206
	hypothetical p	NC_007941:4	0	60hcl	1.58663	6.48674	2.03153	3.36578	5.00E-05	0.00022207	yes	3.65351206
aphA	NMN phospha	NC_007946:4	0	60hcl	46.1308	188.625	2.03172	3.89764	5.00E-05	0.00022207	yes	3.65351206
frwB	PTS system, fr	NC_007946:4	0	60hcl	5.96294	24.4075	2.03323	2.83787	5.00E-05	0.00022207	yes	3.65351206
ydiP	Uncharacteriz	NC_007946:1	0	60hcl	3.72368	15.3434	2.04282	3.69896	5.00E-05	0.00022207	yes	3.65351206
ygjG	Putrescine am	NC_007946:3	0	60hcl	12.9991	53.6418	2.04495	3.91375	5.00E-05	0.00022207	yes	3.65351206
		NC_007946:4	0	60hcl	6.01034	24.8543	2.04798	3.33672	5.00E-05	0.00022207	yes	3.65351206
		NC_007946:4	0	60hcl	9.62039	39.8139	2.04911	3.1793	5.00E-05	0.00022207	yes	3.65351206
	Lipid kinase Y	NC_007946:2	0	60hcl	10.8054	44.8104	2.05209	3.92874	5.00E-05	0.00022207	yes	3.65351206
hdeB	Chaperone Hc	NC_007946:3	0	60hcl	6.65933	27.7208	2.05752	3.10603	5.00E-05	0.00022207	yes	3.65351206
rbsB	Ribose ABC tr	NC_007946:4	0	60hcl	109.941	458.222	2.05931	3.97921	5.00E-05	0.00022207	yes	3.65351206
	Xanthine deh	NC_007946:3	0	60hcl	7.35104	30.9157	2.07232	4.03407	5.00E-05	0.00022207	yes	3.65351206
fucU	L-fucose muta	NC_007946:3	0	60hcl	43.0749	183.073	2.0875	4.15749	5.00E-05	0.00022207	yes	3.65351206
nmpC	Outer membr	NC_007946:1	0	60hcl	1467.28	6258.09	2.09258	3.56401	5.00E-05	0.00022207	yes	3.65351206
traT	IncF plasmid c	NC_007941:1	0	60hcl	250.157	1074.76	2.10311	4.13134	5.00E-05	0.00022207	yes	3.65351206
ompF	Outer membr	NC_007946:9	0	60hcl	358.857	1542.12	2.10344	3.89388	5.00E-05	0.00022207	yes	3.65351206
eutM	Ethanolamine	NC_007946:2	0	60hcl	9.69412	41.7765	2.10751	3.20011	5.00E-05	0.00022207	yes	3.65351206
cdd	Cytidine deam	NC_007946:2	0	60hcl	43.2072	186.633	2.11086	3.6632	5.00E-05	0.00022207	yes	3.65351206
hisJ	Histidine ABC	NC_007946:2	0	60hcl	35.3635	154.675	2.1289	4.27007	5.00E-05	0.00022207	yes	3.65351206
ycjY	hypothetical p	NC_007946:3	0	60hcl	36.3365	159.19	2.13126	4.33299	5.00E-05	0.00022207	yes	3.65351206
pspE	Thiosulfate:cy	NC_007946:1	0	60hcl	18.7791	82.3108	2.13195	3.72734	5.00E-05	0.00022207	yes	3.65351206
yeiL	Regulatory pr	NC_007946:2	0	60hcl	1.71711	7.6033	2.14664	3.07182	5.00E-05	0.00022207	yes	3.65351206
tsx	Nucleoside-sp	NC_007946:4	0	60hcl	516.457	2287.55	2.14708	4.03367	5.00E-05	0.00022207	yes	3.65351206
deoA	Thymidine ph	NC_007946:5	0	60hcl	43.3198	193.878	2.16205	4.26955	5.00E-05	0.00022207	yes	3.65351206
deoC	Deoxyribose-p	NC_007946:5	0	60hcl	38.2375	171.845	2.16804	4.15674	5.00E-05	0.00022207	yes	3.65351206
treA	Trehalase (EC	NC_007946:1	0	60hcl	20.8577	93.9969	2.17203	4.40267	5.00E-05	0.00022207	yes	3.65351206
pntA	NAD(P) transh	NC_007946:1	0	60hcl	142.154	641.462	2.17391	4.1964	5.00E-05	0.00022207	yes	3.65351206
ydgE	Spermidine ex	NC_007946:1	0	60hcl	954.585	4308.49	2.17424	4.26458	5.00E-05	0.00022207	yes	3.65351206
yfbE	UDP-4-amino	NC_007946:2	0	60hcl	69.6764	314.732	2.17538	4.21229	5.00E-05	0.00022207	yes	3.65351206
ilvB	Acetolactate s	NC_007946:4	0	60hcl	24.0659	109.129	2.18098	4.43033	5.00E-05	0.00022207	yes	3.65351206
yaaF	Non-specific r	NC_007946:2	0	60hcl	30.5567	139.015	2.18568	4.4184	5.00E-05	0.00022207	yes	3.65351206
yqjC	Periplasmic p	NC_007946:3	0	60hcl	77.1909	353.922	2.19693	4.31603	5.00E-05	0.00022207	yes	3.65351206
	Putative oxid	NC_007946:3	0	60hcl	2.65146	12.1768	2.19928	4.02757	5.00E-05	0.00022207	yes	3.65351206
yccD	Chaperone-m	NC_007946:1	0	60hcl	91.4913	421.633	2.20428	3.01147	5.00E-05	0.00022207	yes	3.65351206
eutD	Phosphate ac	NC_007946:2	0	60hcl	6.92916	32.6021	2.23421	3.87086	5.00E-05	0.00022207	yes	3.65351206
argT	Lysine-arginin	NC_007946:2	0	60hcl	28.1877	132.642	2.2344	4.31029	5.00E-05	0.00022207	yes	3.65351206
ybaS	Glutaminase (	NC_007946:5	0	60hcl	3.47094	16.3401	2.23502	3.91969	5.00E-05	0.00022207	yes	3.65351206
hdhA	7-alpha-hydr	NC_007946:1	0	60hcl	24.6941	116.869	2.24265	4.32709	5.00E-05	0.00022207	yes	3.65351206
prpR	Propionate ca	NC_007946:3	0	60hcl	2.02399	9.59762	2.24547	3.82138	5.00E-05	0.00022207	yes	3.65351206
ybjP	Uncharacteriz	NC_007946:8	0	60hcl	11.1791	53.0753	2.24723	4.10336	5.00E-05	0.00022207	yes	3.65351206
ybhN	Inner membra	NC_007946:7	0	60hcl	28.1186	133.549	2.24777	4.04911	5.00E-05	0.00022207	yes	3.65351206
aer	Aerotaxis sens	NC_007946:3	0	60hcl	29.4446	139.857	2.24788	4.58259	5.00E-05	0.00022207	yes	3.65351206
icdA	Isocitrate deh	NC_007946:1	0	60hcl	773.588	3685.62	2.25227	3.98389	5.00E-05	0.00022207	yes	3.65351206
yhaM	UPF0597 prot	NC_007946:3	0	60hcl	32.49	155.286	2.25686	4.18016	5.00E-05	0.00022207	yes	3.65351206
yqeC	Accessory pro	NC_007946:3	0	60hcl	1.50774	7.22558	2.26073	3.18217	5.00E-05	0.00022207	yes	3.65351206
galT	Galactose-1-p	NC_007946:7	0	60hcl	48.9714	234.875	2.26188	4.49892	5.00E-05	0.00022207	yes	3.65351206
lysU	Lysyl-tRNA syr	NC_007946:4	0	60hcl	166.483	803.071	2.27015	4.31794	5.00E-05	0.00022207	yes	3.65351206
oppC	Oligopeptide,	NC_007946:1	0	60hcl	99.4152	482.508	2.27902	4.41831	5.00E-05	0.00022207	yes	3.65351206
glpF	Glycerol upta	NC_007946:4	0	60hcl	148.167	719.671	2.28012	3.40953	5.00E-05	0.00022207	yes	3.65351206
	3-hydroxybut	NC_007946:4	0	60hcl	2.26046	11.0188	2.28528	3.66006	5.00E-05	0.00022207	yes	3.65351206
acnA	Aconitate hyd	NC_007946:1	0	60hcl	110.564	539.104	2.28568	4.17708	5.00E-05	0.00022207	yes	3.65351206
sgaB	PTS system, as	NC_007946:4	0	60hcl	11.9569	58.5124	2.2909	3.78529	5.00E-05	0.00022207	yes	3.65351206
	PTS system, gl	NC_007946:3	0	60hcl	5.56371	27.3118	2.29541	4.32425	5.00E-05	0.00022207	yes	3.65351206
yqjE	Phage holin	NC_007946:3	0	60hcl	523.88	2574.09	2.29675	4.3026	5.00E-05	0.00022207	yes	3.65351206
yhaR	2-iminobutan	NC_007946:3	0	60hcl	28.8295	141.667	2.29689	4.47584	5.00E-05	0.00022207	yes	3.65351206

ycjX	Conserved pro	NC_007946:1	0	60hcl	57.7615	285.894	2.3073	4.26575	5.00E-05	0.00022207	yes	3.65351206
glcB	Malate syntha	NC_007946:3	0	60hcl	24.5289	121.498	2.30838	4.54387	5.00E-05	0.00022207	yes	3.65351206
groEL	Heat shock pr	NC_007946:4	0	60hcl	1113.38	5533.68	2.31329	3.64344	5.00E-05	0.00022207	yes	3.65351206
sodB	Superoxide di	NC_007946:1	0	60hcl	134.832	671.608	2.31646	4.64215	5.00E-05	0.00022207	yes	3.65351206
	ABC transport	NC_007946:3	0	60hcl	3.22673	16.2102	2.32876	4.09176	5.00E-05	0.00022207	yes	3.65351206
yhjG	Uncharacteriz	NC_007946:3	0	60hcl	18.2146	91.6209	2.33058	4.51493	5.00E-05	0.00022207	yes	3.65351206
mgsA	Methylglyoxa	NC_007946:1	0	60hcl	91.6709	464.018	2.33965	4.57026	5.00E-05	0.00022207	yes	3.65351206
	hypothetical p	NC_007946:3	0	60hcl	2.20041	11.1918	2.3466	3.21961	5.00E-05	0.00022207	yes	3.65351206
uxaC	Uronate isom	NC_007946:3	0	60hcl	21.1544	107.911	2.35081	4.60214	5.00E-05	0.00022207	yes	3.65351206
narU	Nitrate/nitrite	NC_007946:1	0	60hcl	1.22215	6.23764	2.35158	3.83751	5.00E-05	0.00022207	yes	3.65351206
tdcE	2-ketobutyrat	NC_007946:3	0	60hcl	9.14418	46.7062	2.35269	4.63538	5.00E-05	0.00022207	yes	3.65351206
	UDP-glucose 4	NC_007946:7	0	60hcl	70.9854	362.943	2.35415	4.71078	5.00E-05	0.00022207	yes	3.65351206
ytfR	Galactofuranc	NC_007946:4	0	60hcl	4.37777	22.3844	2.35423	4.3718	5.00E-05	0.00022207	yes	3.65351206
dsdC	D-serine dehy	NC_007946:4	0	60hcl	4.92107	25.3874	2.36707	4.2366	5.00E-05	0.00022207	yes	3.65351206
yhcO	Barstar, ribon	NC_007946:3	0	60hcl	22.8712	118.926	2.37846	4.03391	5.00E-05	0.00022207	yes	3.65351206
yjgB	Cinnamyl alco	NC_007946:4	0	60hcl	14.5357	75.9657	2.38575	4.58052	5.00E-05	0.00022207	yes	3.65351206
	PTS system, II	NC_007946:4	0	60hcl	4.73368	25.0445	2.40346	4.5647	5.00E-05	0.00022207	yes	3.65351206
hmpA	Flavohemoglo	NC_007946:2	0	60hcl	24.4533	129.905	2.40935	4.89355	5.00E-05	0.00022207	yes	3.65351206
udp	Uridine phosp	NC_007946:4	0	60hcl	331.644	1761.97	2.40948	4.2611	5.00E-05	0.00022207	yes	3.65351206
	4-hydroxyphe	NC_007946:4	0	60hcl	2.31367	12.3775	2.41946	4.09669	5.00E-05	0.00022207	yes	3.65351206
ycjQ	Zinc-type alco	NC_007946:1	0	60hcl	1.65655	8.92594	2.42983	4.11608	5.00E-05	0.00022207	yes	3.65351206
acnB	Aconitate hyd	NC_007946:1	0	60hcl	814.524	4396.57	2.43235	3.96622	5.00E-05	0.00022207	yes	3.65351206
yhhJ	Inner membra	NC_007946:3	0	60hcl	63.9861	345.916	2.43459	4.43149	5.00E-05	0.00022207	yes	3.65351206
aldB	Aldehyde deh	NC_007946:4	0	60hcl	11.3089	61.2651	2.43761	4.6835	5.00E-05	0.00022207	yes	3.65351206
	Tripartite tric	NC_007946:4	0	60hcl	10.9203	59.4581	2.44486	4.88137	5.00E-05	0.00022207	yes	3.65351206
glgP	Glycogen pho	NC_007946:3	0	60hcl	53.0803	289.324	2.44644	4.72658	5.00E-05	0.00022207	yes	3.65351206
pykA	Pyruvate kina	NC_007946:1	0	60hcl	115.718	631.864	2.449	4.78284	5.00E-05	0.00022207	yes	3.65351206
dsdC	D-serine dehy	NC_007946:2	0	60hcl	9.11251	49.8477	2.45161	4.61107	5.00E-05	0.00022207	yes	3.65351206
nupG	Nucleoside pe	NC_007946:3	0	60hcl	36.3061	204.633	2.49475	4.72845	5.00E-05	0.00022207	yes	3.65351206
aceB	Malate syntha	NC_007946:4	0	60hcl	14.8546	83.8806	2.49743	4.63338	5.00E-05	0.00022207	yes	3.65351206
ycjR	Sugar phosph	NC_007946:1	0	60hcl	1.6473	9.33257	2.50217	3.91887	5.00E-05	0.00022207	yes	3.65351206
mtlA	PTS system, m	NC_007946:4	0	60hcl	24.9018	141.826	2.5098	4.98122	5.00E-05	0.00022207	yes	3.65351206
ycjM	Uncharacteriz	NC_007946:1	0	60hcl	0.795421	4.56099	2.51956	4.03131	5.00E-05	0.00022207	yes	3.65351206
cadA	Lysine decarb	NC_007946:4	0	60hcl	7.16839	41.3437	2.52795	4.7419	5.00E-05	0.00022207	yes	3.65351206
uxaA	Altronate deh	NC_007946:3	0	60hcl	25.6913	148.356	2.52971	5.03728	5.00E-05	0.00022207	yes	3.65351206
	PTS system, IIA	NC_007946:4	0	60hcl	2.64723	15.29	2.53004	3.50791	5.00E-05	0.00022207	yes	3.65351206
ygeV	Uncharacteriz	NC_007946:3	0	60hcl	9.8802	57.2874	2.53561	4.85797	5.00E-05	0.00022207	yes	3.65351206
narG	Respiratory ni	NC_007946:1	0	60hcl	54.329	315.197	2.53646	3.0167	5.00E-05	0.00022207	yes	3.65351206
ynaF	Universal stre	NC_007946:1	0	60hcl	15.9502	92.827	2.54097	4.5813	5.00E-05	0.00022207	yes	3.65351206
galM	Aldose 1-epim	NC_007946:7	0	60hcl	236.962	1389.04	2.55136	5.00152	5.00E-05	0.00022207	yes	3.65351206
oppA	Oligopeptide	NC_007946:1	0	60hcl	69.5301	408.01	2.5529	4.59688	5.00E-05	0.00022207	yes	3.65351206
tdcC	L-threonine tr	NC_007946:3	0	60hcl	11.4541	67.8203	2.56586	5.00675	5.00E-05	0.00022207	yes	3.65351206
katG	Catalase-pero	NC_007946:4	0	60hcl	112.145	667.991	2.57447	4.63324	5.00E-05	0.00022207	yes	3.65351206
yhjD	Inner membra	NC_007946:3	0	60hcl	20.8552	124.904	2.58234	4.99569	5.00E-05	0.00022207	yes	3.65351206
yiaO	2,3-diketo-L-g	NC_007946:4	0	60hcl	1.65428	9.91276	2.58308	4.20754	5.00E-05	0.00022207	yes	3.65351206
yhjX	Putative resist	NC_007946:3	0	60hcl	34.3496	209.636	2.60952	3.90173	5.00E-05	0.00022207	yes	3.65351206
fucK	L-fuculokinase	NC_007946:3	0	60hcl	7.49914	46.1677	2.62209	5.29559	5.00E-05	0.00022207	yes	3.65351206
ycgT	Phosphoenol	NC_007946:1	0	60hcl	35.9233	221.443	2.62394	4.919	5.00E-05	0.00022207	yes	3.65351206
	Probable deox	NC_007946:3	0	60hcl	23.7668	150.064	2.65855	5.34627	5.00E-05	0.00022207	yes	3.65351206
pfkB	6-phosphofru	NC_007946:1	0	60hcl	47.3918	300.516	2.66473	5.29302	5.00E-05	0.00022207	yes	3.65351206
rspB	Starvation ser	NC_007946:1	0	60hcl	4.78153	30.4404	2.67044	5.1352	5.00E-05	0.00022207	yes	3.65351206
ykgD	Reactive-chlo	NC_007946:3	0	60hcl	6.46036	41.3446	2.67801	5.01021	5.00E-05	0.00022207	yes	3.65351206
ycgC	Phosphoenol	NC_007946:1	0	60hcl	91.0136	586.417	2.68777	5.27782	5.00E-05	0.00022207	yes	3.65351206
yghZ	L-glyceraldeh	NC_007946:3	0	60hcl	11.5803	74.7082	2.68959	5.16799	5.00E-05	0.00022207	yes	3.65351206
ybeL	Uncharacteriz	NC_007946:6	0	60hcl	44.8579	289.708	2.69117	5.1773	5.00E-05	0.00022207	yes	3.65351206
yeiT	NAD-depende	NC_007946:2	0	60hcl	23.5858	152.47	2.69254	5.25136	5.00E-05	0.00022207	yes	3.65351206
dppA	Dipeptide ABC	NC_007946:3	0	60hcl	51.4018	336.445	2.71048	4.87202	5.00E-05	0.00022207	yes	3.65351206
ggt	Gamma-gluta	NC_007946:3	0	60hcl	10.451	68.8038	2.71884	5.32669	5.00E-05	0.00022207	yes	3.65351206
fucI	L-fucose isom	NC_007946:3	0	60hcl	7.9386	52.4829	2.72489	5.54602	5.00E-05	0.00022207	yes	3.65351206
yfcG	Probable glut	NC_007946:2	0	60hcl	5.38292	35.6742	2.72842	4.82108	5.00E-05	0.00022207	yes	3.65351206
dppC	Dipeptide ABC	NC_007946:3	0	60hcl	32.6736	218.255	2.73982	5.08215	5.00E-05	0.00022207	yes	3.65351206
	Hemolysin act	NC_007946:4	0	60hcl	75.6932	506.155	2.74134	5.42239	5.00E-05	0.00022207	yes	3.65351206
clpB	Chaperone pr	NC_007946:2	0	60hcl	125.435	850.712	2.76173	4.73222	5.00E-05	0.00022207	yes	3.65351206
yjcT	D-allose kinas	NC_007946:4	0	60hcl	22.1709	150.703	2.76497	5.47846	5.00E-05	0.00022207	yes	3.65351206
yeaH	UPF0229 prot	NC_007946:1	0	60hcl	5.64124	38.6777	2.77742	4.99848	5.00E-05	0.00022207	yes	3.65351206
inaA	Weak-acid-ind	NC_007946:2	0	60hcl	93.8259	644.656	2.78047	4.03887	5.00E-05	0.00022207	yes	3.65351206

glcG	Hypothetical	NC_007946:3	0	60hcl	24.4521	168.287	2.78289	5.25545	5.00E-05	0.00022207	yes	3.65351206
phoA	Alkaline phos	NC_007946:4	0	60hcl	17.259	119.346	2.78973	5.63824	5.00E-05	0.00022207	yes	3.65351206
	Glycolate deh	NC_007946:3	0	60hcl	7.55742	52.3629	2.79258	5.37679	5.00E-05	0.00022207	yes	3.65351206
idnK	Gluconokinas	NC_007946:4	0	60hcl	4.45077	31.456	2.82121	4.54128	5.00E-05	0.00022207	yes	3.65351206
yccJ	Uncharacteriz	NC_007946:1	0	60hcl	30.8203	218.425	2.82519	4.70166	5.00E-05	0.00022207	yes	3.65351206
cpdB	2',3'-cyclic-nu	NC_007946:4	0	60hcl	25.1542	178.312	2.82553	5.45307	5.00E-05	0.00022207	yes	3.65351206
glpA	Anaerobic gly	NC_007946:2	0	60hcl	37.8466	269.376	2.83138	3.0207	5.00E-05	0.00022207	yes	3.65351206
yqeF	Acetyl-CoA ac	NC_007946:3	0	60hcl	58.4041	419.243	2.84365	5.60652	5.00E-05	0.00022207	yes	3.65351206
oppB	Oligopeptide	NC_007946:1	0	60hcl	31.2804	226.39	2.85548	5.43642	5.00E-05	0.00022207	yes	3.65351206
fumC	Fumarate hyd	NC_007946:1	0	60hcl	13.0272	94.816	2.86361	4.38334	5.00E-05	0.00022207	yes	3.65351206
dppB	Dipeptide ABC	NC_007946:3	0	60hcl	20.6002	153.08	2.89355	5.3781	5.00E-05	0.00022207	yes	3.65351206
ugpB	Glycerol-3-ph	NC_007946:3	0	60hcl	8.34651	62.1862	2.89735	5.55103	5.00E-05	0.00022207	yes	3.65351206
ycgS	Phosphoenol	NC_007946:1	0	60hcl	91.1481	679.227	2.89761	5.80379	5.00E-05	0.00022207	yes	3.65351206
yjdI	Uncharacteriz	NC_007946:4	0	60hcl	59.4738	444.191	2.90085	5.16311	5.00E-05	0.00022207	yes	3.65351206
ycgB	FIG004684: S	NC_007946:1	0	60hcl	4.02713	30.2355	2.90842	5.32148	5.00E-05	0.00022207	yes	3.65351206
ugpQ	Glycerophosp	NC_007946:3	0	60hcl	57.6413	433.421	2.9106	5.49659	5.00E-05	0.00022207	yes	3.65351206
glgA	Glycogen synt	NC_007946:3	0	60hcl	132.561	1005.79	2.9236	5.54453	5.00E-05	0.00022207	yes	3.65351206
yiaG	Antitoxin to R	NC_007946:3	0	60hcl	16.292	124.503	2.93394	4.89029	5.00E-05	0.00022207	yes	3.65351206
ykgC	Putative Dihy	NC_007946:3	0	60hcl	3.84885	29.4583	2.93617	5.43306	5.00E-05	0.00022207	yes	3.65351206
tdcD	Acetate kinase	NC_007946:3	0	60hcl	6.57752	50.6332	2.94447	5.74849	5.00E-05	0.00022207	yes	3.65351206
nagE	PTS system, N	NC_007946:6	0	60hcl	69.3948	535.766	2.9487	5.68421	5.00E-05	0.00022207	yes	3.65351206
glcD	Glycolate deh	NC_007946:3	0	60hcl	10.2282	79.5512	2.95933	5.11489	5.00E-05	0.00022207	yes	3.65351206
yphA	Inner membra	NC_007946:2	0	60hcl	7.74969	60.3664	2.96153	4.99212	5.00E-05	0.00022207	yes	3.65351206
	Transcription	NC_007946:4	0	60hcl	1.4268	11.1416	2.96511	5.12334	5.00E-05	0.00022207	yes	3.65351206
ybaY	Uncharacteriz	NC_007946:4	0	60hcl	67.146	527.733	2.97443	5.66822	5.00E-05	0.00022207	yes	3.65351206
lacY	Lactose perm	NC_007946:3	0	60hcl	2.94538	23.2387	2.98	5.40347	5.00E-05	0.00022207	yes	3.65351206
	D-allose ABC t	NC_007946:4	0	60hcl	5.95041	47.0541	2.98326	5.59378	5.00E-05	0.00022207	yes	3.65351206
agaV	PTS system, N	NC_007946:3	0	60hcl	3.67745	29.4572	3.00184	4.72355	5.00E-05	0.00022207	yes	3.65351206
	hypothetical	NC_007946:2	0	60hcl	14.1524	115.827	3.03285	6.14326	5.00E-05	0.00022207	yes	3.65351206
	Pyridoxine 4-(	NC_007946:1	0	60hcl	8.64245	70.9202	3.03668	5.79579	5.00E-05	0.00022207	yes	3.65351206
ydiA	Phosphoenol	NC_007946:1	0	60hcl	22.2443	183.792	3.04657	6.13225	5.00E-05	0.00022207	yes	3.65351206
frdD	Fumarate red	NC_007946:4	0	60hcl	94.7138	786.173	3.0532	5.96082	5.00E-05	0.00022207	yes	3.65351206
ygaU	Uncharacteriz	NC_007946:2	0	60hcl	30.101	260.382	3.11274	5.92075	5.00E-05	0.00022207	yes	3.65351206
osmE	Osmotically-i	NC_007946:1	0	60hcl	93.1509	806.67	3.11434	5.99137	5.00E-05	0.00022207	yes	3.65351206
papH	hypothetical	NC_007946:4	0	60hcl	28.1011	244.046	3.11845	5.45507	5.00E-05	0.00022207	yes	3.65351206
frdC	Fumarate red	NC_007946:4	0	60hcl	22.3933	195.529	3.12625	5.72629	5.00E-05	0.00022207	yes	3.65351206
ygjL	2,4-dienoyl-C	NC_007946:3	0	60hcl	5.4053	47.2251	3.12711	5.82089	5.00E-05	0.00022207	yes	3.65351206
ucpA	Oxidoreducta	NC_007946:2	0	60hcl	194.38	1739.45	3.16168	6.00942	5.00E-05	0.00022207	yes	3.65351206
fadJ	Enoyl-CoA hyc	NC_007946:2	0	60hcl	24.0284	215.983	3.1681	5.83486	5.00E-05	0.00022207	yes	3.65351206
ybeJ	Glutamate/as	NC_007946:6	0	60hcl	41.0996	373.208	3.18278	5.77549	5.00E-05	0.00022207	yes	3.65351206
ytfQ	Galactofuranc	NC_007946:4	0	60hcl	11.1501	102.417	3.19932	6.00071	5.00E-05	0.00022207	yes	3.65351206
malM	Maltose operc	NC_007946:4	0	60hcl	26.0444	239.801	3.20279	6.17943	5.00E-05	0.00022207	yes	3.65351206
osmC	Peroxiredoxin	NC_007946:1	0	60hcl	22.931	211.233	3.20346	5.91637	5.00E-05	0.00022207	yes	3.65351206
glgX	Limit dextrin	NC_007946:3	0	60hcl	70.7016	655.676	3.21317	5.96534	5.00E-05	0.00022207	yes	3.65351206
dps	DNA protectio	NC_007946:8	0	60hcl	78.4331	751.276	3.25981	6.20432	5.00E-05	0.00022207	yes	3.65351206
ybgO	Uncharacteriz	NC_007946:7	0	60hcl	12.6804	121.813	3.26399	5.86882	5.00E-05	0.00022207	yes	3.65351206
malQ	4-alpha-gluca	NC_007946:3	0	60hcl	21.3832	207.336	3.27742	6.41472	5.00E-05	0.00022207	yes	3.65351206
	UPF0391 mer	NC_007946:5	0	60hcl	42.2542	410.394	3.27985	3.49211	5.00E-05	0.00022207	yes	3.65351206
rihA	Pyrimidine-sp	NC_007946:6	0	60hcl	30.6558	297.951	3.28084	6.54085	5.00E-05	0.00022207	yes	3.65351206
fucO	Lactaldehyde	NC_007946:3	0	60hcl	13.9283	137.08	3.29893	6.47135	5.00E-05	0.00022207	yes	3.65351206
	Putative DNA	NC_007946:2	0	60hcl	11.7051	118.696	3.34206	6.46397	5.00E-05	0.00022207	yes	3.65351206
	Dienelactone	NC_007946:4	0	60hcl	18.938	192.409	3.34482	6.31215	5.00E-05	0.00022207	yes	3.65351206
ugpE	Glycerol-3-ph	NC_007946:3	0	60hcl	6.16408	62.9676	3.35265	6.35914	5.00E-05	0.00022207	yes	3.65351206
galP	Galactose-pro	NC_007946:3	0	60hcl	31.8763	326.049	3.35453	6.48897	5.00E-05	0.00022207	yes	3.65351206
yedE	UPF0394 inne	NC_007946:2	0	60hcl	96.8955	1001.8	3.37002	3.80237	5.00E-05	0.00022207	yes	3.65351206
elaB	ElaB protein	NC_007946:2	0	60hcl	33.8862	353.711	3.3838	6.17393	5.00E-05	0.00022207	yes	3.65351206
yhiX	Transcription	NC_007946:3	0	60hcl	17.5495	183.43	3.38573	6.15588	5.00E-05	0.00022207	yes	3.65351206
ygiW	Protein ygiW	NC_007946:3	0	60hcl	42.2338	444.435	3.3955	6.49349	5.00E-05	0.00022207	yes	3.65351206
nanM	N-acetylneura	NC_007946:4	0	60hcl	2.82302	29.856	3.40271	6.0686	5.00E-05	0.00022207	yes	3.65351206
gltL	Glutamate/as	NC_007946:6	0	60hcl	89.7502	956.538	3.41384	6.44882	5.00E-05	0.00022207	yes	3.65351206
yehZ	Osmoprotecta	NC_007946:2	0	60hcl	12.3785	133.368	3.4295	6.39896	5.00E-05	0.00022207	yes	3.65351206
lysC	Aspartokinase	NC_007946:4	0	60hcl	73.6067	795.843	3.43457	6.61711	5.00E-05	0.00022207	yes	3.65351206
dsdX	D-serine perm	NC_007946:4	0	60hcl	7.78057	84.8577	3.4471	6.24728	5.00E-05	0.00022207	yes	3.65351206
dsdA	D-serine amm	NC_007946:4	0	60hcl	16.4389	181.679	3.4662	6.46336	5.00E-05	0.00022207	yes	3.65351206
ydiZ	Uncharacteriz	NC_007946:1	0	60hcl	14.9172	168.705	3.49945	5.82156	5.00E-05	0.00022207	yes	3.65351206
tdcB	Threonine de	NC_007946:3	0	60hcl	8.89216	103.523	3.54127	6.59004	5.00E-05	0.00022207	yes	3.65351206
yehX	Osmoprotecta	NC_007946:2	0	60hcl	16.3704	192.453	3.55535	6.86558	5.00E-05	0.00022207	yes	3.65351206
rpiR	Transcription	NC_007946:4	0	60hcl	48.6798	577.098	3.56742	6.83348	5.00E-05	0.00022207	yes	3.65351206
	Propionate ca	NC_007946:3	0	60hcl	2.29919	27.3527	3.57248	4.25065	5.00E-05	0.00022207	yes	3.65351206
actP	Acetate perm	NC_007946:4	0	60hcl	65.052	781.253	3.58612	3.57205	5.00E-05	0.00022207	yes	3.65351206
fadE	Acyl-coenzym	NC_007946:2	0	60hcl	9.31626	112.158	3.58963	6.92303	5.00E-05	0.00022207	yes	3.65351206
yjiA	Metal-binding	NC_007946:4	0	60hcl	42.882	517.271	3.59248	6.57235	5.00E-05	0.00022207	yes	3.65351206
yjhA	N-acetylneura	NC_007946:4	0	60hcl	3.42007	41.3064	3.59427	5.85461	5.00E-05	0.00022207	yes	3.65351206

idnO	5-keto-D-gluc	NC_007946:4	0	60hcl	3.91112	47.8701	3.61347	6.50899	5.00E-05	0.00022207	yes	3.65351206
wrbA	NAD(P)H dehy	NC_007946:1	0	60hcl	12.3665	154.048	3.63887	6.68639	5.00E-05	0.00022207	yes	3.65351206
maeB	NADP-depend	NC_007946:2	0	60hcl	94.1011	1179.9	3.6483	6.81905	5.00E-05	0.00022207	yes	3.65351206
dsdA	D-serine amm	NC_007946:2	0	60hcl	23.865	299.79	3.65098	6.75483	5.00E-05	0.00022207	yes	3.65351206
fadA	3-ketoacyl-Co	NC_007946:4	0	60hcl	22.8031	288.522	3.66138	6.8556	5.00E-05	0.00022207	yes	3.65351206
aceA	Isocitrate lyas	NC_007946:4	0	60hcl	20.1712	261.249	3.69506	6.86691	5.00E-05	0.00022207	yes	3.65351206
gcvT	Aminomethyl	NC_007946:3	0	60hcl	115.465	1564.59	3.76026	7.27597	5.00E-05	0.00022207	yes	3.65351206
lacZ	beta-galactosi	NC_007946:3	0	60hcl	3.36907	46.4553	3.78542	7.26288	5.00E-05	0.00022207	yes	3.65351206
yeaG	Uncharacteriz	NC_007946:1	0	60hcl	7.32432	106.665	3.86425	7.16203	5.00E-05	0.00022207	yes	3.65351206
otsA	Alpha,alpha-t	NC_007946:2	0	60hcl	15.0217	221.004	3.87895	6.67666	5.00E-05	0.00022207	yes	3.65351206
sdhC	Succinate deh	NC_007946:7	0	60hcl	531.793	7955.99	3.90311	3.60324	5.00E-05	0.00022207	yes	3.65351206
dsdX	D-serine perm	NC_007946:2	0	60hcl	6.3886	96.4888	3.91679	7.15366	5.00E-05	0.00022207	yes	3.65351206
ydeM	GALNS arylsul	NC_007946:1	0	60hcl	0.684778	10.4134	3.92667	5.515	5.00E-05	0.00022207	yes	3.65351206
ompD	Outer membr	NC_007946:2	0	60hcl	57.3923	882.822	3.94319	7.61836	5.00E-05	0.00022207	yes	3.65351206
tktB	Transketolase	NC_007946:2	0	60hcl	10.7557	165.83	3.94653	7.44558	5.00E-05	0.00022207	yes	3.65351206
agp	Glucose-1-ph	NC_007946:1	0	60hcl	22.6523	350.009	3.94967	7.74035	5.00E-05	0.00022207	yes	3.65351206
dctA	Na+/H+-dicarb	NC_007946:3	0	60hcl	59.9996	928.297	3.95156	7.46834	5.00E-05	0.00022207	yes	3.65351206
talA	Transaldolase	NC_007946:2	0	60hcl	8.50988	132.039	3.95568	7.31643	5.00E-05	0.00022207	yes	3.65351206
yeiM	Pseudouridin	NC_007946:2	0	60hcl	14.0314	219.343	3.96646	7.78681	5.00E-05	0.00022207	yes	3.65351206
gcvH	Glycine cleava	NC_007946:3	0	60hcl	80.3299	1309.48	4.02691	7.92048	5.00E-05	0.00022207	yes	3.65351206
aspA	Aspartate amr	NC_007946:4	0	60hcl	86.4894	1414.88	4.03201	6.95393	5.00E-05	0.00022207	yes	3.65351206
yhiP	Di-tripeptide/	NC_007946:3	0	60hcl	53.0193	870.939	4.03798	7.36444	5.00E-05	0.00022207	yes	3.65351206
gcvP	Glycine dehyd	NC_007946:3	0	60hcl	34.5439	571.055	4.04713	7.85763	5.00E-05	0.00022207	yes	3.65351206
ykgE	Predicted L-la	NC_007946:3	0	60hcl	12.9193	215.479	4.05995	7.83665	5.00E-05	0.00022207	yes	3.65351206
putA	Transcription	NC_007946:1	0	60hcl	15.7142	270.787	4.10702	7.93225	5.00E-05	0.00022207	yes	3.65351206
idnD	L-idonate 5-d	NC_007946:4	0	60hcl	2.75789	48.0184	4.12195	7.42543	5.00E-05	0.00022207	yes	3.65351206
malG	Maltodextrin	NC_007946:4	0	60hcl	8.94847	158.304	4.14491	7.75119	5.00E-05	0.00022207	yes	3.65351206
gabT	Gamma-amin	NC_007946:2	0	60hcl	9.26151	171.197	4.20827	7.95034	5.00E-05	0.00022207	yes	3.65351206
glpK	Glycerol kinas	NC_007946:4	0	60hcl	138.453	2658.02	4.26288	6.40958	5.00E-05	0.00022207	yes	3.65351206
osmY	Osmotically ir	NC_007946:5	0	60hcl	61.0624	1213.74	4.31304	8.01313	5.00E-05	0.00022207	yes	3.65351206
gltA	Citrate syntha	NC_007946:7	0	60hcl	210.734	4274.51	4.34226	7.25882	5.00E-05	0.00022207	yes	3.65351206
lysA	Diaminopime	NC_007946:3	0	60hcl	19.7003	419.415	4.41209	8.32199	5.00E-05	0.00022207	yes	3.65351206
ykgF	Predicted L-la	NC_007946:3	0	60hcl	47.1898	1012.53	4.42334	7.24571	5.00E-05	0.00022207	yes	3.65351206
malP	Maltodextrin	NC_007946:3	0	60hcl	11.3708	244.36	4.4256	8.33946	5.00E-05	0.00022207	yes	3.65351206
poxB	Pyruvate dehy	NC_007946:8	0	60hcl	5.9242	132.673	4.4851	8.26251	5.00E-05	0.00022207	yes	3.65351206
ygaM	ElaB protein	NC_007946:2	0	60hcl	8.4384	189.328	4.48778	7.12163	5.00E-05	0.00022207	yes	3.65351206
sdhB	Succinate deh	NC_007946:7	0	60hcl	184.757	4420.12	4.58039	8.74045	5.00E-05	0.00022207	yes	3.65351206
ygaT	Carbon starva	NC_007946:2	0	60hcl	5.31732	130.408	4.61619	8.41932	5.00E-05	0.00022207	yes	3.65351206
sucC	Succinyl-CoA	NC_007946:7	0	60hcl	448.146	11126.3	4.63387	7.44191	5.00E-05	0.00022207	yes	3.65351206
srlB	PTS system, gl	NC_007946:2	0	60hcl	1.98481	49.4152	4.63788	5.25783	5.00E-05	0.00022207	yes	3.65351206
mdh	Malate dehyd	NC_007946:3	0	60hcl	146.611	3690.82	4.65388	8.45978	5.00E-05	0.00022207	yes	3.65351206
fumA	Fumarate hyd	NC_007946:1	0	60hcl	84.5805	2147.3	4.66606	8.49309	5.00E-05	0.00022207	yes	3.65351206
ygaF	L-2-hydroxygl	NC_007946:2	0	60hcl	2.24622	57.0576	4.66685	7.90486	5.00E-05	0.00022207	yes	3.65351206
sucB	Dihydrolipoar	NC_007946:7	0	60hcl	277.809	7523.98	4.75933	8.27917	5.00E-05	0.00022207	yes	3.65351206
gabD	Succinate-sem	NC_007946:2	0	60hcl	3.05629	83.4152	4.77046	8.66238	5.00E-05	0.00022207	yes	3.65351206
alsA	D-allose ABC t	NC_007946:4	0	60hcl	7.88878	220.422	4.80432	4.05247	5.00E-05	0.00022207	yes	3.65351206
srlD	Sorbitol-6-ph	NC_007946:2	0	60hcl	9.75196	275.421	4.8198	8.82006	5.00E-05	0.00022207	yes	3.65351206
sucA	2-oxoglutarat	NC_007946:7	0	60hcl	109.043	3157.06	4.85561	8.43424	5.00E-05	0.00022207	yes	3.65351206
	Fructose-bisp	NC_007946:2	0	60hcl	3.0772	89.5951	4.86373	8.66367	5.00E-05	0.00022207	yes	3.65351206
srlA	PTS system, gl	NC_007946:2	0	60hcl	6.52207	225.374	5.11085	8.25585	5.00E-05	0.00022207	yes	3.65351206
aldA	Aldehyde deh	NC_007946:1	0	60hcl	36.3492	1262.1	5.11775	9.05523	5.00E-05	0.00022207	yes	3.65351206
yhcH	Putative sugar	NC_007946:3	0	60hcl	52.3465	1967	5.23176	9.01291	5.00E-05	0.00022207	yes	3.65351206
fadB	Enoyl-CoA hyd	NC_007946:4	0	60hcl	7.86709	297.811	5.24242	9.64724	5.00E-05	0.00022207	yes	3.65351206
ppsA	Phosphoenolp	NC_007946:1	0	60hcl	50.4466	1957.45	5.27807	9.60149	5.00E-05	0.00022207	yes	3.65351206
ydeN	N-acetylgalact	NC_007946:1	0	60hcl	1.4234	58.6276	5.36417	9.194	5.00E-05	0.00022207	yes	3.65351206
malF	Maltodextrin	NC_007946:4	0	60hcl	7.05034	305.235	5.43608	10.0803	5.00E-05	0.00022207	yes	3.65351206
tnaB	Low affinity tr	NC_007946:4	0	60hcl	10.7538	470.822	5.45226	9.6035	5.00E-05	0.00022207	yes	3.65351206
dadX	Alanine racem	NC_007946:1	0	60hcl	32.8464	1475.48	5.4893	10.2434	5.00E-05	0.00022207	yes	3.65351206
yjfO	Lipoprotein B	NC_007946:4	0	60hcl	90.4483	4093.5	5.5001	9.82773	5.00E-05	0.00022207	yes	3.65351206
glpQ	Glycerophosp	NC_007946:2	0	60hcl	29.1042	1362.45	5.54883	8.20582	5.00E-05	0.00022207	yes	3.65351206
yjcX	D-allose ABC t	NC_007946:4	0	60hcl	5.81807	311.379	5.74199	10.7326	5.00E-05	0.00022207	yes	3.65351206
acs	Acetyl-CoA syr	NC_007946:4	0	60hcl	8.54905	553.734	6.01728	10.447	5.00E-05	0.00022207	yes	3.65351206
dadA	D-amino acid	NC_007946:1	0	60hcl	25.7358	1686.84	6.0344	10.928	5.00E-05	0.00022207	yes	3.65351206
yeiN	Pseudouridin	NC_007946:2	0	60hcl	10.4674	718.958	6.10194	10.789	5.00E-05	0.00022207	yes	3.65351206
ydjS	Succinylgluta	NC_007946:1	0	60hcl	25.9349	1823.25	6.13548	9.73775	5.00E-05	0.00022207	yes	3.65351206
lamB	Maltoporin (n	NC_007946:4	0	60hcl	12.2808	889.939	6.17923	10.8044	5.00E-05	0.00022207	yes	3.65351206
lldP	L-lactate perm	NC_007946:4	0	60hcl	115.882	8637.93	6.21996	9.50583	5.00E-05	0.00022207	yes	3.65351206
nanT	Sialic acid tra	NC_007946:3	0	60hcl	7.07328	564.489	6.31842	12.3111	5.00E-05	0.00022207	yes	3.65351206
nanA	N-acetylneura	NC_007946:3	0	60hcl	14.7772	1318.59	6.47948	12.2712	5.00E-05	0.00022207	yes	3.65351206
treB	PTS system, tr	NC_007946:4	0	60hcl	16.7015	1829.84	6.7756	11.2748	5.00E-05	0.00022207	yes	3.65351206
glpT	Glycerol-3-ph	NC_007946:2	0	60hcl	13.9531	1588.33	6.83078	8.57722	5.00E-05	0.00022207	yes	3.65351206
treC	Trehalose-6-p	NC_007946:4	0	60hcl	10.2112	1287.02	6.97773	12.4207	5.00E-05	0.00022207	yes	3.65351206
malE	Maltodextrin	NC_007946:4	0	60hcl	3.8844	651.433	7.38978	12.0438	5.00E-05	0.00022207	yes	3.65351206
mglC	Galactose/me	NC_007946:2	0	60hcl	8.50488	1452.94	7.41647	13.5988	5.00E-05	0.00022207	yes	3.65351206
mglB	Galactose/me	NC_007946:2	0	60hcl	12.3157	2212.63	7.48912	12.6276	5.00E-05	0.00022207	yes	3.65351206
malK	Maltose/malt	NC_007946:4	0	60hcl	3.66827	665.303	7.50277	12.4482	5.00E-05	0.00022207	yes	3.65351206
mglA	Galactose/me	NC_007946:2	0	60hcl	1.82592	388.839	7.73441	12.8944	5.00E-05	0.00022207	yes	3.65351206
tnaA	Tryptophanas	NC_007946:4	0	60hcl	11.0363	2580.07	7.86901	11.2442	5.00E-05	0.00022207	yes	3.65351206
yjiy	Pyruvate:H+ s	NC_007946:4	0	60hcl	6.53169	2344.19	8.48742	14.9161	5.00E-05	0.00022207	yes	3.65351206
chaB	Cation transp	NC_007946:1	0	60hcl	8.55338	48.4567	2.50213	4.43726	0.0001	0.0004213	yes	3.37540751
	Uncharacteriz	NC_007946:1	0	60hcl	7.81783	80.1751	3.35831	3.00405	0.0001	0.0004213	yes	3.37540751
ybdD	Uncharacteriz	NC_007946:4	0	60hcl	3.58077	76.2956	4.41326	6.98894	0.0004	0.00145208	yes	2.83800946
	PTS system, III	NC_007946:4	0	60hcl	2.40192	11.2736	2.23069	2.53213	0.0006	0.00207315	yes	2.68336927
gatA	PTS system, ga	NC_007946:2	0	60hcl	0.49783	2.04647	2.03941	1.683	0.01065	0.0261848	yes	1.58195074

C. Genes significantly downregulated in Δ*btsS*Δ*ypdB* 60 minutes after HCl exposure compared to Δ*btsS*Δ*ypdB* at 0 minutes

gene symbol	function	locus	sample_1	sample_2	value_1	value_2	log2(fold_cha	test_stat	p_value	q_value	significant	log10q
nepI	Purine ribonu	NC_007946:4106567-4107923	baseline	60hcl	184.988	46.0056	-2.00755	-4.79153	5.00E-05	0.00031478	yes	3.50199287
rpmI	LSU ribosoma	NC_007946:1835387-1835585	baseline	60hcl	2230.33	554.062	-2.00914	-4.2076	5.00E-05	0.00031478	yes	3.50199287
fis	DNA-binding p	NC_007946:3629226-3629523	baseline	60hcl	1807.95	441.971	-2.03234	-4.86624	5.00E-05	0.00031478	yes	3.50199287
gltP	Proton/glutar	NC_007946:4563875-4565189	baseline	60hcl	1594.01	384.354	-2.05215	-4.78689	5.00E-05	0.00031478	yes	3.50199287
cspG	Cold shock pr	NC_007946:1039734-1039947	baseline	60hcl	6530.97	1572.24	-2.05448	-4.56565	5.00E-05	0.00031478	yes	3.50199287
vacB	3'-to-5' exorib	NC_007946:4678465-4680907	baseline	60hcl	1787.23	421.046	-2.08567	-4.92945	5.00E-05	0.00031478	yes	3.50199287
yghJ	Putative lipop	NC_007946:3318169-3322732	baseline	60hcl	300.544	70.41	-2.09372	-4.91398	5.00E-05	0.00031478	yes	3.50199287
ygfE	Z-ring-associa	NC_007946:3233256-3233586	baseline	60hcl	751.947	175.842	-2.09636	-5.00705	5.00E-05	0.00031478	yes	3.50199287
ybiX	PKHD-type hy	NC_007946:801172-801850	baseline	60hcl	101.102	23.3589	-2.11376	-4.80226	5.00E-05	0.00031478	yes	3.50199287
	Fe2+ ABC tran	NC_007941:10045-12449	baseline	60hcl	1406.84	322.194	-2.12646	-4.94926	5.00E-05	0.00031478	yes	3.50199287
pta	BioD-like N-te	NC_007946:2546887-2549032	baseline	60hcl	1056.24	240.764	-2.13325	-4.93001	5.00E-05	0.00031478	yes	3.50199287
	hypothetical p	NC_007946:4521507-4523060	baseline	60hcl	419.822	95.0985	-2.14228	-4.67675	5.00E-05	0.00031478	yes	3.50199287
ybiL	Ferrichrome-i	NC_007946:802065-804348	baseline	60hcl	233.346	52.5777	-2.14995	-5.03136	5.00E-05	0.00031478	yes	3.50199287
yjeB	Nitrite-sensiti	NC_007946:4678001-4678427	baseline	60hcl	2584.87	579.865	-2.1563	-4.97722	5.00E-05	0.00031478	yes	3.50199287
entC	Isochorismate	NC_007946:608805-609981	baseline	60hcl	364.231	79.6166	-2.19371	-5.17435	5.00E-05	0.00031478	yes	3.50199287
rpmD	LSU ribosoma	NC_007946:3662352-3662532	baseline	60hcl	1568.13	342.42	-2.19521	-4.50354	5.00E-05	0.00031478	yes	3.50199287
deoB	Phosphopent	NC_007946:5043296-5044520	baseline	60hcl	1070.8	233.381	-2.19793	-5.09896	5.00E-05	0.00031478	yes	3.50199287
yjeT	Putative inner	NC_007946:4676197-4676395	baseline	60hcl	175.393	38.0125	-2.20605	-3.7205	5.00E-05	0.00031478	yes	3.50199287
gnsB	GnsA protein	NC_007946:1040340-1040514	baseline	60hcl	1011.74	217.915	-2.21501	-3.93246	5.00E-05	0.00031478	yes	3.50199287
ilvC	Ketol-acid red	NC_007946:4218781-4220257	baseline	60hcl	766.345	163.298	-2.23049	-5.17351	5.00E-05	0.00031478	yes	3.50199287
rbsA	Ribose ABC tra	NC_007946:4194645-4196151	baseline	60hcl	463.621	96.3185	-2.26706	-5.16886	5.00E-05	0.00031478	yes	3.50199287
yhcN	probable expo	NC_007946:3595203-3595467	baseline	60hcl	187.558	38.8645	-2.27081	-4.70796	5.00E-05	0.00031478	yes	3.50199287
yeiE	Transcription	NC_007946:2389944-2390751	baseline	60hcl	267.064	54.4852	-2.29325	-5.39404	5.00E-05	0.00031478	yes	3.50199287
ygjO	23S rRNA (gua	NC_007946:3461344-3462481	baseline	60hcl	419.651	85.479	-2.29555	-5.36986	5.00E-05	0.00031478	yes	3.50199287
asnA	Aspartate--am	NC_007946:4188022-4189015	baseline	60hcl	362.144	73.5537	-2.29969	-5.35691	5.00E-05	0.00031478	yes	3.50199287
fhuC	Ferric hydroxa	NC_007946:175721-179388	baseline	60hcl	2033.6	406.865	-2.32141	-4.74978	5.00E-05	0.00031478	yes	3.50199287
ydhR	Putative mon	NC_007946:1782458-1782764	baseline	60hcl	415.382	82.693	-2.3286	-5.42464	5.00E-05	0.00031478	yes	3.50199287
yjeO	Inner membra	NC_007946:4657525-4657828	baseline	60hcl	146.372	29.1099	-2.33006	-4.84647	5.00E-05	0.00031478	yes	3.50199287
aslA	Arylsulfatase (	NC_007946:4244344-4246000	baseline	60hcl	27.2172	5.39618	-2.33451	-5.3847	5.00E-05	0.00031478	yes	3.50199287
yhdX	Amino acid AE	NC_007946:3638092-3639274	baseline	60hcl	34.4965	6.82109	-2.33837	-5.31699	5.00E-05	0.00031478	yes	3.50199287
napC	Cytochrome c	NC_007946:2434536-2435139	baseline	60hcl	297.721	58.7217	-2.342	-5.34941	5.00E-05	0.00031478	yes	3.50199287
yjaA	Uncharacteriz	NC_007946:4461458-4461842	baseline	60hcl	207.691	40.4787	-2.35921	-5.36761	5.00E-05	0.00031478	yes	3.50199287
chuT	Periplasmic h	NC_007946:3916853-3917687	baseline	60hcl	178.522	34.3873	-2.37616	-5.61291	5.00E-05	0.00031478	yes	3.50199287
dkgB	Methylglyoxal	NC_007946:233914-235629	baseline	60hcl	104.157	19.8438	-2.392	-3.18158	5.00E-05	0.00031478	yes	3.50199287
cspA	Cold shock pr	NC_007946:3987304-3987517	baseline	60hcl	88263.2	16655.5	-2.40581	-5.69038	5.00E-05	0.00031478	yes	3.50199287
appA	Phosphoanhy	NC_007946:1037938-1039449	baseline	60hcl	363.285	66.7492	-2.44428	-5.59391	5.00E-05	0.00031478	yes	3.50199287
yhgG	Ferrous iron-s	NC_007946:3795389-3795626	baseline	60hcl	72.9272	13.3206	-2.4528	-3.7702	5.00E-05	0.00031478	yes	3.50199287
gspL	General secret	NC_007946:3306779-3309498	baseline	60hcl	343.846	60.9963	-2.49497	-5.23539	5.00E-05	0.00031478	yes	3.50199287
gspI	General secret	NC_007946:3309530-3310429	baseline	60hcl	310.865	54.6915	-2.5069	-5.54699	5.00E-05	0.00031478	yes	3.50199287
rhlE	ATP-depender	NC_007946:793815-795177	baseline	60hcl	723.428	125.695	-2.52492	-5.85974	5.00E-05	0.00031478	yes	3.50199287
entE	2,3-dihydroxy	NC_007946:609990-611601	baseline	60hcl	410.026	70.9187	-2.53148	-5.99047	5.00E-05	0.00031478	yes	3.50199287
yegD	Uncharacteriz	NC_007946:2285795-2287148	baseline	60hcl	295.259	50.9516	-2.53478	-5.92999	5.00E-05	0.00031478	yes	3.50199287
napB	Nitrate reduct	NC_007946:2435148-2437140	baseline	60hcl	1319.31	222.529	-2.56772	-5.44709	5.00E-05	0.00031478	yes	3.50199287
rbsC	Ribose ABC tra	NC_007946:4196155-4197121	baseline	60hcl	1169.31	197.121	-2.56851	-5.8701	5.00E-05	0.00031478	yes	3.50199287
yeaI	Diguanylate c	NC_007946:1902776-1904111	baseline	60hcl	17.221	2.90131	-2.56939	-5.39148	5.00E-05	0.00031478	yes	3.50199287
aceE	Pyruvate deh	NC_007946:129245-131909	baseline	60hcl	5951.01	965.428	-2.62389	-6.4047	5.00E-05	0.00031478	yes	3.50199287
glpK	Glycerol kinas	NC_007946:4392711-4394220	baseline	60hcl	604.285	97.9879	-2.62455	-6.04674	5.00E-05	0.00031478	yes	3.50199287
ycgT	Phosphoenol	NC_007946:1328416-1329487	baseline	60hcl	125.694	19.9788	-2.65337	-6.13252	5.00E-05	0.00031478	yes	3.50199287

	PTS system, gl	NC_007946:1202831-1204265	baseline	60hcl	799.892	124.284	-2.68617	-6.29594	5.00E-05	0.00031478	yes	3.50199287
cysG	Precorrin-2 o	NC_007946:3755831-3757205	baseline	60hcl	485.147	74.8413	-2.69651	-6.30589	5.00E-05	0.00031478	yes	3.50199287
pspG	Phage shock p	NC_007946:4510206-4510449	baseline	60hcl	363.658	55.9538	-2.70028	-5.78311	5.00E-05	0.00031478	yes	3.50199287
yhdY	Amino acid AE	NC_007946:3639283-3640387	baseline	60hcl	39.6159	6.05498	-2.70989	-6.0321	5.00E-05	0.00031478	yes	3.50199287
entB	Isochorismata	NC_007946:611614-613218	baseline	60hcl	2273.73	342.687	-2.7301	-6.41163	5.00E-05	0.00031478	yes	3.50199287
gspM	General secret	NC_007946:3306241-3306778	baseline	60hcl	114.904	17.255	-2.73534	-6.11307	5.00E-05	0.00031478	yes	3.50199287
fepA	TonB-depende	NC_007946:594360-596725	baseline	60hcl	560.368	82.3036	-2.76735	-6.3711	5.00E-05	0.00031478	yes	3.50199287
cirA	Colicin I recep	NC_007946:2385987-2387883	baseline	60hcl	586.121	84.3	-2.79759	-6.32524	5.00E-05	0.00031478	yes	3.50199287
deaD	DEAD-box ATP	NC_007946:3525805-3527695	baseline	60hcl	4029.83	571.968	-2.81671	-6.71393	5.00E-05	0.00031478	yes	3.50199287
ackA	Acetate kinase	NC_007946:2545751-2546813	baseline	60hcl	1938.21	273.887	-2.82308	-6.53107	5.00E-05	0.00031478	yes	3.50199287
mntP	Putative mang	NC_007946:1932376-1933749	baseline	60hcl	485.978	68.1493	-2.83412	-4.03417	5.00E-05	0.00031478	yes	3.50199287
aceF	Dihydrolipoar	NC_007946:131923-133816	baseline	60hcl	8744.36	1201.48	-2.86354	-7.07761	5.00E-05	0.00031478	yes	3.50199287
ndh	NADH dehydr	NC_007946:1211046-1212351	baseline	60hcl	683.413	92.225	-2.88953	-6.7595	5.00E-05	0.00031478	yes	3.50199287
ycgC	Phosphoenol	NC_007946:1326344-1327763	baseline	60hcl	360.591	46.6538	-2.9503	-6.89408	5.00E-05	0.00031478	yes	3.50199287
entF	Enterobactin	NC_007946:598048-602145	baseline	60hcl	705.207	88.2842	-2.99782	-2.06221	5.00E-05	0.00031478	yes	3.50199287
aslB	Anaerobic sul	NC_007946:4242951-4244187	baseline	60hcl	168.912	21.0526	-3.0042	-7.11524	5.00E-05	0.00031478	yes	3.50199287
nirB	Nitrite reduct	NC_007946:3752014-3754881	baseline	60hcl	1379.62	165.505	-3.05933	-2.97483	5.00E-05	0.00031478	yes	3.50199287
ybdB	Proofreading	NC_007946:613220-613634	baseline	60hcl	351.009	41.9256	-3.0656	-7.12169	5.00E-05	0.00031478	yes	3.50199287
glnK	Nitrogen regu	NC_007946:486727-487066	baseline	60hcl	37.3919	4.24321	-3.1395	-4.45221	5.00E-05	0.00031478	yes	3.50199287
ybaA	Protein of unk	NC_007946:490801-491155	baseline	60hcl	1688.26	187.699	-3.16905	-7.44964	5.00E-05	0.00031478	yes	3.50199287
ycfJ	hypothetical p	NC_007946:1212577-1213117	baseline	60hcl	505.641	49.0576	-3.36556	-7.75967	5.00E-05	0.00031478	yes	3.50199287
entD	4'-phosphopa	NC_007946:593565-594186	baseline	60hcl	174.724	16.6134	-3.39466	-7.73584	5.00E-05	0.00031478	yes	3.50199287
ycgS	Phosphoenol	NC_007946:1327773-1328406	baseline	60hcl	556.555	48.911	-3.50829	-7.91232	5.00E-05	0.00031478	yes	3.50199287
fruA	PTS system, in	NC_007946:2399767-2401459	baseline	60hcl	3352.91	289.221	-3.53517	-8.24627	5.00E-05	0.00031478	yes	3.50199287
glpD	Aerobic glycer	NC_007946:3814827-3816333	baseline	60hcl	512.084	41.9034	-3.61124	-8.18278	5.00E-05	0.00031478	yes	3.50199287
chuX	Putative hem	NC_007946:3919056-3920174	baseline	60hcl	1456.04	119.085	-3.61199	-8.40576	5.00E-05	0.00031478	yes	3.50199287
fruK	1-phosphofru	NC_007946:2401475-2403544	baseline	60hcl	4513.8	357.099	-3.65995	-8.50635	5.00E-05	0.00031478	yes	3.50199287
yafT	Uncharacteriz	NC_007946:242303-243089	baseline	60hcl	651.822	51.0917	-3.67332	-8.58633	5.00E-05	0.00031478	yes	3.50199287
chuW	Radical SAM f	NC_007946:3917784-3919044	baseline	60hcl	377.981	24.833	-3.92798	-9.25047	5.00E-05	0.00031478	yes	3.50199287
chuU	Hemin ABC tra	NC_007946:3920222-3921982	baseline	60hcl	765.604	39.5242	-4.27579	-9.93698	5.00E-05	0.00031478	yes	3.50199287
yhfC	Selenite- and t	NC_007946:3750571-3751753	baseline	60hcl	308.144	14.6211	-4.39748	-9.968	5.00E-05	0.00031478	yes	3.50199287
	putative mem	NC_007946:3816386-3816992	baseline	60hcl	78.6695	2.13346	-5.20454	-8.10681	5.00E-05	0.00031478	yes	3.50199287
nirC	Nitrite transp	NC_007946:3755006-3755813	baseline	60hcl	601.125	15.9693	-5.23429	-10.8546	5.00E-05	0.00031478	yes	3.50199287
glpA	Anaerobic gly	NC_007946:2488606-2492671	baseline	60hcl	1519.76	33.6047	-5.49904	-10.719	5.00E-05	0.00031478	yes	3.50199287
	hypothetical p	NC_007946:3816994-3817621	baseline	60hcl	47.0434	0.943731	-5.63947	-6.97537	5.00E-05	0.00031478	yes	3.50199287
yaaY	Uncharacteriz	NC_007946:22707-22926	baseline	60hcl	75.8668	8.81849	-3.10487	-3.8714	0.0001	0.00059583	yes	3.22487545
ppdD	Type IV pilin P	NC_007946:119431-119872	baseline	60hcl	8.91938	1.85528	-2.26531	-2.84862	0.0009	0.00417083	yes	2.37977751
ypaA	Pseudogene y	NC_007946:2493835-2494021	baseline	60hcl	57.4076	13.2541	-2.11481	-2.30845	0.0045	0.0163651	yes	1.78608134
yjfL	UPF0719 inne	NC_007946:4683701-4684100	baseline	60hcl	6.78525	1.59681	-2.08721	-2.30811	0.00605	0.021138	yes	1.67493611
	hypothetical p	NC_007946:2869969-2870221	baseline	60hcl	19.3155	3.77405	-2.35557	-2.44044	0.00615	0.0213941	yes	1.66970598

D. Genes significantly upregulated in Δ*btsS*Δ*ypdB* 60 minutes after HCl exposure compared to Δ*btsS*Δ*ypdB* at 0 minutes

gene symbol	function	locus	sample_1	sample_2	value_1	value_2	log2(fold_cha	test_stat	p_value	q_value	significant	log10q
tnaA	Tryptophanas	NC_007946:4150296-4151712	baseline	60hcl	5.12518	1481.54	8.17528	18.3463	5.00E-05	0.00031478	yes	3.50199287
lacZ	beta-galactosi	NC_007946:389116-392191	baseline	60hcl	4.36474	841.902	7.59161	17.7392	5.00E-05	0.00031478	yes	3.50199287
lacY	Lactose perm	NC_007946:387811-389065	baseline	60hcl	3.3723	351.94	6.70545	14.0897	5.00E-05	0.00031478	yes	3.50199287
malK	Maltose/malt	NC_007946:4497477-4498593	baseline	60hcl	12.5183	908.232	6.18096	13.2173	5.00E-05	0.00031478	yes	3.50199287
ppsA	Phosphoenol	NC_007946:1820320-1822699	baseline	60hcl	37.8022	2677.28	6.14615	14.8555	5.00E-05	0.00031478	yes	3.50199287
treB	PTS system, tr	NC_007946:4744604-4746026	baseline	60hcl	49.5222	3319.05	6.06655	14.1382	5.00E-05	0.00031478	yes	3.50199287
malE	Maltodextrin	NC_007946:4495922-4497113	baseline	60hcl	11.735	769.236	6.03453	13.5171	5.00E-05	0.00031478	yes	3.50199287
ydeN	N-acetylgalact	NC_007946:1640459-1642079	baseline	60hcl	1.40697	88.1416	5.96916	11.7481	5.00E-05	0.00031478	yes	3.50199287
lamB	Maltoporin (n	NC_007946:4498664-4500005	baseline	60hcl	19.95	1026.47	5.68516	12.7826	5.00E-05	0.00031478	yes	3.50199287
sbp	Sulfate-bindir	NC_007946:4385795-4386785	baseline	60hcl	58.8798	2686.3	5.51171	13.1242	5.00E-05	0.00031478	yes	3.50199287
cysK	Cysteine synth	NC_007946:2692187-2693159	baseline	60hcl	164.728	6833.27	5.37442	13.0284	5.00E-05	0.00031478	yes	3.50199287
mglB	Galactose/me	NC_007946:2380559-2381558	baseline	60hcl	24.6808	1015.98	5.36334	12.4644	5.00E-05	0.00031478	yes	3.50199287
cbl	Alkanesulfona	NC_007946:2111627-2112578	baseline	60hcl	16.7342	686.103	5.35755	12.2455	5.00E-05	0.00031478	yes	3.50199287
treC	Trehalose-6-p	NC_007946:4742899-4744555	baseline	60hcl	36.0641	1474.47	5.35349	12.4266	5.00E-05	0.00031478	yes	3.50199287
cysD	Sulfate adenyl	NC_007946:3037603-3038512	baseline	60hcl	77.6368	3170.68	5.35191	12.7236	5.00E-05	0.00031478	yes	3.50199287
mglA	Galactose/me	NC_007946:2378978-2380499	baseline	60hcl	4.2577	141.942	5.05909	11.2792	5.00E-05	0.00031478	yes	3.50199287
lacA	Galactoside O	NC_007946:387134-387746	baseline	60hcl	5.98612	195.762	5.03133	10.1662	5.00E-05	0.00031478	yes	3.50199287
	Fructose-bisp	NC_007946:2318079-2319322	baseline	60hcl	3.6847	120.411	5.03028	10.537	5.00E-05	0.00031478	yes	3.50199287
lysA	Diaminopime	NC_007946:3168074-3169337	baseline	60hcl	24.3718	767.383	4.97666	11.457	5.00E-05	0.00031478	yes	3.50199287
dadA	D-amino acid	NC_007946:1310460-1311732	baseline	60hcl	34.5578	1059.47	4.93818	11.5312	5.00E-05	0.00031478	yes	3.50199287
ydjS	Succinylgluta	NC_007946:1859416-1865444	baseline	60hcl	22.499	666.27	4.88817	10.2377	5.00E-05	0.00031478	yes	3.50199287
mglC	Galactose/me	NC_007946:2377952-2378963	baseline	60hcl	17.2689	458.695	4.73128	10.9815	5.00E-05	0.00031478	yes	3.50199287
cysC	Adenylylsulfat	NC_007946:3035569-3037602	baseline	60hcl	233.885	6186.54	4.72526	9.62423	5.00E-05	0.00031478	yes	3.50199287
ygaM	ElaB protein	NC_007946:2955003-2955333	baseline	60hcl	6.98024	171.695	4.62043	7.60099	5.00E-05	0.00031478	yes	3.50199287
tauA	Taurine ABC t	NC_007946:400567-401678	baseline	60hcl	2.32445	53.8851	4.53492	8.59205	5.00E-05	0.00031478	yes	3.50199287
dadX	Alanine racem	NC_007946:1311741-1312812	baseline	60hcl	44.601	970.884	4.44415	10.4046	5.00E-05	0.00031478	yes	3.50199287
tnaB	Low affinity tr	NC_007946:4151803-4153051	baseline	60hcl	9.61412	208.399	4.43805	10.2256	5.00E-05	0.00031478	yes	3.50199287
nanA	N-acetylneura	NC_007946:3584030-3584924	baseline	60hcl	35.8572	760.175	4.406	10.115	5.00E-05	0.00031478	yes	3.50199287
nlpA	Lipoprotein 2	NC_007946:4105193-4106012	baseline	60hcl	40.2363	803.469	4.31967	10.1058	5.00E-05	0.00031478	yes	3.50199287
malF	Maltodextrin	NC_007946:4494224-4495769	baseline	60hcl	15.8979	314.201	4.30478	9.86767	5.00E-05	0.00031478	yes	3.50199287
fliY	L-cystine ABC	NC_007946:2023331-2024132	baseline	60hcl	181.481	3508.3	4.27288	10.2096	5.00E-05	0.00031478	yes	3.50199287
cysI	Sulfite reduct	NC_007946:3041150-3044662	baseline	60hcl	359.096	6494.12	4.17669	9.88672	5.00E-05	0.00031478	yes	3.50199287
gabD	Succinate-sen	NC_007946:2946131-2947580	baseline	60hcl	3.60057	65.0133	4.17444	9.00936	5.00E-05	0.00031478	yes	3.50199287
nanT	Sialic acid tra	NC_007946:3582431-3583922	baseline	60hcl	14.5605	256.22	4.13725	9.44467	5.00E-05	0.00031478	yes	3.50199287
mdh	Malate dehyd	NC_007946:3592996-3593935	baseline	60hcl	143.177	2442.67	4.09258	9.78391	5.00E-05	0.00031478	yes	3.50199287
ygaT	Carbon starva	NC_007946:2943843-2944821	baseline	60hcl	4.78789	81.2121	4.08423	8.61301	5.00E-05	0.00031478	yes	3.50199287
ygaF	L-2-hydroxygl	NC_007946:2944840-2946109	baseline	60hcl	2.17672	36.7494	4.07749	8.06788	5.00E-05	0.00031478	yes	3.50199287
tdcA	Threonine cat	NC_007946:3492032-3492971	baseline	60hcl	14.2673	234.533	4.03901	7.84437	5.00E-05	0.00031478	yes	3.50199287
poxB	Pyruvate deh	NC_007946:870289-872008	baseline	60hcl	5.96781	96.7826	4.01947	9.25942	5.00E-05	0.00031478	yes	3.50199287
glcD	Glycolate deh	NC_007946:3329089-3331632	baseline	60hcl	8.33222	134.115	4.00862	8.85595	5.00E-05	0.00031478	yes	3.50199287
cysA	Sulfate and th	NC_007946:2698537-2702349	baseline	60hcl	453.324	7246.26	3.99862	9.21778	5.00E-05	0.00031478	yes	3.50199287
osmY	Osmotically in	NC_007946:5035341-5035947	baseline	60hcl	63.1905	999.376	3.98325	9.38684	5.00E-05	0.00031478	yes	3.50199287
ytjA	UPF0391 mer	NC_007946:5036073-5036235	baseline	60hcl	27.5188	434.521	3.98093	4.25668	5.00E-05	0.00031478	yes	3.50199287
yciW	Uncharacteriz	NC_007946:1469907-1471035	baseline	60hcl	19.8118	311.66	3.97554	9.16115	5.00E-05	0.00031478	yes	3.50199287
yeiM	Pseudouridin	NC_007946:2396100-2397330	baseline	60hcl	19.9561	294.125	3.88153	8.98436	5.00E-05	0.00031478	yes	3.50199287
fumA	Fumarate hyd	NC_007946:1727160-1728807	baseline	60hcl	123.29	1793.78	3.86287	9.12103	5.00E-05	0.00031478	yes	3.50199287
yjfO	Lipoprotein B	NC_007946:4688163-4688493	baseline	60hcl	341.432	4905.3	3.84467	8.38402	5.00E-05	0.00031478	yes	3.50199287
gabT	Gamma-amin	NC_007946:2947593-2948874	baseline	60hcl	10.5646	150.814	3.83546	8.74429	5.00E-05	0.00031478	yes	3.50199287
srlB	PTS system, gl	NC_007946:2985754-2986126	baseline	60hcl	3.42157	48.2018	3.81636	5.36691	5.00E-05	0.00031478	yes	3.50199287
ydeM	GALNS arylsul	NC_007946:1639250-1640408	baseline	60hcl	0.986942	13.8202	3.80767	6.20318	5.00E-05	0.00031478	yes	3.50199287
srlA	PTS system, gl	NC_007946:2984224-2985744	baseline	60hcl	17.3758	236.001	3.76364	7.75653	5.00E-05	0.00031478	yes	3.50199287
acs	Acetyl-CoA sy	NC_007946:4554807-4556766	baseline	60hcl	8.02536	106.896	3.73549	8.07464	5.00E-05	0.00031478	yes	3.50199287
sucC	Succinyl-CoA	NC_007946:730480-732516	baseline	60hcl	804.019	10681.8	3.73179	8.59949	5.00E-05	0.00031478	yes	3.50199287
gltA	Citrate syntha	NC_007946:720772-722229	baseline	60hcl	192.239	2523.4	3.71439	8.81829	5.00E-05	0.00031478	yes	3.50199287
ybiK	Isoaspartyl an	NC_007946:827782-830606	baseline	60hcl	111.897	1419.42	3.66505	8.05596	5.00E-05	0.00031478	yes	3.50199287
yeiN	Pseudouridin	NC_007946:2397444-2399312	baseline	60hcl	104.338	1275.21	3.6114	8.16307	5.00E-05	0.00031478	yes	3.50199287
cysH	Phosphoaden	NC_007946:3040342-3041077	baseline	60hcl	139.513	1675.25	3.58591	8.50442	5.00E-05	0.00031478	yes	3.50199287
talA	Transaldolase	NC_007946:2728309-2729260	baseline	60hcl	10.3073	122.811	3.5747	8.19096	5.00E-05	0.00031478	yes	3.50199287
yehX	Osmoprotecta	NC_007946:2357701-2359778	baseline	60hcl	13.8232	161.658	3.54778	8.25082	5.00E-05	0.00031478	yes	3.50199287
tktB	Transketolase	NC_007946:2729279-2731283	baseline	60hcl	13.6561	158.945	3.54091	8.35047	5.00E-05	0.00031478	yes	3.50199287
sucB	Dihydrolipoa	NC_007946:729169-730387	baseline	60hcl	551.364	6279.18	3.5095	8.37111	5.00E-05	0.00031478	yes	3.50199287
srlD	Sorbitol-6-ph	NC_007946:2986129-2986909	baseline	60hcl	25.7836	289.294	3.48801	8.0452	5.00E-05	0.00031478	yes	3.50199287
yeaG	Uncharacteriz	NC_007946:1899158-1901093	baseline	60hcl	8.98419	94.8648	3.40041	7.96965	5.00E-05	0.00031478	yes	3.50199287
yedE	UPF0394 inne	NC_007946:2032283-2033719	baseline	60hcl	121.964	1278.14	3.38952	4.63813	5.00E-05	0.00031478	yes	3.50199287
aldA	Aldehyde deh	NC_007946:1563132-1564572	baseline	60hcl	38.4062	402.475	3.38949	7.81209	5.00E-05	0.00031478	yes	3.50199287
sucA	2-oxoglutarat	NC_007946:726353-729155	baseline	60hcl	243.096	2509.74	3.36794	8.04698	5.00E-05	0.00031478	yes	3.50199287
otsA	Alpha,alpha-t	NC_007946:2003945-2006145	baseline	60hcl	16.2924	164.016	3.33157	7.08333	5.00E-05	0.00031478	yes	3.50199287
malG	Maltodextrin	NC_007946:4493319-4494210	baseline	60hcl	13.2817	133.264	3.32677	7.61448	5.00E-05	0.00031478	yes	3.50199287
yhcH	Putative suga	NC_007946:3580361-3582384	baseline	60hcl	84.7499	837.005	3.30395	6.84666	5.00E-05	0.00031478	yes	3.50199287
narU	Nitrate/nitrite	NC_007946:1611398-1612787	baseline	60hcl	0.897518	8.69554	3.27626	5.54624	5.00E-05	0.00031478	yes	3.50199287
putA	Transcription	NC_007946:1061850-1065813	baseline	60hcl	28.6046	266.283	3.21864	7.61608	5.00E-05	0.00031478	yes	3.50199287
osmC	Peroxiredoxir	NC_007946:1623535-1624095	baseline	60hcl	23.679	218.281	3.20451	7.15611	5.00E-05	0.00031478	yes	3.50199287
glcG	Hypothetical	NC_007946:3327446-3327851	baseline	60hcl	29.8341	273.869	3.19845	7.11412	5.00E-05	0.00031478	yes	3.50199287
phoA	Alkaline phos	NC_007946:415983-417399	baseline	60hcl	21.2989	195.112	3.19545	7.53022	5.00E-05	0.00031478	yes	3.50199287

yfcG	Probable glut	NC_007946:2552761-2553409	baseline	60hcl	4.2091	38.5059	3.1935	6.0802	5.00E-05	0.00031478	yes	3.50199287
ygbE	Inner membra	NC_007946:3035196-3035520	baseline	60hcl	49.1117	446.331	3.18397	7.18378	5.00E-05	0.00031478	yes	3.50199287
gcvT	Aminomethyl	NC_007946:3227217-3228312	baseline	60hcl	206.292	1864.04	3.17567	7.50091	5.00E-05	0.00031478	yes	3.50199287
agp	Glucose-1-ph	NC_007946:1052796-1054038	baseline	60hcl	42.4049	373.519	3.13888	7.38468	5.00E-05	0.00031478	yes	3.50199287
		NC_007946:4204571-4207495	baseline	60hcl	17.1686	149.952	3.12666	6.34479	5.00E-05	0.00031478	yes	3.50199287
pspE	Thiosulfate:cy	NC_007946:1489005-1489320	baseline	60hcl	11.3013	98.1346	3.11827	5.51251	5.00E-05	0.00031478	yes	3.50199287
lldP	L-lactate perm	NC_007946:4039261-4042880	baseline	60hcl	113.495	980.376	3.11071	6.16295	5.00E-05	0.00031478	yes	3.50199287
		NC_007946:230502-233426	baseline	60hcl	17.2174	148.625	3.10974	6.31579	5.00E-05	0.00031478	yes	3.50199287
		NC_007946:4458262-4461186	baseline	60hcl	17.3529	148.849	3.1006	6.28902	5.00E-05	0.00031478	yes	3.50199287
phxI	Pyridoxine 4-(	NC_007946:1551361-1552222	baseline	60hcl	10.5267	89.9594	3.09522	7.06921	5.00E-05	0.00031478	yes	3.50199287
		NC_007946:4323845-4326769	baseline	60hcl	17.4527	148.699	3.09088	6.27569	5.00E-05	0.00031478	yes	3.50199287
sdhB	Succinate deh	NC_007946:725276-725993	baseline	60hcl	455.746	3807.66	3.06261	7.19583	5.00E-05	0.00031478	yes	3.50199287
idnD	L-idonate 5-d	NC_007946:4775081-4776113	baseline	60hcl	4.53153	37.5984	3.0526	6.51352	5.00E-05	0.00031478	yes	3.50199287
ybaS	Glutaminase (	NC_007946:527065-527998	baseline	60hcl	4.18905	34.7209	3.05111	6.22037	5.00E-05	0.00031478	yes	3.50199287
gcvH	Glycine cleava	NC_007946:3226804-3227194	baseline	60hcl	175.942	1448.35	3.04123	7.0403	5.00E-05	0.00031478	yes	3.50199287
	hypothetical p	NC_007946:2200667-2201813	baseline	60hcl	15.7578	127.424	3.0155	7.11303	5.00E-05	0.00031478	yes	3.50199287
ykgC	Putative Dihy	NC_007946:338641-339967	baseline	60hcl	4.55972	36.7105	3.00918	6.65968	5.00E-05	0.00031478	yes	3.50199287
malM	Maltose opero	NC_007946:4500327-4501248	baseline	60hcl	28.5455	227.805	2.99647	6.93425	5.00E-05	0.00031478	yes	3.50199287
		NC_007946:228523-230065	baseline	60hcl	25.2002	200.44	2.99166	6.01404	5.00E-05	0.00031478	yes	3.50199287
yhiE	Transcription	NC_007946:3925144-3925672	baseline	60hcl	1.27869	10.0983	2.98137	3.73724	5.00E-05	0.00031478	yes	3.50199287
		NC_007946:4456366-4457908	baseline	60hcl	26.6103	209.454	2.97658	5.97707	5.00E-05	0.00031478	yes	3.50199287
		NC_007946:4321857-4323399	baseline	60hcl	26.8587	209.583	2.96406	5.95525	5.00E-05	0.00031478	yes	3.50199287
ycgB	FIG004684: S	NC_007946:1308571-1310104	baseline	60hcl	4.30803	33.5657	2.96189	6.6594	5.00E-05	0.00031478	yes	3.50199287
		NC_007946:4202675-4204217	baseline	60hcl	26.687	207.677	2.96013	5.96649	5.00E-05	0.00031478	yes	3.50199287
maeB	NADP-depend	NC_007946:2725741-2728021	baseline	60hcl	122.745	948.398	2.94983	6.92982	5.00E-05	0.00031478	yes	3.50199287
gcvP	Glycine dehyc	NC_007946:3223813-3226687	baseline	60hcl	82.2836	621.267	2.91654	6.82333	5.00E-05	0.00031478	yes	3.50199287
glcF	Glycolate deh	NC_007946:3327855-3329079	baseline	60hcl	9.19422	69.0502	2.90885	6.69727	5.00E-05	0.00031478	yes	3.50199287
ycbN	FMNH2-depe	NC_007946:999327-1001997	baseline	60hcl	8.77493	63.4864	2.85499	5.70646	5.00E-05	0.00031478	yes	3.50199287
yahO	hypothetical p	NC_007946:376440-376716	baseline	60hcl	6.06977	43.4751	2.84048	3.82506	5.00E-05	0.00031478	yes	3.50199287
yehZ	Osmoprotecta	NC_007946:2359784-2360702	baseline	60hcl	18.5408	132.679	2.83917	6.65588	5.00E-05	0.00031478	yes	3.50199287
ygiW	Protein ygiW	NC_007946:3386639-3387032	baseline	60hcl	59.6221	423.23	2.82752	6.57516	5.00E-05	0.00031478	yes	3.50199287
aceA	Isocitrate lyas	NC_007946:4465334-4466639	baseline	60hcl	10.9889	77.577	2.81959	6.4846	5.00E-05	0.00031478	yes	3.50199287
yeiL	Regulatory pr	NC_007946:2395335-2396034	baseline	60hcl	2.402	16.5076	2.78083	4.73525	5.00E-05	0.00031478	yes	3.50199287
hdhA	7-alpha-hydro	NC_007946:1737528-1738296	baseline	60hcl	24.7763	169.351	2.77299	6.55143	5.00E-05	0.00031478	yes	3.50199287
	hypothetical p	NC_007946:3862242-3862728	baseline	60hcl	1.55074	10.4683	2.755	3.54313	5.00E-05	0.00031478	yes	3.50199287
fadB	Enoyl-CoA hyc	NC_007946:4315110-4317300	baseline	60hcl	9.86539	66.3883	2.75048	6.31251	5.00E-05	0.00031478	yes	3.50199287
	Hemolysin act	NC_007946:4854178-4855945	baseline	60hcl	80.7687	541.932	2.74624	6.47738	5.00E-05	0.00031478	yes	3.50199287
gsiB	Oligopeptide	NC_007946:830655-832164	baseline	60hcl	55.5108	370.987	2.74053	6.49071	5.00E-05	0.00031478	yes	3.50199287
yhiX	Transcription	NC_007946:3931765-3932590	baseline	60hcl	20.6254	137.148	2.73324	6.45683	5.00E-05	0.00031478	yes	3.50199287
glcB	Malate syntha	NC_007946:3325253-3327425	baseline	60hcl	28.4192	187.732	2.72374	6.36452	5.00E-05	0.00031478	yes	3.50199287
yghZ	L-glyceraldeh	NC_007946:3358722-3359763	baseline	60hcl	15.854	104.622	2.72228	6.2922	5.00E-05	0.00031478	yes	3.50199287
xasA	Probable glut	NC_007946:1628572-1630108	baseline	60hcl	4.08922	26.4904	2.69557	5.96569	5.00E-05	0.00031478	yes	3.50199287
yddH	NAD(P)H-flavi	NC_007946:1601992-1602562	baseline	60hcl	2.22642	14.4169	2.69496	4.10002	5.00E-05	0.00031478	yes	3.50199287
rstA	Two-compone	NC_007946:1722588-1723308	baseline	60hcl	44.1495	284.708	2.68902	6.36966	5.00E-05	0.00031478	yes	3.50199287
wrbA	NAD(P)H dehy	NC_007946:1054323-1054920	baseline	60hcl	36.4736	234.502	2.68468	6.12026	5.00E-05	0.00031478	yes	3.50199287
ygaU	Uncharacteriz	NC_007946:2951195-2951645	baseline	60hcl	38.7703	248.512	2.68029	6.22466	5.00E-05	0.00031478	yes	3.50199287
gsiD	Oligopeptide	NC_007946:833104-834016	baseline	60hcl	52.3067	335.131	2.67966	6.33014	5.00E-05	0.00031478	yes	3.50199287
ybaY	Uncharacteriz	NC_007946:489508-490081	baseline	60hcl	55.5007	352.743	2.66804	6.32489	5.00E-05	0.00031478	yes	3.50199287
papH	hypothetical p	NC_007946:4795816-4796065	baseline	60hcl	28.1167	178.299	2.66479	5.11888	5.00E-05	0.00031478	yes	3.50199287
hdeA	Chaperone Hc	NC_007946:3923186-3923519	baseline	60hcl	32.1947	204.109	2.66445	5.68008	5.00E-05	0.00031478	yes	3.50199287
yiaG	Antitoxin to R	NC_007946:3986733-3987024	baseline	60hcl	15.8439	100.066	2.65895	4.88024	5.00E-05	0.00031478	yes	3.50199287
melA	alpha-galacto	NC_007946:4615663-4617666	baseline	60hcl	12.0335	75.9111	2.65726	4.6857	5.00E-05	0.00031478	yes	3.50199287
lysC	Aspartokinase	NC_007946:4484429-4485779	baseline	60hcl	128.131	805.808	2.65282	6.20404	5.00E-05	0.00031478	yes	3.50199287
elaB	ElaB protein	NC_007946:2516741-2517047	baseline	60hcl	54.136	336.854	2.63746	5.84272	5.00E-05	0.00031478	yes	3.50199287
ggt	Gamma-gluta	NC_007946:3846333-3848067	baseline	60hcl	10.9927	68.0776	2.63063	6.22796	5.00E-05	0.00031478	yes	3.50199287
ydiZ	Uncharacteriz	NC_007946:1842113-1842404	baseline	60hcl	24.6178	152.341	2.62954	5.27859	5.00E-05	0.00031478	yes	3.50199287
yjfN	hypothetical p	NC_007946:4687739-4688027	baseline	60hcl	24.0667	147.634	2.61691	4.68752	5.00E-05	0.00031478	yes	3.50199287
yjhA	N-acetylneura	NC_007946:4903517-4904066	baseline	60hcl	2.88944	17.6599	2.61162	4.13401	5.00E-05	0.00031478	yes	3.50199287
		NC_007946:3641652-3644576	baseline	60hcl	24.2763	146.245	2.59076	5.22497	5.00E-05	0.00031478	yes	3.50199287
yphA	Inner membra	NC_007946:2815094-2815517	baseline	60hcl	8.27241	49.7548	2.58845	4.84281	5.00E-05	0.00031478	yes	3.50199287
idnO	5-keto-D-gluc	NC_007946:4774293-4775058	baseline	60hcl	5.73914	34.2709	2.57808	5.33624	5.00E-05	0.00031478	yes	3.50199287
	hypothetical p	NC_007941:42627-43797	baseline	60hcl	3.37388	20.1428	2.57779	5.36041	5.00E-05	0.00031478	yes	3.50199287
fucO	Lactaldehyde	NC_007946:3086369-3087521	baseline	60hcl	16.7506	99.617	2.57218	6.06505	5.00E-05	0.00031478	yes	3.50199287
		NC_007946:2873816-2875358	baseline	60hcl	35.4251	210.239	2.56918	5.09101	5.00E-05	0.00031478	yes	3.50199287
		NC_007946:2870538-2873462	baseline	60hcl	26.5324	155.897	2.55476	5.11489	5.00E-05	0.00031478	yes	3.50199287
hdeB	Chaperone Hc	NC_007946:3922744-3923083	baseline	60hcl	12.3008	71.8115	2.54546	4.57448	5.00E-05	0.00031478	yes	3.50199287
clpB	Chaperone pr	NC_007946:2875800-2878113	baseline	60hcl	136.044	792.982	2.54321	5.6967	5.00E-05	0.00031478	yes	3.50199287
dps	DNA protectio	NC_007946:811080-811584	baseline	60hcl	129.422	753.937	2.54236	5.98471	5.00E-05	0.00031478	yes	3.50199287
		NC_007946:3696659-3698201	baseline	60hcl	36.6472	211.028	2.52566	5.04292	5.00E-05	0.00031478	yes	3.50199287
ydgE	Spermidine ex	NC_007946:1713250-1713932	baseline	60hcl	610.96	3499.74	2.5181	5.79437	5.00E-05	0.00031478	yes	3.50199287
		NC_007946:3693381-3696305	baseline	60hcl	26.8428	153.64	2.51694	5.03185	5.00E-05	0.00031478	yes	3.50199287
carB	Carbamoyl-ph	NC_007946:32708-35930	baseline	60hcl	91.4928	521.607	2.51123	5.70401	5.00E-05	0.00031478	yes	3.50199287
		NC_007946:3645022-3646564	baseline	60hcl	36.1924	206.272	2.51079	5.00782	5.00E-05	0.00031478	yes	3.50199287
	Putative DNA	NC_007946:297786-301886	baseline	60hcl	17.8401	101.385	2.50665	5.8735	5.00E-05	0.00031478	yes	3.50199287
ydiA	Phosphoenol	NC_007946:1823031-1823865	baseline	60hcl	34.8723	197.072	2.49857	5.96687	5.00E-05	0.00031478	yes	3.50199287
mtfA	Protein MtfA	NC_007946:2068901-2069699	baseline	60hcl	18.9017	106.235	2.49068	5.68042	5.00E-05	0.00031478	yes	3.50199287
cysM	Cysteine synth	NC_007946:2697491-2698349	baseline	60hcl	286.783	1603.63	2.48331	5.83709	5.00E-05	0.00031478	yes	3.50199287
sdhC	Succinate deh	NC_007946:722866-725261	baseline	60hcl	1058.21	5888.91	2.47638	3.01338	5.00E-05	0.00031478	yes	3.50199287
nanM	N-acetylneura	NC_007946:4902391-4903498	baseline	60hcl	3.03531	16.6047	2.45167	4.82355	5.00E-05	0.00031478	yes	3.50199287
ssuB	Alkanesulfona	NC_007946:997760-999319	baseline	60hcl	12.926	70.7025	2.45148	5.63519	5.00E-05	0.00031478	yes	3.50199287

dapB	4-hydroxy-tet	NC_007946:30265-31087	baseline	60hcl	101.431	553.066	2.44695	5.7794	5.00E-05	0.00031478	yes	3.50199287
yliE	c-di-GMP pho	NC_007946:834192-836541	baseline	60hcl	11.8298	63.9009	2.43341	5.72481	5.00E-05	0.00031478	yes	3.50199287
yhiP	Di-tripeptide/	NC_007946:3902654-3904124	baseline	60hcl	140.736	758.565	2.43028	5.60329	5.00E-05	0.00031478	yes	3.50199287
gsiC	Oligopeptide	NC_007946:832181-833102	baseline	60hcl	90.1109	482.945	2.42208	5.71671	5.00E-05	0.00031478	yes	3.50199287
gadB	Glutamate de	NC_007946:1630263-1631664	baseline	60hcl	6.84907	36.0941	2.39779	5.46785	5.00E-05	0.00031478	yes	3.50199287
ytfQ	Galactofuranc	NC_007946:4729779-4730736	baseline	60hcl	12.4541	65.5469	2.39591	5.587	5.00E-05	0.00031478	yes	3.50199287
ybaT	Inner membra	NC_007946:528000-529293	baseline	60hcl	15.3795	80.2839	2.3841	5.5652	5.00E-05	0.00031478	yes	3.50199287
ompD	Outer membr	NC_007946:2035008-2036091	baseline	60hcl	143.789	748.555	2.38015	5.56495	5.00E-05	0.00031478	yes	3.50199287
yicL	Uncharacteriz	NC_007946:4104266-4105190	baseline	60hcl	38.0661	195.651	2.3617	5.54386	5.00E-05	0.00031478	yes	3.50199287
ugpB	Glycerol-3-ph	NC_007946:3852252-3853569	baseline	60hcl	6.86525	35.1951	2.35799	5.32868	5.00E-05	0.00031478	yes	3.50199287
yqeF	Acetyl-CoA ac	NC_007946:3174848-3176030	baseline	60hcl	83.0146	423.397	2.35057	5.5067	5.00E-05	0.00031478	yes	3.50199287
tdcB	Threonine del	NC_007946:3490944-3491934	baseline	60hcl	40.4741	204.701	2.33845	4.6398	5.00E-05	0.00031478	yes	3.50199287
rspB	Starvation ser	NC_007946:1693398-1694418	baseline	60hcl	6.3082	31.8287	2.33503	5.1485	5.00E-05	0.00031478	yes	3.50199287
tauB	Taurine ABC t	NC_007946:401690-404130	baseline	60hcl	25.5434	128.626	2.33216	5.65896	5.00E-05	0.00031478	yes	3.50199287
malP	Maltodextrin	NC_007946:3802882-3805276	baseline	60hcl	55.9152	280.888	2.32868	5.32632	5.00E-05	0.00031478	yes	3.50199287
yehV	HTH-type tran	NC_007946:2356086-2356818	baseline	60hcl	10.4178	52.3314	2.32862	5.21921	5.00E-05	0.00031478	yes	3.50199287
dctA	Na+/H+-dicart	NC_007946:3948779-3949967	baseline	60hcl	130.212	651.013	2.32183	5.42732	5.00E-05	0.00031478	yes	3.50199287
bssR	Biofilm regula	NC_007946:839461-839845	baseline	60hcl	16.0697	80.2442	2.32005	4.58887	5.00E-05	0.00031478	yes	3.50199287
ybhN	Inner membra	NC_007946:784485-787441	baseline	60hcl	22.6427	112.876	2.31763	5.32217	5.00E-05	0.00031478	yes	3.50199287
slp	Starvation lip	NC_007946:3911723-3912290	baseline	60hcl	15.4128	76.0801	2.30339	4.98141	5.00E-05	0.00031478	yes	3.50199287
yjgB	Cinnamyl alcc	NC_007946:4776896-4777916	baseline	60hcl	11.8898	58.4312	2.29701	5.29159	5.00E-05	0.00031478	yes	3.50199287
yeaH	UPF0229 prot	NC_007946:1901205-1902489	baseline	60hcl	6.8922	33.4997	2.28111	5.16354	5.00E-05	0.00031478	yes	3.50199287
ybeL	Uncharacteriz	NC_007946:656868-657351	baseline	60hcl	70.0156	338.756	2.2745	5.31012	5.00E-05	0.00031478	yes	3.50199287
ydaM	Diguanylate c	NC_007946:1523718-1525011	baseline	60hcl	5.34015	25.6799	2.26569	5.08453	5.00E-05	0.00031478	yes	3.50199287
fadE	Acyl-coenzym	NC_007946:273357-275802	baseline	60hcl	9.74792	46.5649	2.25608	5.23444	5.00E-05	0.00031478	yes	3.50199287
ugpE	Glycerol-3-ph	NC_007946:3850425-3852155	baseline	60hcl	5.66538	26.9717	2.2512	4.74472	5.00E-05	0.00031478	yes	3.50199287
acnB	Aconitate hyd	NC_007946:137801-140399	baseline	60hcl	655.613	3108.09	2.24511	5.43615	5.00E-05	0.00031478	yes	3.50199287
rpiR	Transcription	NC_007946:4586464-4587355	baseline	60hcl	166.461	784.91	2.23734	4.88777	5.00E-05	0.00031478	yes	3.50199287
glgA	Glycogen synt	NC_007946:3828761-3831490	baseline	60hcl	162.054	755.908	2.22173	5.19943	5.00E-05	0.00031478	yes	3.50199287
groEL	Heat shock pr	NC_007946:4643136-4644783	baseline	60hcl	1136.62	5299.81	2.22118	5.0868	5.00E-05	0.00031478	yes	3.50199287
ycdW	Glyoxylate/hy	NC_007946:1142852-1143791	baseline	60hcl	37.5288	174.762	2.21932	5.27437	5.00E-05	0.00031478	yes	3.50199287
ybgO	Uncharacteriz	NC_007946:720250-720625	baseline	60hcl	14.3904	66.8205	2.21519	4.28316	5.00E-05	0.00031478	yes	3.50199287
idnK	Gluconokinas	NC_007946:4776329-4776893	baseline	60hcl	8.9714	41.546	2.2113	4.44526	5.00E-05	0.00031478	yes	3.50199287
xylF	D-xylose ABC t	NC_007946:3996982-3997975	baseline	60hcl	2.30159	10.6357	2.20822	4.15974	5.00E-05	0.00031478	yes	3.50199287
ygeV	Uncharacteriz	NC_007946:3182853-3184632	baseline	60hcl	14.6952	67.8803	2.20764	5.12992	5.00E-05	0.00031478	yes	3.50199287
	NAD-depende	NC_007946:1564613-1565615	baseline	60hcl	7.04252	32.4644	2.20469	4.93949	5.00E-05	0.00031478	yes	3.50199287
glgX	Limit dextrin	NC_007946:3831507-3835664	baseline	60hcl	106.731	489.333	2.19684	5.15296	5.00E-05	0.00031478	yes	3.50199287
	Transcription	NC_007946:4878455-4879022	baseline	60hcl	39.2651	179.72	2.19444	4.37078	5.00E-05	0.00031478	yes	3.50199287
osmE	Osmotically-i	NC_007946:1855379-1855706	baseline	60hcl	125.604	573.685	2.19138	5.1321	5.00E-05	0.00031478	yes	3.50199287
	hypothetical p	NC_007946:1260134-1260515	baseline	60hcl	8.96942	40.6397	2.1798	3.80755	5.00E-05	0.00031478	yes	3.50199287
araC	Arabinose ope	NC_007946:72225-73071	baseline	60hcl	49.3549	222.086	2.16986	5.09656	5.00E-05	0.00031478	yes	3.50199287
ydcT	ABC transport	NC_007946:1583894-1584908	baseline	60hcl	4.88081	21.9179	2.16692	4.631	5.00E-05	0.00031478	yes	3.50199287
	Lipid kinase Y	NC_007946:2310811-2311711	baseline	60hcl	10.5988	47.3054	2.15811	4.88849	5.00E-05	0.00031478	yes	3.50199287
yeeO	Uncharacteriz	NC_007946:2109869-2111321	baseline	60hcl	41.6843	185.107	2.15078	5.05817	5.00E-05	0.00031478	yes	3.50199287
icdA	Isocitrate deh	NC_007946:1240102-1241353	baseline	60hcl	722.112	3199.01	2.14733	5.06833	5.00E-05	0.00031478	yes	3.50199287
ydjY	Hypothetical	NC_007946:1867577-1868255	baseline	60hcl	22.9547	101.65	2.14675	4.82189	5.00E-05	0.00031478	yes	3.50199287
yebF	Small secrete	NC_007946:1956721-1957078	baseline	60hcl	176.824	762.299	2.10804	5.07212	5.00E-05	0.00031478	yes	3.50199287
acnA	Aconitate hyd	NC_007946:1456763-1459439	baseline	60hcl	92.8645	396.762	2.09507	4.88874	5.00E-05	0.00031478	yes	3.50199287
katE	Catalase KatE-	NC_007946:1847532-1849794	baseline	60hcl	19.8614	84.4472	2.08808	4.90202	5.00E-05	0.00031478	yes	3.50199287
yafM	Transposase a	NC_007946:279539-280037	baseline	60hcl	5.23216	21.9761	2.07046	3.61071	5.00E-05	0.00031478	yes	3.50199287
	Putative oxid	NC_007946:324308-325451	baseline	60hcl	3.61497	15.1395	2.06626	4.34576	5.00E-05	0.00031478	yes	3.50199287
cysB	Cys regulon tr	NC_007946:1454801-1455776	baseline	60hcl	126.914	530.131	2.06249	4.88198	5.00E-05	0.00031478	yes	3.50199287
ompT	Protease VII ((	NC_007946:571058-572012	baseline	60hcl	102.62	425.522	2.05192	4.85192	5.00E-05	0.00031478	yes	3.50199287
carA	Carbamoyl-pl	NC_007946:31542-32691	baseline	60hcl	112.489	465.092	2.04774	4.7832	5.00E-05	0.00031478	yes	3.50199287
sfaA	Type-1 fimbria	NC_007946:1099350-1100043	baseline	60hcl	88.7175	361.617	2.02717	4.86877	5.00E-05	0.00031478	yes	3.50199287
	Transcription	NC_007946:4095996-4097550	baseline	60hcl	1.97976	8.01115	2.01668	4.08535	5.00E-05	0.00031478	yes	3.50199287
fumC	Fumarate hyd	NC_007946:1724676-1727018	baseline	60hcl	16.1377	65.3001	2.01665	3.60863	5.00E-05	0.00031478	yes	3.50199287
glgP	Glycogen pho	NC_007946:3826295-3828743	baseline	60hcl	61.4926	247.412	2.00843	4.63755	5.00E-05	0.00031478	yes	3.50199287
ydjN	L-cystine upta	NC_007946:1845648-1847040	baseline	60hcl	531.925	2136.32	2.00583	4.72589	5.00E-05	0.00031478	yes	3.50199287
ycdO	Ferrous iron t	NC_007946:1068851-1069979	baseline	60hcl	353.737	1419.17	2.0043	4.67414	5.00E-05	0.00031478	yes	3.50199287
rspA	Mannonate de	NC_007946:1694429-1695644	baseline	60hcl	8.44886	33.8386	2.00184	4.58044	5.00E-05	0.00031478	yes	3.50199287
yaiB	Anti-adapter p	NC_007946:415622-415883	baseline	60hcl	6.79842	51.8752	2.93177	3.99061	0.0001	0.00059583	yes	3.22487545
yodD	Uncharacteriz	NC_007946:2051083-2051311	baseline	60hcl	14.7727	77.7661	2.39621	3.67849	0.0001	0.00059583	yes	3.22487545
ygcW	Uncharacteriz	NC_007946:3052251-3053037	baseline	60hcl	1.15058	5.04425	2.13228	3.05636	0.00025	0.00135088	yes	2.86938323
erf	Phage recomb	NC_007946:2633924-2634913	baseline	60hcl	4.54113	18.8762	2.05544	2.99671	0.0003	0.00158053	yes	2.80119726
ygfJ	Molybdenum	NC_007946:3193826-3194405	baseline	60hcl	2.19316	8.87707	2.01707	2.94496	0.0003	0.00158053	yes	2.80119726
ydcK	FIG005189: p	NC_007946:1572207-1573719	baseline	60hcl	5.10131	21.7732	2.09362	2.69678	0.00055	0.00272213	yes	2.56509114
	PTS system, II	NC_007946:4095499-4095970	baseline	60hcl	1.87592	9.74271	2.37673	3.05545	0.0006	0.00293333	yes	2.53263908
chaB	Cation transp	NC_007946:1346366-1346597	baseline	60hcl	9.48457	38.9731	2.03882	2.71502	0.00115	0.00522063	yes	2.28227709
rmf	Ribosome mo	NC_007946:1013034-1013202	baseline	60hcl	16.6612	135.898	3.02795	3.28505	0.00205	0.00860398	yes	2.06530061
prpR	Propionate ca	NC_007946:378064-378403	baseline	60hcl	1.73177	12.3743	2.83703	2.97825	0.00225	0.00925899	yes	2.03343638

E. Genes significantly downregulated in Δ*btsS*Δ*ypdB* at 0 minutes after HCl exposure compared to WT at 0 minutes

gene symbol	function	locus	sample_1	sample_2	value_1	value_2	log2(fold_cha	test_stat	p_value	q_value	significant	log10q
fmlD	mannose-spec	NC_007946:1646442-1647357	wt	btssypdb	18.9155	4.39693	-2.105	-3.91785	5.00E-05	0.0008048	yes	3.09431203
proP	L-Proline/Gly	NC_007946:4604243-4605746	wt	btssypdb	1156.94	262.548	-2.13966	-5.9709	5.00E-05	0.0008048	yes	3.09431203
fimG	Type 1 fimbra	NC_007946:1647416-1647671	wt	btssypdb	88.596	17.0722	-2.37559	-3.75319	5.00E-05	0.0008048	yes	3.09431203
rpsT	SSU ribosoma	NC_007946:22341-22527	wt	btssypdb	1654.88	254.793	-2.69933	-5.06302	5.00E-05	0.0008048	yes	3.09431203
	Transcription	NC_007946:1590193-1590367	wt	btssypdb	93.8494	12.0501	-2.9613	-2.62835	0.00095	0.0110806	yes	1.95543672

F. Genes significantly upregulated in Δ*btsS*Δ*ypdB* at 0 minutes after HCl exposure compared to WT at 0 minutes

gene symbol	function	locus	sample_1	sample_2	value_1	value_2	log2(fold_cha	test_stat	p_value	q_value	significant	log10q
glpA	Anaerobic gly	NC_007946:2488606-2492671	wt	btssypdb	37.1728	1445.97	5.28164	10.285	5.00E-05	0.0008048	yes	3.09431203
narG	Respiratory ni	NC_007946:1353988-1360651	wt	btssypdb	53.0861	1734.02	5.02965	7.26871	5.00E-05	0.0008048	yes	3.09431203
frdC	Fumarate red	NC_007946:4651175-4651571	wt	btssypdb	21.907	513.933	4.55211	9.49045	5.00E-05	0.0008048	yes	3.09431203
frdD	Fumarate red	NC_007946:4650805-4651165	wt	btssypdb	92.4924	1718.57	4.21573	10.4596	5.00E-05	0.0008048	yes	3.09431203
nirC	Nitrite transp	NC_007946:3755006-3755813	wt	btssypdb	37.2028	571.528	3.94134	10.1076	5.00E-05	0.0008048	yes	3.09431203
napB	Nitrate reduct	NC_007946:2435148-2437140	wt	btssypdb	84.9571	1254.53	3.88427	9.34496	5.00E-05	0.0008048	yes	3.09431203
rbsC	Ribose ABC tra	NC_007946:4196155-4197121	wt	btssypdb	88.3573	1114.35	3.65671	9.74631	5.00E-05	0.0008048	yes	3.09431203
yjjI	Uncharacteriz	NC_007946:5038422-5040909	wt	btssypdb	22.9336	284.826	3.63455	7.52979	5.00E-05	0.0008048	yes	3.09431203
glpT	Glycerol-3-ph	NC_007946:2486975-2488334	wt	btssypdb	13.6443	163.481	3.58275	8.48124	5.00E-05	0.0008048	yes	3.09431203
rbsA	Ribose ABC tra	NC_007946:4194645-4196151	wt	btssypdb	38.1663	440.787	3.52971	9.51666	5.00E-05	0.0008048	yes	3.09431203
narK	Nitrate/nitrite	NC_007946:1352204-1353596	wt	btssypdb	56.5284	565.4	3.32222	7.07303	5.00E-05	0.0008048	yes	3.09431203
yeiN	Pseudouridin	NC_007946:2397444-2399312	wt	btssypdb	10.1734	99.4394	3.28902	7.16859	5.00E-05	0.0008048	yes	3.09431203
napC	Cytochrome c	NC_007946:2434536-2435139	wt	btssypdb	29.5917	283.735	3.26128	7.56461	5.00E-05	0.0008048	yes	3.09431203
rbsB	Ribose ABC tra	NC_007946:4197145-4198036	wt	btssypdb	107.255	1027.37	3.25984	8.92738	5.00E-05	0.0008048	yes	3.09431203
nirB	Nitrite reduct	NC_007946:3752014-3754881	wt	btssypdb	151.289	1312.61	3.11706	3.58629	5.00E-05	0.0008048	yes	3.09431203
rbsD	D-ribose pyran	NC_007946:4194218-4194638	wt	btssypdb	54.677	470.974	3.10664	7.37119	5.00E-05	0.0008048	yes	3.09431203
ykgF	Predicted L-la	NC_007946:342304-344420	wt	btssypdb	46.0632	381.888	3.05146	7.14126	5.00E-05	0.0008048	yes	3.09431203
ykgE	Predicted L-la	NC_007946:341574-342294	wt	btssypdb	12.607	103.005	3.03042	6.62226	5.00E-05	0.0008048	yes	3.09431203
cdd	Cytidine deam	NC_007946:2373053-2373938	wt	btssypdb	42.3641	334.129	2.97949	7.058	5.00E-05	0.0008048	yes	3.09431203
nikA	Nickel ABC tra	NC_007946:3880155-3885071	wt	btssypdb	128.796	1011.99	2.97404	5.73473	5.00E-05	0.0008048	yes	3.09431203
fruK	1-phosphofru	NC_007946:2401475-2403544	wt	btssypdb	574.872	4298.46	2.90251	7.64849	5.00E-05	0.0008048	yes	3.09431203
dmsA	Anaerobic din	NC_007946:948909-951132	wt	btssypdb	7.77218	57.9056	2.89731	6.98298	5.00E-05	0.0008048	yes	3.09431203
yhbV	Uncharacteriz	NC_007946:3522323-3523202	wt	btssypdb	21.4017	159.101	2.89414	6.48938	5.00E-05	0.0008048	yes	3.09431203
frdB	Fumarate red	NC_007946:4651581-4654117	wt	btssypdb	115.998	862.213	2.89394	5.35808	5.00E-05	0.0008048	yes	3.09431203
yjcX	D-allose ABC t	NC_007946:4585470-4586412	wt	btssypdb	5.67699	38.6391	2.76686	5.607	5.00E-05	0.0008048	yes	3.09431203
katG	Catalase-pero	NC_007946:4418149-4420330	wt	btssypdb	109.631	732.647	2.74046	7.63914	5.00E-05	0.0008048	yes	3.09431203
dmsB	Anaerobic din	NC_007946:951142-951760	wt	btssypdb	12.4947	80.3464	2.68492	5.75901	5.00E-05	0.0008048	yes	3.09431203
yaaY	Uncharacteriz	NC_007946:22707-22926	wt	btssypdb	11.4042	72.787	2.67412	3.15778	5.00E-05	0.0008048	yes	3.09431203
aspA	Aspartate amr	NC_007946:4639002-4640439	wt	btssypdb	84.7494	534.092	2.65581	6.79096	5.00E-05	0.0008048	yes	3.09431203
fruA	PTS system, in	NC_007946:2399767-2401459	wt	btssypdb	529.175	3190.57	2.59199	6.80506	5.00E-05	0.0008048	yes	3.09431203
ycgS	Phosphoenol	NC_007946:1327773-1328406	wt	btssypdb	89.0372	530.303	2.57434	6.60819	5.00E-05	0.0008048	yes	3.09431203
yhgG	Ferrous iron-s	NC_007946:3795389-3795626	wt	btssypdb	12.0849	69.6197	2.52629	3.44622	5.00E-05	0.0008048	yes	3.09431203
adhE	Acetaldehyde	NC_007946:1370514-1373190	wt	btssypdb	109.269	602.845	2.4639	6.69139	5.00E-05	0.0008048	yes	3.09431203
udp	Uridine phosp	NC_007946:4297304-4298069	wt	btssypdb	324.612	1781.62	2.4564	6.58805	5.00E-05	0.0008048	yes	3.09431203
glpQ	Glycerophosp	NC_007946:2485894-2486971	wt	btssypdb	28.4015	152.155	2.4215	5.99602	5.00E-05	0.0008048	yes	3.09431203
yhbU	Uncharacteriz	NC_007946:3521319-3522315	wt	btssypdb	30.223	157.486	2.38151	4.68396	5.00E-05	0.0008048	yes	3.09431203
fdnH	Formate dehy	NC_007946:1617232-1618763	wt	btssypdb	31.5014	161.665	2.35952	5.57753	5.00E-05	0.0008048	yes	3.09431203
nrfB	Cytochrome c	NC_007946:4558638-4560826	wt	btssypdb	12.1942	62.0395	2.34699	4.85656	5.00E-05	0.0008048	yes	3.09431203
malP	Maltodextrin	NC_007946:3802882-3805276	wt	btssypdb	11.0866	53.2804	2.26478	5.59508	5.00E-05	0.0008048	yes	3.09431203
deoA	Thymidine ph	NC_007946:5041922-5043245	wt	btssypdb	42.2944	201.701	2.25368	5.98733	5.00E-05	0.0008048	yes	3.09431203
hypB	[NiFe] hydrog	NC_007946:3010093-3013357	wt	btssypdb	69.5023	328.088	2.23895	4.18228	5.00E-05	0.0008048	yes	3.09431203
	Putative trans	NC_007946:3885676-3886423	wt	btssypdb	5.59553	25.1289	2.167	4.1557	5.00E-05	0.0008048	yes	3.09431203
fdnG	Formate dehy	NC_007946:1614172-1617220	wt	btssypdb	21.6554	96.4869	2.15561	5.06853	5.00E-05	0.0008048	yes	3.09431203
tdcB	Threonine deh	NC_007946:3490944-3491934	wt	btssypdb	8.68018	38.669	2.15538	4.48808	5.00E-05	0.0008048	yes	3.09431203
manZ	PTS system, m	NC_007946:1930583-1931435	wt	btssypdb	162.774	708.094	2.12107	5.90022	5.00E-05	0.0008048	yes	3.09431203
deoC	Deoxyribose-p	NC_007946:5041065-5041845	wt	btssypdb	37.3904	162.113	2.11626	5.1019	5.00E-05	0.0008048	yes	3.09431203
feoB	Ferrous iron t	NC_007946:3793057-3795379	wt	btssypdb	80.723	347.871	2.1075	5.62992	5.00E-05	0.0008048	yes	3.09431203
glpK	Glycerol kinas	NC_007946:4392711-4394220	wt	btssypdb	135.117	575.055	2.08949	5.91345	5.00E-05	0.0008048	yes	3.09431203
rbsK	Ribokinase (EC	NC_007946:4198146-4199091	wt	btssypdb	147.509	624.619	2.08217	5.78168	5.00E-05	0.0008048	yes	3.09431203
manY	PTS system, m	NC_007946:1929770-1930571	wt	btssypdb	141.807	587.8	2.0514	5.65476	5.00E-05	0.0008048	yes	3.09431203
fhlA	Formate hydr	NC_007946:3013430-3015509	wt	btssypdb	10.1112	41.5905	2.0403	4.98069	5.00E-05	0.0008048	yes	3.09431203
manX	PTS system, m	NC_007946:1928736-1929708	wt	btssypdb	103.825	426.944	2.0399	5.59534	5.00E-05	0.0008048	yes	3.09431203
gntT	High-affinity g	NC_007946:3799427-3800744	wt	btssypdb	14.9278	60.4564	2.01789	4.86137	5.00E-05	0.0008048	yes	3.09431203
dmsC	Anaerobic din	NC_007946:951761-952625	wt	btssypdb	21.2416	85.6738	2.01196	4.7691	5.00E-05	0.0008048	yes	3.09431203
alsA	D-allose ABC t	NC_007946:4583587-4585432	wt	btssypdb	7.68415	52.3111	2.76716	2.47578	0.0001	0.00151278	yes	2.82022423
	hypothetical p	NC_007946:2599397-2599553	wt	btssypdb	61.6005	282.563	2.19756	1.5222	0.0012	0.0133392	yes	1.87487022
ykgH	Uncharacteriz	NC_007946:344661-345330	wt	btssypdb	0.730061	3.82137	2.388	2.58188	0.0013	0.0143321	yes	1.84369017
napA	Periplasmic ni	NC_007946:2437146-2440377	wt	btssypdb	164.635	713.626	2.11589	2.2651	0.00175	0.0184829	yes	1.73322989

G. Genes significantly downregulated in Δ*btsS*Δ*ypdB* at 60 minutes after HCl exposure compared to WT at 60 minutes after HCl exposure

gene symbol	function	locus	sample_1	sample_2	value_1	value_2	log2(fold_cha	test_stat	p_value	q_value	significant	logq
yeiH	UPF0324 inne	NC_007946:2390924-2391974	wt	btssypdb	121.654	28.9642	-2.07044	-3.83855	5.00E-05	0.00156496	yes	2.80549676
	D-allose ABC t	NC_007946:4582852-4583560	wt	btssypdb	49.7935	11.0228	-2.17546	-4.26254	5.00E-05	0.00156496	yes	2.80549676
fadB	Enoyl-CoA hyc	NC_007946:4315110-4317300	wt	btssypdb	313.992	66.49	-2.23952	-3.59131	5.00E-05	0.00156496	yes	2.80549676
glcC	Glycolate util	NC_007946:3331891-3332656	wt	btssypdb	456.987	91.4465	-2.32115	-3.94205	5.00E-05	0.00156496	yes	2.80549676
yeiE	Transcription	NC_007946:2389944-2390751	wt	btssypdb	287.143	54.8043	-2.38941	-4.43492	5.00E-05	0.00156496	yes	2.80549676
dsdX	D-serine perm	NC_007946:2639114-2640452	wt	btssypdb	101.594	19.2286	-2.40148	-4.04062	5.00E-05	0.00156496	yes	2.80549676
acs	Acetyl-CoA syı	NC_007946:4554807-4556766	wt	btssypdb	583.139	106.945	-2.44697	-3.6212	5.00E-05	0.00156496	yes	2.80549676
yjiA	Metal-binding	NC_007946:4961908-4962865	wt	btssypdb	549.576	94.1855	-2.54474	-4.19428	5.00E-05	0.00156496	yes	2.80549676
dsdX	D-serine perm	NC_007946:4862477-4863815	wt	btssypdb	89.3477	13.7135	-2.70383	-4.58033	5.00E-05	0.00156496	yes	2.80549676
glpA	Anaerobic gly	NC_007946:2488606-2492671	wt	btssypdb	288.082	33.9213	-3.08621	-3.4399	5.00E-05	0.00156496	yes	2.80549676
lldP	L-lactate perm	NC_007946:4039261-4042880	wt	btssypdb	9121.86	978.563	-3.22059	-3.82636	5.00E-05	0.00156496	yes	2.80549676
ycgT	Phosphoenol	NC_007946:1328416-1329487	wt	btssypdb	233.846	20.1036	-3.54003	-6.42444	5.00E-05	0.00156496	yes	2.80549676
inaA	Weak-acid-ind	NC_007946:2485041-2485692	wt	btssypdb	689.124	55.5631	-3.63256	-4.65043	5.00E-05	0.00156496	yes	2.80549676
ycgC	Phosphoenol	NC_007946:1326344-1327763	wt	btssypdb	620.402	46.8584	-3.72682	-6.53652	5.00E-05	0.00156496	yes	2.80549676
ycgS	Phosphoenol	NC_007946:1327773-1328406	wt	btssypdb	718.119	49.1693	-3.86839	-7.18638	5.00E-05	0.00156496	yes	2.80549676
kgtP	Alpha-ketoglu	NC_007946:2865744-2867312	wt	btssypdb	306.544	20.5249	-3.90065	-6.54854	5.00E-05	0.00156496	yes	2.80549676
glpD	Aerobic glyce	NC_007946:3814827-3816333	wt	btssypdb	771.493	42.2163	-4.19178	-4.71115	5.00E-05	0.00156496	yes	2.80549676
glpQ	Glycerophosp	NC_007946:2485894-2486971	wt	btssypdb	1452.9	55.7603	-4.70356	-6.47908	5.00E-05	0.00156496	yes	2.80549676
glpK	Glycerol kina	NC_007946:4392711-4394220	wt	btssypdb	2830.63	98.4906	-4.84499	-6.53601	5.00E-05	0.00156496	yes	2.80549676
	putative mem	NC_007946:3816386-3816992	wt	btssypdb	62.5978	2.15004	-4.86368	-5.89352	5.00E-05	0.00156496	yes	2.80549676
glpT	Glycerol-3-ph	NC_007946:2486975-2488334	wt	btssypdb	1696.75	55.12	-4.94405	-5.99708	5.00E-05	0.00156496	yes	2.80549676
	hypothetical p	NC_007946:3816994-3817621	wt	btssypdb	36.2588	0.950009	-5.25424	-5.92279	5.00E-05	0.00156496	yes	2.80549676
yjiY	Pyruvate:H+ s	NC_007946:4963196-4965311	wt	btssypdb	2485.41	8.13369	-8.25536	-13.9387	5.00E-05	0.00156496	yes	2.80549676
alsA	D-allose ABC t	NC_007946:4583587-4585432	wt	btssypdb	233.266	39.1353	-2.57543	-2.1065	0.0001	0.00292279	yes	2.53420239
yhjX	Putative resis	NC_007946:3978054-3979263	wt	btssypdb	224.021	28.7207	-2.96347	-3.71696	0.0001	0.00292279	yes	2.53420239
glpF	Glycerol upta	NC_007946:4394242-4395088	wt	btssypdb	768.509	134.168	-2.51802	-2.92623	0.00025	0.00658113	yes	2.18169953
ybdD	Uncharacteriz	NC_007946:4962875-4963079	wt	btssypdb	81.1235	2.72923	-4.89355	-4.48901	0.00105	0.0229327	yes	1.63954481

H. Genes significantly upregulated in Δ*btsS*Δ*ypdB* at 60 minutes after HCl exposure compared to WT at 60 minutes after HCl exposure

gene symbol	function	locus	sample_1	sample_2	value_1	value_2	log2(fold_cha	test_stat	p_value	q_value	significant	logq
cysD	Sulfate adenyl	NC_007946:3037603-3038512	wt	btssypdb	4.07606	3187.4	9.61099	16.3872	5.00E-05	0.00156496	yes	2.80549676
cysI	Sulfite reduct	NC_007946:3041150-3044662	wt	btssypdb	16.3234	6522.69	8.64238	14.3289	5.00E-05	0.00156496	yes	2.80549676
cysC	Adenylylsulfat	NC_007946:3035569-3037602	wt	btssypdb	24.0683	6217.21	8.01299	11.6927	5.00E-05	0.00156496	yes	2.80549676
sbp	Sulfate-bindir	NC_007946:4385795-4386785	wt	btssypdb	10.477	2701.2	8.01023	14.0914	5.00E-05	0.00156496	yes	2.80549676
cysA	Sulfate and th	NC_007946:2698537-2702349	wt	btssypdb	44.3492	7283.94	7.35967	12.1074	5.00E-05	0.00156496	yes	2.80549676
cysH	Phosphoaden	NC_007946:3040342-3041077	wt	btssypdb	10.7847	1683.5	7.28634	13.0968	5.00E-05	0.00156496	yes	2.80549676
cbl	Alkanesulfona	NC_007946:2111627-2112578	wt	btssypdb	10.5236	690.054	6.03501	10.8297	5.00E-05	0.00156496	yes	2.80549676
ydjN	L-cystine upta	NC_007946:1845648-1847040	wt	btssypdb	47.2998	2144.42	5.50261	9.53274	5.00E-05	0.00156496	yes	2.80549676
yciW	Uncharacteriz	NC_007946:1469907-1471035	wt	btssypdb	7.85041	313.491	5.31951	9.78958	5.00E-05	0.00156496	yes	2.80549676
cysK	Cysteine synth	NC_007946:2692187-2693159	wt	btssypdb	300.145	6870.48	4.51668	7.09947	5.00E-05	0.00156496	yes	2.80549676
tauA	Taurine ABC t	NC_007946:400567-401678	wt	btssypdb	2.66415	54.0831	4.34343	7.98691	5.00E-05	0.00156496	yes	2.80549676
lacZ	beta-galactosi	NC_007946:389116-392191	wt	btssypdb	48.9879	847.052	4.11195	6.59001	5.00E-05	0.00156496	yes	2.80549676
nirB	Nitrite reduct	NC_007946:3752014-3754881	wt	btssypdb	10.7185	167.328	3.9645	3.05189	5.00E-05	0.00156496	yes	2.80549676
lacY	Lactose perm	NC_007946:387811-389065	wt	btssypdb	24.4958	353.787	3.85228	6.74652	5.00E-05	0.00156496	yes	2.80549676
nlpA	Lipoprotein 2	NC_007946:4105193-4106012	wt	btssypdb	56.4658	807.78	3.83851	6.46211	5.00E-05	0.00156496	yes	2.80549676
fliY	L-cystine ABC	NC_007946:2023331-2024132	wt	btssypdb	254.62	3526.86	3.79197	6.37328	5.00E-05	0.00156496	yes	2.80549676
lacA	Galactoside O	NC_007946:387134-387746	wt	btssypdb	14.6127	196.743	3.75101	7.04914	5.00E-05	0.00156496	yes	2.80549676
yjiD	YjiD protein	NC_007946:4919312-4919696	wt	btssypdb	3.90433	47.3423	3.59998	5.34289	5.00E-05	0.00156496	yes	2.80549676
cysM	Cysteine synth	NC_007946:2697491-2698349	wt	btssypdb	133.377	1609.09	3.59267	6.25375	5.00E-05	0.00156496	yes	2.80549676
ycbN	FMNH2-deper	NC_007946:999327-1001997	wt	btssypdb	6.31704	63.8065	3.33638	5.91002	5.00E-05	0.00156496	yes	2.80549676
ygbE	Inner membra	NC_007946:3035196-3035520	wt	btssypdb	46.1435	448.727	3.28164	6.36478	5.00E-05	0.00156496	yes	2.80549676
narK	Nitrate/nitrite	NC_007946:1352204-1353596	wt	btssypdb	191.096	1827.17	3.25724	4.83058	5.00E-05	0.00156496	yes	2.80549676
tdcA	Threonine cat	NC_007946:3492032-3492971	wt	btssypdb	29.6486	237.139	2.9997	4.15667	5.00E-05	0.00156496	yes	2.80549676
yfiD	Autonomous	NC_007946:2857631-2858015	wt	btssypdb	714.921	5230.62	2.87113	4.58957	5.00E-05	0.00156496	yes	2.80549676
yhbU	Uncharacteriz	NC_007946:3521319-3522315	wt	btssypdb	17.8088	119.813	2.75013	4.75461	5.00E-05	0.00156496	yes	2.80549676
adiY	Transcription	NC_007946:4610909-4611671	wt	btssypdb	3.50868	23.1103	2.71954	4.98985	5.00E-05	0.00156496	yes	2.80549676
ybiK	Isoaspartyl an	NC_007946:827782-830606	wt	btssypdb	216.71	1427.29	2.71944	4.04677	5.00E-05	0.00156496	yes	2.80549676
fdnG	Formate dehy	NC_007946:1614172-1617220	wt	btssypdb	18.5018	109.237	2.56173	4.4821	5.00E-05	0.00156496	yes	2.80549676
		NC_007946:230502-233426	wt	btssypdb	25.4825	150.278	2.56006	3.54341	5.00E-05	0.00156496	yes	2.80549676
ygiP	Transcription	NC_007946:3433133-3434166	wt	btssypdb	3.638	21.2219	2.54434	4.4603	5.00E-05	0.00156496	yes	2.80549676
		NC_007946:4458262-4461186	wt	btssypdb	26.1093	150.508	2.52721	3.49023	5.00E-05	0.00156496	yes	2.80549676
		NC_007946:4204571-4207495	wt	btssypdb	26.3847	151.622	2.52271	3.48525	5.00E-05	0.00156496	yes	2.80549676
cdh	CDP-diacylgly	NC_007946:4386891-4387647	wt	btssypdb	26.0066	149.31	2.52136	4.81742	5.00E-05	0.00156496	yes	2.80549676
		NC_007946:4323845-4326769	wt	btssypdb	26.3787	150.353	2.51091	3.46467	5.00E-05	0.00156496	yes	2.80549676
		NC_007946:3641652-3644576	wt	btssypdb	26.2074	147.871	2.4963	3.43836	5.00E-05	0.00156496	yes	2.80549676
		NC_007946:3693381-3696305	wt	btssypdb	27.5956	155.349	2.493	3.44949	5.00E-05	0.00156496	yes	2.80549676
		NC_007946:2870538-2873462	wt	btssypdb	28.1001	157.628	2.48788	3.43676	5.00E-05	0.00156496	yes	2.80549676
yfeK	Uncharacteriz	NC_007946:2697120-2697489	wt	btssypdb	14.8169	82.7963	2.48232	4.72098	5.00E-05	0.00156496	yes	2.80549676
napA	Periplasmic n	NC_007946:2437146-2440377	wt	btssypdb	124.289	669.898	2.43024	1.93446	5.00E-05	0.00156496	yes	2.80549676
ynfK	Dethiobiotin	NC_007946:1705819-1707649	wt	btssypdb	75.3798	398.969	2.40403	3.37872	5.00E-05	0.00156496	yes	2.80549676
	Transcription	NC_007946:4878455-4879022	wt	btssypdb	34.381	181.582	2.40094	3.82707	5.00E-05	0.00156496	yes	2.80549676
		NC_007946:228523-230065	wt	btssypdb	39.1724	202.692	2.37138	3.39016	5.00E-05	0.00156496	yes	2.80549676
		NC_007946:3696659-3698201	wt	btssypdb	41.8851	213.391	2.34899	3.3716	5.00E-05	0.00156496	yes	2.80549676
		NC_007946:4321857-4323399	wt	btssypdb	41.6083	211.936	2.34868	3.3526	5.00E-05	0.00156496	yes	2.80549676
gsiB	Oligopeptide	NC_007946:830655-832164	wt	btssypdb	73.3481	372.647	2.34498	4.11065	5.00E-05	0.00156496	yes	2.80549676
		NC_007946:4456366-4457908	wt	btssypdb	41.935	211.813	2.33656	3.34455	5.00E-05	0.00156496	yes	2.80549676
		NC_007946:2873816-2875358	wt	btssypdb	42.1402	212.588	2.33479	3.35038	5.00E-05	0.00156496	yes	2.80549676
		NC_007946:3645022-3646564	wt	btssypdb	41.5749	208.577	2.3268	3.33083	5.00E-05	0.00156496	yes	2.80549676
ansB	L-asparaginas	NC_007946:3277237-3278284	wt	btssypdb	79.5289	398.844	2.32627	3.39642	5.00E-05	0.00156496	yes	2.80549676
dcuC	C4-dicarboxyl	NC_007946:637032-638418	wt	btssypdb	5.90645	29.5241	2.32153	4.03836	5.00E-05	0.00156496	yes	2.80549676
		NC_007946:4202675-4204217	wt	btssypdb	42.2669	209.997	2.31277	3.31334	5.00E-05	0.00156496	yes	2.80549676
tauB	Taurine ABC t	NC_007946:401690-404130	wt	btssypdb	26.1961	129.236	2.30259	4.47517	5.00E-05	0.00156496	yes	2.80549676
feoA	Ferrous iron t	NC_007946:3792813-3793041	wt	btssypdb	88.0045	427.182	2.2792	3.9831	5.00E-05	0.00156496	yes	2.80549676
cysB	Cys regulon tr	NC_007946:1454801-1455776	wt	btssypdb	111.229	532.659	2.25968	3.93564	5.00E-05	0.00156496	yes	2.80549676
gsiC	Oligopeptide	NC_007946:832181-833102	wt	btssypdb	104.242	484.714	2.21719	3.955	5.00E-05	0.00156496	yes	2.80549676
yicL	Uncharacteriz	NC_007946:4104266-4105190	wt	btssypdb	42.3606	196.908	2.21673	4.0987	5.00E-05	0.00156496	yes	2.80549676
yggM	Putative alph	NC_007946:3276113-3277121	wt	btssypdb	7.3187	33.6208	2.1997	4.0128	5.00E-05	0.00156496	yes	2.80549676
gsiD	Oligopeptide	NC_007946:833104-834016	wt	btssypdb	73.3844	336.427	2.19675	4.0392	5.00E-05	0.00156496	yes	2.80549676
	FIG00732456	NC_007946:4877096-4878433	wt	btssypdb	22.2451	94.3547	2.0846	3.35411	5.00E-05	0.00156496	yes	2.80549676
yhbV	Uncharacteriz	NC_007946:3522323-3523202	wt	btssypdb	17.4535	73.6575	2.07731	3.7707	5.00E-05	0.00156496	yes	2.80549676
ssuB	Alkanesulfona	NC_007946:997760-999319	wt	btssypdb	17.4232	71.0412	2.02764	4.05995	5.00E-05	0.00156496	yes	2.80549676

References

1. Foxman, B. (2010). The epidemiology of urinary tract infection. Nature Reviews Urology *7*, 653-660. 10.1038/nrurol.2010.190.
2. Medina, M., and Castillo-Pino, E. (2019). An introduction to the epidemiology and burden of urinary tract infections. Therapeutic advances in urology *11*, 1756287219832172-1756287219832172. 10.1177/1756287219832172.
3. Flores-Mireles, A.L., Walker, J.N., Caparon, M., and Hultgren, S.J. (2015). Urinary tract infections: epidemiology, mechanisms of infection and treatment options. Nature reviews. Microbiology *13*, 269-284. 10.1038/nrmicro3432.
4. Foxman, B. (2003). Epidemiology of urinary tract infections: incidence, morbidity, and economic costs. Dis Mon *49*, 53-70. 10.1067/mda.2003.7.
5. Eberly, A.R., Beebout, C.J., Carmen Tong, C.M., Van Horn, G.T., Green, H.D., Fitzgerald, M.J., De, S., Apple, E.K., Schrimpe-Rutledge, A.C., Codreanu, S.G., et al. (2020). Defining a Molecular Signature for Uropathogenic versus Urocolonizing Escherichia coli: The Status of the Field and New Clinical Opportunities. J Mol Biol *432*, 786-804. 10.1016/j.jmb.2019.11.008.
6. Geerlings Suzanne, E. (2016). Clinical Presentations and Epidemiology of Urinary Tract Infections. Microbiology Spectrum *4*, 10.1128/microbiolspec.uti-0002-2012. 10.1128/microbiolspec.uti-0002-2012.
7. Nicolle, L.E., Gupta, K., Bradley, S.F., Colgan, R., DeMuri, G.P., Drekonja, D., Eckert, L.O., Geerlings, S.E., Köves, B., Hooton, T.M., et al. (2019). Clinical Practice Guideline for the Management of Asymptomatic Bacteriuria: 2019 Update by the Infectious Diseases Society of Americaa. Clin Infect Dis *68*, 1611-1615. 10.1093/cid/ciz021.
8. Baerheim, A. (2012). Empirical treatment of uncomplicated cystitis. Scandinavian Journal of Primary Health Care *30*, 1-2. 10.3109/02813432.2012.649629.
9. Trautner, B.W., and Grigoryan, L. (2014). Approach to a positive urine culture in a patient without urinary symptoms. Infect Dis Clin North Am *28*, 15-31. 10.1016/j.idc.2013.09.005.
10. Deltourbe, L., Lacerda Mariano, L., Hreha, T.N., Hunstad, D.A., and Ingersoll, M.A. (2022). The impact of biological sex on diseases of the urinary tract. Mucosal Immunology *15*, 857-866. 10.1038/s41385-022-00549-0.
11. Stapleton, A.E. (2016). The Vaginal Microbiota and Urinary Tract Infection. Microbiology spectrum *4*, 10.1128/microbiolspec.UTI-0025-2016. 10.1128/microbiolspec.UTI-0025-2016.
12. Forde, B.M., Roberts, L.W., Phan, M.-D., Peters, K.M., Fleming, B.A., Russell, C.W., Lenherr, S.M., Myers, J.B., Barker, A.P., Fisher, M.A., et al. (2019). Population dynamics of an Escherichia coli ST131 lineage during recurrent urinary tract infection. Nature Communications *10*, 3643. 10.1038/s41467-019-11571-5.
13. Chen, S.L., Wu, M., Henderson, J.P., Hooton, T.M., Hibbing, M.E., Hultgren, S.J., and Gordon, J.I. (2013). Genomic Diversity and Fitness of E. coli Strains Recovered from the Intestinal and Urinary Tracts of Women with Recurrent Urinary Tract Infection. Science Translational Medicine *5*, 184ra160-184ra160. 10.1126/scitranslmed.3005497.
14. Song, J., Bishop, B.L., Li, G., Grady, R., Stapleton, A., and Abraham, S.N. (2009). TLR4-mediated expulsion of bacteria from infected bladder epithelial cells. Proceedings of the National Academy of Sciences *106*, 14966-14971. 10.1073/pnas.0900527106.

15. Abraham, S.N., and Miao, Y. (2015). The nature of immune responses to urinary tract infections. Nature Reviews Immunology *15*, 655-663. 10.1038/nri3887.
16. Lewis Adam, J., Richards Amanda, C., and Mulvey Matthew, A. (2016). Invasion of Host Cells and Tissues by Uropathogenic Bacteria. Microbiology Spectrum *4*, 10.1128/microbiolspec.uti-0026-2016. 10.1128/microbiolspec.uti-0026-2016.
17. Justice, S.S., Hunstad, D.A., Seed, P.C., and Hultgren, S.J. (2006). Filamentation by Escherichia coli subverts innate defenses during urinary tract infection. Proc Natl Acad Sci U S A *103*, 19884-19889.
18. Hunstad, D.A., and Justice, S.S. (2010). Intracellular lifestyles and immune evasion strategies of uropathogenic Escherichia coli. Annu Rev Microbiol *64*, 203-221. 10.1146/annurev.micro.112408.134258.
19. Beebout, C.J., Robertson, G.L., Reinfeld, B.I., Blee, A.M., Morales, G.H., Brannon, J.R., Chazin, W.J., Rathmell, W.K., Rathmell, J.C., Gama, V., and Hadjifrangiskou, M. (2022). Uropathogenic Escherichia coli subverts mitochondrial metabolism to enable intracellular bacterial pathogenesis in urinary tract infection. Nature Microbiology *7*, 1348-1360. 10.1038/s41564-022-01205-w.
20. Russell, S.K., Harrison, J.K., Olson, B.S., Lee, H.J., O'Brien, V.P., Xing, X., Livny, J., Yu, L., Roberson, E.D.O., Bomjan, R., et al. (2023). Uropathogenic Escherichia coli infection-induced epithelial trained immunity impacts urinary tract disease outcome. Nat Microbiol. 10.1038/s41564-023-01346-6.
21. Yu, L., O'Brien, V.P., Livny, J., Dorsey, D., Bandyopadhyay, N., Colonna, M., Caparon, M.G., Roberson, E.D., Hultgren, S.J., and Hannan, T.J. (2019). Mucosal infection rewires TNFα signaling dynamics to skew susceptibility to recurrence. Elife *8*. 10.7554/eLife.46677.
22. Wiles, T.J., Kulesus, R.R., and Mulvey, M.A. (2008). Origins and virulence mechanisms of uropathogenic Escherichia coli. Experimental and molecular pathology *85*, 11-19. 10.1016/j.yexmp.2008.03.007.
23. Russo, T.A., Stapleton, A., Wenderoth, S., Hooton, T.M., and Stamm, W.E. (1995). Chromosomal restriction fragment length polymorphism analysis of Escherichia coli strains causing recurrent urinary tract infections in young women. J Infect Dis *172*, 440-445.
24. Navas-Nacher, E.L., Dardick, F., Venegas, M.F., Anderson, B.E., Schaeffer, A.J., and Duncan, J.L. (2001). Relatedness of Escherichia coli colonizing women longitudinally. Mol Urol *5*, 31-36. 10.1089/109153601750124285.
25. Chow, A.W., Percival-Smith, R., Bartlett, K.H., Goldring, A.M., and Morrison, B.J. (1986). Vaginal colonization with Escherichia coli in healthy women. Determination of relative risks by quantitative culture and multivariate statistical analysis. Am J Obstet Gynecol *154*, 120-126.
26. Obata-Yasuoka, M., Ba-Thein, W., Tsukamoto, T., Yoshikawa, H., and Hayashi, H. (2002). Vaginal Escherichia coli share common virulence factor profiles, serotypes and phylogeny with other extraintestinal E. coli. Microbiology *148*, 2745-2752. https://doi.org/10.1099/00221287-148-9-2745.
27. Clermont, O., Christenson, J.K., Denamur, E., and Gordon, D.M. (2013). The Clermont Escherichia coli phylo-typing method revisited: improvement of specificity and detection of new phylo-groups. Environ Microbiol Rep *5*, 58-65. 10.1111/1758-2229.12019.

28. Larsen Mette, V., Cosentino, S., Rasmussen, S., Friis, C., Hasman, H., Marvig Rasmus, L., Jelsbak, L., Sicheritz-Pontén, T., Ussery David, W., Aarestrup Frank, M., and Lund, O. (2020). Multilocus Sequence Typing of Total-Genome-Sequenced Bacteria. Journal of Clinical Microbiology *50*, 1355-1361. 10.1128/jcm.06094-11.
29. Breland, E.J., Eberly, A.R., and Hadjifrangiskou, M. (2017). An Overview of Two-Component Signal Transduction Systems Implicated in Extra-Intestinal Pathogenic E. coli Infections. Front Cell Infect Microbiol *7*, 162. 10.3389/fcimb.2017.00162.
30. André, A.C., Debande, L., and Marteyn, B.S. (2021). The selective advantage of facultative anaerobes relies on their unique ability to cope with changing oxygen levels during infection. Cellular Microbiology *23*, e13338. https://doi.org/10.1111/cmi.13338.
31. Friedman, E.S., Bittinger, K., Esipova, T.V., Hou, L., Chau, L., Jiang, J., Mesaros, C., Lund, P.J., Liang, X., FitzGerald, G.A., et al. (2018). Microbes vs. chemistry in the origin of the anaerobic gut lumen. Proceedings of the National Academy of Sciences *115*, 4170-4175. 10.1073/pnas.1718635115.
32. Donaldson, G.P., Lee, S.M., and Mazmanian, S.K. (2016). Gut biogeography of the bacterial microbiota. Nature Reviews Microbiology *14*, 20-32. 10.1038/nrmicro3552.
33. Conway, T., and Cohen, P.S. (2015). Commensal and Pathogenic Escherichia coli Metabolism in the Gut. Microbiology Spectrum *3*. doi:10.1128/microbiolspec.MBP-0006-2014.
34. Zeng, M.Y., Inohara, N., and Nuñez, G. (2017). Mechanisms of inflammation-driven bacterial dysbiosis in the gut. Mucosal Immunology *10*, 18-26. 10.1038/mi.2016.75.
35. Lupp, C., Robertson, M.L., Wickham, M.E., Sekirov, I., Champion, O.L., Gaynor, E.C., and Finlay, B.B. (2007). Host-Mediated Inflammation Disrupts the Intestinal Microbiota and Promotes the Overgrowth of Enterobacteriaceae. Cell Host & Microbe *2*, 119-129. https://doi.org/10.1016/j.chom.2007.06.010.
36. Castro, J., Machado, D., and Cerca, N. (2016). Escherichia coli and Enterococcus faecalis are able to incorporate and enhance a pre-formed Gardnerella vaginalis biofilm. Pathogens and Disease *74*, ftw007. 10.1093/femspd/ftw007.
37. Donders, G.G., Vereecken, A., Bosmans, E., Dekeersmaecker, A., Salembier, G., and Spitz, B. (2002). Definition of a type of abnormal vaginal flora that is distinct from bacterial vaginosis: aerobic vaginitis. BJOG *109*, 34-43.
38. Donders, G.G.G., Bellen, G., Grinceviciene, S., Ruban, K., and Vieira-Baptista, P. (2017). Aerobic vaginitis: no longer a stranger. Research in Microbiology *168*, 845-858. https://doi.org/10.1016/j.resmic.2017.04.004.
39. Ma, X., Wu, M., Wang, C., Li, H., Fan, A., Wang, Y., Han, C., and Xue, F. (2022). The pathogenesis of prevalent aerobic bacteria in aerobic vaginitis and adverse pregnancy outcomes: a narrative review. Reproductive Health *19*, 21. 10.1186/s12978-021-01292-8.
40. Wang, Z.J., Joe, B.N., Coakley, F.V., Zaharchuk, G., Busse, R., and Yeh, B.M. (2008). Urinary oxygen tension measurement in humans using magnetic resonance imaging. Acad Radiol *15*, 1467-1473. 10.1016/j.acra.2008.04.013.
41. Eberly, A.R., Floyd, K.A., Beebout, C.J., Colling, S.J., Fitzgerald, M.J., Stratton, C.W., Schmitz, J.E., and Hadjifrangiskou, M. (2017). Biofilm Formation by Uropathogenic Escherichia coli Is Favored under Oxygen Conditions That Mimic the Bladder Environment. Int J Mol Sci *18*. 10.3390/ijms18102077.

42. Boyanova, L., Marteva-Proevska, Y., Markovska, R., Yordanov, D., and Gergova, R. (2022). Urinary tract infections: Should we think about the anaerobic cocci? Anaerobe *77*, 102509. https://doi.org/10.1016/j.anaerobe.2021.102509.
43. Floyd, K.A., Mitchell, C.A., Eberly, A.R., Colling, S.J., Zhang, E.W., DePas, W., Chapman, M.R., Conover, M., Rogers, B.R., Hultgren, S.J., and Hadjifrangiskou, M. (2016). The UbiI (VisC) Aerobic Ubiquinone Synthase Is Required for Expression of Type 1 Pili, Biofilm Formation, and Pathogenesis in Uropathogenic Escherichia coli. J Bacteriol *198*, 2662-2672. 10.1128/JB.00030-16.
44. Beebout, C.J., Eberly, A.R., Werby, S.H., Reasoner, S.A., Brannon, J.R., De, S., Fitzgerald, M.J., Huggins, M.M., Clayton, D.B., Cegelski, L., and Hadjifrangiskou, M. (2019). Respiratory Heterogeneity Shapes Biofilm Formation and Host Colonization in Uropathogenic Escherichia coli. MBio *10*. 10.1128/mBio.02400-18.
45. Mann, R., Mediati, D.G., Duggin, I.G., Harry, E.J., and Bottomley, A.L. (2017). Metabolic Adaptations of Uropathogenic E. coli in the Urinary Tract. Frontiers in cellular and infection microbiology *7*, 241-241. 10.3389/fcimb.2017.00241.
46. Miller, E.A., Beasley, D.E., Dunn, R.R., and Archie, E.A. (2016). Lactobacilli Dominance and Vaginal pH: Why Is the Human Vaginal Microbiome Unique? Front Microbiol *7*, 1936. 10.3389/fmicb.2016.01936.
47. Ravel, J., Gajer, P., Abdo, Z., Schneider, G.M., Koenig, S.S.K., McCulle, S.L., Karlebach, S., Gorle, R., Russell, J., Tacket, C.O., et al. (2011). Vaginal microbiome of reproductive-age women. Proceedings of the National Academy of Sciences *108*, 4680-4687. 10.1073/pnas.1002611107.
48. Mendling, W. (2016). Vaginal Microbiota. In Microbiota of the Human Body: Implications in Health and Disease, A. Schwiertz, ed. (Springer International Publishing), pp. 83-93. 10.1007/978-3-319-31248-4_6.
49. Lund, P.A., De Biase, D., Liran, O., Scheler, O., Mira, N.P., Cetecioglu, Z., Fernández, E.N., Bover-Cid, S., Hall, R., Sauer, M., and O'Byrne, C. (2020). Understanding How Microorganisms Respond to Acid pH Is Central to Their Control and Successful Exploitation. Frontiers in Microbiology *11*.
50. Foster, J.W. (2004). Escherichia coli acid resistance: tales of an amateur acidophile. Nature Reviews Microbiology *2*, 898-907. 10.1038/nrmicro1021.
51. Chang, Y.-Y., and Cronan, J.E. (1999). Membrane cyclopropane fatty acid content is a major factor in acid resistance of Escherichia coli. Molecular Microbiology *33*, 249-259. https://doi.org/10.1046/j.1365-2958.1999.01456.x.
52. Chang, Y.-Y., Eichel, J., and Cronan John, E. (2000). Metabolic Instability of Escherichia coli Cyclopropane Fatty Acid Synthase Is Due to RpoH-Dependent Proteolysis. Journal of Bacteriology *182*, 4288-4294. 10.1128/jb.182.15.4288-4294.2000.
53. Yuk, H.-G., and Marshall Douglas, L. (2004). Adaptation of Escherichia coli O157:H7 to pH Alters Membrane Lipid Composition, Verotoxin Secretion, and Resistance to Simulated Gastric Fluid Acid. Applied and Environmental Microbiology *70*, 3500-3505. 10.1128/AEM.70.6.3500-3505.2004.
54. Gray, M.J., Wholey, W.Y., Wagner, N.O., Cremers, C.M., Mueller-Schickert, A., Hock, N.T., Krieger, A.G., Smith, E.M., Bender, R.A., Bardwell, J.C., and Jakob, U. (2014). Polyphosphate is a primordial chaperone. Mol Cell *53*, 689-699. 10.1016/j.molcel.2014.01.012.

55. Gray Michael, J. (2019). Inorganic Polyphosphate Accumulation in Escherichia coli Is Regulated by DksA but Not by (p)ppGpp. Journal of Bacteriology *201*, 10.1128/jb.00664-00618. 10.1128/jb.00664-18.
56. Foster, P.L. (2007). Stress-induced mutagenesis in bacteria. Crit Rev Biochem Mol Biol *42*, 373-397.
57. delaVega, A.L., and Delcour, A.H. (1995). Cadaverine induces closing of E. coli porins. The EMBO Journal *14*, 6058-6065-6065. https://doi.org/10.1002/j.1460-2075.1995.tb00294.x.
58. Samartzidou, H., Mehrazin, M., Xu, Z., Benedik Michael, J., and Delcour Anne, H. (2003). Cadaverine Inhibition of Porin Plays a Role in Cell Survival at Acidic pH. Journal of Bacteriology *185*, 13-19. 10.1128/jb.185.1.13-19.2003.
59. Gajiwala, K.S., and Burley, S.K. (2000). HDEA, a periplasmic protein that supports acid resistance in pathogenic enteric bacteria11Edited by P. E. Wright. Journal of Molecular Biology *295*, 605-612. https://doi.org/10.1006/jmbi.1999.3347.
60. Malki, A., Le, H.-T., Milles, S., Kern, R., Caldas, T., Abdallah, J., and Richarme, G. (2008). Solubilization of Protein Aggregates by the Acid Stress Chaperones HdeA and HdeB*. Journal of Biological Chemistry *283*, 13679-13687. https://doi.org/10.1074/jbc.M800869200.
61. Dahl, J.U., Koldewey, P., Salmon, L., Horowitz, S., Bardwell, J.C., and Jakob, U. (2015). HdeB functions as an acid-protective chaperone in bacteria. J Biol Chem *290*, 65-75. 10.1074/jbc.M114.612986.
62. Mujacic, M., and Baneyx, F. (2007). Chaperone Hsp31 Contributes to Acid Resistance in Stationary-Phase Escherichia coli. Applied and Environmental Microbiology *73*, 1014-1018. 10.1128/AEM.02429-06.
63. Calhoun, L.N., and Kwon, Y.M. (2011). Structure, function and regulation of the DNA-binding protein Dps and its role in acid and oxidative stress resistance in Escherichia coli: a review. Journal of Applied Microbiology *110*, 375-386. https://doi.org/10.1111/j.1365-2672.2010.04890.x.
64. Ceci, P., Ilari, A., Falvo, E., and Chiancone, E. (2003). The Dps Protein of Agrobacterium tumefaciens Does Not Bind to DNA but Protects It toward Oxidative Cleavage: X-RAY CRYSTAL STRUCTURE, IRON BINDING, AND HYDROXYL-RADICAL SCAVENGING PROPERTIES*. Journal of Biological Chemistry *278*, 20319-20326. https://doi.org/10.1074/jbc.M302114200.
65. Martinez, A., and Kolter, R. (1997). Protection of DNA during oxidative stress by the nonspecific DNA-binding protein Dps. J Bacteriol *179*, 5188-5194.
66. Ilari, A., Ceci, P., Ferrari, D., Rossi, G.L., and Chiancone, E. (2002). Iron Incorporation into Escherichia coli Dps Gives Rise to a Ferritin-like Microcrystalline Core*. Journal of Biological Chemistry *277*, 37619-37623. https://doi.org/10.1074/jbc.M206186200.
67. Maurer, L.M., Yohannes, E., Bondurant, S.S., Radmacher, M., and Slonczewski, J.L. (2005). pH Regulates Genes for Flagellar Motility, Catabolism, and Oxidative Stress in Escherichia coli K-12. Journal of Bacteriology *187*, 304. 10.1128/JB.187.1.304-319.2005.
68. Gorden, J., and Small, P.L. (1993). Acid resistance in enteric bacteria. Infect Immun *61*, 364-367.

69. Small, P., Blankenhorn, D., Welty, D., Zinser, E., and Slonczewski, J.L. (1994). Acid and base resistance in Escherichia coli and Shigella flexneri: role of rpoS and growth pH. Journal of Bacteriology *176*, 1729-1737. 10.1128/jb.176.6.1729-1737.1994.
70. Lin, J., Lee, I.S., Frey, J., Slonczewski, J.L., and Foster, J.W. (1995). Comparative analysis of extreme acid survival in Salmonella typhimurium, Shigella flexneri, and Escherichia coli. Journal of Bacteriology *177*, 4097. 10.1128/jb.177.14.4097-4104.1995.
71. Castanie-Cornet, M.P., Penfound, T.A., Smith, D., Elliott, J.F., and Foster, J.W. (1999). Control of acid resistance in Escherichia coli. Journal of bacteriology *181*, 3525-3535. 10.1128/JB.181.11.3525-3535.1999.
72. De Biase, D., and Pennacchietti, E. (2012). Glutamate decarboxylase-dependent acid resistance in orally acquired bacteria: function, distribution and biomedical implications of the gadBC operon. Molecular Microbiology *86*, 770-786. https://doi.org/10.1111/mmi.12020.
73. Ma, D., Lu, P., and Shi, Y. (2013). Substrate Selectivity of the Acid-activated Glutamate/γ-Aminobutyric acid (GABA) Antiporter GadC from Escherichia coli*. Journal of Biological Chemistry *288*, 15148-15153. https://doi.org/10.1074/jbc.M113.474502.
74. Tsai, M.F., McCarthy, P., and Miller, C. (2013). Substrate selectivity in glutamate-dependent acid resistance in enteric bacteria. Proc Natl Acad Sci U S A *110*, 5898-5902. 10.1073/pnas.1301444110.
75. Richard, H., and Foster John, W. (2004). Escherichia coli Glutamate- and Arginine-Dependent Acid Resistance Systems Increase Internal pH and Reverse Transmembrane Potential. Journal of Bacteriology *186*, 6032-6041. 10.1128/JB.186.18.6032-6041.2004.
76. Mates Aaron, K., Sayed Atef, K., and Foster John, W. (2007). Products of the Escherichia coli Acid Fitness Island Attenuate Metabolite Stress at Extremely Low pH and Mediate a Cell Density-Dependent Acid Resistance. Journal of Bacteriology *189*, 2759-2768. 10.1128/jb.01490-06.
77. Lawson, A., and Quinn, A.G. (1967). Studies on amino acid decarboxylases in Escherichia coli. Biochemical Journal *105*, 483-490. 10.1042/bj1050483.
78. Andréll, J., Hicks, M.G., Palmer, T., Carpenter, E.P., Iwata, S., and Maher, M.J. (2009). Crystal Structure of the Acid-Induced Arginine Decarboxylase from Escherichia coli: Reversible Decamer Assembly Controls Enzyme Activity. Biochemistry *48*, 3915-3927. 10.1021/bi900075d.
79. Wang, S., Yan, R., Zhang, X., Chu, Q., and Shi, Y. (2014). Molecular mechanism of pH-dependent substrate transport by an arginine-agmatine antiporter. Proceedings of the National Academy of Sciences *111*, 12734. 10.1073/pnas.1414093111.
80. Tetsch, L., Koller, C., Haneburger, I., and Jung, K. (2008). The membrane-integrated transcriptional activator CadC of Escherichia coli senses lysine indirectly via the interaction with the lysine permease LysP. Molecular Microbiology *67*, 570-583. https://doi.org/10.1111/j.1365-2958.2007.06070.x.
81. Rauschmeier, M., Schüppel, V., Tetsch, L., and Jung, K. (2014). New Insights into the Interplay Between the Lysine Transporter LysP and the pH Sensor CadC in Escherichia Coli. Journal of Molecular Biology *426*, 215-229. https://doi.org/10.1016/j.jmb.2013.09.017.

82. Sabo, D.L., Boeker, E.A., Byers, B., Waron, H., and Fischer, E.H. (1974). Purification and physical properties of inducible Escherichia coli lysine decarboxylase. Biochemistry *13*, 662-670. 10.1021/bi00701a005.
83. Applebaum, D., Sabo, D.L., Fischer, E.H., and Morris, D.R. (1975). Biodegradative ornithine decarboxylase of Escherichia coli. Purification, properties, and pyridoxal 5'-phosphate binding site. Biochemistry *14*, 3675-3681. 10.1021/bi00687a025.
84. Kashiwagi, K., Suzuki, T., Suzuki, F., Furuchi, T., Kobayashi, H., and Igarashi, K. (1991). Coexistence of the genes for putrescine transport protein and ornithine decarboxylase at 16 min on Escherichia coli chromosome. Journal of Biological Chemistry *266*, 20922-20927. https://doi.org/10.1016/S0021-9258(18)54798-0.
85. Applebaum, D.M., Dunlap, J.C., and Morris, D.R. (1977). Comparison of the biosynthetic and biodegradative ornithine decarboxylases of Escherichia coli. Biochemistry *16*, 1580-1584. 10.1021/bi00627a008.
86. Lu, P., Ma, D., Chen, Y., Guo, Y., Chen, G.-Q., Deng, H., and Shi, Y. (2013). L-glutamine provides acid resistance for Escherichia coli through enzymatic release of ammonia. Cell research *23*, 635-644. 10.1038/cr.2013.13.
87. Pennacchietti, E., D'Alonzo, C., Freddi, L., Occhialini, A., and De Biase, D. (2018). The Glutaminase-Dependent Acid Resistance System: Qualitative and Quantitative Assays and Analysis of Its Distribution in Enteric Bacteria. Frontiers in microbiology *9*, 2869-2869. 10.3389/fmicb.2018.02869.
88. Zschiedrich, C.P., Keidel, V., and Szurmant, H. (2016). Molecular Mechanisms of Two-Component Signal Transduction. J Mol Biol *428*, 3752-3775. 10.1016/j.jmb.2016.08.003.
89. Stock, A.M., Robinson, V.L., and Goudreau, P.N. (2000). Two-component signal transduction. Annual Review of Biochemistry *69*, 183-215. 10.1146/annurev.biochem.69.1.183.
90. Capra, E.J., and Laub, M.T. (2012). Evolution of Two-Component Signal Transduction Systems. Annual Review of Microbiology *66*, 325-347. 10.1146/annurev-micro-092611-150039.
91. Laub, M.T., and Goulian, M. (2007). Specificity in two-component signal transduction pathways. Annu Rev Genet *41*, 121-145. 10.1146/annurev.genet.41.042007.170548.
92. Eguchi, Y., Ishii, E., Hata, K., and Utsumi, R. (2011). Regulation of Acid Resistance by Connectors of Two-Component Signal Transduction Systems in Escherichia coli. Journal of Bacteriology *193*, 1222. 10.1128/JB.01124-10.
93. Nishino, K., Inazumi, Y., and Yamaguchi, A. (2003). Global analysis of genes regulated by EvgA of the two-component regulatory system in Escherichia coli. Journal of bacteriology *185*, 2667-2672. 10.1128/jb.185.8.2667-2672.2003.
94. Sen, H., Aggarwal, N., Ishionwu, C., Hussain, N., Parmar, C., Jamshad, M., Bavro, V.N., and Lund, P.A. (2017). Structural and Functional Analysis of the Escherichia coli Acid-Sensing Histidine Kinase EvgS. Journal of bacteriology *199*, e00310-00317. 10.1128/JB.00310-17.
95. Ma, Z., Gong, S., Richard, H., Tucker, D.L., Conway, T., and Foster, J.W. (2003). GadE (YhiE) activates glutamate decarboxylase-dependent acid resistance in Escherichia coli K-12. Molecular Microbiology *49*, 1309-1320. https://doi.org/10.1046/j.1365-2958.2003.03633.x.
96. Zwir, I., Shin, D., Kato, A., Nishino, K., Latifi, T., Solomon, F., Hare, J.M., Huang, H., and Groisman, E.A. (2005). Dissecting the PhoP regulatory network of Escherichia

coli and Salmonella enterica. Proceedings of the National Academy of Sciences of the United States of America *102*, 2862. 10.1073/pnas.0408238102.
97. Sheikh, S.W., Ali, A., Ahsan, A., Shakoor, S., Shang, F., and Xue, T. (2021). Insights into Emergence of Antibiotic Resistance in Acid-Adapted Enterohaemorrhagic Escherichia coli. Antibiotics *10*. 10.3390/antibiotics10050522.
98. Battesti, A., Majdalani, N., and Gottesman, S. (2011). The RpoS-Mediated General Stress Response in Escherichia coli. Annual Review of Microbiology *65*, 189-213. 10.1146/annurev-micro-090110-102946.
99. Groisman Eduardo, A., Duprey, A., and Choi, J. (2021). How the PhoP/PhoQ System Controls Virulence and Mg2+ Homeostasis: Lessons in Signal Transduction, Pathogenesis, Physiology, and Evolution. Microbiology and Molecular Biology Reviews *85*, 10.1128/mmbr.00176-00120. 10.1128/mmbr.00176-20.
100. Price, S.B., Wright, J.C., DeGraves, F.J., Castanie-Cornet, M.-P., and Foster, J.W. (2004). Acid resistance systems required for survival of Escherichia coli O157:H7 in the bovine gastrointestinal tract and in apple cider are different. Applied and environmental microbiology *70*, 4792-4799. 10.1128/AEM.70.8.4792-4799.2004.
101. Bower Jean, M., and Mulvey Matthew, A. (2006). Polyamine-Mediated Resistance of Uropathogenic Escherichia coli to Nitrosative Stress. Journal of Bacteriology *188*, 928-933. 10.1128/jb.188.3.928-933.2006.
102. Purkerson, J.M., Everett, C.A., and Schwartz, G.J. (2022). Ammonium chloride-induced acidosis exacerbates cystitis and pyelonephritis caused by uropathogenic E. coli. Physiological Reports *10*, e15471. https://doi.org/10.14814/phy2.15471.
103. Lund, P., Tramonti, A., and De Biase, D. (2014). Coping with low pH: molecular strategies in neutralophilic bacteria. FEMS Microbiology Reviews *38*, 1091-1125. 10.1111/1574-6976.12076.
104. Yamamoto, S., Tsukamoto, T., Terai, A., Kurazono, H., Takeda, Y., and Yoshida, O. (1997). Genetic Evidence Supporting the Fecal-Perineal-Urethral Hypothesis in Cystitis Caused by Escherichia Coli. The Journal of Urology *157*, 1127-1129. https://doi.org/10.1016/S0022-5347(01)65154-1.
105. Bergholz, T.M., and Whittam, T.S. (2007). Variation in acid resistance among enterohaemorrhagic Escherichia coli in a simulated gastric environment. Journal of Applied Microbiology *102*, 352-362. https://doi.org/10.1111/j.1365-2672.2006.03099.x.
106. Kanjee, U., and Houry, W.A. (2013). Mechanisms of acid resistance in Escherichia coli. Annu Rev Microbiol *67*, 65-81. 10.1146/annurev-micro-092412-155708.
107. Lin, J., Smith, M.P., Chapin, K.C., Baik, H.S., Bennett, G.N., and Foster, J.W. (1996). Mechanisms of acid resistance in enterohemorrhagic Escherichia coli. Applied and Environmental Microbiology *62*, 3094.
108. De Biase, D., and Lund, P.A. (2015). Chapter Two - The Escherichia coli Acid Stress Response and Its Significance for Pathogenesis. In Advances in Applied Microbiology, S. Sariaslani, and G.M. Gadd, eds. (Academic Press), pp. 49-88. https://doi.org/10.1016/bs.aambs.2015.03.002.
109. Selvarasu, S., Ow, D.S.-W., Lee, S.Y., Lee, M.M., Oh, S.K.-W., Karimi, I.A., and Lee, D.-Y. (2009). Characterizing Escherichia coli DH5α growth and metabolism in a complex medium using genome-scale flux analysis. Biotechnology and Bioengineering *102*, 923-934. 10.1002/bit.22119.

110. Cicchillo, R.M., Baker, M.A., Schnitzer, E.J., Newman, E.B., Krebs, C., and Booker, S.J. (2004). Escherichia coli L-Serine Deaminase Requires a [4Fe-4S] Cluster in Catalysis. Journal of Biological Chemistry *279*, 32418-32425. 10.1074/jbc.M404381200.
111. Zhang, X., and Newman, E. (2008). Deficiency in l-serine deaminase results in abnormal growth and cell division of Escherichia coli K-12. Molecular Microbiology *69*, 870-881. 10.1111/j.1365-2958.2008.06315.x.
112. Vining, L.C., and Magasanik, B. (1981). Serine utilization by Klebsiella aerogenes. Journal of bacteriology *146*, 647-655. 10.1128/jb.146.2.647-655.1981.
113. Chaussee, M.S., Somerville, G.A., Reitzer, L., and Musser, J.M. (2003). Rgg coordinates virulence factor synthesis and metabolism in Streptococcus pyogenes. Journal of bacteriology *185*, 6016-6024. 10.1128/JB.185.20.6016-6024.2003.
114. Mulvey, M.A., Schilling, J.D., and Hultgren, S.J. (2001). Establishment of a persistent Escherichia coli reservoir during the acute phase of a bladder infection. Infect Immun *69*, 4572-4579.
115. Hannan, T.J., Totsika, M., Mansfield, K.J., Moore, K.H., Schembri, M.A., and Hultgren, S.J. (2012). Host–pathogen checkpoints and population bottlenecks in persistent and intracellular uropathogenic Escherichia coli bladder infection. FEMS Microbiology Reviews *36*, 616-648. 10.1111/j.1574-6976.2012.00339.x.
116. Spaulding, C.N., Klein, R.D., Ruer, S., Kau, A.L., Schreiber, H.L., Cusumano, Z.T., Dodson, K.W., Pinkner, J.S., Fremont, D.H., Janetka, J.W., et al. (2017). Selective depletion of uropathogenic E. coli from the gut by a FimH antagonist. Nature *546*, 528-532. 10.1038/nature22972.
117. O'Hanlon, D.E., Come, R.A., and Moench, T.R. (2019). Vaginal pH measured in vivo: lactobacilli determine pH and lactic acid concentration. BMC Microbiol *19*, 13. 10.1186/s12866-019-1388-8.
118. Matsuzaki, T., Scotcher, D., Darwich, A.S., Galetin, A., and Rostami-Hodjegan, A. (2019). Towards Further Verification of Physiologically-Based Kidney Models: Predictability of the Effects of Urine-Flow and Urine-pH on Renal Clearance. Journal of Pharmacology and Experimental Therapeutics *368*, 157. 10.1124/jpet.118.251413.
119. Simerville, J.A., Maxted Wc Fau - Pahira, J.J., and Pahira, J.J. Urinalysis: a comprehensive review.
120. Murphy, K.C., and Campellone, K.G. (2003). Lambda Red-mediated recombinogenic engineering of enterohemorrhagic and enteropathogenic E. coli. BMC Mol Biol *4*, 11.
121. Steiner, B.D., Eberly, A.R., Hurst, M.N., Zhang, E.W., Green, H.D., Behr, S., Jung, K., and Hadjifrangiskou, M. (2018). Evidence of Cross-Regulation in Two Closely Related Pyruvate-Sensing Systems in Uropathogenic Escherichia coli. The Journal of Membrane Biology *251*, 65-74. 10.1007/s00232-018-0014-2.
122. Fried, L., Behr, S., and Jung, K. (2013). Identification of a target gene and activating stimulus for the YpdA/YpdB histidine kinase/response regulator system in Escherichia coli. J Bacteriol *195*, 807-815. 10.1128/JB.02051-12.
123. Pfaffl, M.W. (2001). A new mathematical model for relative quantification in real-time RT–PCR. Nucleic Acids Research *29*, e45-e45. 10.1093/nar/29.9.e45.
124. Kraxenberger, T., Fried, L., Behr, S., and Jung, K. (2012). First insights into the unexplored two-component system YehU/YehT in Escherichia coli. J Bacteriol *194*, 4272-4284. 10.1128/JB.00409-12.

125. Kannan, G., Wilks, J.C., Fitzgerald, D.M., Jones, B.D., BonDurant, S.S., and Slonczewski, J.L. (2008). Rapid acid treatment of Escherichia coli: transcriptomic response and recovery. BMC Microbiology *8*, 37. 10.1186/1471-2180-8-37.
126. Chen, S.L., Hung, C.-S., Xu, J., Reigstad, C.S., Magrini, V., Sabo, A., Blasiar, D., Bieri, T., Meyer, R.R., Ozersky, P., et al. (2006). Identification of genes subject to positive selection in uropathogenic strains of Escherichia coli: A comparative genomics approach. Proceedings of the National Academy of Sciences *103*, 5977-5982. 10.1073/pnas.0600938103.
127. Fried, L., Behr, S., and Jung, K. (2013). Identification of a Target Gene and Activating Stimulus for the YpdA/YpdB Histidine Kinase/Response Regulator System in Escherichia coli. Journal of Bacteriology *195*, 807. 10.1128/JB.02051-12.
128. Shin, D., Lee, E.J., Huang, H., and Groisman, E.A. (2006). A positive feedback loop promotes transcription surge that jump-starts Salmonella virulence circuit. Science *314*, 1607-1609. 10.1126/science.1134930.
129. Behr, S., Kristoficova, I., Witting, M., Breland, E.J., Eberly, A.R., Sachs, C., Schmitt-Kopplin, P., Hadjifrangiskou, M., and Jung, K. (2017). Identification of a High-Affinity Pyruvate Receptor in Escherichia coli. Scientific Reports *7*, 1388. 10.1038/s41598-017-01410-2.
130. Newman, E.B., Dumont, D., and Walker, C. (1985). In vitro and in vivo activation of L-serine deaminase in Escherichia coli K-12. Journal of Bacteriology *162*, 1270.
131. Su, H., and Newman, E.B. (1991). A novel L-serine deaminase activity in Escherichia coli K-12. Journal of bacteriology *173*, 2473-2480.
132. Zhang, X., El-Hajj Ziad, W., and Newman, E. (2010). Deficiency in l-Serine Deaminase Interferes with One-Carbon Metabolism and Cell Wall Synthesis in Escherichia coli K-12. Journal of Bacteriology *192*, 5515-5525. 10.1128/JB.00748-10.
133. Shao, Z., and Newman, E.B. (1993). Sequencing and characterization of the sdaB gene from Escherichia coli K-12. European Journal of Biochemistry *212*, 777-784. https://doi.org/10.1111/j.1432-1033.1993.tb17718.x.
134. Takahashl, N., Saito, K., Schachtele, C.F., and Yamada, T. (1997). Acid tolerance and acid-neutralizing activity of Porphyromonas gingivalis, Prevotella intermedia and Fusobacterium nucleatum. Oral Microbiology and Immunology *12*, 323-328. https://doi.org/10.1111/j.1399-302X.1997.tb00733.x.
135. Scott, D.R., Marcus, E.A., Weeks, D.L., and Sachs, G. (2002). Mechanisms of acid resistance due to the urease system of Helicobacter pylori. Gastroenterology *123*, 187-195. 10.1053/gast.2002.34218.
136. Persson, K., Petersson, U., Johansson, C., Demirel, I., and Kruse, R. (2022). Transcriptional alterations in bladder epithelial cells in response to infection with different morphological states of uropathogenic Escherichia coli. Scientific Reports *12*, 486. 10.1038/s41598-021-04396-0.
137. Magliano, E., Grazioli, V., Deflorio, L., Leuci, A.I., Mattina, R., Romano, P., and Cocuzza, C.E. (2012). Gender and Age-Dependent Etiology of Community-Acquired Urinary Tract Infections. The Scientific World Journal *2012*, 349597. 10.1100/2012/349597.

138. Zhang, L., Foxman, B., and Marrs, C. (2002). Both Urinary and Rectal Escherichia coli Isolates Are Dominated by Strains of Phylogenetic Group B2. Journal of Clinical Microbiology *40*, 3951-3955. 10.1128/jcm.40.11.3951-3955.2002.
139. Nielsen, K.L., Stegger, M., Kiil, K., Godfrey, P.A., Feldgarden, M., Lilje, B., Andersen, P.S., and Frimodt-Møller, N. (2017). Whole-genome comparison of urinary pathogenic Escherichia coli and faecal isolates of UTI patients and healthy controls. International Journal of Medical Microbiology *307*, 497-507. https://doi.org/10.1016/j.ijmm.2017.09.007.
140. Yamamoto, S., Tsukamoto T Fau - Terai, A., Terai A Fau - Kurazono, H., Kurazono H Fau - Takeda, Y., Takeda Y Fau - Yoshida, O., and Yoshida, O. Genetic evidence supporting the fecal-perineal-urethral hypothesis in cystitis caused by Escherichia coli.
141. Thomas-White, K., Forster, S.C., Kumar, N., Van Kuiken, M., Putonti, C., Stares, M.D., Hilt, E.E., Price, T.K., Wolfe, A.J., and Lawley, T.D. (2018). Culturing of female bladder bacteria reveals an interconnected urogenital microbiota. Nature Communications *9*, 1557. 10.1038/s41467-018-03968-5.
142. Fallingborg, J. Intraluminal pH of the human gastrointestinal tract.
143. Brannon, J.A.-O., Dunigan, T.L., Beebout, C.A.-O., Ross, T., Wiebe, M.A., Reynolds, W.S., and Hadjifrangiskou, M.A.-O. Invasion of vaginal epithelial cells by uropathogenic Escherichia coli.
144. Juárez Tomás, M.S., Ocaña, V.S., Wiese, B., and Nader-Macías, M.E. (2003). Growth and lactic acid production by vaginal Lactobacillus acidophilus CRL 1259, and inhibition of uropathogenic Escherichia coli. Journal of Medical Microbiology *52*, 1117-1124. https://doi.org/10.1099/jmm.0.05155-0.
145. O'Hanlon, D.E., Come, R.A., and Moench, T.R. (2019). Vaginal pH measured in vivo: lactobacilli determine pH and lactic acid concentration. BMC Microbiology *19*, 13. 10.1186/s12866-019-1388-8.
146. Miao, Y., Li, G., Zhang, X., Xu, H., and Abraham, Soman N. (2015). A TRP Channel Senses Lysosome Neutralization by Pathogens to Trigger Their Expulsion. Cell *161*, 1306-1319. https://doi.org/10.1016/j.cell.2015.05.009.
147. Iyer, R., Williams, C., and Miller, C. (2003). Arginine-Agmatine Antiporter in Extreme Acid Resistance in Escherichia coli. Journal of Bacteriology *185*, 6556. 10.1128/JB.185.22.6556-6561.2003.
148. Auger, E.A., and Bennett, G.N. (1989). Regulation of lysine decarboxylase activity in Escherichia coli K-12. Archives of Microbiology *151*, 466-468. 10.1007/BF00416608.
149. Mulvey Matthew, A., Schilling Joel, D., and Hultgren Scott, J. (2001). Establishment of a Persistent Escherichia coli Reservoir during the Acute Phase of a Bladder Infection. Infection and Immunity *69*, 4572-4579. 10.1128/IAI.69.7.4572-4579.2001.
150. Guckes, K.R., Kostakioti M Fau - Breland, E.J., Breland Ej Fau - Gu, A.P., Gu Ap Fau - Shaffer, C.L., Shaffer Cl Fau - Martinez, C.R., 3rd, Martinez Cr 3rd Fau - Hultgren, S.J., Hultgren Sj Fau - Hadjifrangiskou, M., and Hadjifrangiskou, M. Strong cross-system interactions drive the activation of the QseB response regulator in the absence of its cognate sensor.
151. Wiebe Michelle, A., Brannon John, R., Steiner Bradley, D., Bamidele, A., Schrimpe-Rutledge Alexandra, C., Codreanu Simona, G., Sherrod Stacy, D., McLean John, A., and Hadjifrangiskou, M. (2022). Serine Deamination Is a New Acid Tolerance Mechanism

Observed in Uropathogenic Escherichia coli. mBio *13*, e02963-02922. 10.1128/mbio.02963-22.
152. Wright, K.J., Seed, P.C., and Hultgren, S.J. (2007). Development of intracellular bacterial communities of uropathogenic Escherichia coli depends on type 1 pili. Cellular Microbiology *9*, 2230-2241. https://doi.org/10.1111/j.1462-5822.2007.00952.x.
153. Mulvey, M.A., Lopez-Boado, Y.S., Wilson, C.L., Roth, R., Parks, W.C., Heuser, J., and Hultgren, S.J. (1998). Induction and Evasion of Host Defenses by Type 1-Piliated Uropathogenic Escherichia coli. Science *282*, 1494-1497. 10.1126/science.282.5393.1494.
154. Schembri, M.A., Kjaergaard, K., Sokurenko, E.V., and Klemm, P. (2001). Molecular Characterization of the Escherichia coli FimH Adhesin. The Journal of Infectious Diseases *183*, S28-S31. 10.1086/318847.
155. Hayes, B.W., and Abraham, S.N. (2016). Innate Immune Responses to Bladder Infection. Microbiol Spectr *4*. 10.1128/microbiolspec.UTI-0024-2016.
156. Justice, S.S., Hung, C., Theriot, J.A., Fletcher, D.A., Anderson, G.G., Footer, M.J., and Hultgren, S.J. (2004). Differentiation and developmental pathways of uropathogenic Escherichia coli in urinary tract pathogenesis. Proc Natl Acad Sci U S A *101*, 1333-1338. 10.1073/pnas.0308125100.
157. Lacerda Mariano, L., Rousseau, M., Varet, H., Legendre, R., Gentek, R., Saenz Coronilla, J., Bajenoff, M., Gomez Perdiguero, E., and Ingersoll, M.A. Functionally distinct resident macrophage subsets differentially shape responses to infection in the bladder. Science Advances *6*, eabc5739. 10.1126/sciadv.abc5739.
158. Yu, L., O'Brien, V.P., Livny, J., Dorsey, D., Bandyopadhyay, N., Colonna, M., Caparon, M.G., Roberson, E.D.O., Hultgren, S.J., and Hannan, T.J. (2019). Mucosal infection rewires TNFα signaling dynamics to skew susceptibility to recurrence. eLife *8*, e46677. 10.7554/eLife.46677.
159. Martinez, J.J., Mulvey, M.A., Schilling, J.D., Pinkner, J.S., and Hultgren, S.J. (2000). Type 1 pilus-mediated bacterial invasion of bladder epithelial cells. The EMBO Journal *19*, 2803-2812. https://doi.org/10.1093/emboj/19.12.2803.
160. Bishop, B.L., Duncan, M.J., Song, J., Li, G., Zaas, D., and Abraham, S.N. (2007). Cyclic AMP–regulated exocytosis of Escherichia coli from infected bladder epithelial cells. Nature Medicine *13*, 625-630. 10.1038/nm1572.
161. Naskar, M., Parekh, V.P., Abraham, M.A., Alibasic, Z., Kim, M.J., Suk, G., Noh, J.H., Ko, K.Y., Lee, J., Kim, C., et al. (2023). α-Hemolysin promotes uropathogenic E. coli persistence in bladder epithelial cells via abrogating bacteria-harboring lysosome acidification. PLOS Pathogens *19*, e1011388. 10.1371/journal.ppat.1011388.
162. Steinberg, T.H. (1994). Cellular Transport of Drugs. Clinical Infectious Diseases *19*, 916-921. 10.1093/clinids/19.5.916.
163. Ciak, J., and Hahn, F.E. (1966). Chloroquine: Mode of Action. Science *151*, 347-349. 10.1126/science.151.3708.347.
164. Paetzold, S., Lourido, S., Raupach, B., and Zychlinsky, A. (2007). Shigella flexneri Phagosomal Escape Is Independent of Invasion. Infection and Immunity *75*, 4826-4830. 10.1128/iai.00454-07.
165. Shaffer, C.L., Zhang, E.W., Dudley, A.G., Dixon, B.R.E.A., Guckes, K.R., Breland, E.J., Floyd, K.A., Casella, D.P., Algood, H.M.S., Clayton, D.B., and Hadjifrangiskou, M. (2016). Purine Biosynthesis Metabolically Constrains Intracellular Survival of

Uropathogenic Escherichia coli. Infection and immunity *85*, e00471-00416. 10.1128/IAI.00471-16.
166. Knodler, L.A., Nair, V., and Steele-Mortimer, O. (2014). Quantitative Assessment of Cytosolic Salmonella in Epithelial Cells. PLOS ONE *9*, e84681. 10.1371/journal.pone.0084681.
167. Mauvezin, C., and Neufeld, T.P. (2015). Bafilomycin A1 disrupts autophagic flux by inhibiting both V-ATPase-dependent acidification and Ca-P60A/SERCA-dependent autophagosome-lysosome fusion. Autophagy *11*, 1437-1438. 10.1080/15548627.2015.1066957.
168. Bower Jean, M., Gordon-Raagas Hannah, B., and Mulvey Matthew, A. (2009). Conditioning of Uropathogenic Escherichia coli for Enhanced Colonization of Host. Infection and Immunity *77*, 2104-2112. 10.1128/iai.01200-08.
169. Di Martino, M.L., Campilongo, R., Casalino, M., Micheli, G., Colonna, B., and Prosseda, G. (2013). Polyamines: Emerging players in bacteria–host interactions. International Journal of Medical Microbiology *303*, 484-491. https://doi.org/10.1016/j.ijmm.2013.06.008.
170. Jiang, J., Wang, W., Sun, F., Zhang, Y., Liu, Q., and Yang, D. (2021). Bacterial infection reinforces host metabolic flux from arginine to spermine for NLRP3 inflammasome evasion. Cell Reports *34*. 10.1016/j.celrep.2021.108832.
171. Nakamura, A., Kurihara, S., Takahashi, D., Ohashi, W., Nakamura, Y., Kimura, S., Onuki, M., Kume, A., Sasazawa, Y., Furusawa, Y., et al. (2021). Symbiotic polyamine metabolism regulates epithelial proliferation and macrophage differentiation in the colon. Nature Communications *12*, 2105. 10.1038/s41467-021-22212-1.
172. Chakraborty, S., Mizusaki, H., and Kenney, L.J. (2015). A FRET-Based DNA Biosensor Tracks OmpR-Dependent Acidification of Salmonella during Macrophage Infection. PLOS Biology *13*, e1002116. 10.1371/journal.pbio.1002116.
173. Chakraborty, S., and Kenney, L.J. (2018). A New Role of OmpR in Acid and Osmotic Stress in Salmonella and E. coli. Frontiers in microbiology *9*, 2656-2656. 10.3389/fmicb.2018.02656.
174. Miao, J., Willems Hubertine, M.E., and Peters Brian, M. (2021). Exogenous Reproductive Hormones nor Candida albicans Colonization Alter the Near Neutral Mouse Vaginal pH. Infection and Immunity *89*, 10.1128/iai.00550-00520. 10.1128/iai.00550-20.
175. Wolfarth, A.A., Smith, T.M., VanInsberghe, D., Dunlop, A.L., Neish, A.S., Corwin, E.J., and Jones, R.M. (2020). A Human Microbiota-Associated Murine Model for Assessing the Impact of the Vaginal Microbiota on Pregnancy Outcomes. Frontiers in Cellular and Infection Microbiology *10*. 10.3389/fcimb.2020.570025.
176. Mejia, M.E., Mercado-Evans, V., Zulk, J.J., Ottinger, S., Ruiz, K., Ballard, M.B., Fowler, S.W., Britton, R.A., and Patras, K.A. (2023). Vaginal microbial dynamics and pathogen colonization in a humanized microbiota mouse model. npj Biofilms and Microbiomes *9*, 87. 10.1038/s41522-023-00454-9.
177. Hung, C.-S., Dodson, K.W., and Hultgren, S.J. (2009). A murine model of urinary tract infection. Nature Protocols *4*, 1230-1243. 10.1038/nprot.2009.116.
178. Kristoficova, I., Vilhena, C., Behr, S., and Jung, K. (2018). BtsT, a Novel and Specific Pyruvate/H⁺ Symporter in <span class="named-content genus-species"

id="named-content-1">Escherichia coli. Journal of Bacteriology *200*, e00599-00517. 10.1128/JB.00599-17.
179. Kraxenberger, T., Fried, L., Behr, S., and Jung, K. (2012). First Insights into the Unexplored Two-Component System YehU/YehT in Escherichia coli. Journal of Bacteriology *194*, 4272. 10.1128/JB.00409-12.
180. Trapnell, C., Roberts, A., Goff, L., Pertea, G., Kim, D., Kelley, D.R., Pimentel, H., Salzberg, S.L., Rinn, J.L., and Pachter, L. (2012). Differential gene and transcript expression analysis of RNA-seq experiments with TopHat and Cufflinks. Nature Protocols *7*, 562-578. 10.1038/nprot.2012.016.
181. Li, D. (2019). Computational Biology. In H. Husi, ed. Chaptere 6: Statistical Methods for RNA Sequencing Data Analysis. Codon Publications.
182. Witkin Steven, S., Mendes-Soares, H., Linhares Iara, M., Jayaram, A., Ledger William, J., and Forney Larry, J. (2013). Influence of Vaginal Bacteria and d- and l-Lactic Acid Isomers on Vaginal Extracellular Matrix Metalloproteinase Inducer: Implications for Protection against Upper Genital Tract Infections. mBio *4*, 10.1128/mbio.00460-00413. 10.1128/mbio.00460-13.
183. Chen, X., Lu, Y., Chen, T., and Li, R. (2021). The Female Vaginal Microbiome in Health and Bacterial Vaginosis. Frontiers in Cellular and Infection Microbiology *11*. 10.3389/fcimb.2021.631972.
184. Abbe, C., and Mitchell, C.M. (2023). Bacterial vaginosis: a review of approaches to treatment and prevention. Frontiers in Reproductive Health *5*. 10.3389/frph.2023.1100029.
185. Gilbert, N.M., O'Brien, V.P., and Lewis, A.L. (2017). Transient microbiota exposures activate dormant Escherichia coli infection in the bladder and drive severe outcomes of recurrent disease. PLOS Pathogens *13*, e1006238. 10.1371/journal.ppat.1006238.
186. Singhal, R., and Shah, Y.M. (2020). Oxygen battle in the gut: Hypoxia and hypoxia-inducible factors in metabolic and inflammatory responses in the intestine. Journal of Biological Chemistry *295*, 10493-10505. 10.1074/jbc.REV120.011188.
187. Hayes, E.T., Wilks, J.C., Sanfilippo, P., Yohannes, E., Tate, D.P., Jones, B.D., Radmacher, M.D., BonDurant, S.S., and Slonczewski, J.L. (2006). Oxygen limitation modulates pH regulation of catabolism and hydrogenases, multidrug transporters, and envelope composition in Escherichia coli K-12. BMC microbiology *6*, 89-89. 10.1186/1471-2180-6-89.
188. Wanner, B.L. (1992). Is cross regulation by phosphorylation of two-component response regulator proteins important in bacteria? J Bacteriol *174*, 2053-2058.
189. Mike, L.A., Choby, J.E., Brinkman, P.R., Olive, L.Q., Dutter, B.F., Ivan, S.J., Gibbs, C.M., Sulikowski, G.A., Stauff, D.L., and Skaar, E.P. (2014). Two-component system cross-regulation integrates Bacillus anthracis response to heme and cell envelope stress. PLoS Pathog *10*, e1004044. 10.1371/journal.ppat.1004044.
190. Guckes, K.R., Breland, E.J., Zhang, E.W., Hanks, S.C., Gill, N.K., Algood, H.M., Schmitz, J.E., Stratton, C.W., and Hadjifrangiskou, M. (2017). Signaling by two-component system noncognate partners promotes intrinsic tolerance to polymyxin B in uropathogenic Escherichia coli. Sci Signal *10*. 10.1126/scisignal.aag1775.

191. van der Ploeg, J.R., Eichhorn, E., and Leisinger, T. (2001). Sulfonate-sulfur metabolism and its regulation in Escherichia coli. Archives of Microbiology *176*, 1-8. 10.1007/s002030100298.
192. Rowbury, R.J. (1997). Regulatory components, including integration host factor, CysB and H-NS, that influence pH responses in Escherichia coli. Letters in Applied Microbiology *24*, 319-328. https://doi.org/10.1046/j.1472-765X.1997.00065.x.
193. Takagi, H., and Ohtsu, I. (2017). l-Cysteine Metabolism and Fermentation in Microorganisms. In Amino Acid Fermentation, A. Yokota, and M. Ikeda, eds. (Springer Japan), pp. 129-151. 10.1007/10_2016_29.
194. Kawano, Y., Suzuki, K., and Ohtsu, I. (2018). Current understanding of sulfur assimilation metabolism to biosynthesize l-cysteine and recent progress of its fermentative overproduction in microorganisms. Applied Microbiology and Biotechnology *102*, 8203-8211. 10.1007/s00253-018-9246-4.
195. Kredich Nicholas, M. (2008). Biosynthesis of Cysteine. EcoSal Plus *3*, 10.1128/ecosalplus.1123.1126.1121.1111. 10.1128/ecosalplus.3.6.1.11.
196. Heieck, K., Arnold, N.D., and Brück, T.B. (2023). Metabolic stress constrains microbial L-cysteine production in Escherichia coli by accelerating transposition through mobile genetic elements. Microbial Cell Factories *22*, 10. 10.1186/s12934-023-02021-5.
197. Ohtsu, I., Wiriyathanawudhiwong, N., Morigasaki, S., Nakatani, T., Kadokura, H., and Takagi, H. (2010). The l-Cysteine/l-Cystine Shuttle System Provides Reducing Equivalents to the Periplasm in Escherichia coli*. Journal of Biological Chemistry *285*, 17479-17487. https://doi.org/10.1074/jbc.M109.081356.
198. Shabayek, S., and Spellerberg, B. (2017). Acid Stress Response Mechanisms of Group B Streptococci. Frontiers in Cellular and Infection Microbiology *7*. 10.3389/fcimb.2017.00395.
199. Liu, Y., Tang, H., Lin, Z., and Xu, P. (2015). Mechanisms of acid tolerance in bacteria and prospects in biotechnology and bioremediation. Biotechnology Advances *33*, 1484-1492. https://doi.org/10.1016/j.biotechadv.2015.06.001.
200. Wilks, J.C., and Slonczewski, J.L. (2007). pH of the Cytoplasm and Periplasm of Escherichia coli: Rapid Measurement by Green Fluorescent Protein Fluorimetry. Journal of Bacteriology *189*, 5601. 10.1128/JB.00615-07.
201. Kitko, R.D., Wilks, J.C., Garduque, G.M., and Slonczewski, J.L. (2010). Osmolytes Contribute to pH Homeostasis of Escherichia coli. PLOS ONE *5*, e10078. 10.1371/journal.pone.0010078.
202. Llopis, J., McCaffery, J.M., Miyawaki, A., Farquhar, M.G., and Tsien, R.Y. (1998). Measurement of cytosolic, mitochondrial, and Golgi pH in single living cells with green fluorescent proteins. Proceedings of the National Academy of Sciences *95*, 6803. 10.1073/pnas.95.12.6803.
203. Slonczewski, J.L., Fujisawa M Fau - Dopson, M., Dopson M Fau - Krulwich, T.A., and Krulwich, T.A. Cytoplasmic pH measurement and homeostasis in bacteria and archaea.
204. Brameyer, S., Schumacher, K., Kuppermann, S., and Jung, K. (2022). Division of labor and collective functionality in Escherichia coli under acid stress. Communications Biology *5*, 327. 10.1038/s42003-022-03281-4.
205. Aquino, P., Honda, B., Jaini, S., Lyubetskaya, A., Hosur, K., Chiu, J.G., Ekladious, I., Hu, D., Jin, L., Sayeg, M.K., et al. (2017). Coordinated regulation of acid resistance in Escherichia coli. BMC Syst Biol *11*, 1. 10.1186/s12918-016-0376-y.

206. Stim-Herndon, K.P., Flores, T.M., and Bennett, G.N. (1996). Molecular characterization of adiY, a regulatory gene which affects expression of the biodegradative acid-induced arginine decarboxylase gene (adiA) of Escherichia coli. Microbiology *142*, 1311-1320. https://doi.org/10.1099/13500872-142-5-1311.
207. Behr, S., Heermann, R., and Jung, K. (2016). Insights into the DNA-binding mechanism of a LytTR-type transcription regulator. Bioscience Reports *36*. 10.1042/BSR20160069.
208. Guckes, K.R., Breland, E.J., Zhang, E.W., Hanks, S.C., Gill, N.K., Algood, H.M., Schmitz, J.E., Stratton, C.W., and Hadjifrangiskou, M. Signaling by two-component system noncognate partners promotes intrinsic tolerance to polymyxin B in uropathogenic Escherichia coli. LID - 10.1126/scisignal.aag1775 [doi] LID - eaag1775.
209. Breland, E.J., Zhang, E.W., Bermudez, T., Martinez, C.R., 3rd, and Hadjifrangiskou, M. The Histidine Residue of QseC Is Required for Canonical Signaling between QseB and PmrB in Uropathogenic Escherichia coli. LID - 10.1128/JB.00060-17 [doi] LID - e00060-17.
210. Kostakioti, M., Hadjifrangiskou M Fau - Pinkner, J.S., Pinkner Js Fau - Hultgren, S.J., and Hultgren, S.J. QseC-mediated dephosphorylation of QseB is required for expression of genes associated with virulence in uropathogenic Escherichia coli.
211. Ouellette, S.P., Karimova, G., Davi, M., and Ladant, D. (2017). Analysis of Membrane Protein Interactions with a Bacterial Adenylate Cyclase–Based Two-Hybrid (BACTH) Technique. Current Protocols in Molecular Biology *118*, 20.12.21-20.12.24. 10.1002/cpmb.36.